AD-A060 204 CIVIL ENGINEERING LAB (NAVY) PORT HUFNEME CALIF F/G 8/11
A PROBABILISTIC PROCEDURE FOR ESTIMATING SEISMIC LOADING BASED --ETC(U)
AUG 78 J M FERRITTO
UNCLASSIFIED CEL-TR-867 NL

1 OF 3
AD A060 204

AD A060204

LEVEL II

12 55

DDC
RECEIVED
OCT 23 1978
F

R867

DDC FILE COPY

TECHNICAL REPORT
CIVIL ENGINEERING LABORATORY

Naval Construction Battalion Center, Port Hueneme, California 93043

A PROBABILISTIC PROCEDURE FOR ESTIMATING SEISMIC LOADING BASED ON HISTORIC AND GEOLOGIC DATA

By

J. M. Ferritto

August 1978

Sponsored by

NAVAL MATERIAL COMMAND

Approved for public release; distribution unlimited.

78 10 19 063

Unclassified

SECURITY CLASSIFICATION OF THIS PAGE (When Data Entered)

REPORT DOCUMENTATION PAGE

READ INSTRUCTIONS BEFORE COMPLETING FORM

1. REPORT NUMBER: TR-867	2. GOVT ACCESSION NO.: DN 887007
3. RECIPIENT'S CATALOG NUMBER: Rept.	
4. TITLE (and Subtitle): A PROBABILISTIC PROCEDURE FOR ESTIMATING SEISMIC LOADING BASED ON HISTORIC AND GEOLOGIC DATA	5. TYPE OF REPORT & PERIOD COVERED: Final Oct 1977 – Sep 1978
	6. PERFORMING ORG. REPORT NUMBER
7. AUTHOR(s): J. M. Ferritto	8. CONTRACT OR GRANT NUMBER(s)
9. PERFORMING ORGANIZATION NAME AND ADDRESS: CIVIL ENGINEERING LABORATORY, Naval Construction Battalion Center, Port Hueneme, California 93043	10. PROGRAM ELEMENT, PROJECT, TASK AREA & WORK UNIT NUMBERS: 61152N; Z-R000-01-165
11. CONTROLLING OFFICE NAME AND ADDRESS: Naval Material Command, Washington, D.C. 20360	12. REPORT DATE: August 1978
	13. NUMBER OF PAGES: 240
14. MONITORING AGENCY NAME & ADDRESS (if different from Controlling Office): ZR000 01	15. SECURITY CLASS. (of this report): Unclassified
	15a. DECLASSIFICATION/DOWNGRADING SCHEDULE

16. DISTRIBUTION STATEMENT (of this Report): ZR000 01 165

Approved for public release; distribution unlimited.

17. DISTRIBUTION STATEMENT (of the abstract entered in Block 20, if different from Report)

18. SUPPLEMENTARY NOTES

19. KEY WORDS (Continue on reverse side if necessary and identify by block number)

Earthquake, ground motion, acceleration, response spectra, seismic risk.

20. ABSTRACT (Continue on reverse side if necessary and identify by block number)

This report describes a procedure for estimating site ground motion based on the historic data base of earthquakes adjusted to incorporate fault slip data. Procedures are given for determining site acceleration magnitude and duration for various confidence levels. Seismic risk analysis techniques are discussed. The report contains background material required for an understanding of the procedure.

DD FORM 1 JAN 73 1473 EDITION OF 1 NOV 65 IS OBSOLETE

Unclassified

SECURITY CLASSIFICATION OF THIS PAGE (When Data Entered)

391111

78 10 19 063

Library Card

Civil Engineering Laboratory
A PROBABILISTIC PROCEDURE FOR ESTIMATING SEISMIC LOADING BASED ON HISTORIC AND GEOLOGIC DATA
(Final), by J. M. Ferritto
TR-867 240 pp illus August 1978 Unclassified

1. Earthquake movement 2. Seismic analysis I. Z-R000-01-165

This report describes a procedure for estimating site ground motion based on the historic data base of earthquakes adjusted to incorporate fault slip data. Procedures are given for determining site acceleration magnitude and duration for various confidence levels. Seismic risk analysis techniques are discussed. The report contains background material required for an understanding of the procedure.

CONTENTS

CONTENTS (Con't)

ACCESSION for
NTIS White Section
DDC Buff Section
UNANNOUNCED
JUSTIFICATION
BY
DISTRIBUTION/AVAILABILITY CODES
SPECIAL
A

PREFACE

NAVFAC Instruction 11012.138, 24 October 1975, has specified that, for buildings designated as "critical buildings," a site seismicity study be performed, in lieu of the lateral load coefficients provided in NAVFAC P355, Seismic Design of Buildings, April 1973. Acceleration response spectra developed from the study shall be used to determine the magnitude of the lateral loads. This report is intended to provide a methodology and automated procedure for computing site microzonation studies and recurrence data needed for design.

This report cites the works of many authors. Much of the material is included here to give the reader adequate background to understand the developments and assumptions made. In particular, the work of Krinitzsky (1974) was cited verbatim in many places.

The report is organized into nine chapters. Chapter 1 gives the reader an introduction into earthquake causes, types of faults and associated behavior. Chapter 2 gives dimensional relationships between faults and magnitude. Such information is used in later sections. Chapter 3 discusses fault movement and geologic slip rates as a procedure for estimating earthquake recurrence. Chapter 4 discusses the historic earthquake data base and its limitations. Chapter 5 presents stochastic procedures for treating earthquake data. Chapter 6 presents earthquake site-induced ground motion as a function of epicentral distance and magnitude. Chapter 7 draws upon the previous sections as background and presents an automated procedure for determining a probabilistic estimation of site acceleration based on the historic data base and adjusted to consider geologic data. The confidence limits of

the estimate are given. Such a process is the first step in specification of a design level earthquake loading. Chapter 8 provides the second step - the preparation of response spectra. Chapter 9 discusses risk analysis and an approach for economic selection of design criteria.

CHAPTER 1 - EARTHQUAKES AND FAULTING

Plate Tectonics

The United States is located on the North America plate, the western portion of which mets the Pacific plate. The interaction of these two plates is responsible for the high seismic activity which has in the past and continues now to take place in the Western United States. Plate tectonic theory has explained much of the geologic activity. Also explained in terms of plate tectonic theory is the seismic activity experienced in the Central and Eastern parts of the United States. This midplate activity can be very destructive.

Figure 1-1 shows a cross section of the earth. The lithosphere, composed largely of basalt, extends to an average depth of about 100 km. Below the lithosphere is the asthenosphere which extends to a depth of 400 km. Because its upper portion is partially molten, seismic velocity in that region is decreased. The lithospheric plates are able to "float" on this plastic layer. Not all of the asthenosphere is molten; however, there is a rigid portion.

Most seismic activity is located at plate boundaries and, therefore, boundaries are of considerable interest. Walper (1976) is quoted in the following paragraph:

> Three kinds of plate boundaries can be distinguished by the three principal modes of interaction between adjacent plates, and distinctive types of plate margins are identified with each: (a) divergent or spreading boundaries with constructive or accreting plate margins; (b) convergent or collision boundaries with destructive or consuming margins; and

(c) transform or transcursion boundaries that form margins known as conservative because there is no gain or loss of crust [Figure 1-2].

Geologic Faults and Earthquakes

Since the San Francisco earthquake of 1906 and the subsequent work on the elastic rebound theory of earthquakes, general agreement has been reached on the close relationship between earthquakes and geologic faults. Most tectonic earthquakes of the type that cause major structural damage are associated with fracture on a fault. Plate motion causes stress in the earth's rock crust. Earthquakes occur when the strength of the fault can no longer withstand the stress that has built up. Fault plane solutions and earthquake mechanism studies have contributed to a consistent picture of the earthquake generation process which satisfactorily explains most of the observed facts.

Krinitzsky (1974) states:

> A fault is a shear rupture in the earth along which opposite faces have been displaced relative to each other. Relative motion is parallel to the fault itself. *** † A rupture without relative displacement is termed a joint.
>
> The basic kinds of faults discussed above are illustrated schematically in *** [Figure 1-3 showing appropriate terminology]. They are defined in the following paragraphs.
>
> a. Strike slip. Strike is the line of direction in a horizontal plane produced by intersection by a fault plane. Movement along this line *** [Figure 1-3a] is strike slip. Such faults are usually high angle, that is near to vertical. *** The direction of movement is designated as right lateral

†Asterisks (***) indicate deleted material in quoted passages.

or left lateral depending on the direction (right or left) the opposite side has moved when one faces the fault. *** The movement shown in *** [Figure 1-3a] is left lateral.

b. Normal. A normal fault *** [Figure 1-3b] is one in which the hanging wall (the overlying side of the fault) has moved downward relative to the footwall (the underlying side of the fault). For hanging wall and footwall *** [see Figure 1-4]. This movement results from horizontal tension. *** It is also called a gravity fault. Note that AB in *** [Figure 1-3b] is slip, AC is throw, and BC is heave.

c. Thrust or reverse. This is a fault *** [Figure 1-3c] in which the hanging wall has moved upward relative to the footwall. It is caused by horizontal compression. *** Its movement AB is slip, AC is throw, and BC is heave.

Most faults are combinations of strike slip and one or the other of the above. Also, the fault plane itself is likely to be curved. Blocks may be rotated relative to each other.

Components of movement *** [Figure 1-3d] are staged as AB, net slip; AE or CB, strike slip; AC or EB, dip slip; AD, throw; and DC, heave.

The fault trace *** [Figure 1-4] is the line of the fault at the surface. The strike of the fault is measured in a horizontal plane as degrees of deviation of its direction from north. The dip is measured in degrees from the horizontal plane to the fault plane and is given a directional component that is perpendicular to the fault strike.

Features commonly associated with normal faults are shown schematically in *** [Figure 1-5]. Step faults are blocks that are sheared like slices. The lowermost block is a graben. An isolated high block is a horst.

> The movements illustrated in *** [Figure 1-3] are highly simplified. In nature they may be very complex with secondary and tertiary slippages related to primary fault movements.

Some misunderstandings have occurred – and perhaps some significant differences of opinion – about the direct relationship between geologic faults and the earthquake hazard. There is much evidence dating from 1906 to suggest that destructive ground shaking is not necessarily at a maximum in the immediate vicinity of the causative fault (Hudson, 1972). More often than not, the maximum destructive ground shaking is observed to be some miles from the fault, as can be explained by a number of the features of the generation and propagation of seismic waves. Classical photographs of the 1906 major movements along the San Andreas fault, for example, show horizontal surface displacements of as much as 15 feet passing several feet from a small wood-frame house that received no significant damage. Similarly, during the San Fernando earthquake of 9 February 1971, a 5-foot vertical fault scarp passed directly through a wooden barn just a few hundred feet from a single-story residence. The barn was severely damaged, but no significant structural damage to the house was noted (Hudson, 1972). The San Fernando earthquake also furnished numerous examples of surface faulting passing through heavily populated areas. Although severe structural deformation, with a resulting economic loss, occurred in numerous cases, catastrophic collapses leading to loss of life and serious injury were not directly associated with these surface breaks. Hazardous collapses were in all cases the consequence of severe ground shaking, which is pervasive over a large area and is not limited to the vicinity of faults.

The focus or hypocenter is the point within the earth's crust where the initial rupture occurs and from which the first waves are released. The projection of this point to the ground surface is the epicenter. The epicenter and hypocenter do not necessarily indicate the center of total energy release of the earthquake but rather the point where the

seismic energy waves were first created. For small earthquakes the center of total energy release and the epicenter are not far apart because the fault break length is short; however, this is not the case for large earthquakes. The majority of earthquakes in the United States have had relatively shallow focal depths (0 to 40 km). In California, earthquakes have occurred in regions where surface fault patterns were clearly visible. In the Puget Sound area, earthquakes are focused at deeper locations within the earth's crust so that a surface rupture is not observable. In the eastern United States, the relationship to surface rupture has not been identified (Bolt, 1970; Newmark and Rosenblueth, 1971).

A fault undergoing tectonic creep, or one with abrupt displacement, causes changes in the terrain it crosses. Very distinctive patterns are produced where active faults cross streams, such as landslides. The ongoing geologic process causes scarps, trenches, sag ponds and stream offsets. Figure 1-6 shows a landform with an active fault (Wesson et al., 1975).

Estimates of the maximum size and frequency of earthquakes on a fault are based on the geologically determined slip rate and the historic record of ground deformation (where available), the seismic history of the fault and surrounding tectonic region, a geological evaluation of the tectonic setting, and empirically derived relationships between earthquake magnitude and fault length.

Surface Effects of Fault Movements

When faults are considered, the assumption is commonly made that the creation of entirely new faults by an earthquake is unlikely (Krinitzsky, 1974). Significant surface faults and their activity may be found by proper geologic investigations. Cluff, Slemmons, and Waggoner (1970) have illustrated schematically the character of typical surface effects by faults. These are shown in Figures 1-7 to 1-9.

Strike-Slip Faults. Strike-slip faults are usually steep, nearly vertical. Figure 1-7 shows the damage that is associated with strike-slip movement. Some fault displacement pre-exists, and movement occurs along the pre-existing plane. There is very little vertical component of movement; hence, there are negligible topographic effects other than the slip itself. Krinitzsky (1974) describes types of faults below:

> The San Andreas is a nearly vertical strike-slip fault that in recent times has had a cumulative displacement of many kilometers. It has manifested this activity by pronounced effects on the [regional] drainage. Where it passes through mountainous country, for example in the Santa Cruz Mountains, the drainage has cut a valley along the active trace of the fault. In the Carrizo Plain of southern California, *** the fault has had a dramatic effect in turning drainage that crosses the fault. The displaced drainage now is joined in a dogleg along the fault trace. This is a measure of the displacement that has occurred since the drainage was developed. Though drainage history has never been dated precisely, interpretations are possible of the manner of movement in recent times.
>
> Strike slip faults [usually] tend to have greater continuity along their fault traces than do other faults. Also, strike-slip faults will occur within narrower fault zones. Along the San Andreas the full zone in some places is as much as 1.6 to 3.3 km wide. However, the most recent and most pronounced fault movement is likely to be on single, identifiable planes. A recurrence of movement has a high probability of being along the same plane. Thus, the trace of movement along a strike-slip fault is predictable to a far larger extent than for other types of faults.

Various portions of Krinitzsky (1974) are quoted below:

Landslides. Where fault movements are postulated near an engineering site, the hazard from landslides should be evaluated as a special category. They may be produced in association with faults or, more commonly, they may be triggered elsewhere by earthquakes. Loose, saturated debris, or jointed rock with weakened planes, on steep slopes are susceptible and have contributed to spectacular landslides in the past.

Normal Faults. Normal faults *** [Figure 1-8] have more pronounced topographic effects. The downdropped block breaks along the dragged lip and forms secondary displacements in addition to those on the major plane. Damage by fault displacement is concentrated in the downdropped block. The upthrown block may remain relatively intact. This assumes that movement is confined to a single major fault plane. Normal faulting is susceptible also to multiple-plane steplike displacements.

Thrust Faults. Thrust faults *** [Figure 1-9] tend to break up in the upthrown block. The downthrown block remains intact, except that near the face of the major fault plane there is landsliding. Field measurement of the amount of thrusting often is difficult because of this destruction of the fault plane. The breakage in the upthrown block tends to be highly arcuate and irregular. Thrust faults are likely to occur along multiple planes.

Thrust faults may occur along a mountain front by activation of a scarp-forming process, such as that which occurred during the San Fernando earthquake of 1971. Such movement is to some degree predictable. However, thrust faults may also occur in very complex and often unpredictable associations. A thrust fault occurred at Hanning Bay during

the Alaska earthquake of 1964. It raised the bay floor and cut across an adjacent ridge. The ridge contains a notch that had been developed during earlier movements.

Geological, Seismological, and Soils Investigations and Fault Activity

The objective of the geological investigation is to establish the lithology, stratigraphy, structure, and history of the general region. Tectonic structures underlying the region must be identified, and any evidence of fault activity determined. The seismological investigation compiles a listing of all earthquakes of record which may have affected the general area of the site. The magnitude of the earthquakes, epicenter locations, dynamic characteristics, and durations of the resulting ground motion are determined. Epicenters within about 200 miles of the proposed site are of particular significance. Geological fault structures within this approximate radius should be studied.

The type of information required includes identification and delineation of those faults that are active; that is, capable of generating earthquakes. Information about recency of faulting is useful in designating particular faults as active for specific land uses. Designation of a fault as active can be based on the assumption that the more recent the faulting (geologic time) the more likely that the fault will undergo intermittent displacement in the geologically near future. Movement is presumed less likely to occur in the immediate future (50 years) along faults that have progressively longer geologic periods of demonstrated quiescence. Because of the apparent great range in frequency of movement, there is no agreement at present on the length of geologic time pertinent to evaluation of the near-future behavior of faults. Selection of the timespan used to designate faults as active from age of latest movement has been influenced by the potential consequence of seismic shaking of surface faulting on the specific structure. The greater the risk to be incurred, the longer the timespan that must be

considered. Displacement during Holocene time* is a generally accepted criterion of activity for many land uses. This timespan is probably inadequate, however, to assure recognition of all active faults. Historic offsets have occurred along faults, such as the White Wolf fault in southern California, that had no previously recognized evidence of Holocene faulting. Wentworth and Yerkes (1971) state that evidence of displacement during late Quaternary time (the past several hundred thousand years) should be considered evidence that a fault is probably active for low seismicity regions.

To quote Krinitzsky (1974) further:

> Fault movements have occurred throughout geologic time. The oldest geologic strata, it may be supposed, are the most faulted but this is not a general condition. However, faults which moved in the past will not necessarily move again in the present.
>
> *** faults [,for an engineering analysis,] are either active or inactive. Active means that a fault may move at some time in the near future. In engineering [terms], it means it may occur during the life of a structure. Inactive means that it will not.
>
> *** The Atomic Energy Commission [1973b] has developed a set of guidelines. ***:
>
> a. Datable movement during the past 35,000 yr. (The limit of reliable radiocarbon dating.)
> b. Datable movement more than once in the past 500,000 yr. (Marine terraces on the West Coast.)
> c. Structural interrelation whereby a fault can be shown to move if movement occurs on a different fault with proven activity.

*The most recent geologic time unit - beginning of the last glacial retreat 12,000 to 20,000 years ago to the present.

d. Instrumentally determined macroseismic activity relatable to a fault.

e. Projection of a proven active fault through or into areas where all evidence of the fault or its activity is obscured, as by thick alluvium.

The International Atomic Energy Agency [1972] adds two additional criteria:

a. Evidence of creep movement along a fault (creep is slow displacement not necessarily accompanied by macroearthquakes).

b. Topographic evidence of surface rupture, surface warping, or offset of geomorphic features.

They would further classify active faults on a geomorphic basis as follows:

Class A - High rate of movement, greater than 1 m per 1000 yr

Class B - Topography shows clear evidence of dislocation

Class C - Topography shows indistinct evidence of dislocation

Class D - No evidence of amount or rate of dislocation on which quantitative assessment can be based, but fault is considered capable of causing surface faulting.

In general engineering practice a fault is considered to be active if there is displacement within Holocene *** deposits regardless of datable evidence. (Examples: fault displacements within surface gravels, alluvium, or glacial outwash.) *** All of the criteria above are indicative of a present-day hazard from renewed movement along a fault, and they are sufficient to identify a fault as active.

Geophysical and Geological Investigation

A general description of the types of tasks performed in geophysical and geological investigations will be given here as given in Krinitzsky (1974).

Background Information.

Background information, *** which *** [may be] assembled and studied *** includes:

a. Imagery. Air photos and other [photos].

b. General geology. Available maps and reports on the rock and soil types, ages, tectonic history.

c. Seismicity. Historic record.

d. Mapped faults.

* * * * * * *

Air Inspection. An efficient way to begin is to overfly the area in a helicopter or small plane and inspect the terrain carefully for whatever evidences can be found. Early morning and late afternoon hours are best, since long shadows may reveal faults that might otherwise be missed. The faults should be scanned for appearances of fresh displacements and a notation made for checking the displacements on the ground. The prime concern in checking faults for earthquake risk is to determine the presence or absence of activity along the faults.

Ground Inspection. Criteria for determining recent fault activity are:

a. Scarps. Freshness of fault breaks; displacements of surficial gravels or soil layers.

b. Turned drainage.

c. Sag ponds.

d. Other hydrologic anomalies. Springs; lines of greenery in arid areas; groundwater barriers.

e. Land displacement. Anomalous displaced land blocks; drowned trees.

f. Tilted trees. Bends in trees along fault zones. Bends may be related to recent movements. Tree rings may help to date fault movements.

g. Sandblows. To determine inclusive areas of large earthquake disturbance.

h. Harrowed ground. Intricate breakage of ground by earth shaking; usually on local topographic highs.

Associations. The information above must be placed in context with:

a. Historic seismic events. A caution is that reported epicenters are sometimes unreliable. They should be rechecked wherever they contribute to important judgments on location of fault movements.

b. Structural trends. An area of doubtful activity may be determined to be a continuation of a structural trend in which elsewhere there is proven activity. Activity may be inferred by association and through projection.

Dating. Dating calls for imaginative and resourceful approaches. Some of the more common are:

a. Stratigraphic displacements. Borings may show net displacements in young deposits of known age. Rates of movement may be postulated for such faults.

b. Effects of datable geomorphic features. Breaks in marine terraces of known ages. Displacements in datable alluvial sediments or glacial deposits. Similarly, these may give average rates of fault movement.

c. Paleontology and palynology. Age dating of fossils in displaced layers.

d. Radiocarbon dating. Age dating of organic matter (peat, wood, bones, etc.) in sag ponds, scarp detritus, and displaced layers. Often such dating can be related to specific earthquake events.

e. Paleomagnetism. Magnetic dating with relation to polar wandering during recent times.

f. Uranium disequilibrium. Disintegration of radioactive uranium with time.

g. Potassium-argon. Particularly useful for displaced volcanic rocks.

h. Other. Associations with young cinder cones, presence of fresh scarps without datable associations, etc.

Mapping. Mapping should include as much as can be determined of the following information:

a. Geometry of fault movement.

b. Age of most recent movement.

c. Frequency of movement or rate of movement.

d. Reliability of interpretation.

e. Projected activity beneath masking deposits.

f. Association with landslides. In particular, one must be certain that landslides are not mistaken for fault movements.

* * * * * * *

Borings.

Correlations between borings provide a direct method for examining a site closely for fault planes.

Caution must be exercised in determining the lithology from the need to interpolate between bore holes.

Trenching. Trenching offers a procedure for uncovering faults not seen at the surface.

Strain Measurement. This is principally a research technique consisting of installation of strain measuring gages.

Geodetic Surveys. Precision surveying of a series of monuments on opposite sides of a fault is used to measure fault movement.

Geophysical investigations include the following:

Bouguer Gravity Survey. A regional survey of the earth's gravity in which corrections have been made for the effects of topography. Anomalies are indicative of changes in the mass properties of rocks where something unusual has happened in the earth's crust. This approach does not identify specific faults, but may help delineate areas of faulting in the subsurface.

Magnetic Survey. A magnetic survey explores local changes in the earth's magnetic field. The results are affected by changes of rock types (iron content) revealing abrupt changes such as those which take place where there is movement.

Seismographic and Electrical Resistivity Surveys. These are the various techniques for passing energy through rocks and monitoring changes in rock properties. The property changes occur from either stratification or inhomogeneities in the rock mass or from displacements in the rock mass.

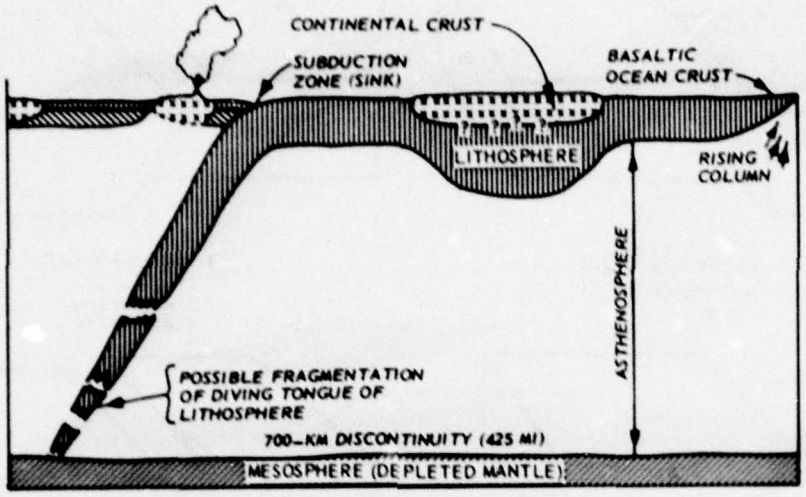

Figure 1-1. Schematic cross section of earth structure (from Walper, 1976).

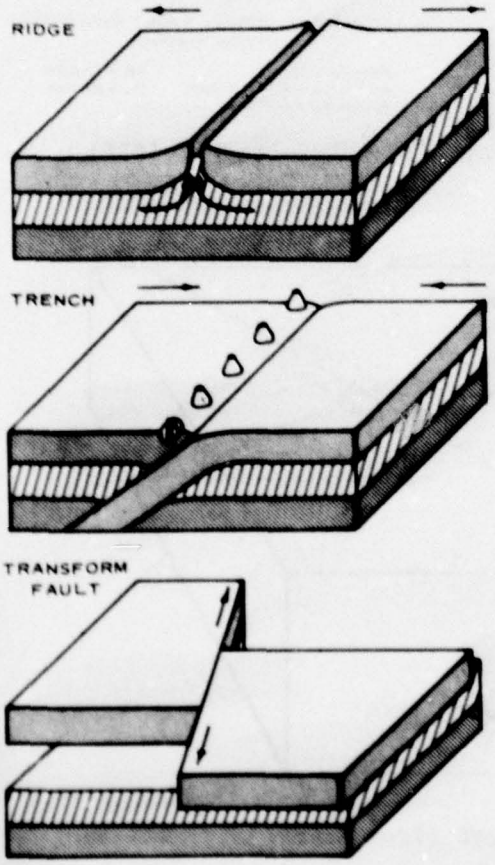

a. Divergent or spreading boundary

b. Convergent or collision boundary

c. Transform or transcursion boundary

Figure 1-2. The three kinds of boundaries between plates (from Walper, 1976).

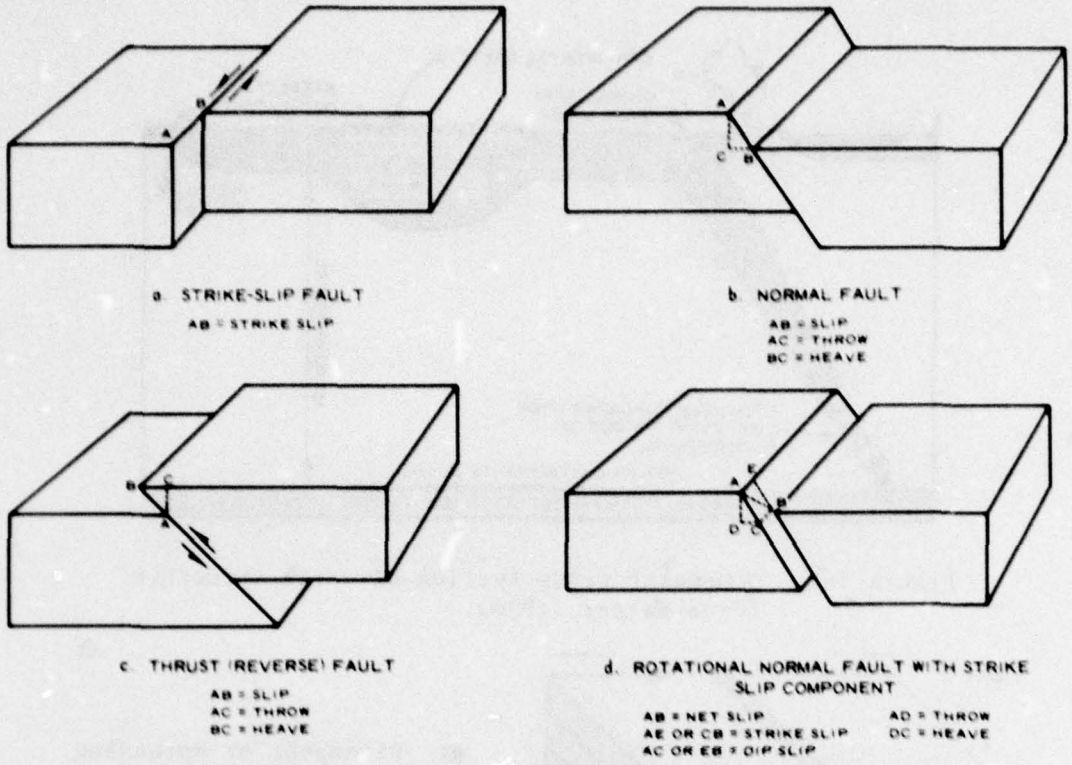

Figure 1-3. Fault terminology (from Krinitzsky, 1974).

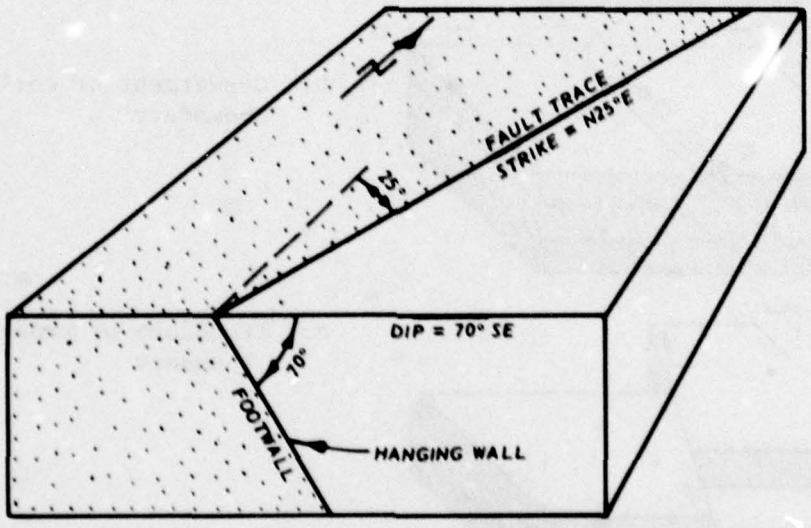

Figure 1-4. Fault measurement (from Krinitzsky, 1974).

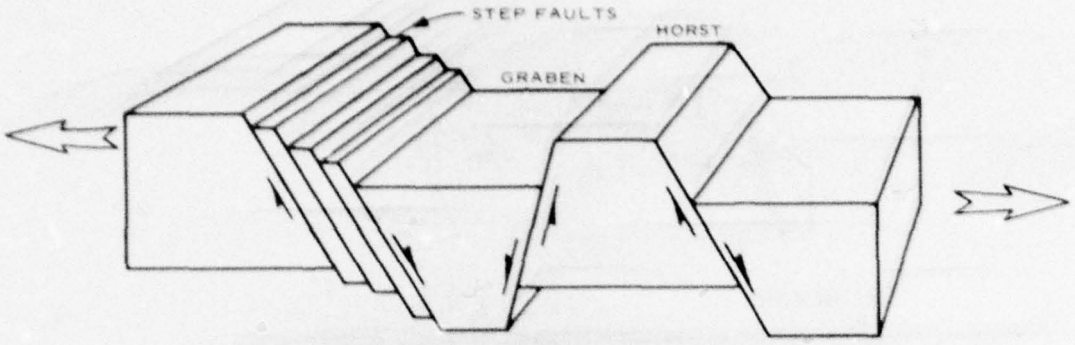

Figure 1-5. Fault block features associated with normal faults (from Krinitzsky, 1974).

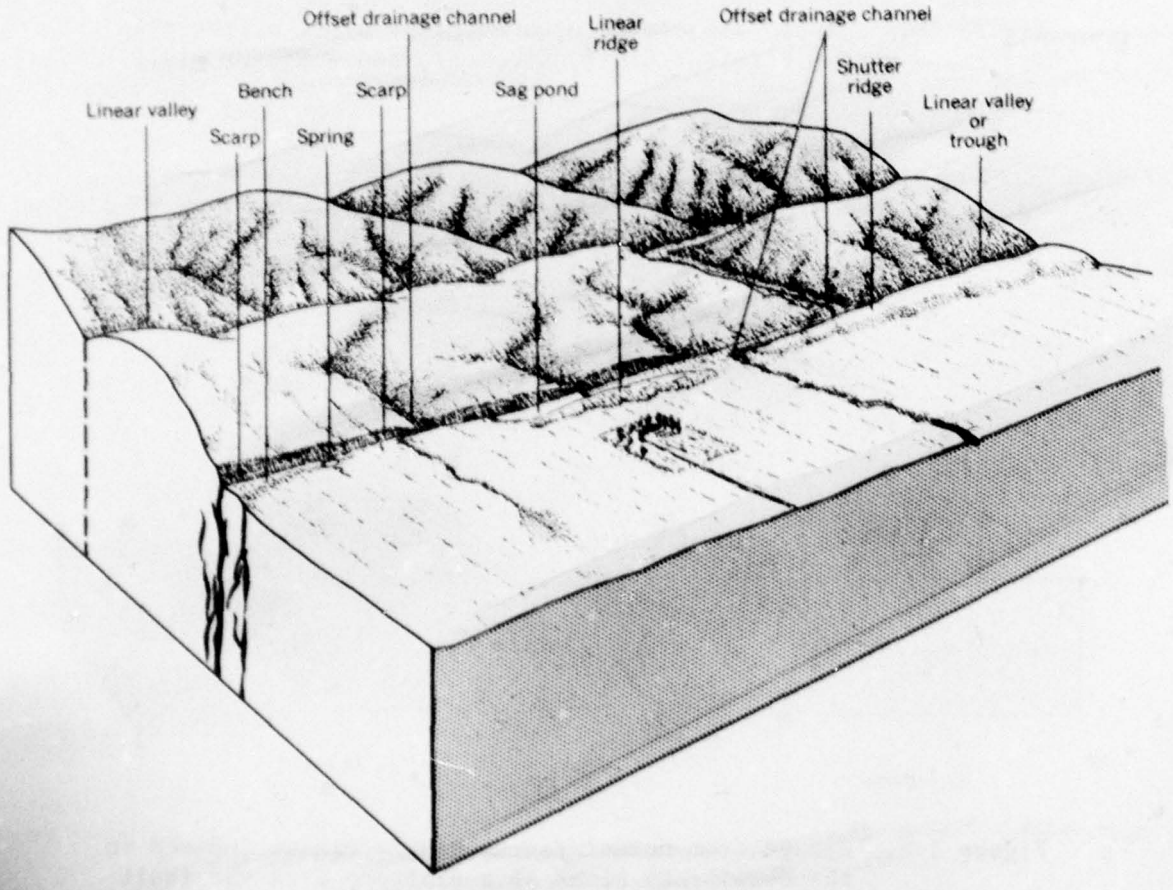

Figure 1-6. Landforms developed along recently active strike-slip faults (after U.S. Geological Survey, 1975).

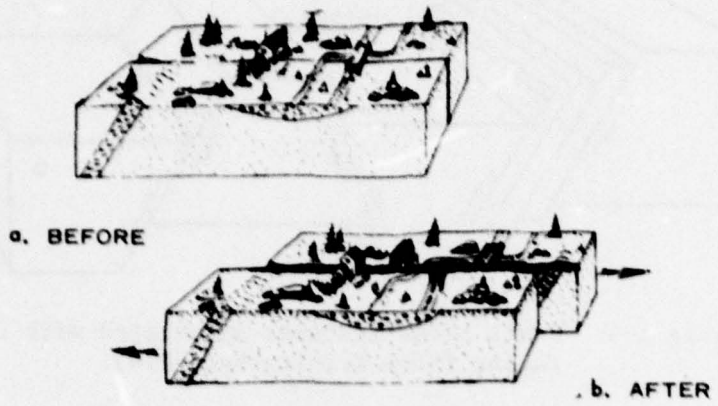

Figure 1-7. Damage associated with movement along strike-slip fault (after Cluff, Slemmons, and Waggoner, 1970).

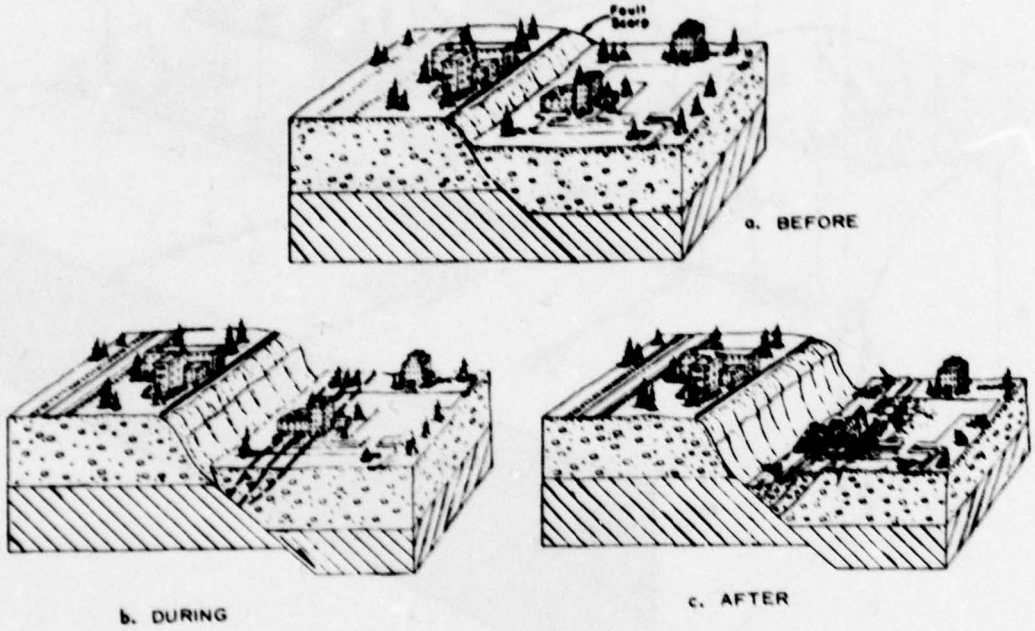

Figure 1-8. Damage from normal fault; displacements induced in the downthrown block at a distance from the fault trace (after Cluff, Slemmons, and Waggoner, 1970).

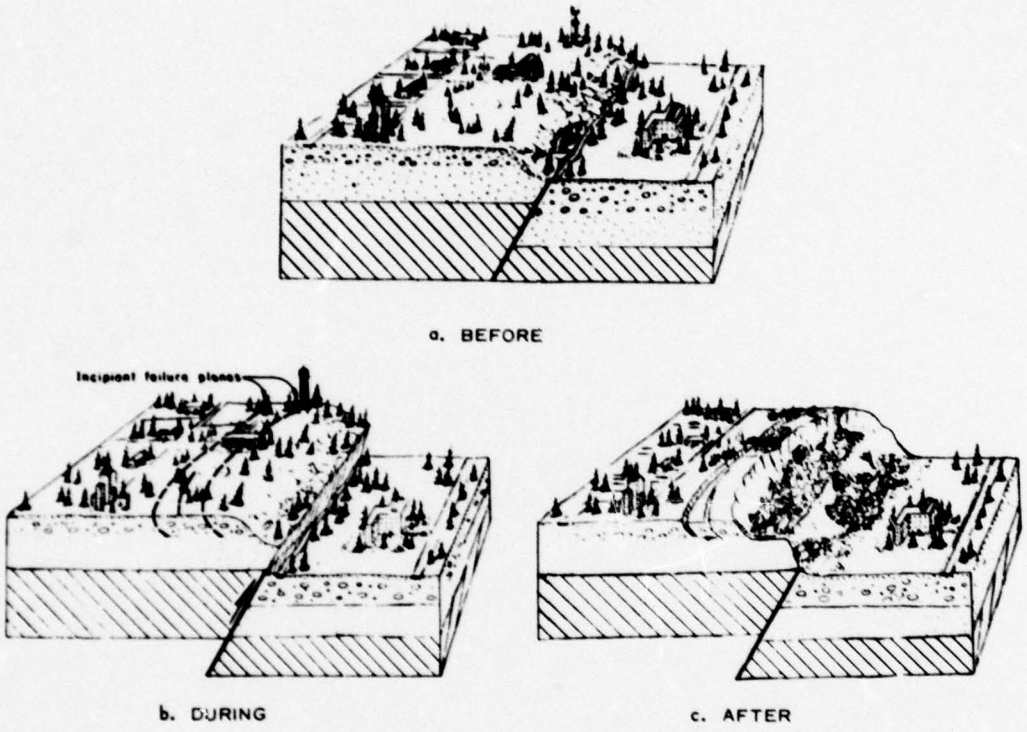

Figure 1-9. Damage from thrust (reverse) fault; earth displacements induced on the upthrown block at a distance from the fault trace (after Cluff, Slemmons, and Waggoner, 1970).

CHAPTER 2 – DIMENSIONAL RELATIONSHIP BETWEEN FAULTS AND EARTHQUAKE MAGNITUDE

Earthquake Magnitude

Engineers may define a design earthquake for a site in terms of the earthquake magnitude M and the strength of ground motion. Factors which influence the selection of a design earthquake are the length of geologic fault structures, the relationship of the fault to the regional tectonic structure, the geologic history of displacement along the structure and the seismic history of the region.

The design earthquake in engineering terms is a specification of levels of ground motion that the project is required to survive successfully with an avoidance of loss of life and acceptable damage and loss of service. A design earthquake on a statistical basis considers the probability of the recurrence of a historical event.

Earthquake magnitudes may be specified in terms of a design level earthquake which can reasonably be expected to occur during the life of the structure. As such, this represents a service load which the structure must withstand without significant structural damage or interruption of required operation. A second level of earthquake magnitude is a maximum credible event for which the structure must not collapse; however, significant structural damage may occur. The inelastic behavior of the structure must be limited to insure the prevention of collapse and catastrophic loss of life.

The selection of a magnitude level may be based on:

1. Known design-level and maximum-credible earthquake magnitudes associated with a fault whose seismicity has been estimated

PRECEDING PAGE BLANK

2. Specification of probability of occurrence for a given life of the structure (such as having a 10% chance of being exceeded in 25 years, NAVFAC criteria)

3. Specification of required level of ground motion as in a code provision

4. Fault length empirical relationships

Earthquake magnitude can be related to length of fault for shallow depth earthquakes. Data have been plotted by Seed et al. (1969), Krinitzsky (1974), Housner (1965), and Tocher (1958) to provide the curves indicated (Figure 2-1). It is important to note that in some regions, correlations of these types are of little value since many of the important geologic features may be deeply buried by weathered materials.

Magnitude as measured on the Richter scale is calculated from a standard earthquake, one which provides a maximum trace amplitude of 1 μm on a standard Wood-Anderson torsion seismograph at a distance of 100 km. Magnitude is the $\log_{10}$ of the ratio of the amplitude of any earthquake at the standard distance to that of the standard earthquake. Each full numeral step in the scale (two to three, for example) represents an energy increase of about 32 times. Experience with past earthquakes is presently the only useful basis for relating fault length and motion to magnitudes of associated earthquakes.

Fault Length and Earthquake Magnitude

A useful insight into the relationship between earthquake magnitude and length of observed fault slippage was presented by Iida (1965). He grouped faults of all types and obtained the plot shown in Figure 2-2. He presents a spread of points for which upper and lower boundaries are drawn. Iida's spread of values should be kept in mind when one considers the linear relationships that have been suggested by numerous authors.

Figure 2-1 shows several such relationships that were compiled by the Bureau of Reclamation (1972) and reported by Krinitzsky (1974). They differ from each other only to a minor extent. The curves appear to be least reliable for low earthquake magnitudes. Krinitzsky (1974) is quoted below:

> [Figure 2-3] illustrates the concept that a small earthquake may radiate displacements around a focus (that point which is the center of the earthquake and the origin of its elastic waves) without breaking the surface in any consistent manner. In fact it may not break the surface at all. The energy release can be accommodated largely or totally in the subsurface.
>
> The spread of related data is explored further in *** [Figure 2-4]. The dashed lines were drawn to encompass a spread of worldwide earthquake events gathered by Ambraseys and Tchalenko [1968] ***. In addition, a selection of large earthquakes generated specifically by thrust faults is shown from U. S. Geological Survey (USGS) data. From the Ambraseys and Tchalenko [1968] data there is a lower limit, or cutoff, at magnitude 5.4 below which surface rupture has no significance in relation to magnitude. Fault movements below magnitude 5.4, with very few exceptions, are contained in the subsurface as shown in *** [Figure 2-3]. The corollary to this is that if <u>any</u> active surface fault movement is found, no matter how short it is, it might be evidence for an earthquake capability of greater than magnitude 5.4.
>
> Thrust faults *** present a more difficult problem. They are capable of huge irregularities between magnitude and surface rupture even for large earthquakes (magnitudes greater than 7). In fact their greatest irregularity may be in the largest events. This may result from energy release by breakage along multiple parallel planes, much more so than is the case in slippages of other types of faults. Thus, where

magnitudes are to be estimated for thrust faults, one must be prepared to apply values that can represent strong earthquakes, though the fault lengths may not be exceptional.

Fault Length and Displacement

Figure 2-5 shows the maximum surface rupture on main faults typical of the United States with superimposed lines best fit of world and North America data (Bonilla, 1967 and 1970). Maximum surface displacement is related to earthquake magnitude in Figure 2-6 (Bonilla, 1970). The displacements are total displacement measured after the earthquake and thus may have a large amount of creep displacement included. This data is limited and should be used only as a guide to minimums.

Figure 2-7 shows minor branch and secondary faults associated with a major fault. Bonilla (1967) relates displacement on a minor fault to the major fault. Figure 2-8 shows an envelope of the data.

The broad scatter shown by the data is partly due to (1) the variety of field conditions in the areas where the observations of faulting were made, (2) the inadequacy of the length of surface fault rupture as a measure of the length of faulting at depth, and (3) theoretical limitations.

Bonilla and Buchanan (1970) combined the data, "the study of the relationships between surface fault displacement, surface fault rupture, and earthquake magnitude" to produce Figure 2-9. "Again, the data have very large spreads." Boundaries were added by Krinitzsky (1974). More recent work by Mark and Bonilla (1977) reevaluated the data taking fault type into account. The results are shown in Figures 2-10, 2-11, and 2-12.

It is important to note the spread in the data. Krinitzsky (1974) concludes "Any fault break in competent rock, no matter how small, should be taken as indicative of the capability for at least a 5.4 earthquake." It is important that consideration be given to the local seismic history and the behavior of other analogous faults.

Absence of Surface Faults

Consideration should be given to the possibility of not identifying all the faults in a region which may be active. This is especially true in central and eastern United States. To account for this a "floating earthquake" (one that may be assumed capable of occurring anywhere in the region) should be considered (Krinitzsky, 1974).

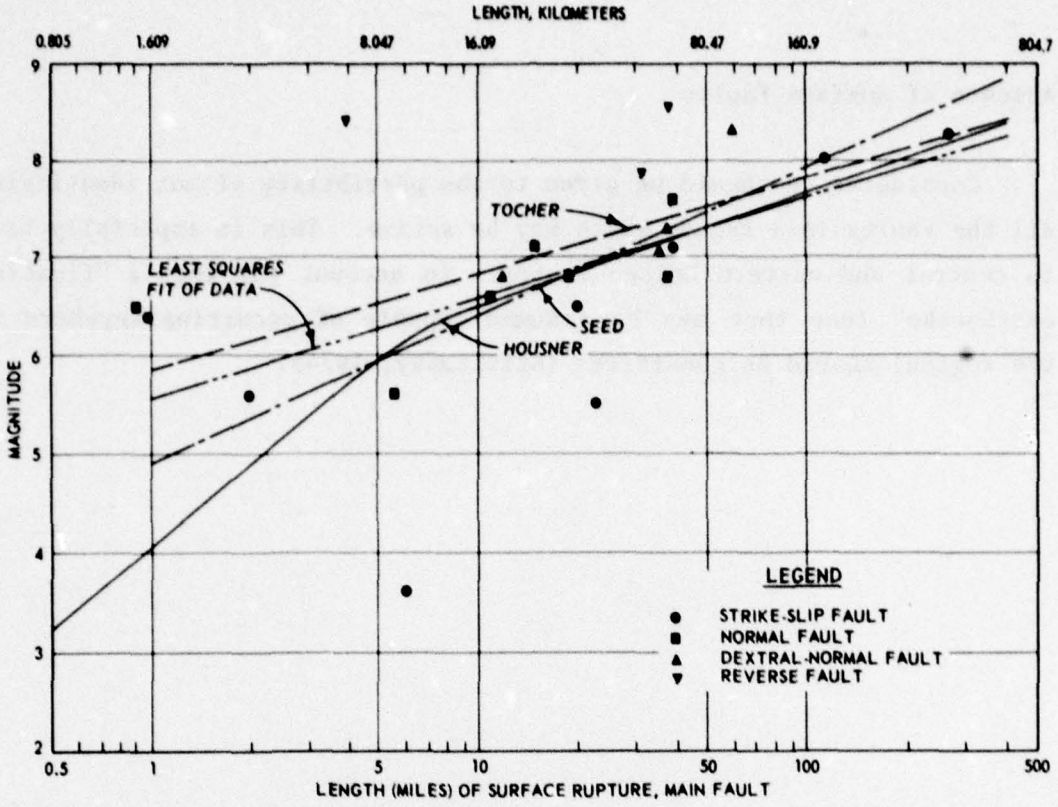

Figure 2-1. Earthquake magnitude versus length of surface rupture (from Krinitzsky, 1974).

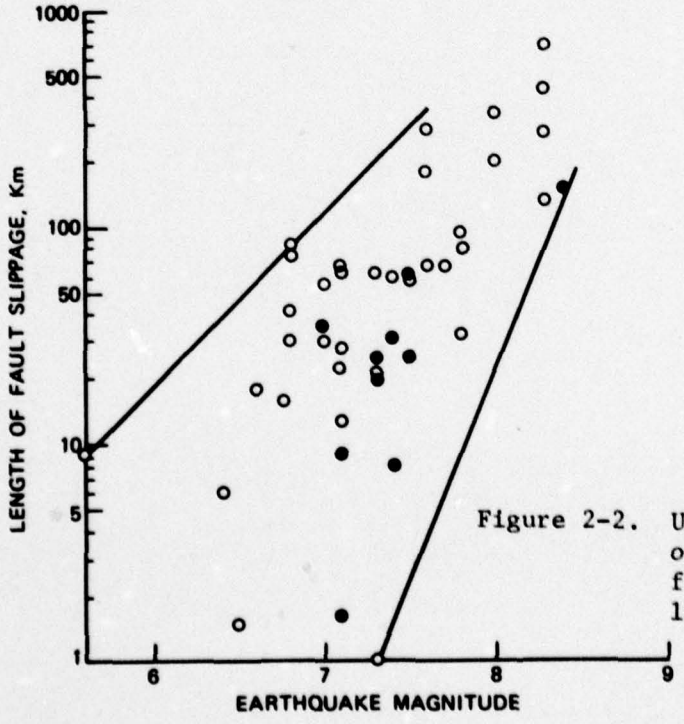

Figure 2-2. Upper and lower boundaries of earthquake magnitude and fault slippage (from Iida, 1965).

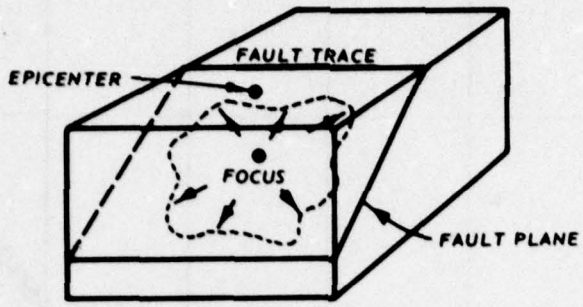

Figure 2-3. Concept of a spreading fault movement that occurs during an earthquake (from Krinitzsky, 1974).

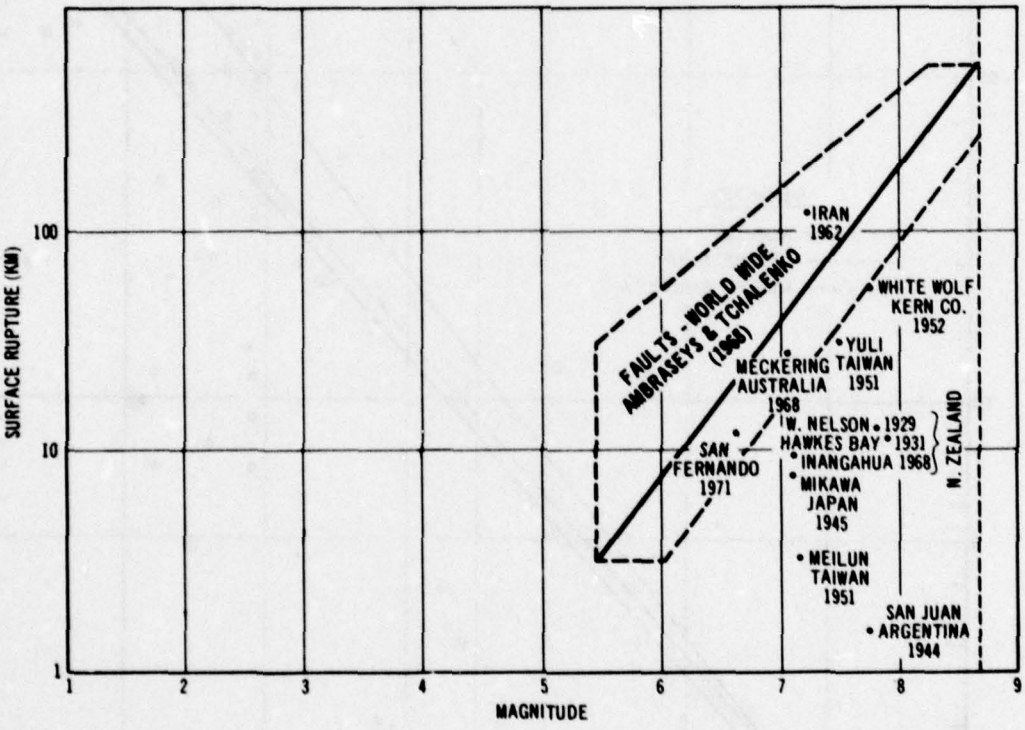

Figure 2-4. Spread in magnitude versus surface rupture in data assembled by Ambraseys and Tchalenko plus data on selected thrust faults from the U.S. Geological Survey (from Krinitzsky, 1974).

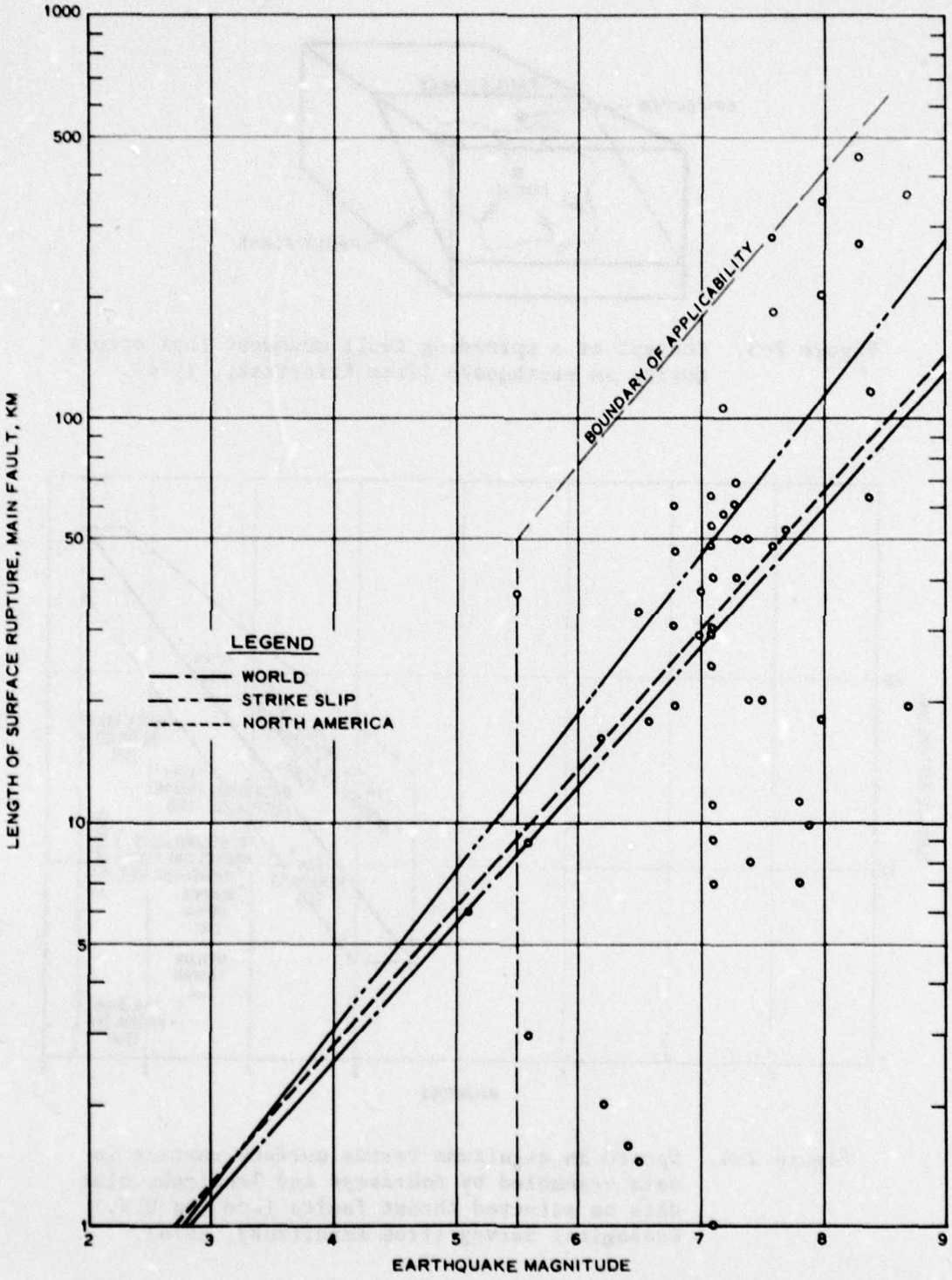

Figure 2-5. Length of surface rupture on main fault as related to earthquake magnitude (from Bonilla and Buchanan, 1970; boundary of applicability added).

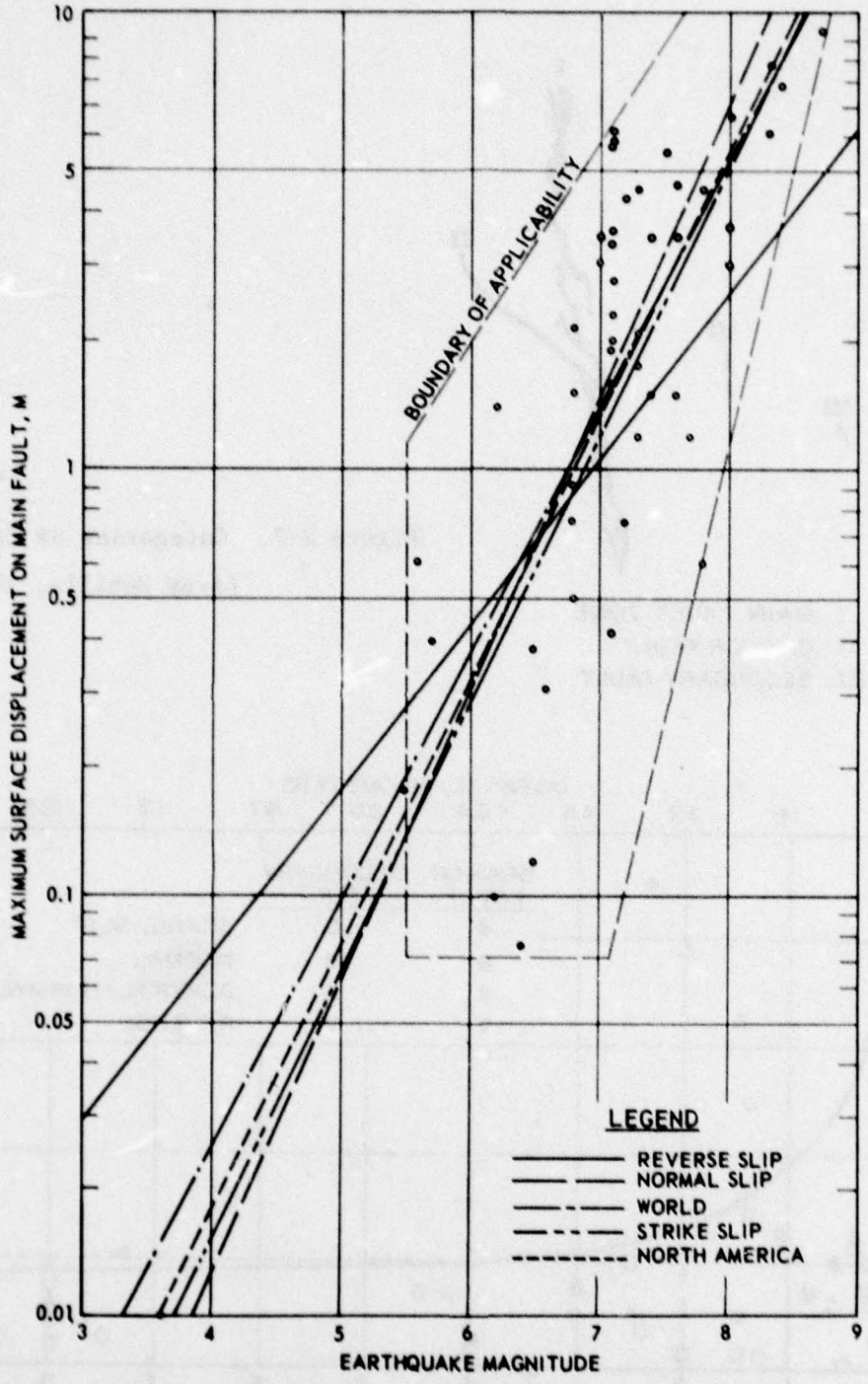

Figure 2-6. Maximum surface displacement on main fault as related to earthquake magnitude (from Bonilla and Buchanan, 1970; boundary of applicability added).

I. MAIN FAULT ZONE
II. BRANCH FAULT
III. SECONDARY FAULT

Figure 2-7. Categories of faults (from Bonilla, 1967).

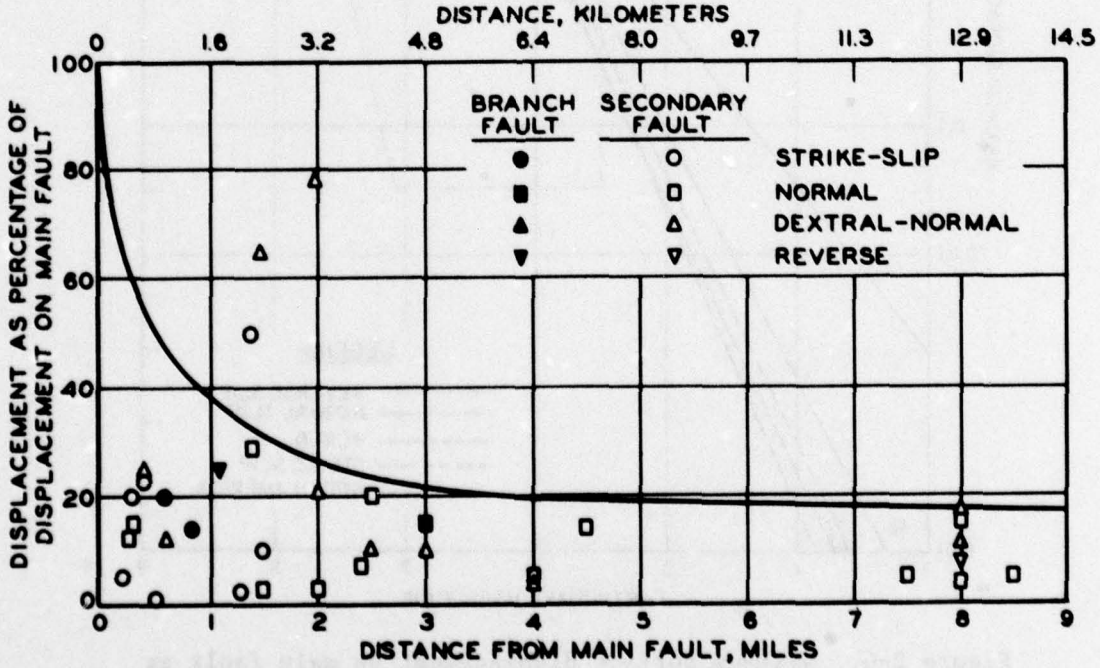

Figure 2-8. Displacement on associated faults as percentage of displacement on main fault (from Bonilla, 1967).

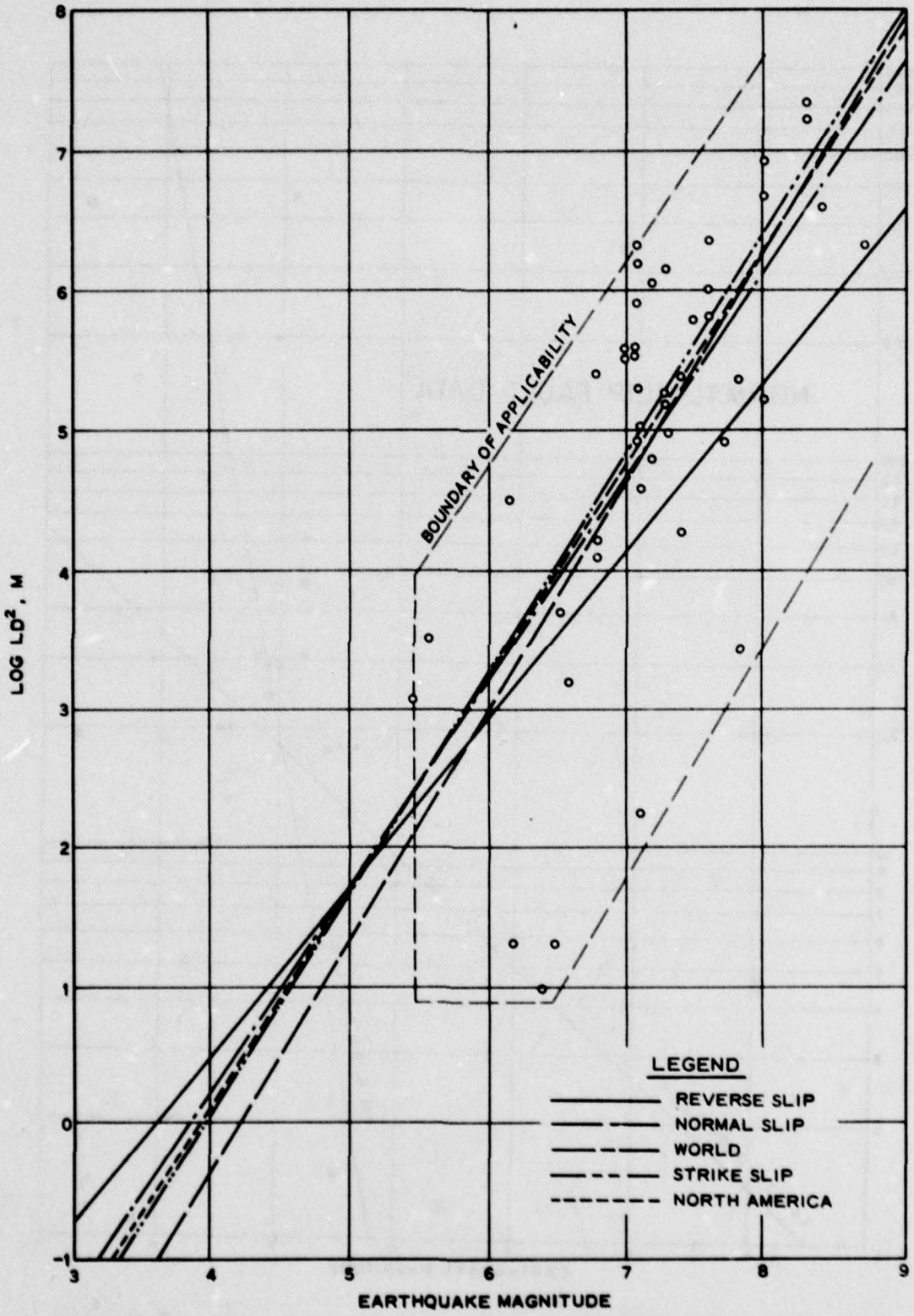

Figure 2-9. Relation of earthquake magnitude to surface length times square of surface displacement (from Bonilla and Buchanan, 1970; boundary of applicability added).

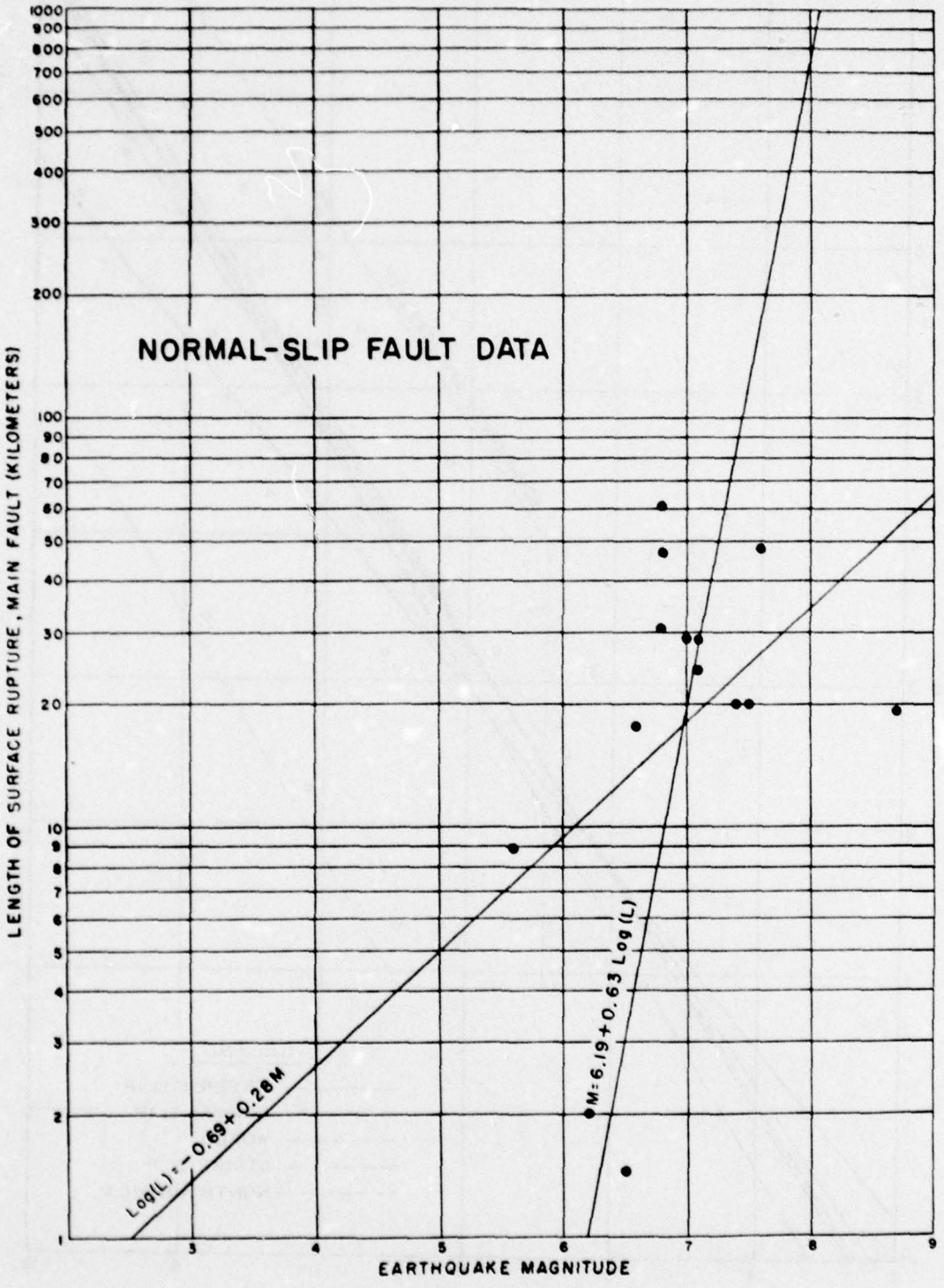

Figure 2-10. Normal-slip fault data (from Mark and Bonilla, 1977).

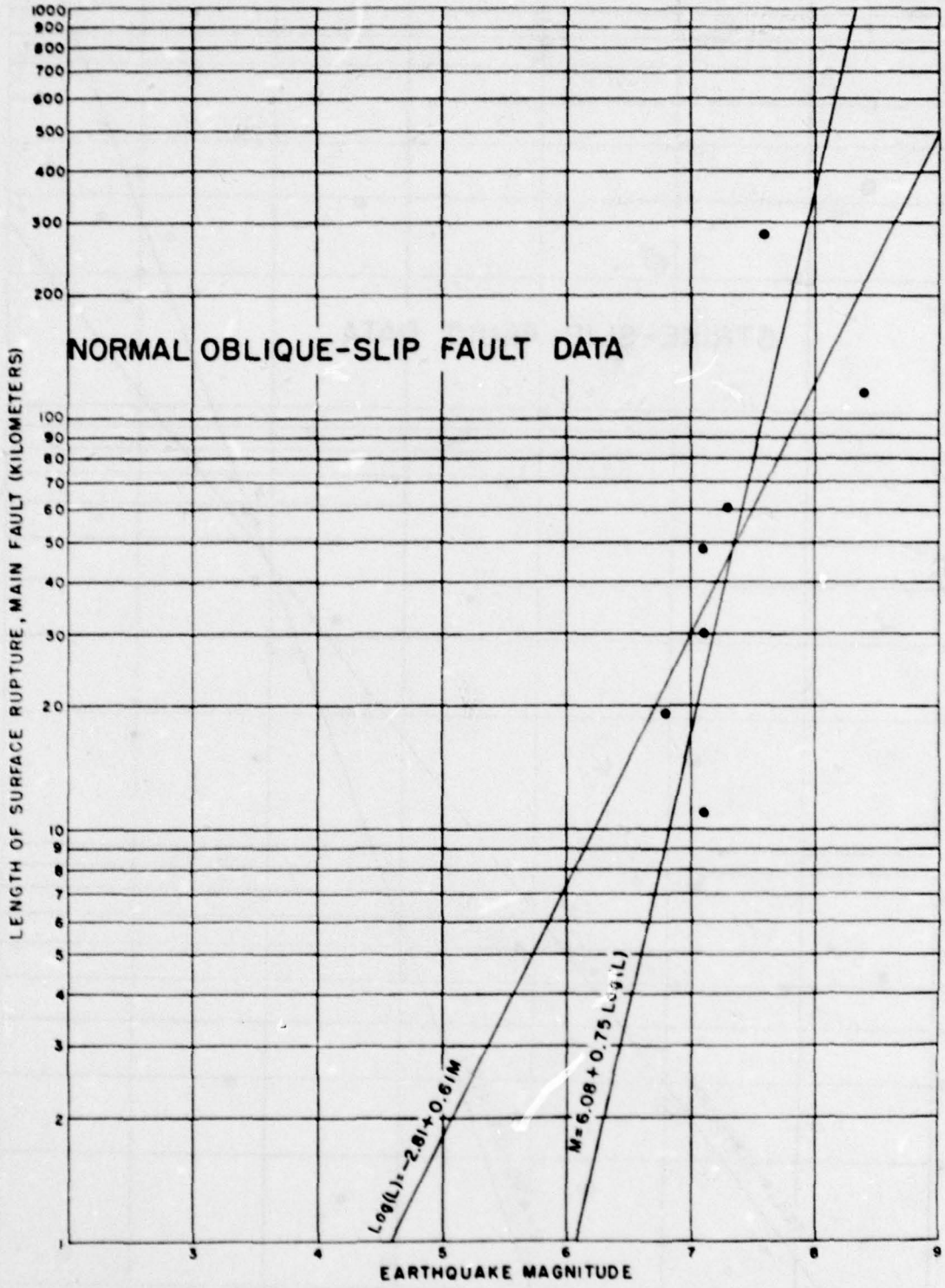

Figure 2-11. Normal oblique-slip fault data (from Mark and Bonilla, 1977).

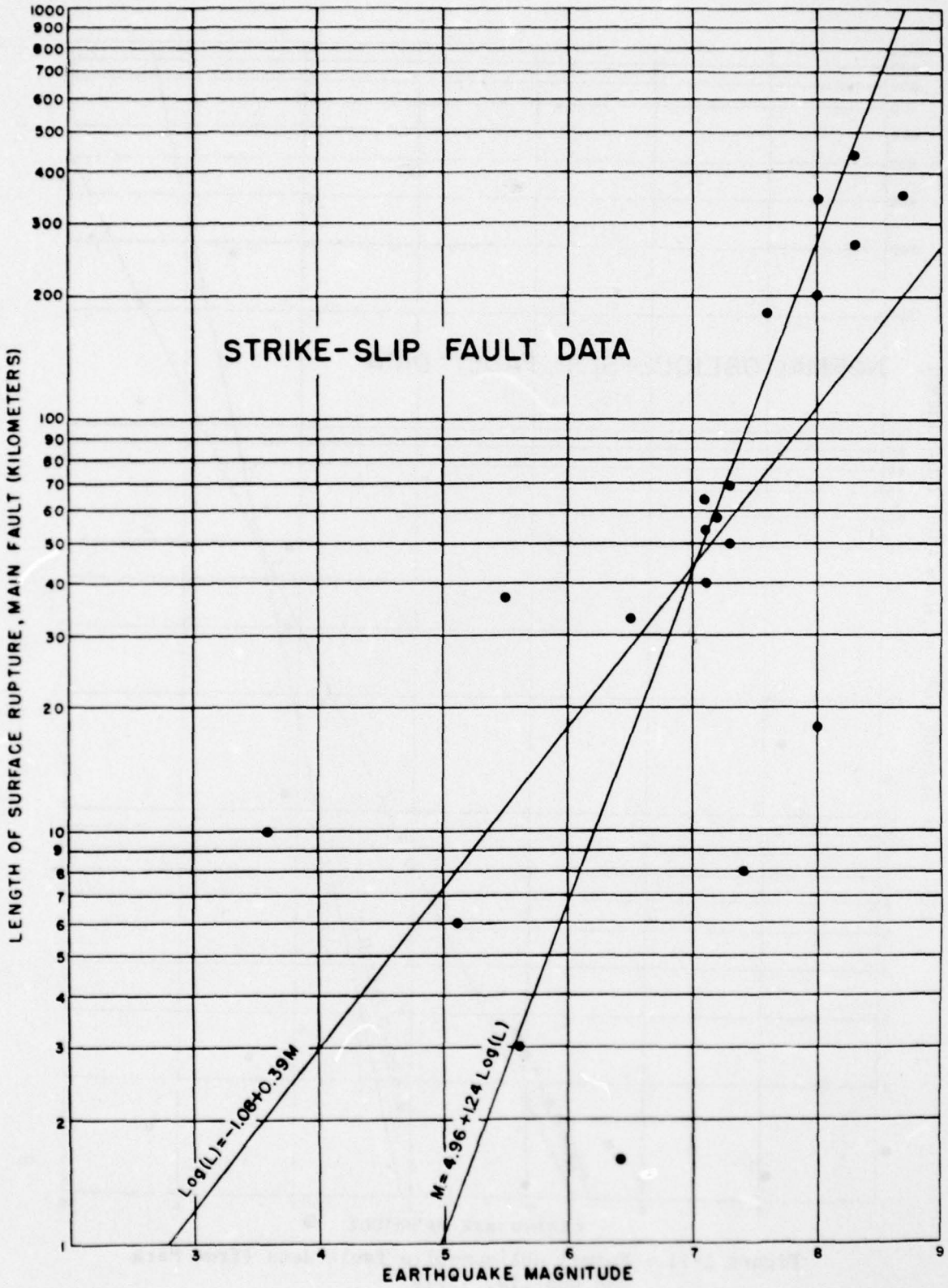

Figure 2-12. Strike-slip fault data (from Mark and Bonilla, 1977).

CHAPTER 3 - FAULT MOVEMENT

Prediction of Fault Movement

Prediction of movement along specific fault zones is being studied by many researchers throughout the world. Their chief approaches thus far are given in the following paragraphs taken from Krinitzsky (1974) and quoted below.

Field Strains

Where faults move, they are the visible displacements that occur within much larger areas in which crustal strain takes place. It is known that the Niigata earthquake was preceded by vertical movements that went on at a steady rate for half a century. Fifteen years before the earthquake the movement became more rapid for about 10 yr. Then there were 5 yr of very little movement that ended with the earthquake. Studies of elastic strain accumulation may prove to be a guide to predicting fault movements ***.

Dilation

Fault zones, or the areas closely adjacent to major faults, may dilate measurably prior to relief of stresses by slippage. Monitoring the progress of dilation by [level surveys] adjacent to specific faults may identify critical stages that preceded movement.

Seismologists in the USSR found premonitory changes in the ratio V_p/V_s of microearthquakes prior to moderate size earthquakes in Central Asia *** [where] *** V_p is the compressional velocity and V_s is the shear velocity. *** Corroborative results were reported in the Adirondack Mountains of New

York and similar anomalies were found to have preceded the San Fernando, California, earthquake of February 1971. Tectonic strain produces a steady increase in stress until dilatancy occurs. *** the forming of many small cracks *** takes place at lesser stress levels than those necessary *** [for rupture]. Initially, there is an increase in pore volume without a corresponding increase in pore fluid and V_p drops. V_s is not affected by pore fluids so that V_p/V_s also decreases. As water flows into the new cracks, the ratio will return to normal and pore pressure will build up. With continuing tectonic stress and the buildup of pore pressure, an earthquake will result.

Creep

Similarly, creep, or slow movements of faults without earthquakes, may indicate the gradual relief of stress ***. [It may indicate] the partial relief of a locked condition that will later break and move abruptly. Clear identification of the significance of creep is not yet possible, but creep may in time be related to earthquake potential.

Microearthquakes

Numerous small earthquakes along active fault zones may indicate the approach of a large event, but this is an [inconclusive] relationship. Of use, perhaps, is the plotting of microearthquakes. They may show a geographical spread that, correlated with historic earthquakes, can suggest the most probable locations for future events.

They may, however, indicate only aftershocks of a previous large event.

Stress- and Strain-related Effects

The physical properties of rocks are affected by the levels of stress and strain they are undergoing. Thus electrical resistivity, magnetism, piezoelectricity, the

transmission of seismic waves, the emission of radon, and possibly other factors [may show changes] as rocks approach the stage in which fault slippage is about to happen.

Geologically Determined Slip Rates

The offset of distinctive rock units establishes the rate of fault movement within fairly wide bounds. Commonly these offsets average the rate of movement over millions of years, and sudden slip cannot be distinguished from creep. Data for the San Andreas fault suggest an average slip rate of 1-2 cm/yr (0.4-0.8 in./yr) over the last 20 million years. But to predict movements in the immediate future, the most recent few hundreds to thousands of years are the most important (Wesson et al., 1975).

The history and rate of fault movement have been obtained within this brief time period in a few special circumstances in southern California using absolute age dating techniques.

Figure 3-1 is a simplified sketch of a trench wall showing vertical deformation of initially flat-lying sediments and sedimentary contacts associated with predominantly horizontal movement on the Coyote Creek fault of southern California (from Clark et al., 1972). The trench, dug shortly after the 1968 Borrego Mountain earthquake, crosses a branching break of the fault zone along which about 50 mm (2 in.) of vertical displacement and about the same amount of horizontal displacement took place during the earthquake. Deposits at points A, B, and C were dated radiometrically. The vertical displacement of the sedimentary contacts plotted against the age of the corresponding deposits yields an average rate of vertical deformation of about 0.5 mm/yr (0.02 in./yr) for the past 3,000 years. This suggests a recurrence interval for earthquakes the size of the 1968 event of about 200 years (Clark et al., 1972) (Figure 3-2).

Recurrence Intervals From Geologic Slip Rates

Wallace (1970) presented an approach which has been used by Lamar et al. (1973). The recurrence interval at a point can be estimated by

$$R_x = \frac{D}{S - C} \qquad (3\text{-}1)$$

where D = displacement
S = long-term strain rate
C = tectonic creep rate

Lamar et al. present the following quoted discussion.

> The following assumptions are made: (1) Slip on faults occurs incrementally during earthquakes and will continue at the same rate as that determined from geodetic data and offset of geologic units. (2) Elastic strain accumulates between earthquakes; the displacement during an earthquake represents the release of this accumulated elastic strain. (3) Tectonic creep is aseismic slip which reduces the accumulation of elastic strain available for release during earthquakes. *** Recurrence intervals determined by Eq. 3-1 represent a long-term average; there is however, evidence of significant local (Ambraseys, 1970) and worldwide (Davies and Brune, 1971) time variations in the level of seismic activity.

For most faults, creep can be evaluated. Therefore, as an expedient, Equation 3-1 is simplified as

$$R_x = \frac{D}{S} \qquad (3\text{-}2)$$

Equation 3-2 is thought appropriate when the rupture length is large compared to the distance of the site to the fault. When this is not the case, Equation 3-2 is multiplied by the ratio of length of rupture to total fault length to account for the spatial distribution.

Application of Slip Rate to Compute Recurrence Data

Lamar et al. (1973) have investigated the recurrence data for six faults in the southern California area. Their data are summarized in Table 3-1. The displacement, D, used in Equation 3-2 to calculate recurrence intervals at a given point on a fault were derived from Bonilla and Buchanan (1970), except in the case of the White Wolf and Sierra Madre faults. For these two faults historic displacements were available, and they deviated significantly from the least-squares-fit curve for reverse faults.

Quoting from Lamar et al. (1973):

> The determination of long-term slip rates and recurrence intervals provides a new approach to earthquake hazard assessment. The results can be strikingly different from those based on the historic earthquake record. For example, the *** Garlock fault, which has not caused damaging historic movement, may have accumulated sufficient elastic strain for a destructive earthquake. On the other hand, historic ruptures on faults such as the *** San Fernando, have released [some] accumulated elastic strain, so that a destructive earthquake [may be less probable] for the next few hundred years [depending on the amount of strain release and buildup]. The recurrence intervals in Table [3-1] must be considered tentative and are subject to revision as new information becomes available. For the most part, slip rates are poorly known, and the

curves relating magnitude to surface displacement and rupture length are based on meager data with considerable scatter. More accurate age-dates of offset strata on faults are needed, and additional studies following earthquakes throughout the world are required to refine the empirical relations between magnitude, surface displacement and rupture length. This research offers the prospect of more quantitative assessments of earthquake risk.

Table 3-1. Recurrence Intervals on Selected Faults in Southern California [from Lamar et al., 1973, edited by Southern California Section of the Association of Engineering Geologists]

Fault	Slip Rate (cm/yr)	Length (km)	Recurrence Intervals (yr) at a Point on Fault (R_x)			Recurrence Intervals (yr) over Length of Fault (R_t)		
			M 6	M 7	M 8	M 6	M 7	M 8
Northwest Trend Right-Slip								
San Andreas (southern segment)	3	500	10	40	200*	.3-1	3-10	40-100*
San Jacinto Fault System	0.3	440	100*	400*	2000	4-10*	40-100*	400-1000
Whittier-Elsinore-Agua Caliente-Laguna Salada	0.08	260	300	2000	6000	20-90	200-900	3000-6000
Northeast Trend Left-Slip								
Big Pine	0.2	95	100	600*	3000	20-100	300-600*	3000
Garlock	0.8	250	30	200	600	2-10	30-90	300-600
Reverse and Thrust								
White Wolf	0.04	53	1000	2000*	4000	200-900	1000-2000*	4000
Sierra Madre Fault System	0.8	90	100*	300*	800	30-100*	100-300*	800

*Most likely, based on historic record.

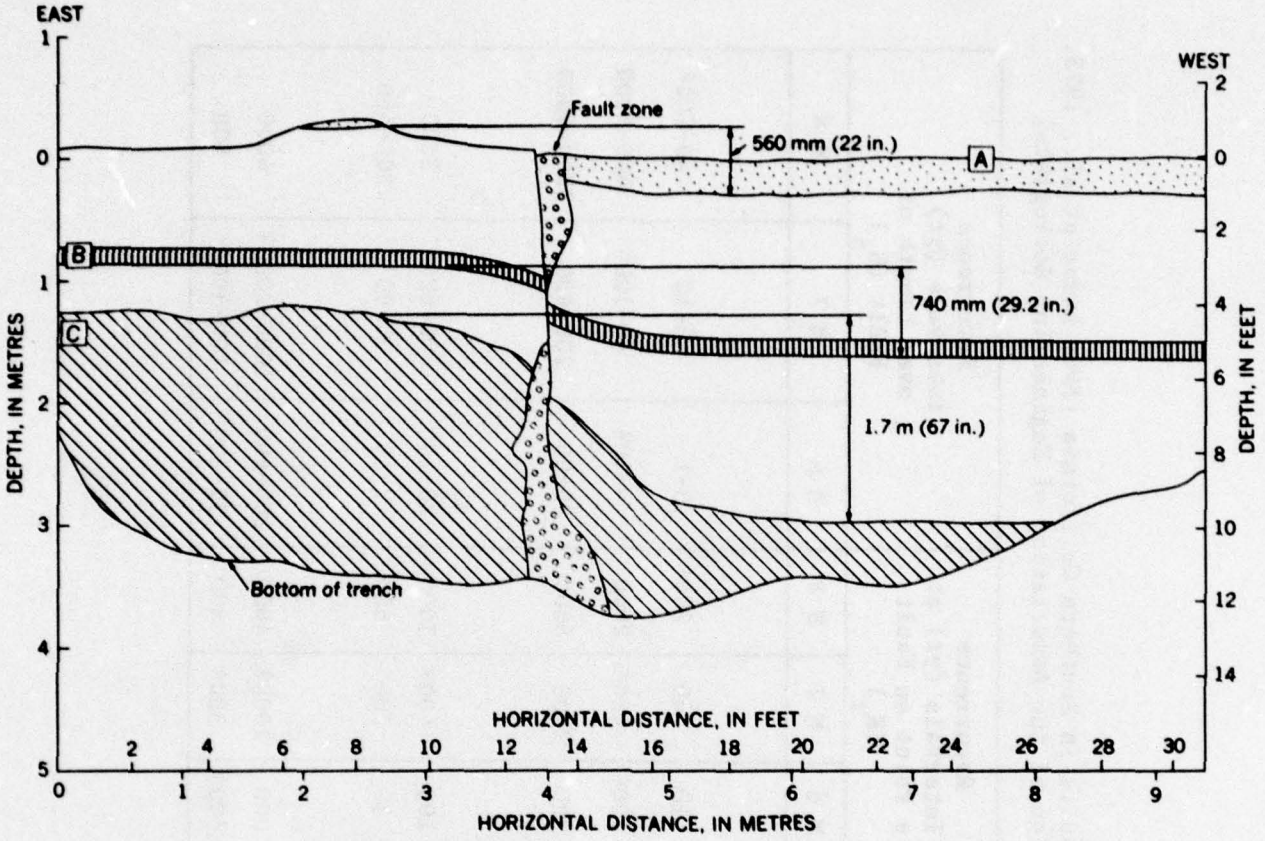

Figure 3-1. Sketch of trench wall (from Clark et al., 1972).

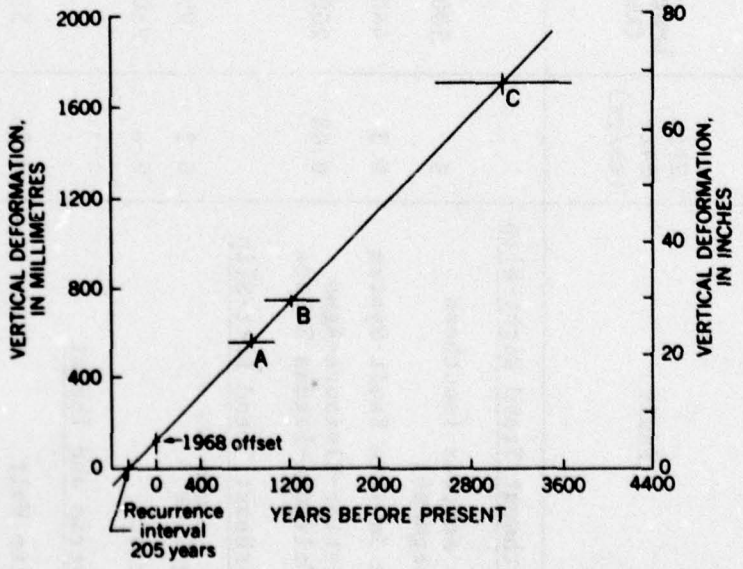

Figure 3-2. Estimated recurrence data (from Clark et al., 1972).

CHAPTER 4 - SEISMOLOGICAL STUDIES OF FAULTS

Introduction

The National Oceanic and Atmospheric Administration's (NOAA) National Geophysical and Solar-Terrestial Data Center in Boulder, Colorado, maintains a file of earthquake data in computer format.

This earthquake data file is a magnetic tape file of earthquake origin times, locations, magnitudes, and related information on effects that have been compiled from many sources. It is a useful tool for providing searches of the seismicity of selected regions, for preparing lists of earthquakes of given characteristics (large magnitude, intensity, tsunami, etc.), for plotting maps, and for making statistical studies. It is updated as new earthquake data become available in machine-readable form.

The earthquake data file (sometimes called hypocenter data file) contains information on approximately 116,000 earthquakes for the period June 11, 1638, through December 31, 1974. The file includes for each event the date, origin time, geographic location, focal depth, magnitude, and intensity when available. It contains additional information on the source of the data, quality factors, associated phenomena (tsunami, volcanism, faulting, etc.), and seismic region number. In addition to earthquakes, the file contains about 500 phenomena that have surface effects similar to earthquakes, including known or suspected explosions and associated collapse phenomena, coal bumps, rockbursts, quarry blasts, and other earth disturbances. At present, data for the 1638-1899 period are practically limited to earthquakes in the United States, a few hundred in number, which had a maximum intensity of 5 or greater. A number of data fields for some events are unfilled because

the information is not available. Information on cultural effects, intensity, and other phenomena associated with the event has been included for earthquakes in the United States. This information has sometimes been entered for non-United States earthquakes, particularly since May 1968, although significant gaps still exist.

The quality of epicenter determinations varies significantly with the time period studied. Before 1900 locations are usually noninstrumentally determined and are given as the center of the macroseismic effects. Most instrumental epicenters prior to 1961, excluding local earthquakes in California, were located to the nearest 1/4 or 1/2 degree of latitude and longitude. Reliable information on the quality of many epicenter determinations is lacking. Beginning in 1960, epicenters have been determined by computer, and the accuracy is generally better. However, although stated to tenths or hundredths of a degree, the location accuracy is usually a few tenths of a degree. Since May 1968, the latitude and longitude values for most events have been listed to three decimal places. This precision is not intended to reflect the accuracy of the location of events except for local California earthquakes and special epicenter determinations. Where several sources have determined an epicenter for the same earthquake, one solution has been designated as the most reliable. Usually it is the source believed to contain the best data set for the earthquake. In come cases, data from two sources were combined to provide a more complete record.

Magnitudes from a number of different sources are included in the earthquake data file. Gutenberg and Richter (1954) and Richter (1958) discuss the development of the magnitude scale. Many magnitudes published by Gutenberg and Richter (1954) were later revised by Richter (1958). The revised magnitudes are used in the file even though the source is identified as Gutenberg and Richter (1954). The concept of earthquake magnitude is not restricted to one value. Several definitions are possible, depending on which seismic waves are measured. Three different magnitude scales, BODY WAVE (MB), SURFACE WAVE (MS), and LOCAL (ML), are distinguished in this file. In addition another data

field, OTHER MAGNITUDE, has been included when it was unclear which scale was used. Richter (1958) and other modern seismology references provide detailed discussions of this topic. The different scales do not give exactly comparable results, and different values frequently are given for the same earthquake. It is common practice to average the individual magnitudes from different stations to get a more uniform value within each scale (MB, MS, and to a lesser extent ML).

In general, the file contains earthquakes of magnitude 4.0 or less only for the United States region and for areas within dense seismic station networks. However, no claim is made for the statistical homogeneity of these events. Inclusion of earthquakes of magnitude 4.0 to 5.0 also is influenced by the proximity of seismic stations to the source or epicenter.

A maximum intensity is listed for many of the earthquakes. Each is assigned according to the Modified Mercalli Intensity Scale of 1931. Some of these values have been converted from reported intensities on other scales.

Correction of Epicenters

Early records of earthquakes may show inaccurate epicentral locations. Also magnitudes or intensities may differ from values that would now be assigned. As an example, Krinitzsky (1974) reports the following:

> The location of an NOAA listed earthquake of 15 May 1909 in southern Saskatchewan is shown in [Figure 4-1]. It has a maximum intensity of VIII and is the largest recorded event in this general area. Its location was made when seismograph stations were few, and those that operated were far less accurate than they are today. The intensity of VIII was assigned on the basis of the large felt area.

The event was checked by referring to the newspaper accounts of this time. This was not too formidable a task. State archives, state university collections, and national archives often have collections of local newspapers gathered in central depositories. One may request microfilm copies of these papers for the dates of interest, review them, and assign intensity values based on their descriptions. This exercise provided intensities for more than 50 communities though this was, and still is, a thinly populated area. The resulting iso-intensity map shows there was no intensity VIII. The greatest was VI. Also the region of VI had its center to the east by about 1 deg from the NOAA location. In [Figure 4-1] the revised location is shown in relation to three other earthquakes of 1956, 1968, and 1972. Their locations were accurate to begin with because of better instrumental capability. One is associated with a seismically interpreted fault that also agrees with a geologically mapped fault. Its trend is toward the three other events. Thus the revised location for the 1909 event helps to interpret a fault trend.

Seismic Arrays

Seismometers have been installed near known active faults to record microearthquakes. Figures 4-2 and 4-3 show the location of recorded microearthquakes for a year and major fault zones in California. The events recorded ranged in magnitude from 0.5 to 1.5. The figures show areas where the microearthquakes closely trace the faults. There are also regions where few microearthquakes occurred. The San Andreas fault north of the Sargent fault exhibits less activity than southern portions, perhaps indicating it is locked. However, sufficient microearthquakes have occurred to show the continuation of the fault. It may be reasoned that small failures might occur before a major rupture

occurs; alternatively, the large number of microearthquakes demonstrate active creep which may be sufficient to prevent sizable strain accumulation and preclude a large event.

Since earthquakes are associated with faults, it might be thought that they should precisely overlay the fault location. This is not the case because the distribution of seismometers is uneven and has changed with time. There are limitations in the accuracy of the techniques used to locate epicenters, principally from variations in the assumed propagation velocities. Further explanation for the location of epicenters being off their associated fault comes from the simplified model used to locate them. This is explained in Figure 4-4. Note that the center of earthquake energy is located at the focus. For an inclined fault, the surface location (epicenter) is a distance removed from the surface fault location. It is only in vertical faults that one might expect the epicenter to lie on the fault.

Krinitzsky (1974) concludes that earthquakes can be related to existing faults and that the possibility of formation of new faults should not be considered in design. Large earthquakes require fault breaks of considerable distance. The uncertainties that occur in the association of earthquakes with faults can occur only for small events. Generally in the western United States the extent of geologic investigation precludes the omission of a large fault remaining unknown. However, there are uncertainties associated with eastern earthquakes. For example, causative faults responsible for the New Madrid earthquakes of 1811 and 1812 have not yet been identified. This may be the result of insufficient geologic investigations. The importance of considering the extent and quality of geologic investigations is evident.

Limitations to Historic Data

A period of demonstrated quiescence over a geological time period indicates inactivity of the fault and probable continued inactivity. However, inactivity over a period of historic recording (50 to 100

years) does not imply future inactivity. Rather it may point to a region which is locked and through which a major fault rupture may propagate. The last two earthquakes producing damage in southern California (Arvin-Tehachapi, 1952, and San Fernando, 1971) occurred on faults lacking historic activity. With the exception of the San Jacinto fault system, every known event greater than magnitude 6 in southern California occurred on a fault without prior historic activity. Caution must be exercised to recognize that the accuracy of an incomplete data base is very limited when extrapolated for return periods greatly exceeding the length of the period of recorded data. Furthermore, aftershocks must be distinguished from main shocks. An area having recently undergone a large event releasing strain built up for hundreds or thousands of years is probably safe against that size release in the near future. Thus a recent large event on a fault might actually indicate safety in the immediate future rather than an indication of activity. A single event by itself cannot give an accurate measure of return time.

Krinitzsky (1974) is quoted below:

> In the United States the history of earthquake activity is greatly truncated. At best the record covers less than 350 years. This it does in very few places. For most of the country it is about 150 years. This, however, is general earthquake history and not the record of movement on specific faults or in fault zones. In other parts of the world the record for both earthquake history and interpreted fault activity is better.
>
> N. N. Ambraseys *** [1971] has studied the record of damaging earthquakes for the past two millennia in some portions of the Near East. [Figure 4-5] *** shows the cumulative distribution during this time of damaging earthquakes along (a) the Border Zone, which is a northeast-southwest trend of faults that extends toward the Dead Sea along the border of Israel; and (b) the Anatolian Zone that is roughly

an east-west zone of faulting. It intersects with the Border Zone. Ambraseys points out that during the first five centuries the Border Zone was quiescent while the Anatolian Zone was active. For the following six centuries the pattern was reversed only to be reversed again during the eleventh century. In this case there is a factor of dependence of activity along one zone on that of the other. The two join to encompass a miniplate, and movement tends to shift from one side to another on a cyclical basis. This tends to discredit the validity of probabilistic projections based only on a short history.

Also, as noted in Krinitzsky (1974) there are likely to be:

*** variations in rates of slippage along various segments of *any one long active fault or fault zone.* This is known to be the case along the San Andreas. During its relatively short historic period, it was noted that major earthquakes moved from place to place along the fault. Portions that once moved, notably the segment that slipped during the San Francisco earthquake of 1906, have become locked while slippages occurred elsewhere. [Figure 4-6] is a schematic statement of variations in rates of slippage in inches per year, as given by Brown and Wallace (1968). The slippage is that which has occurred during an interval of 60 years. Though this is instructive of irregularities in the rates of movement, it is not intended as a guide to the future. If anything, the future is very likely to be different. The segment between Cholame and Camp Dix appears to be in a locked position. Stresses are building up. One day this segment will rupture suddenly.

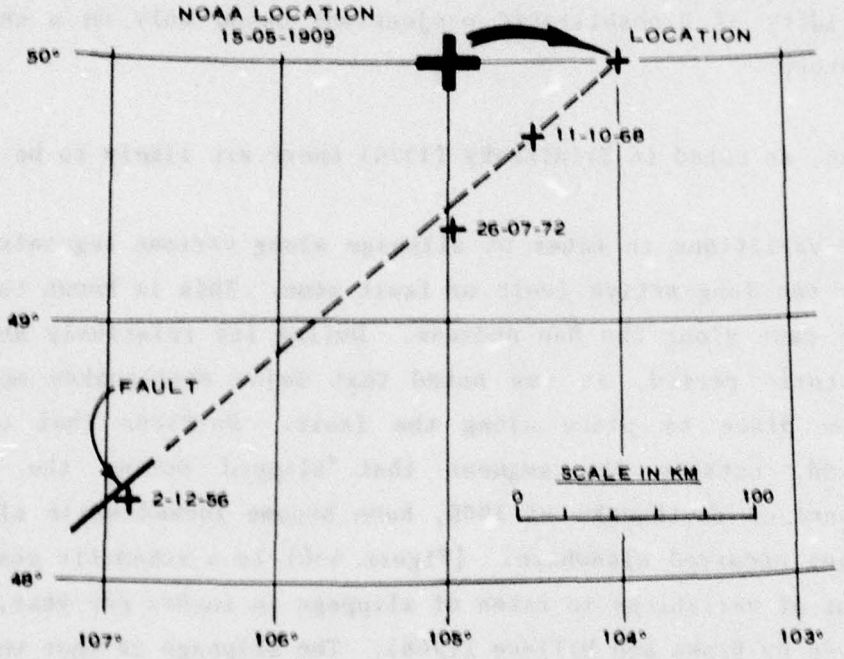

Figure 4-1. Revised epicentral location used as a clue to suggest association with a projected fault trend (from Krinitzsky, 1974).

Figure 4-2. Microearthquakes recorded during 1970 (U.S. Geological Survey), indicating fault trends shown in Figure 4-3 (from Krinitzsky, 1974).

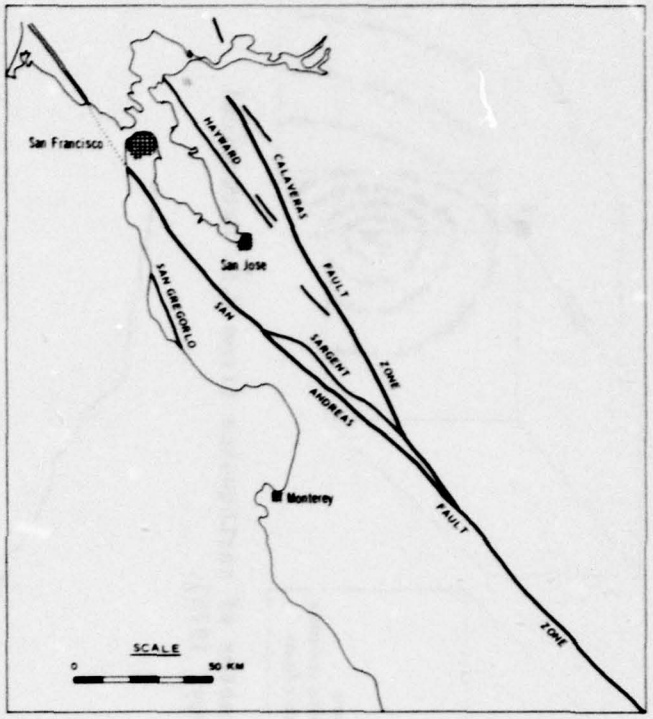

Figure 4-3. Major fault zones in central California mapped by U.S. Geological Survey (from Krinitzsky, 1974).

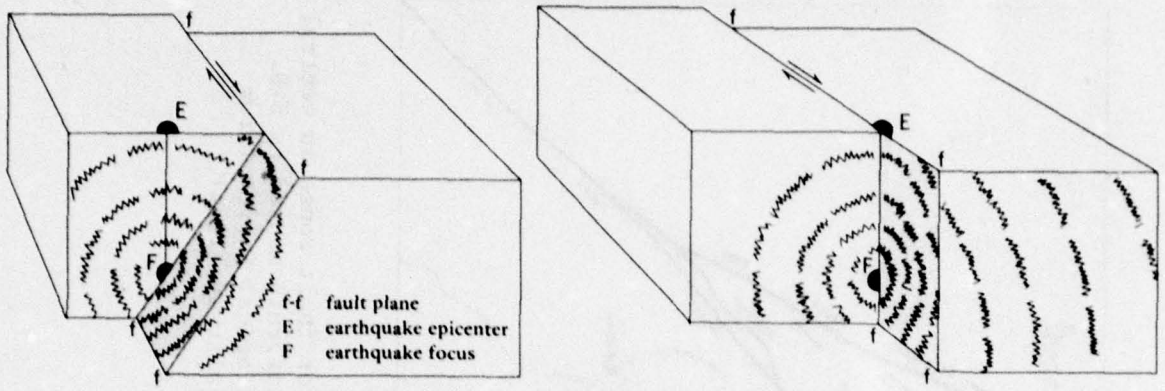

Figure 4-4. Epicenter of earthquakes (from U.S. Geological Survey, 1975).

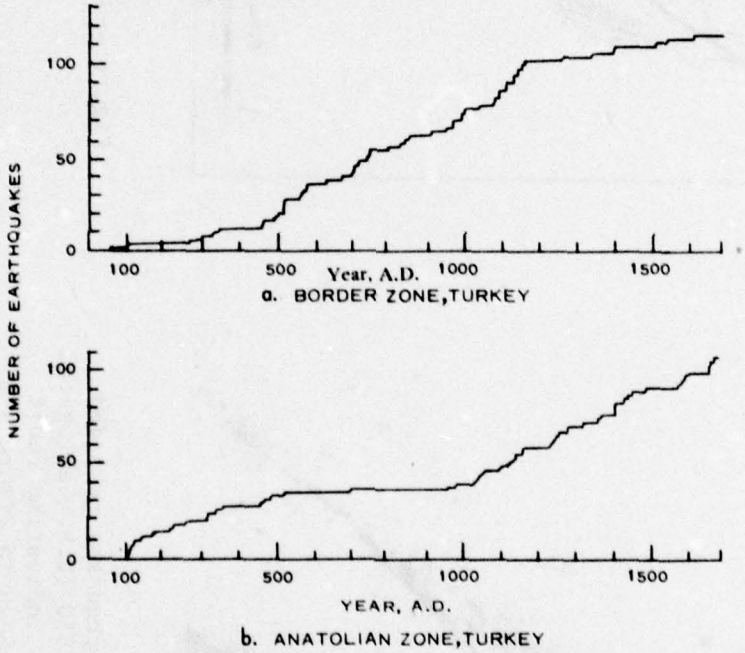

Figure 4-5. Time distribution of damaging earthquakes in Turkey (from Ambraseys in Nature, 1971).

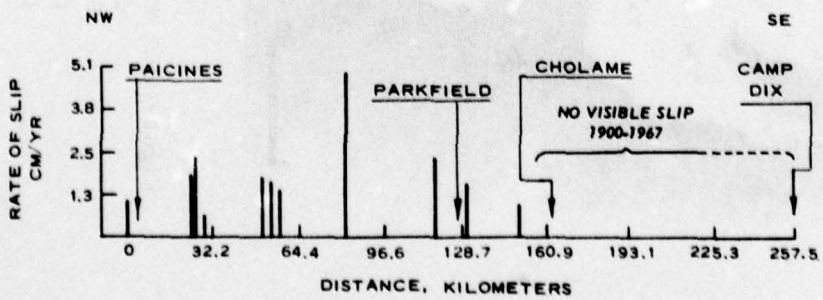

Figure 4-6. Variation in rate of slippage along the San Andreas fault (from Brown and Wallace, 1968).

CHAPTER 5 – STOCHASTIC APPROACH TO EARTHQUAKE DATA

Earthquake Models

Oliveira (1975) summarizes as follows:

> The generation of earthquakes as related to the geotectonic mechanisms of faults and the timing, intensity and location of future earthquakes, cannot be predicted with certainty in a deterministic way. *** The generation of earthquakes in space and time falls under the general category of stochastic processes *** [Cox and Miller, 1970; Lomnitz, 1974].
>
> [Time Distribution.] Both the Markov and Poisson representations are used to simulate the occurrence of earthquakes generated in time. These representations are stochastic point processes. The Markov model differs from the Poisson model in that the occurrences of new events depend on past events whereas in the latter model these occurrences are independent of past events. Results obtained using these two models differ somewhat. The Markov model, better adjusted to the elastic rebound theory *** [Reid (1911)], has some drawbacks due to difficulty in setting the initial conditions and requires more numerical treatment. The Poisson model, on the other hand, does not always agree with experimental data for small magnitude earthquakes, because it ignores the tendency of earthquakes to cluster in space and time *** [Knopoff, 1964]. Nevertheless, the Poisson model seems to give adequate results in many situations except for cases of very large

return periods and cases when analysing structures that have just been damaged [Rosenblueth, 1973]. Emphasis is given to the Poisson model in the present treatment.

* * * * * * *

$$p_N(n,\lambda t) = \frac{e^{-\lambda t}(\lambda t)^n}{n!}, \qquad [(5\text{-}1)]$$

where p_N = the probabilty of occurrence of n events of a given magnitude range

λ = the mean rate of occurences per unit of time t

The probability of the amount of time between two consecutive events is given by the exponential law

$$p_T(t) = \lambda\, e^{-\lambda t} \qquad 0 \leq t \leq \infty \qquad [(5\text{-}2)]$$

Cornel (1974), Esteva (1968), and Milne and Davenport (1969) have, at least for main shocks, verified the Poisson model favorably; however, Knopoff (1964) reports after testing different regions in the world the Poisson model is inadequate to explain the time distribution of low magnitude shocks. Small magnitude earthquakes may contribute heavily to the general seismic risk, rendering the Poisson model inadequate. A more refined model of generation should then be used. In seismic risk analysis the Poisson model is generally an acceptable approach except when working with return periods of several thousand years or in analyzing one structure that has just been damaged (Oliveira, 1975). The Poisson distribution is intended to be used with National Bureau of Standards Seismicity Tables (Culver et al., 1975). The main deficiency of the simple Poisson model is that it ignores the tendency of earthquakes to come in groups which are often triggered by a large main shock; magnitude is treated as a separate independent phenomenon.

Figure 5-1 gives the probability of not exceeding specified values during the life of a facility.

An improvement over the Poisson distribution is the Weinbull distribution suggested by Chou and Fisher (1975)

$$P(t) = 1 - e^{-ut^{\gamma}} \tag{5-3}$$

where u and γ are scale and shape parameters, respectively. Several methods are available to estimate the parameters. The maximum-likelihood method is recommended because it utilizes the available information in the most appropriate manner. The shape factor γ is estimated by solving the general equation:

$$\frac{n}{\gamma} + \sum_{i=1}^{n} (\ln t_i) - n \left[\frac{\sum_{i=1}^{n} (t_i^{\gamma} \ln t_i)}{\sum_{i=1}^{n} (t^{\gamma})} \right] = 0 \tag{5-4}$$

and the scale parameter μ is obtained by equating:

$$\mu = \frac{n}{\sum_{i=1}^{n} (t_i^{\gamma})} \tag{5-5}$$

where n is the size of the sample and t_i is the time interval involved.

A graphical method of plotting historic earthquake data is very useful and widely used in practice. A new random variable is introduced as $Z = \ln(\mu t^{\gamma})$, and

$$F(Z) = 1 - e^{-e^{Z}} \tag{5-6}$$

The list of earthquake occurrence data is arranged in groups of intensity or magnitude ranges. Within each group of earthquake events of the same magnitude range the data are ordered by time intervals between occurrences, the most frequent first. The plotting position of any data point within a group is $[t_i, F(i)]$ where t_i is the i^{th} longest time interval and

$$F(i) = \frac{i}{n + 1} \tag{5-7}$$

where i = position on the list; i.e., first, second, etc.
n = total number of events in the group

The parameters μ and γ are determined by the intercept and slope, respectively, of the plotted data following the relationship:

$$Z_i = \ln \mu + \gamma \ln t_i \tag{5-8}$$

where t_i is the i^{th} longest time interval and Z_i is given by

$$\ln\ln\left[\frac{1}{1 - F(Z)}\right] \tag{5-9}$$

or

$$\ln\ln\left(\frac{n + 1}{n - i + 1}\right) \tag{5-10}$$

When $\gamma = 1$, the Weibull distribution is equivalent to the Poisson distribution.

Magnitude Distribution. The number of earthquakes of magnitude $\geq m$ to be expected in a given interval of time can be translated into a random variable using an exponential distribution. This distribution is similar to a Poisson distribution; however, it is continuous rather than discrete.

The magnitude distribution is exponentially related to magnitude through a parameter β. The probability density function is

$$f(m) = \beta e^{-\beta(m-m_o)} \qquad (5\text{-}11)$$

and the cumulative distribution function is

$$F_M(m) = 1 - e^{-\beta(m-m_o)} \qquad m \geq m_o \qquad [(5\text{-}12)]$$

where $\beta = b \log_e 10$

m_o = a constant defined by the lower magnitude limit

b = the coefficient of Richter's law of magnitudes ($\log_{10} \lambda_m = a - bm$). (See Site Recurrence below).

Oliveira (1975) states "Experimental data show that the linear form, $\log_{10} \lambda_m = a - bm$, of Richter's law does not hold for very large magnitudes. This suggests the use of truncation at a certain value of magnitude, m_1, or the introduction of a quadratic term (Merz and Cornell, 1973)." Table 5-1 summarizes the probability law of magnitudes for the above three cases.

Seismic Risk

The occurrence and magnitude mechanisms defined above characterize the generation of earthquakes in time and intensity. Randomness in space is another very important consideration in assessing seismic risk. Earthquake activity might be connected with the presence of faults. Only geological and geotectonic considerations associated with the past history of occurrences of earthquakes can characterize the distribution laws of epicentral locations. Spatial correlations among earthquake source zones have been detected in several seismic areas (Ferraes, 1973). Sophisticated models have been developed to take into account, simultaneously, space and time generation (Lomnitz, 1974).

If each source zone is considered to have a constant mean rate of occurrence λ_i, following a Poisson probability law, the set of all independent source zones will generate another Poisson process with mean rate $\lambda = \Sigma\lambda_i$ (the sources can be reduced to point sources). This principle has been used in studies of risk analysis at a site.

From the Poisson model of occurrences and the exponential type distribution of magnitudes it is possible to show that the extreme distribution of magnitude follows an extreme type I distribution (Gumbel, 1958) of the form

$$G_M(m) = \exp - \lambda e^{-\beta(m-m_o)} \qquad m \geqq m_o \tag{5-13}$$

Site Recurrence

Historical events within a distance around the site can be tabulated to evaluate the site regional seismicity. This gives an average measure of the earthquake proneness of a geographic area and is usually discussed in terms of an earthquake recurrence equation of the form

$$\log_{10} N = a - b\,m \tag{5-14}$$

where N = number of earthquakes per year exceeding a magnitude m
a = seismicity constant for an area
b = constant for an area

The tabulated historical data may be arranged according to magnitude, normalized to 1 year by dividing by the timespan covered, and the number of events greater than a magnitude m plotted against m. This graph, plotted on semilog graph paper, can be used to evaluate the coefficients a and b.

Some specific recurrence plots for major faults having historic activity are available in the literature (e.g., Environmental Development Agency, 1975). With this data it is possible to develop probabil-

ity of occurrence data for selection of a design and collapse-level earthquake magnitude. The distance of the site to the fault is important in determining the site motion as will be shown later.

Nuttli (1974) has compiled recurrence information for the central United States. The recurrence equation for the region of his study covering the states of Illinois, Indiana, Kentucky, Tennessee, Mississippi, Arkansas, and Missouri is

$$\log N = 3.55 - 0.87(\pm 0.11)m \qquad (5\text{-}15)$$

where N is the number of earthquakes per year occurring in the magnitude range m ± 0.2. This indicates a return period of 6.3 years for a magnitude 5 earthquake, 47 years for a magnitude 6 earthquake, and 347 years for a magnitude 7 earthquake.

The National Bureau of Standards (Culver et al., 1975) has published a guide for the evaluation of earthquake hazards. This guide contains tables which contain the coefficients a and b and an effective site distance for 1/2-degree squares of the entire United States. This data was developed considering the seismicity of each sector and averages the results of the sector. When specific recurrence data is available for a specific fault within 200 miles of the site, the actual fault data and distance to the site should be used.

A probability distribution may be applied to recurrence data to determine the probability of occurrence of a specified magnitude event in a number of years (the Poisson model is the most common as noted earlier). The cumulative probability of occurrence of an event ≥ m in time t is

$$P(t) = 1 - e^{-\lambda(m)t} \qquad (5\text{-}16)$$

where $\lambda(m)$ is the rate of occurrence of an event ≥ m determined from the recurrence plots.

Table 5-1. Magnitude Distribution Law (from Oliveira, 1975)

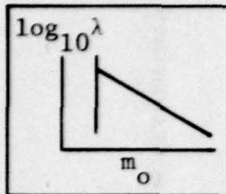	$\log_{10}\lambda = \begin{cases} a \\ a - bm \end{cases}$	$F_M(m) = \begin{cases} 0 \\ 1 - e^{-\beta(m-m_o)} \end{cases}$	$m < m_o$ $m > m_o$
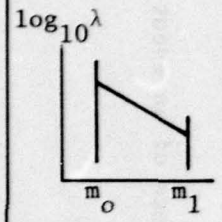	$\log_{10}\lambda = \begin{cases} a \\ a - b(m-m_o) \\ 0 \end{cases}$	$F_M(m) = \begin{cases} 0 \\ \dfrac{1 - e^{-(b \log_e 10)(m-m_o)}}{1 - e^{-(b \log_e 10)(m_1-m_o)}} \\ 1 \end{cases}$	$m < m_o$ $m_o \leq m \leq m_1$ $m > m_1$
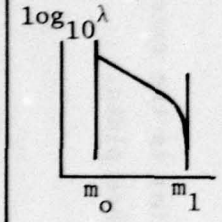	$\log_{10}\lambda = \begin{cases} a \\ a + b'_1(m-m_o) \\ + b'_2(m-m_o)^2 \\ 0 \end{cases}$	$F_M(m) = \begin{cases} 0 \\ \dfrac{1 - e^{\beta_1(m-m_o) + \beta_2(m^2-m^2_o)}}{1 - e^{\beta_1(m_1-m_o) + \beta_2(m_1^2-m_o^2)}} \\ 1 \end{cases}$ $\beta_{1,2} = b'_{1,2} \log_e 10$	$m < m_o$ $m_o \leq m \leq m_1$ $m > m_1$

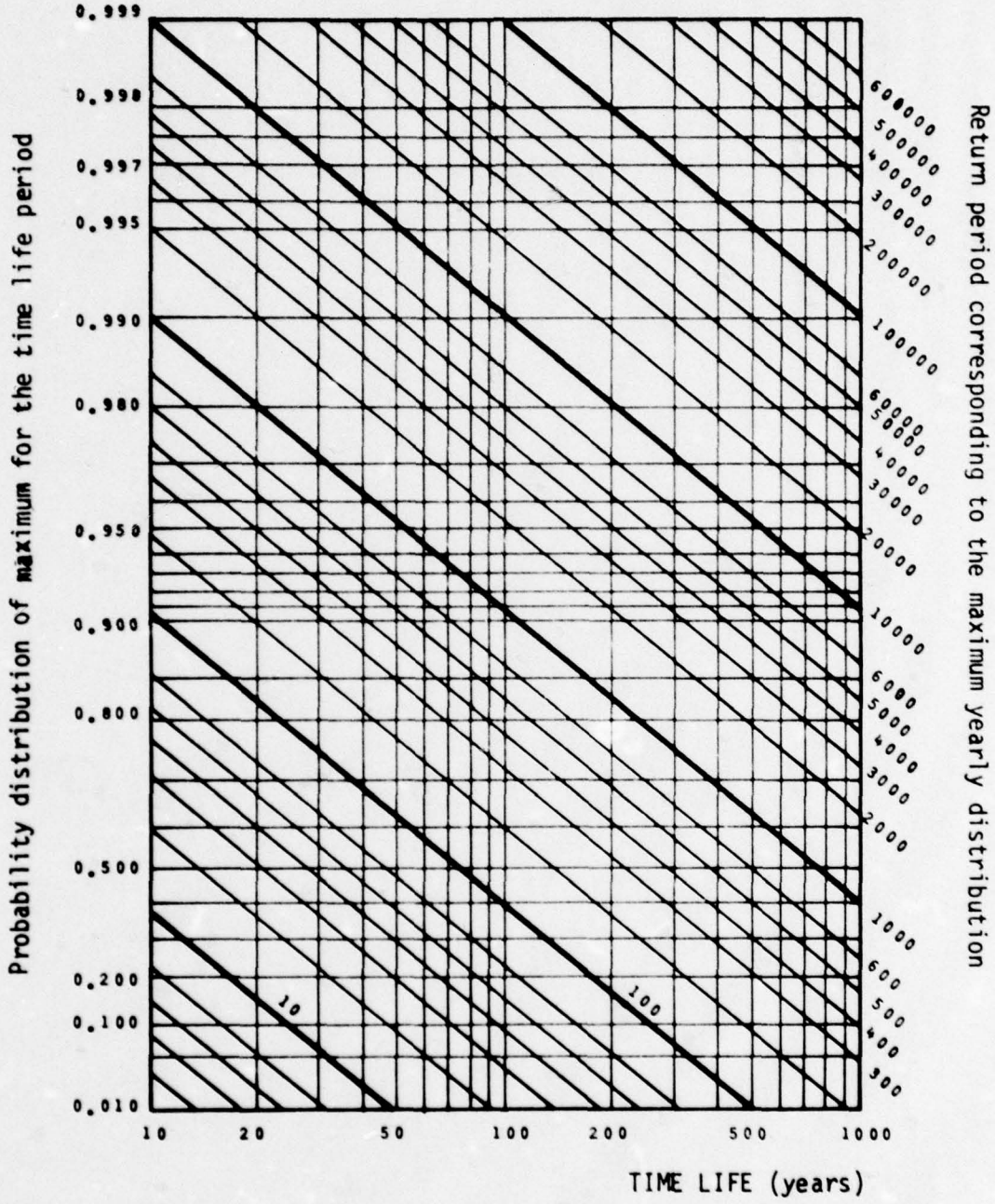

Figure 5-1. Conversion factors as function of probability of not exceeding y-values and of life-time (from Oliveira, 1975).

CHAPTER 6 - GROUND MOTION

Earthquake-Induced Ground Motion Levels

The rupture of a fault generates body waves propagating within the earth and surface waves propagating on the surface. The body waves are composed of dilational, longitudinal, compressional waves and distortional, transverse, shear waves, both vertical and horizontal. The surface waves are waves which involve a surface layer in horizontal transverse vibration and Rayleigh waves comprising vibration in retrograde orbit. Each of these types of waves propagates at its own velocity and arrives at specific locations at different times. Body waves travel fastest through the higher velocity mediums at depth (bedrock). The waves tend to be refracted toward the vertical as they propagate upward through increasingly softer materials near the surface. (This follows from Snell's law because shallower layers generally have lower wave velocities.)

Thus, shear waves tend to approach the surface traveling in the vertical direction and vibrating in a horizontal plane. Most structures are well-designed for vertical loads by use of standard safety factors. However, horizontal shear waves induce motions and load in the structure in the horizontal plane. Strong motion accelerograms show that vertical accelerations are often about two-thirds as large as horizontal vibrations. For this reason, vertically propagating, horizontal motions are considered of greatest importance and most work has centered on understanding them.

Rock motions beneath a particular site will depend upon the energy released along the fault (characterized by the magnitude of the earth-

PRECEDING PAGE BLANK

quake and type of fault and the distance of the site from the zone of energy release). Figure 6-1 shows the factors affecting seismic wave transmission.

Having the estimated magnitude of a seismic event and its distance from the site of interest, it is then possible to predict ground motions.

In order to estimate the response of any point on the surface, it is necessary to determine the surface topography and the underlying rock configurations. The types of soils and their characteristics determine the soil response under dynamic loading. It is important to consider the mechanism of underlying soil deposits and the transfer mechanisms to the surface. (For earthquake engineering purposes, bedrock may be loosely defined as a material exhibiting a shear wave velocity of 2,500 ft/sec or greater.) However, ground motion prediction is an inexact procedure; this will be discussed below.

Western United States

Several correlations are available to relate earthquake magnitude, distance from causative fault, and peak acceleration. An early correlation by Housner (1965) estimated peak acceleration for seismic motions experienced at the ground surface. At that time the influence of overlying soils on the peak accelerations could not be evaluated. Peak accelerations represented by these curves are not, therefore, directly applicable to the bedrock level.

A study by Schnabel and Seed (1972) evaluated the peak rock outcrop motions. The curves given in Figure 6-2 resulted from this study and relate peak rock acceleration with earthquake magnitude and distance from causative fault.

Seed et al. (1975) show that for the range from 20 to 250 km all measured accelerogram peak data from 6.5 magnitude earthquakes tends to lie within a band of two standard deviations (Figure 6-3). Prediction

at closer distances is based on extrapolation. Figures 6-4 and 6-5 show similar data for stiff soil conditions and deep cohesionless sites. Figure 6-6 compares acceleration in rock to acceleration in various soil profiles.

Trifunac and Brady (1975a) suggest that peaks of ground motion may be scaled by the following, where A_{max} is in./sec^2

$$\log_{10}[A_{max}] = M + \log_{10}[A_o(R)] + \log_{10}[A_o(M)]$$

They characterize site conditions s as

0 = alluvium
1 = intermediate
2 = basement rock

Tables 6-1 and 6-2 give values of $\log_{10}[A_o(R)]$ and $\log_{10}[A_o(M)]$. They extend the applicability of the equation to include confidence level p, site condition s, and component direction v (v = 0 for horizontal, v = 1 for vertical) as follows

$$\log_{10}[A_o(M,p,s,v)] = a\,p + b\,M + c + d\,s + e\,v + f\,M^2$$

The following coefficients in the expression are results of a least-squares-fit to available strong motion data.

$$= ap + bM + c + ds + ev + fM^2 - f(M - M_{max})^2 \qquad M \leq M_{max}$$

$$\log_{10}[A_o(M,p,s,v)] = ap + bM + c + ds + ev + fM^2 \qquad M_{max} \leq M \leq M_{min}$$

$$= ap + bM_{min} + c + ds + ev + fM_{min}^2 \qquad M \geq M_{min}$$

where
$a = -0.898$
$b = -1.789$
$c = 6.217$
$d = 0.060$
$e = 0.331$
$f = 0.186$
Total N Data = 227
$M_{min} = 4.80$
$M_{max} = 7.5$

The Trifunac and Brady (1975b) equation results in ground motions (Tables 6-3 and 6-4) near the fault much greater than Seed's estimates (Figures 6-2 and 6-6).

Page et al. (1972) reviewed ground motion records where the distance to fault was accurately known. They found that peak acceleration attenuates with distance r at a rate in the range $r^{-1.5}$ to $r^{-2.0}$ at distances beyond 10 km for magnitude 5, about 20 km for magnitude 6, and 40 km for magnitude 7 (Figure 6-7). For distances less than 10 km there are no strong motion data for shocks larger than magnitude 6. They estimate the near fault, free-field, horizontal ground motion in Table 6-5. The free-field peak acceleration values close to the fault are

higher than those estimated by Schnabel and Seed (1972). This table reflects the analysis of the 6.6-magnitude 1971 San Fernando earthquake's Pacoima Dam record. Motions for magnitudes greater than this were extrapolated considering that peak acceleration increased with magnitude and that near-fault peak acceleration is proportional to the effective stress causing slippage.

Table 6-6 (after McGuire, 1976) summarizes different attenuation equations developed for ground motions. Figure 6-8 (after Donovan, 1974) compares some of the attenuation equations for a magnitude 6.5 earthquake with measured data for the 1971 San Fernando earthquake. Although site conditions are not defined, other than as soil or rock, it is clear that there is a range in predictions of motion at a given distance. The estimation of ground motion is still an imperfect procedure with upper and lower bounds differing as much as 100% from mean predictions demonstrating the statistical spread in the data. Since no single relationship has been shown to give more reliable results than any other, it is recommended that the data presented in this section be reviewed to select the methodology most compatible with the intended usage, site characteristics, and importance of the structure.

Central and Eastern United States

Insofar as its effects on landform are concerned, the most destructive earthquakes in North America, since its settlement by Europeans, occurred in the New Madrid fault zone between December 1811 and February 1812 (Nuttli and Zellweg, 1974; Nuttli, 1973a, b, c, and 1974). This area includes southeast Missouri, northeast Arkansas, western Tennessee, western Kentucky and southern Illinois. However, in this region the occurrence of earthquakes is very infrequent. The historical data is limited to less than 200 years. Thus, it is possible that there are regions in the United States that have not experienced a destructive earthquake in the past 200 years but might suffer one in the next 100

years. There is a significant lack in strong motion records in the eastern and central United States. Since most of the recorded data for the United States have come from California, the characteristics of the accelerograms reflect seismologic and geologic conditions different from those of the east and central parts of the country. The tectonic forces in California are dominated by the San Andreas fault system, a strike-slip fault more than 600 miles long, and no comparable fault system exists elsewhere in the United States.

Nuttli has compiled a list of earthquakes in the central United States since 1843. He concludes that the attenuation rate of motion with distance is less in the central United States, and consequently a given magnitude earthquake is felt over a larger area. Nuttli (1973b) defines geographic regions (Figure 6-9) and associates maximum credible earthquakes of 7.2 with region 1, 6.2 with region 2, and 5.7 with region 3. He further adds however, that there is no place in the central United States that can be considered completely aseismic.

For region 1 the maximum credible earthquake is equal to that of the three largest earthquakes of the 1811-1812 New Madrid sequence. Since the attenuation with distance is less in the central United States, the earthquakes can be expected to be more destructive. Earthquake surface waves are dispersed which result in an increase in the time duration of the wave motion with an increase in epicentral distance. This is not a problem in California because strong attenuation of wave energy with distance reduces the motion to low levels at distances at which dispersion becomes important. The weak attenuation in the central United States produces prolonged shaking of as much as 1 or 2 minutes at distances of a few hundred miles. Further, there is a danger of developing resonant conditions for structures with natural periods of oscillation near those of the predominant surface motion. Nuttli has estimated the acceleration with distance for region 1 (7.2 magnitude) as shown in Figure 6-10. The acceleration given in Figure 6-10 for 0.3, 1, and 3 cps waves are the resultants of vertical and horizontal components of the sustained maximum surface wave motion.

(The resultant is the vector sum of two horizontal and one vertical components.) This work notes the attenuation as a function of wave frequency. If the horizontal motion is considered as two-thirds of the resultant, Figure 6-2 can be plotted as shown in Figure 6-10 to compare Western attenuation with Central attenuation. As can be seen for distances of less than 60 miles (100 km) there is fair agreement. Within these distances attenuation is controlled by geometric spreading rather than absorption so that the attenuation does not vary much with geographic area. However, at greater distances, lower level, long-duration shaking may be a significant problem, causing liquefaction.

Table 6-7 from Nuttli (1973a) gives displacement velocity and acceleration resultant data for hard rock ground motion. It is important to note that the active fault zones in the central United States are not well-delineated, in contrast to those in California. There is no known evidence of surficial fault breakage for any central United States earthquake except possibly those of 1811 and 1812.

Earthquake Characteristics

In developing a ground motion prediction, it is necessary to define the distance from the point of interest to the fault under consideration. If the fault break is short in length and the site is located a considerable distance from the fault, the significant distance from the site to the zone of energy release can be expressed by the epicentral distance. In the case of a long fault this can be grossly misleading. The rupture of the fault propagates along its length. When the site is close to a fault the distance should consider the release of energy as the rupture propagates along the fault length. In such a case, the distance to the site from the zone of energy release is more appropriately characterized by the shortest distance to the causative fault rather than the distance to the epicenter. To give perspective to this, consider Table 6-8 which gives an indication of magnitude and length of slipped fault.

After the design earthquake magnitudes and site ground motion levels have been defined by the geological and seismological studies, characteristics of the earthquake motions must be defined for use in engineering studies. Time-motion records may be used with complex computer programs as input to analyses which predict the response of overlying soils.

The important characteristics of the acceleration record are its duration, predominant period, and peak acceleration. A present practice is to scale acceleration from an existing suitable record to provide earthquake time histories. The general problem of scaling earthquake records is treated by Seed, Idriss and Kiefer (1969). The acceleration is linearly scaled to provide the design peak accelerations.

The duration of strong motion has been related in a general way to fault length and the time required for the fault to shear, which can also be related to earthquake magnitude. Figure 6-11 provides a relationship between duration of strong motion and earthquake magnitude developed by Lee and Chan (1972). Note the definition of duration on the graph. Data from Page et al. (1972) for near fault horizontal motion is given in Table 6-4. Studies by Bolt (1974) and Kobayashi (1974) have developed similar duration versus magnitude correlations (Figures 6-12 and 6-13). In general the studies presented in Figures 6-11, 6-12, and 6-13 show good agreement. Duration defined as motion greater than 0.05g can be estimated by an average of the data shown. The rate of rupture is believed to be on the order of magnitude of 2 miles per second so that, for example, a magnitude 7 earthquake resulting from a 25-mile (40 km) fault break would have at least 12.5 seconds duration. Nuttli (1973c) suggests that Central United States earthquakes do not have the same duration (of felt motion) characteristics as Western earthquakes as a result of the increased dispersion effects and weak attenuation. However, for distances less than 100 miles from the fault this may not be significant.

Figure 6-14 provides a relationship between predominant periods of maximum acceleration, earthquake magnitude, and distance from the causative fault. The scarcity of close-in data results in a constant period

for a given earthquake magnitude out to a distance of 25 miles (40 km) from the causative fault. Figueroa (1960), however, indicates a very wide scatter in predominant period data out to a distance of 50 miles (80 km).

An acceleration time history for use in seismic design studies can also be generated with desired characteristics by use of random number programs shaped to the desired spectral characteristics.

Scaling an individual earthquake record has the disadvantage that each record is representative of a specific event and site. Each individual record will be deficient in some response frequencies. An ensemble of scaled earthquake records can be used as a better average of the individual records. Scaled artificial earthquake records that do not exhibit a specific bias can also be used. Procedures for selecting an ensemble of real or artificial records are provided in Werner (1970) and Guzman and Jennings (1975a and b).

Seismic Studies

As an example of available seismic studies, Greensfelder (1974) shows contours of possible peak acceleration from active faults using the attenuation after Schnabel and Seed (1972). The probability of occurrence is not considered other than the fact that the faults considered active include Quaternary movement. Algermissen and Perkins (1976) developed a similar map for the entire United States. This may assist in predicting site motion. However, the relatively large area coverage of the maps may not be sufficiently detailed for specific site studies.

Discussion

An in-depth geological and seismological investigation is desirable at proposed sites to locate faults and evaluate the site soil profile. When historical data is available the design earthquake magnitude should be determined in terms of the structure life and earthquake recurrence.

For engineering analysis, use of the Poisson model should be adequate. Figure 6-10 shows that although the attenuation in Central and Eastern United States is less than in the West within the range less than 60 miles (100 km), Figure 6-2 is probably adequate since this is the range of most engineering interest. The earthquake duration can be approximated from Figures 6-11, 6-12, and 6-13.

Table 6-1. $\text{Log}_{10}A_o(R)$ Versus Epicentral Distance R

R (km)	$-\log_{10}A_o(R)$	R (km)	$-\log_{10}A_o(R)$	R (km)	$-\log_{10}A_o(R)$	R (km)	$-\log_{10}A_o(R)$
0	1.400	120	3.135	330	4.164	540	4.817
5	1.500	130	3.182	340	4.209	550	4.835
10	1.605	140	3.230	350	4.253	560	4.853
15	1.716	150	3.279	360	4.295	570	4.869
20	1.833	160	3.328	370	4.336	580	4.885
25	1.955	170	3.378	380	4.376	590	4.900
30	2.078	180	3.429	390	4.414		
35	2.199	190	3.480	400	4.451		
40	2.314	200	3.530	410	4.485		
45	2.421	210	3.581	420	4.518		
50	2.517	220	3.631	430	4.549		
55	2.603	230	3.680	440	4.579		
60	2.679	240	3.729	450	4.607		
65	2.746	250	3.779	460	4.634		
70	2.805	260	3.827	470	4.660		
80	2.920	270	3.877	480	4.685		
85	2.958	280	3.926	490	4.709		
90	2.989	290	3.975	500	4.732		
95	3.020	300	4.024	510	4.755		
100	3.044	310	4.072	520	4.776		
110	3.089	320	4.119	530	4.797		

Table 6-2. Means and Standard Deviations of the Logarithm of the Magnitude-Dependent Scaling Function $A_o(M)$

Magnitude	Site Classification	Vertical Acceleration (cm/s^2)		Horizontal Acceleration (cm/s^2)		No. of Data Used	
		$\log A_o$	σ	$\log A_o$	σ	Vertical	Horizontal
4.0 - 4.9	0	1.80	0.036	1.38	0.309	3	6
	1	1.39	0.519	1.07	0.368	2	4
	2	-	-	-	-		
5.0 - 5.9	0	1.83	0.494	1.56	0.503	24	47
	1	1.94	0.253	1.54	0.313	15	30
	2	1.60	0.213	1.41	0.390	2	4
6.0 - 6.9	0	2.21	0.270	1.94	0.278	82	164
	1	2.25	0.253	1.94	0.205	34	68
	2	2.25	0.332	2.05	0.331	12	24
7.0 - 7.9	0	3.21	0.107	2.87	0.163	7	14
	1	-	-	-	-		
	2	-	-	-	-		

Table 6-3. Mean Value (Intermediate Site) (from Ferritto and Forrest, 1977)

Magnitude	Distance (miles)									
	5	10	15	20	25	30	35	40	45	50
2.400	.000	.000	.000	.000	.000	.000	.000	.000	.000	.000
2.600	.000	.000	.000	.000	.000	.000	.000	.000	.000	.000
2.800	.001	.000	.000	.000	.000	.000	.000	.000	.000	.000
3.000	.001	.001	.000	.000	.000	.000	.000	.000	.000	.000
3.200	.001	.001	.001	.000	.000	.000	.000	.000	.000	.000
3.400	.002	.001	.001	.001	.000	.000	.000	.000	.000	.000
3.600	.003	.002	.001	.001	.001	.000	.000	.000	.000	.000
3.800	.005	.003	.002	.001	.001	.001	.000	.000	.000	.000
4.000	.008	.006	.004	.002	.001	.001	.001	.001	.000	.000
4.200	.013	.009	.006	.004	.002	.002	.001	.001	.001	.001
4.400	.021	.014	.009	.006	.004	.003	.002	.001	.001	.001
4.600	.033	.022	.014	.009	.006	.004	.003	.002	.002	.001
4.800	.052	.035	.022	.014	.009	.006	.005	.004	.003	.002
5.000	.082	.054	.035	.022	.014	.010	.007	.005	.004	.004
5.200	.123	.082	.052	.033	.022	.015	.011	.008	.007	.005
5.400	.179	.119	.076	.049	.032	.022	.016	.012	.010	.008
5.600	.252	.168	.108	.068	.044	.030	.022	.017	.014	.011
5.800	.343	.228	.146	.093	.060	.041	.030	.023	.018	.015
6.000	.451	.300	.193	.122	.079	.054	.039	.030	.024	.020

(continued)

Table 6-3. Continued

Magnitude	Distance (miles)									
	5	10	15	20	25	30	35	40	45	50
6.200	.573	.381	.245	.155	.101	.069	.050	.038	.031	.025
6.400	.704	.468	.300	.191	.124	.085	.061	.047	.038	.031
6.600	.835	.555	.356	.226	.147	.100	.073	.056	.045	.036
6.800	.957	.636	.408	.259	.168	.115	.084	.064	.052	.042
7.000	1.061	.705	.452	.287	.186	.128	.093	.071	.057	.046
7.200	1.135	.754	.484	.308	.200	.136	.099	.076	.061	.050
7.400	1.174	.780	.501	.318	.206	.141	.102	.079	.063	.051
7.600	1.179	.783	.503	.320	.207	.142	.103	.079	.063	.052
7.800	1.178	.783	.503	.319	.207	.142	.103	.079	.063	.051
8.000	1.178	.782	.502	.319	.207	.142	.103	.079	.063	.051
8.200	1.177	.782	.502	.319	.207	.142	.103	.079	.063	.051
8.400	1.177	.782	.502	.319	.207	.141	.103	.079	.063	.051

(continued)

Table 6-3. Continued

Magnitude	Distance (miles)									
	55	60	65	70	75	80	85	90	95	100
2.400	.000	.000	.000	.000	.000	.000	.000	.000	.000	.000
2.600	.000	.000	.000	.000	.000	.000	.000	.000	.000	.000
2.800	.000	.000	.000	.000	.000	.000	.000	.000	.000	.000
3.000	.000	.000	.000	.000	.000	.000	.000	.000	.000	.000
3.200	.000	.000	.000	.000	.000	.000	.000	.000	.000	.000
3.400	.000	.000	.000	.000	.000	.000	.000	.000	.000	.000
3.600	.000	.000	.000	.000	.000	.000	.000	.000	.000	.000
3.800	.000	.000	.000	.000	.000	.000	.000	.000	.000	.000
4.000	.000	.000	.000	.000	.000	.000	.000	.000	.000	.000
4.200	.001	.000	.000	.000	.000	.000	.000	.000	.000	.000
4.400	.001	.001	.001	.001	.001	.001	.000	.000	.000	.000
4.600	.001	.001	.001	.001	.001	.001	.001	.001	.001	.001
4.800	.002	.002	.002	.002	.001	.001	.001	.001	.001	.001
5.000	.003	.003	.003	.002	.002	.002	.002	.002	.002	.001
5.200	.005	.004	.004	.004	.003	.003	.003	.003	.002	.002
5.400	.007	.006	.006	.005	.005	.004	.004	.004	.003	.003
5.600	.010	.009	.008	.007	.007	.006	.006	.006	.005	.004
5.800	.013	.012	.011	.010	.009	.008	.008	.007	.006	.006
6.000	.017	.016	.014	.013	.012	.011	.010	.009	.008	.008

(continued)

Table 6-3. Continued

Magnitude	Distance (miles)									
	55	60	65	70	75	80	85	90	95	100
6.200	.022	.020	.018	.017	.015	.014	.013	.012	.011	.010
6.400	.027	.024	.022	.020	.019	.017	.016	.014	.013	.012
6.600	.032	.029	.026	.024	.022	.020	.019	.017	.016	.014
6.800	.037	.033	.030	.028	.026	.023	.021	.020	.018	.016
7.000	.041	.036	.033	.031	.028	.026	.024	.022	.020	.018
7.200	.004	.039	.036	.033	.030	.028	.025	.023	.021	.019
7.400	.045	.040	.037	.034	.031	.029	.026	.024	.022	.020
7.600	.045	.041	.037	.034	.031	.029	.026	.024	.022	.020
7.800	.045	.041	.037	.034	.031	.029	.026	.024	.022	.020
8.000	.045	.041	.037	.034	.031	.029	.026	.024	.022	.020
8.200	.045	.040	.037	.034	.031	.029	.026	.024	.022	.020
8.400	.045	.040	.037	.034	.031	.029	.026	.024	.022	.020

Table 6-4. Standard Deviation (Intermediate Site) (from Ferritto and Forrest, 1977)

Magnitude	Distance (miles)									
	5	10	15	20	25	30	35	40	45	50
2.400	.000	.000	.000	.000	.000	.000	.000	.000	.000	.000
2.600	.000	.000	.000	.000	.000	.000	.000	.000	.000	.000
2.800	.001	.000	.000	.000	.000	.000	.000	.000	.000	.000
3.000	.001	.001	.000	.000	.000	.000	.000	.000	.000	.000
3.200	.001	.001	.001	.000	.000	.000	.000	.000	.000	.000
3.400	.002	.001	.001	.001	.000	.000	.000	.000	.000	.000
3.600	.003	.002	.001	.001	.001	.000	.000	.000	.000	.000
3.800	.005	.004	.002	.001	.001	.001	.000	.000	.000	.000
4.000	.008	.006	.004	.002	.001	.001	.001	.001	.000	.000
4.200	.013	.009	.006	.004	.002	.002	.001	.001	.001	.001
4.400	.021	.014	.009	.006	.004	.003	.002	.001	.001	.001
4.600	.034	.022	.014	.009	.006	.004	.003	.002	.002	.001
4.800	.053	.035	.023	.014	.009	.006	.005	.004	.003	.002
5.000	.083	.055	.035	.023	.015	.010	.007	.006	.004	.004
5.200	.125	.083	.054	.034	.022	.015	.011	.008	.007	.005
5.400	.183	.121	.078	.050	.032	.022	.016	.012	.010	.008
5.600	.257	.171	.110	.070	.045	.031	.022	.017	.014	.011
5.800	.350	.233	.149	.095	.062	.042	.031	.023	.019	.015
6.000	.460	.306	.196	.125	.081	.055	.040	.031	.025	.020

(continued)

Table 6-4. Continued

Magnitude	Distance (miles)									
	5	10	15	20	25	30	35	40	45	50
6.200	.585	.389	.249	.159	.103	.070	.051	.039	.031	.026
6.400	.718	.477	.306	.195	.126	.086	.063	.048	.039	.031
6.600	.852	.566	.363	.231	.150	.102	.074	.057	.046	.037
6.800	.976	.649	.416	.265	.172	.117	.085	.065	.053	.043
7.000	1.082	.719	.461	.293	.190	.130	.094	.073	.058	.047
7.200	1.158	.769	.494	.314	.204	.139	.101	.078	.062	.051
7.400	1.198	.796	.511	.325	.211	.144	.104	.080	.064	.052
7.600	1.202	.799	.513	.326	.211	.145	.105	.081	.065	.053
7.800	1.202	.798	.513	.326	.211	.144	.105	.081	.065	.053
8.000	1.201	.798	.512	.326	.211	.144	.105	.081	.065	.052
8.200	1.200	.798	.512	.325	.211	.144	.105	.080	.065	.052
8.400	1.200	.797	.512	.325	.211	.144	.105	.080	.065	.052

(continued)

Table 6-4. Continued

Magnitude	Distance (miles)									
	55	60	65	70	75	80	85	90	95	100
2.400	.000	.000	.000	.000	.000	.000	.000	.000	.000	.000
2.600	.000	.000	.000	.000	.000	.000	.000	.000	.000	.000
2.800	.000	.000	.000	.000	.000	.000	.000	.000	.000	.000
3.000	.000	.000	.000	.000	.000	.000	.000	.000	.000	.000
3.200	.000	.000	.000	.000	.000	.000	.000	.000	.000	.000
3.400	.000	.000	.000	.000	.000	.000	.000	.000	.000	.000
3.600	.000	.000	.000	.000	.000	.000	.000	.000	.000	.000
3.800	.000	.000	.000	.000	.000	.000	.000	.000	.000	.000
4.000	.000	.000	.000	.000	.000	.000	.000	.000	.000	.000
4.200	.001	.000	.000	.000	.000	.000	.000	.000	.000	.000
4.400	.001	.001	.001	.001	.001	.001	.000	.000	.000	.000
4.600	.001	.001	.001	.001	.001	.001	.001	.001	.001	.001
4.800	.002	.002	.002	.002	.001	.001	.001	.001	.001	.001
5.000	.003	.003	.003	.002	.002	.002	.002	.002	.002	.001
5.200	.005	.004	.004	.004	.003	.003	.003	.003	.002	.002
5.400	.007	.006	.006	.005	.005	.004	.004	.004	.003	.003
5.600	.010	.009	.008	.007	.007	.006	.006	.005	.005	.004
5.800	.013	.012	.011	.010	.009	.009	.008	.007	.007	.006
6.000	.018	.016	.015	.013	.012	.011	.010	.009	.009	.008

(continued)

Table 6-4. Continued

Magnitude	Distance (miles)									
	55	60	65	70	75	80	85	90	95	100
6.200	.022	.020	.018	.017	.016	.014	.013	.012	.011	.010
6.400	.028	.025	.023	.021	.019	.018	.016	.015	.013	.012
6.600	.033	.029	.027	.025	.023	.021	.019	.017	.016	.015
6.800	.037	.034	.031	.028	.026	.024	.022	.020	.018	.017
7.000	.042	.037	.034	.031	.029	.026	.024	.022	.020	.018
7.200	.044	.040	.037	.034	.031	.028	.026	.024	.022	.020
7.400	.046	.041	.038	.035	.032	.029	.027	.024	.022	.020
7.600	.046	.041	.038	.035	.032	.029	.027	.025	.022	.020
7.800	.046	.041	.038	.035	.032	.029	.027	.025	.022	.020
8.000	.046	.041	.038	.035	.032	.029	.027	.025	.022	.020
8.200	.046	.041	.038	.035	.032	.029	.027	.025	.022	.020
8.400	.046	.041	.038	.035	.032	.029	.027	.025	.022	.020

Table 6-5. Near-Fault Horizontal Ground Motion

Magnitude	Acceleration (g) Peak Absolute Values				Velocity (cm/s) Peak Absolute Values			Displacement (cm)	Duration[a] (s)
	1st Peak	2nd Peak	5th Peak	10th Peak	1st Peak	2nd Peak	3rd Peak		
8.5	1.25	1.15	1.00	0.75	150	130	110	100	90
8.0	1.20	1.10	0.95	0.70	145	125	105	85	60
7.5	1.15	1.00	0.85	0.65	135	115	100	70	40
7.0	1.05	0.90	0.75	0.55	120	100	85	55	25
6.5	*0.90*[b]	*0.75*	*0.60*	*0.45*	*100*	*80*	*70*	*40*	*17*
5.5	*0.45*	*0.30*	*0.20*	*0.15*	*50*	*40*	*30*	*15*	*10*

[a] Time interval between first and last peaks of absolute acceleration equal to or greater than 0.05 g.

[b] Italic values are based on instrumental data.

Notes — 1. The values in this table are for a single horizontal component of motion at a distance of a few (3-5) km of the causative fault; are for sites at which ground motion is not strongly altered by extreme contrasts in the elastic properties within the local geologic section or by the presence of structures; and contain no factor relating to the nature or importance of the structure being designed.

2. The values of acceleration may be exceeded if there is appreciable high-frequency (higher than 8 Hz) energy.

3. The values of displacement are for dynamic ground displacements from which spectral components with periods greater than 10 to 15 seconds are removed.

Table 6-6. Summary of Published Attenuation Functions (from McGuire, 1976)

Reference	Data Source	Distance Parameter	Dependent Variable	Equation	Standard Deviation
Blume (1966)	Southern California	Epicentral distance Δ (mi)	Peak ground acceleration a_g (g)	$a_g = \frac{a_o}{1+(\Delta/h)^2}$ where a_o is epicentral acceleration, h is focal depth	Not reported
Brazee (1972)	United States east of long. 106°W	Epicentral distance Δ (mi)	Distance over which a Modified Mercalli intensity is felt	$\text{Log } \Delta = a_I + b_I I_e$ where I_e is epicentral intensity, a_I and b_I are tabulated	Not reported
Cloud and Perez (1971)	North and South America	Epicentral distance or distance to fault Δ (mi)	Maximum single component ground acceleration a_g (g)	$a_g = 3.0 - 2 \log(\Delta+43)$ $a_g = 3.5 - 2 \log(\Delta+80)$	Not reported
Cornell and Merz (1974)	Northeastern United States, rock sites	Epicentral distance Δ (mi)	Modified Mercalli intensity	$I = 2.6 + I_e - 1.3 \ln \Delta$ $\Delta \geq 10$ mi	$\sigma_I = 0.2$
	Northwestern United States, all sites	------do------	------do------	$I = 3.1 + I_e - 1.3 \ln \Delta$ $\Delta \geq 10$ mi where I_e is epicentral intensity	$\sigma_I = 0.5$
Donovan (1974)	San Fernando, rock sites	Distance to energy center R (km)	Peak ground acceleration a_g (gals)	$a_g = 12.783 \times 10^6 (R+25)^{-2.77}$	Not reported
	San Fernando, soil sites	------do------	------do------	$a_g = 2.054 \times 10^5 (R+25)^{-1.83}$	Not reported
	San Fernando, all sites	------do------	------do------	$a_g = 5.165 \times 10^5 (R+25)^{-2.04}$	$\sigma_{\ln a_g} = 0.481$
	---do---	------do------	------do------	$a_g = 1.84 \times 10^4 R^{-1.42}$	Not reported

continued

Table 6-6. Continued

Reference	Data Source	Distance Parameter	Dependent Variable	Equation	Standard Deviation
Donovan (1974) (continued)	Western North America, Japan, Papua-New Guinea	------do------	------do------	$a_g=1080\ e^{-0.5M}(R+25)^{-1.32}$	$\sigma_{\ln a_g}=0.707$
Donovan (1973)	Worldwide	Hypocentral distance, epicentral distance, or distance to fault R (km)	Peak ground acceleration a_g (gals)	$a_g=1320\ e^{0.58M}(R+25)^{-1.52}$	$\sigma_{\ln a_g}=0.84$
Duke and others (1972)	San Fernando, all sites	Distance to energy center R (km)	Peak ground acceleration a_g (g)	$a_g=\frac{6.69}{R}e^{-0.0097R}$	$\sigma_{a_g}=0.052$ g
	---do---	------do------	Spectral acceleration s_g (g)	$s_g=\frac{5.34}{R}e^{-0.0068R}$	$\sigma_{s_g}=0.053$ g
Esteva (1970)	See reference	Hypocentral distance R (km)	Peak ground acceleration a_g (gals)	$a_g=1230\ e^{0.8M}(R+25)^{-2}$	$\sigma_{\ln a_g}=1.2$
	---do---	------do------	Peak ground velocity v_g (cm/sec)	$v_g=15\ e^{M}(R+0.17\ e^{0.59M})^{-1.7}$	$\sigma_{\ln v_g}=0.84$
Esteva and Rosenblueth (1964)	West Coast of United States	Hypocentral distance R (km)	Peak ground acceleration a_g (gals)	$a_g=2000\ e^{0.8M}R^{-2}$	See reference
	---do---	------do------	Peak ground velocity v_g (cm/sec)	$v_g=20\ e^{M}\ R^{-1.7}$	See reference
Esteva and Villaverde (1974)	Western United States	Hypocentral distance R (km)	Peak ground acceleration a_g (gals)	$a_g=5600\ e^{0.8M}(R+40)^{-2}$	$\sigma_{\ln a_g}=0.64$
	---do---	------do------	Peak ground velocity v_g (cm/sec)	$v_g=32\ e^{M}(R+25)^{-1.7}$	$\sigma_{\ln v_g}=0.74$

continued

Table 6-6. Continued

Reference	Data Source	Distance Parameter	Dependent Variable	Equation	Standard Deviation
Esteva and Villaverde (1974)	Western United States	Hypocentral distance R (km)	Maximum average spectral acceleration $\bar{A}$ (gals)	$\bar{A}=69600\ e^{0.8M}(R+70)^{-2}$	$\sigma_{\ln \bar{A}}=0.75$
	---do---	------do------	Maximum average spectral velocity $\bar{V}$ (cm/sec)	$\bar{V}=250\ e^{M}(R+60)^{-1.7}$	$\sigma_{\ln \bar{V}}=0.64$
Gupta and Nuttli (1975)	Central United States	Epicentral distance to isoseismal Δ (km)	Modified Mercalli intensity	$I=I_e+3.7-0.0011\ \Delta$ $-2.7 \log \Delta$ where I_e is epicentral intensity	Not reported
Gutenberg and Richter (1956)	California	Epicentral distance	Peak ground acceleration	Graphical	Not reported
Housner (1965)	Western United States, and Central and South America	Distance to fault	Peak ground acceleration	Graphical	Not reported
Howell and Schultz (1975)	California coast	Epicentral distance to isoseismal Δ (km)	Modified Mercalli intensity	$I=I_e+0.874-0.422 \ln \Delta$ $-0.0186\ \Delta$	$\sigma_I=0.64$
	---do---	------do------	Logarithm of Modified Mercalli intensity	$\ln I=\ln I_e+0.16-0.0763 \ln \Delta$ $-0.0023\ \Delta$	$\sigma_I=0.44$
	Rocky Mountains, Washington, Oregon	Epicentral distance to isoseismal Δ (km)	Modified Mercalli intensity	$I=I_e+1.802-0.628 \ln \Delta$ $-0.009\ \Delta$	$\sigma_I=0.61$
	---do---	------do------	Logarithm of Modified Mercalli intensity	$\ln I=\ln I_e+0.322-0.1098 \ln \Delta$ $-0.0012\ \Delta$	$\sigma_I=0.47$

continued

Table 6-6. Continued

Reference	Data Source	Distance Parameter	Dependent Variable	Equation	Standard Deviation
Howell and Schultz (1975) (continued)	Central and Eastern United States and Canada	Epicentral distance to isoseismal Δ (km)	Modified Mercalli intensity	$I=I_e+3.278-0.989 \ln \Delta -0.0029 \Delta$	$\sigma_I=0.64$
	---do---	------do------	Logarithm of Modified Mercalli intensity	$\ln I=\ln I_e+0.480-0.139 \ln \Delta -0.00075 \Delta$ where I_e is epicentral intensity	$\sigma_I=0.43$
			(Other forms of equations examined and reported also)		
McGuire (1974)	West Coast of United States	Hypocentral distance R (km)	Peak ground acceleration a_g (gals)	$a_g=472 \times 10^{0.28M}(R+25)^{-1.3}$	$\sigma_{\log a_g}=0.222$
	---do---	------do------	Peak ground velocity v_g (cm/sec)	$v_g=5.64 \times 10^{0.40M}(R+25)^{-1.2}$	$\sigma_{\log v_g}=0.273$
	---do---	------do------	Peak ground displacement d_g (cm)	$d_g=0.393 \times 10^{0.43M}(R+25)^{-0.88}$	$\sigma_{\log d_g}=0.330$
	---do---	------do------	Spectral velocity (T=1 sec, ζ=0.02) s (in/sec)	$s=0.428 \times 10^{0.38M}(R+25)^{-0.59}$	$\sigma_{\log s}=0.274$
			(Spectral attenuation equations given for other periods and dampings also.)		
Mickey (1971)	See reference	Hypocentral distance, R (km)	Peak particle acceleration a (g)	$a=3.04 \times 10^{0.74m-4}R^{-1.4}$	See reference
	---do---	------do------	Peak particle velocity v (cm/sec)	$v=4.06 \times 10^{0.88m-3}R^{-1.5}$	---do---
	---do---	------do------	Peak particle displacement d (cm)	$d=5.66 \times 10^{1.1m-5}R^{-1.2}$ where m is body-wave magnitude	---do---

continued

Table 6-6. Continued

Reference	Data Source	Distance Parameter	Dependent Variable	Equation	Standard Deviation
Milne and Davenport (1969)	Western United States, Central America, Chile	Epicentral distance Δ (km)	Peak ground acceleration a_g (g)	$a_g = \frac{0.69\, e^{1.64M}}{1.1\, e^{1.1M} + \Delta^2}$	Not reported
	Eastern Canada	------do------	Modified Mercalli intensity	$I=I_7-9.66-0.0037\,\Delta +1.38\,M+0.00528\,\Delta\,M$ where I_7 is site intensity of M=7 event at distance Δ	$\sigma_I=0.53$
Neumann (1954)	West Coast of United States	Epicentral distance Δ (mi)	Modified Mercalli intensity	$I=I_e+0.15-3.17 \log R$ $R \geq 1.12$ miles where I_e is epicentral intensity	Not reported
Nuttli (1973a)	Central United States	Epicentral distance	Vertical particle acceleration, velocity, and displacement at 3 frequencies for Rayleigh waves	Graphical and tabular for various earthquakes	Not reported
Nuttli (1973b)	Central United States	Epicentral distance	Sustained ground acceleration, velocity, and displacement at 3 frequencies for surface waves	Graphical and tabular	Not reported
Orphal and Lahoud (1974)	California	Hypocentral distance R (km)	Peak ground acceleration a_g (g)	$a_g=0.066\times10^{0.4M}R^{-1.39}$	See reference
	California and nuclear explosions	-----do-----	Peak ground velocity v_g (cm/sec)	$v_g=0.726\times10^{0.52M}R^{-1.34}$	----do----
	---do----	-----do-----	Peak ground displacement d_g (cm)	$d_g=0.0471\times10^{0.57M}R^{-1.18}$	----do----

continued

Table 6-6. Continued

Reference	Data Source	Distance Parameter	Dependent Variable	Equation	Standard Deviation
Rasmussen and others (1974)	Puget Sound, Washington	Epicentral distance	Modified Mercalli intensity	Graphical; data and limits given for each earthquake	Not calculated; data shown
Schnabel and Seed (1973)	Western United States	Distance to fault	Peak ground acceleration	Graphical	Not reported
Stepp (1971)	Puget Sound, Washington	Hypocentral distance to isoseismal R (km)	Modified Mercalli intensity	$I=I_e-2.017 \log(R/h) -0.008(R/h)$ where I_e is epicentral intensity, h is focal depth	Not reported

Table 6-7. Design Earthquake for Regions 1, 2, and 3[a]

Distance (miles)	0.3-Hz Waves			1-Hz Waves			3-Hz Waves		
	Displacement (cm)	Particle Velocity (cm/s)	Acceleration (g)	Displacement (cm)	Particle Velocity (cm/s)	Acceleration (g)	Displacement (cm)	Particle Velocity (cm/s)	Acceleration (g)
Region 1									
5	120 - 260	260 - 540	0.56 - 1.1	12 - 21	78 - 140	0.48 - 0.88	1.2 - 2.4	26 - 52	0.54 - 1.1
10	120	260	0.56	12	78	0.48	1.2	26	0.54
15	80	170	0.35	8.2	54	0.34	0.80	17	0.35
20	60	130	0.26	6.3	42	0.26	0.60	12	0.26
25	48	100	0.21	5.2	35	0.22	0.47	9.8	0.21
35	34	72	0.15	3.9	26	0.16	0.39	6.7	0.14
50	24	50	0.10	2.8	19	0.12	0.21	4.4	0.095
75	15	32	0.066	2.0	13	0.083	0.12	2.5	0.055
100	11	23	0.047	1.6	10	0.065	0.072	1.7	0.037
150	6.5	14	0.029	1.1	6.8	0.044	0.043	0.85	0.019
200	4.6	9.8	0.020	0.80	5.2	0.033	0.026	0.53	0.012
300	2.7	5.7	0.012	0.52	3.4	0.021	0.012	0.24	0.005
Region 2									
5	12 - 26	26 - 54	0.056 - 0.11	1.2 - 2.1	7.8 - 14	0.048 - 0.088	0.12 - 0.24	2.6 - 5.2	0.054 - 0.11
10	12	26	0.056	1.2	7.8	0.048	0.12	2.6	0.054
15	8.0	17	0.035	0.82	5.4	0.034	0.080	1.7	0.035
20	6.0	13	0.026	0.63	4.2	0.026	0.060	1.2	0.026
25	4.8	10	0.021	0.52	3.5	0.022	0.047	0.98	0.021
35	3.4	7.2	0.015	0.39	2.6	0.016	0.039	0.67	0.014
50	2.4	5.0	0.010	0.28	1.9	0.012	0.021	0.44	0.0095
75	1.5	3.2	0.0066	0.20	1.3	0.0083	0.012	0.25	0.0055

continued

Table 6-7. Continued

Distance (miles)	0.3-Hz Waves			1-Hz Waves			3-Hz Waves		
	Displacement (cm)	Particle Velocity (cm/s)	Acceleration (g)	Displacement (cm)	Particle Velocity (cm/s)	Acceleration (g)	Displacement (cm)	Particle Velocity (cm/s)	Acceleration (g)
Region 2 (continued)									
100	1.1	2.3	0.0047	0.16	1.0	0.0065	0.0072	0.17	0.0037
150	0.65	1.4	0.0029	0.11	0.68	0.0044	0.0043	0.085	0.0019
200	0.46	0.98	0.0020	0.080	0.52	0.0033	0.0026	0.053	0.0012
300	0.27	0.57	0.0012	0.052	0.34	0.0021	0.0012	0.024	0.0005
Region 3									
5	4.0 - 8.6	8.6 - 18	0.019 - 0.037	0.40 - 0.70	2.6 - 4.7	0.016 - 0.029	0.040 - 0.080	0.86 - 1.7	0.018 - 0.037
10	4.0	8.6	0.019	0.40	2.6	0.016	0.040	0.86	0.018
15	2.7	5.7	0.012	0.27	1.8	0.011	0.027	0.57	0.012
20	2.0	4.3	0.0087	0.21	1.4	0.0087	0.020	0.40	0.0087
25	1.6	3.3	0.0070	0.17	1.2	0.0073	0.016	0.33	0.0070
35	1.1	2.4	0.0050	0.13	0.87	0.0053	0.013	0.22	0.0047
50	0.80	1.7	0.0033	0.093	0.63	0.0040	0.0070	0.15	0.0032
75	0.50	1.1	0.0022	0.067	0.43	0.0028	0.0040	0.083	0.0018
100	0.37	0.77	0.0016	0.053	0.33	0.0022	0.0024	0.057	0.0012
150	0.22	0.47	0.00097	0.037	0.23	0.0015	0.0014	0.028	0.00063
200	0.15	0.33	0.00067	0.027	0.17	0.0011	0.00087	0.018	0.00040
300	0.090	0.19	0.00040	0.017	0.11	0.0007	0.00040	0.008	0.00017

[a] The hard-rock ground motions (displacement, particle velocity, and acceleration) are the vector resultants of the vertical and horizontal components of the sustained maximum surface wave motion. At distances of 75 miles, the duration of this motion will be as much as 30 s. At distances of 100 miles and greater, the duration can be as much as 1 to 2 minutes, generally increasing with increasing epicentral distance.

AD-A060 204 CIVIL ENGINEERING LAB (NAVY) PORT HUFNEME CALIF F/G 8/11
A PROBABILISTIC PROCEDURE FOR ESTIMATING SEISMIC LOADING BASED --ETC(U)
AUG 78 J M FERRITTO

UNCLASSIFIED CEL-TR-867 NL

2 OF 3
AD
A060 204

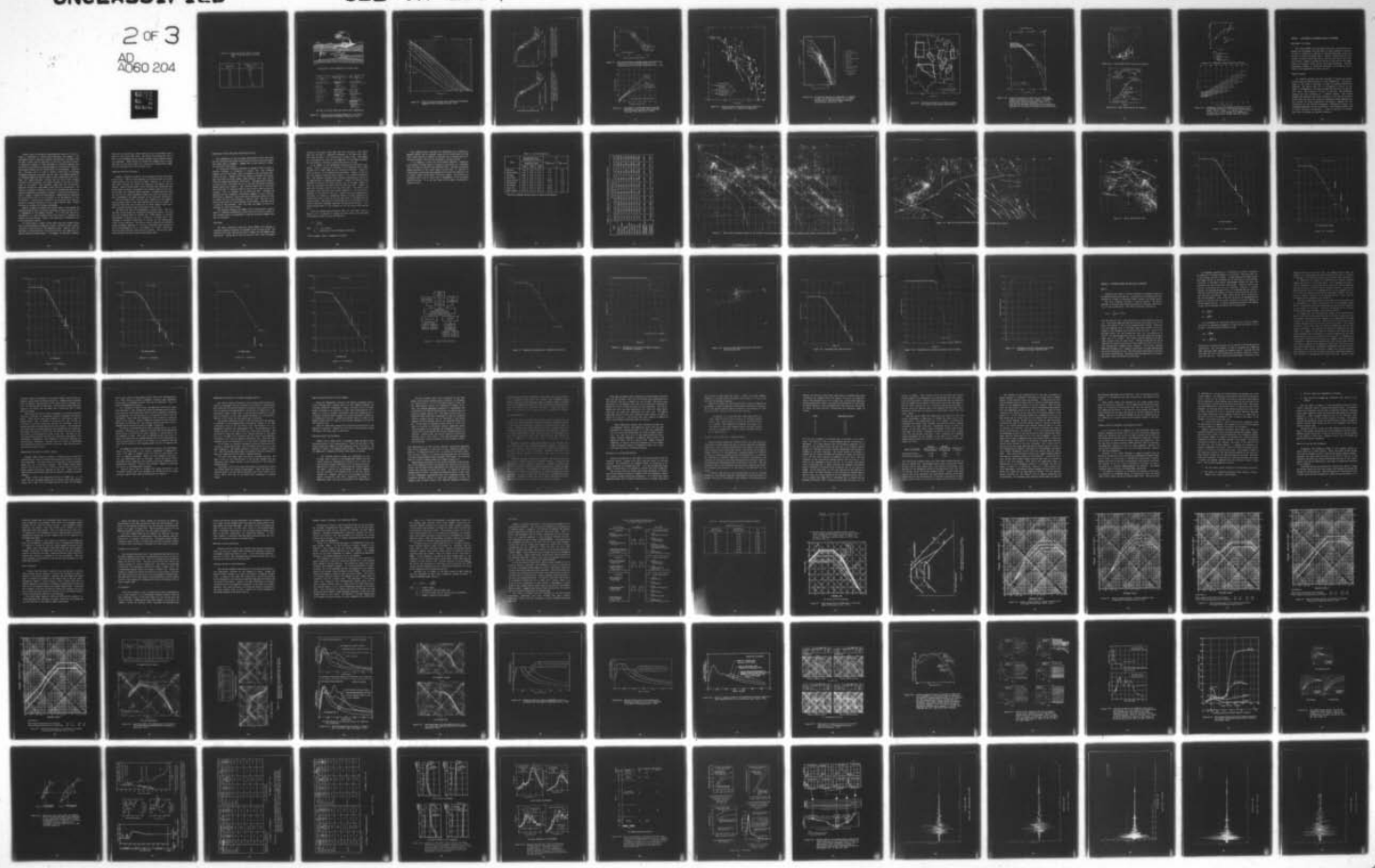

Table 6-8. Magnitude Versus Length of Slipped Faults (from Ferritto and Forrest, 1977)

Magnitude	Length of Slip (miles)
8.8	1,000
8.5	530
8.0	190
7.0	25
6.0	5
5.0	2.1
4.0	0.83

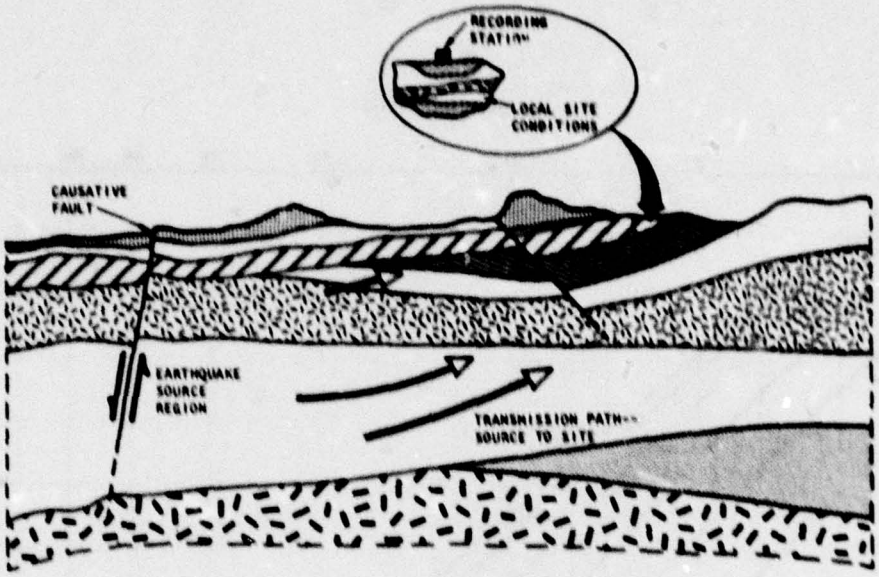

(a) Generation and transmission of seismic waves.

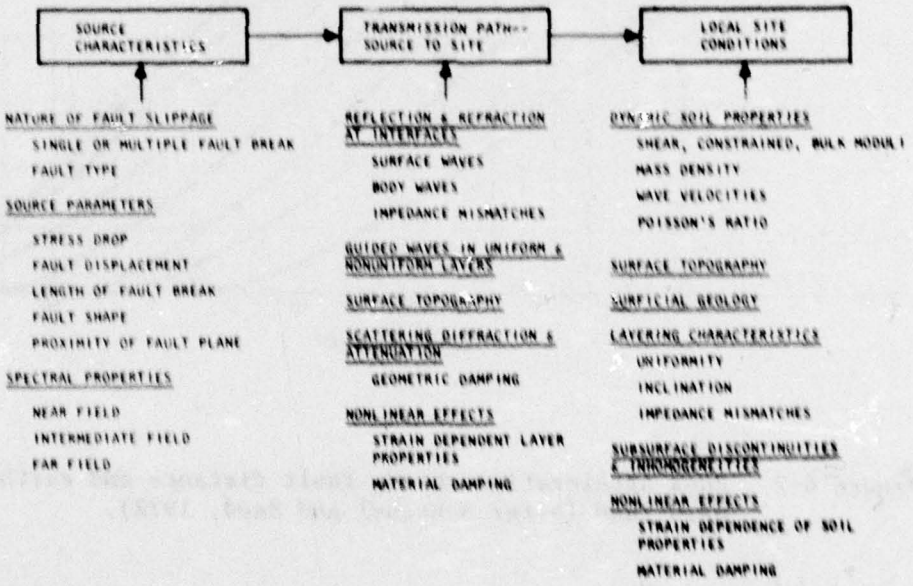

(b) List of factors affecting seismic wave transmission.

Figure 6-1. Factors affecting ground shaking at a site (from Shannon-Wilson and Agbabian Associates, 1975).

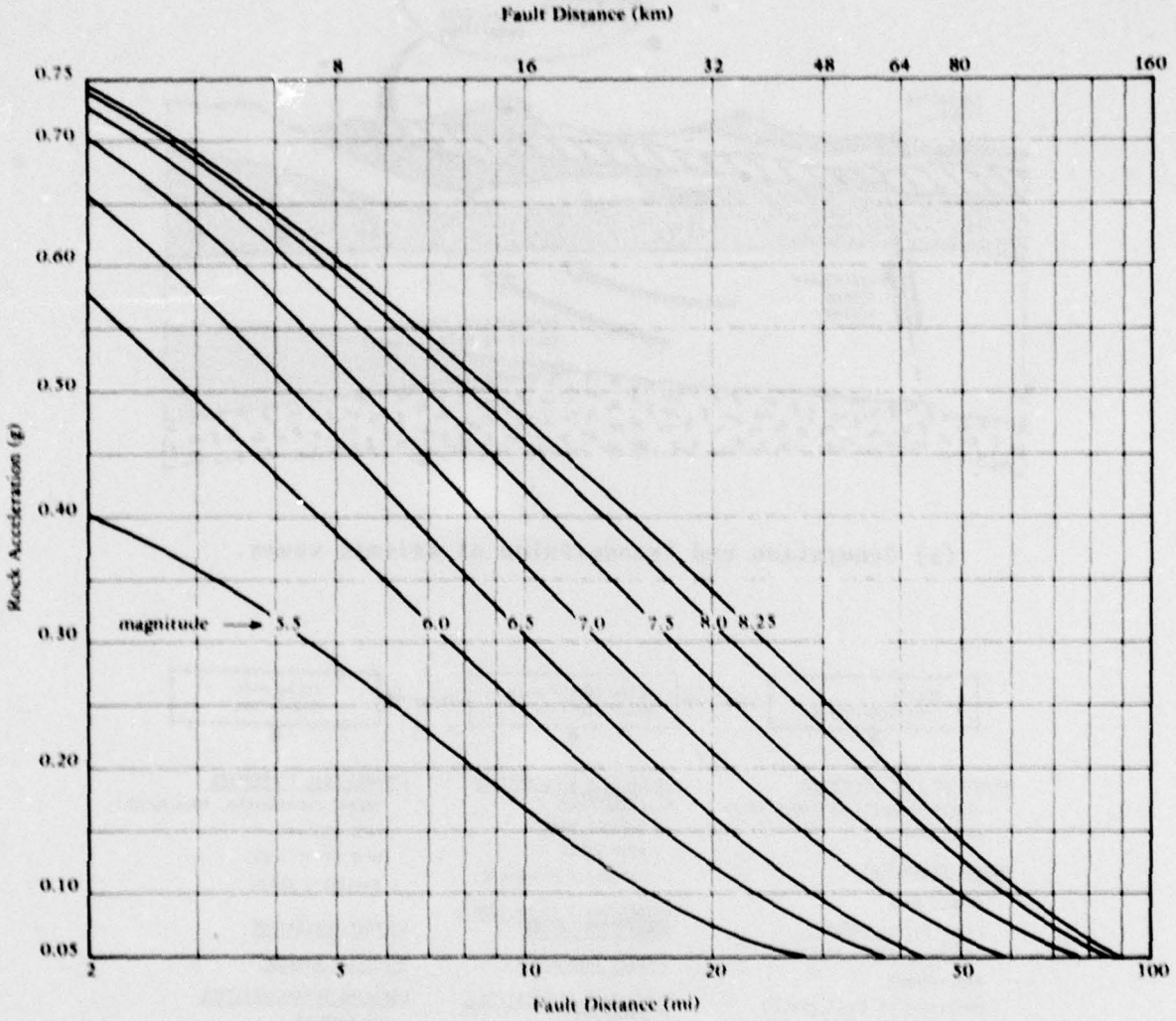

Figure 6-2. Rock acceleration versus fault distance and earthquake magnitude (after Schnabel and Seed, 1972).

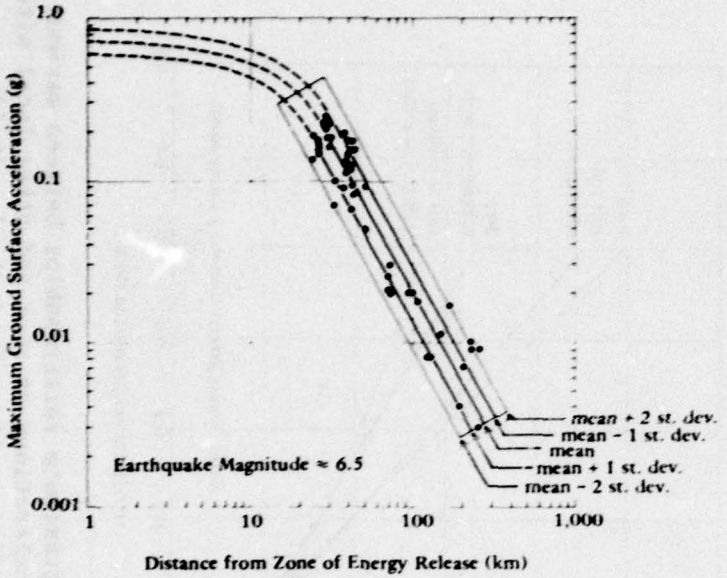

Figure 6-3. Relationship between maximum ground acceleration and distance from zone of energy release for rock sites (from Seed et al., 1975).

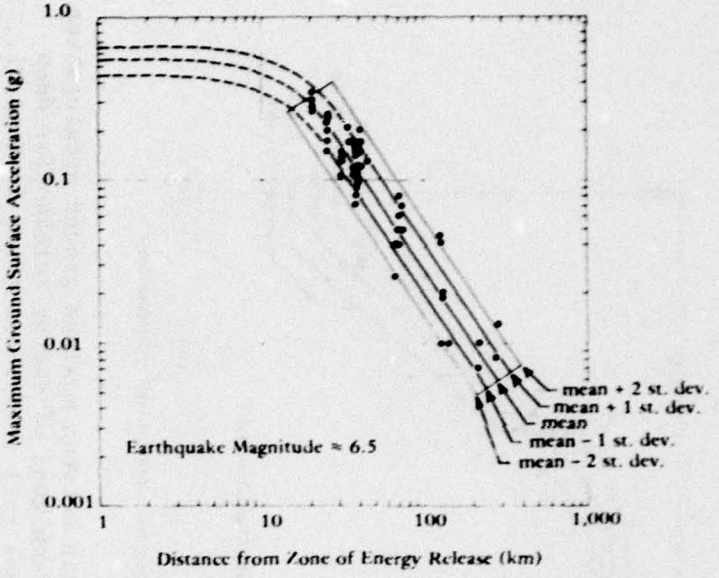

Figure 6-4. Relationship between maximum ground acceleration and distance from zone of energy release for stiff soil conditions (from Seed et al., 1975).

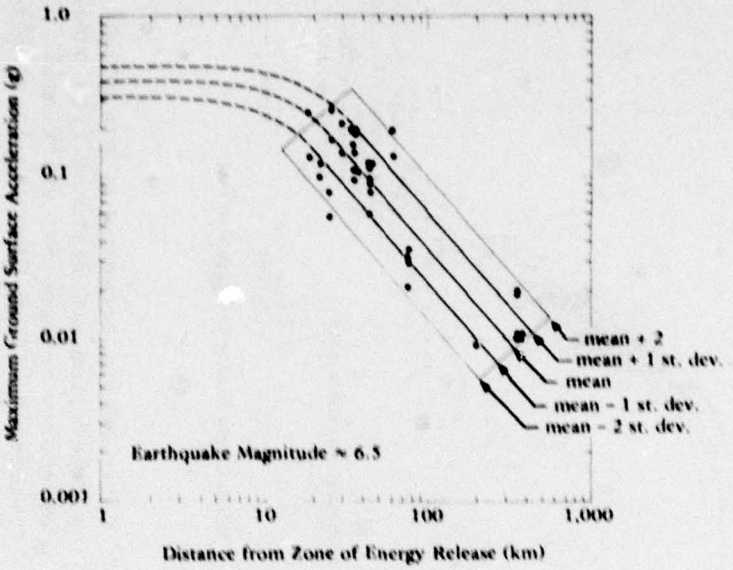

Figure 6-5. Relationship between maximum ground acceleration and distance from zone of energy release for deep cohesionless soil conditions (from Seed et al., 1975).

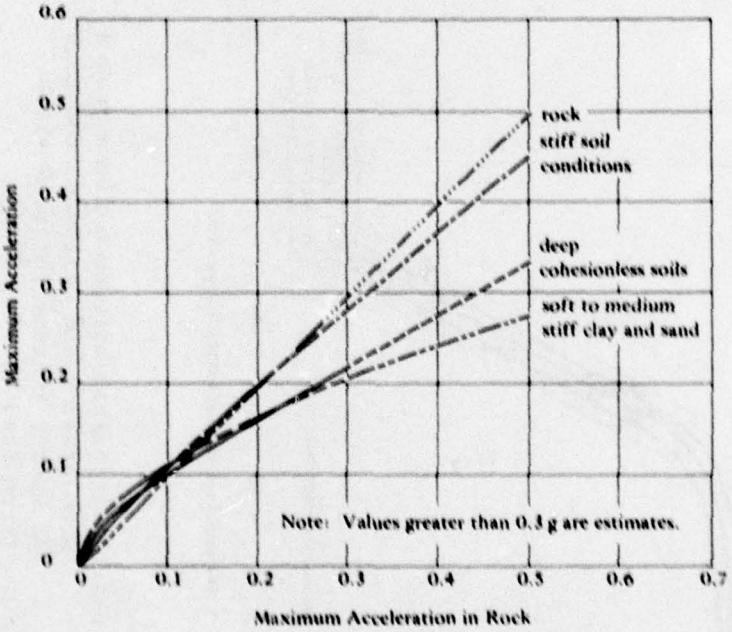

Figure 6-6. Approximate relationships between maximum accelerations on rock and other local site conditions (from Seed et al., 1975).

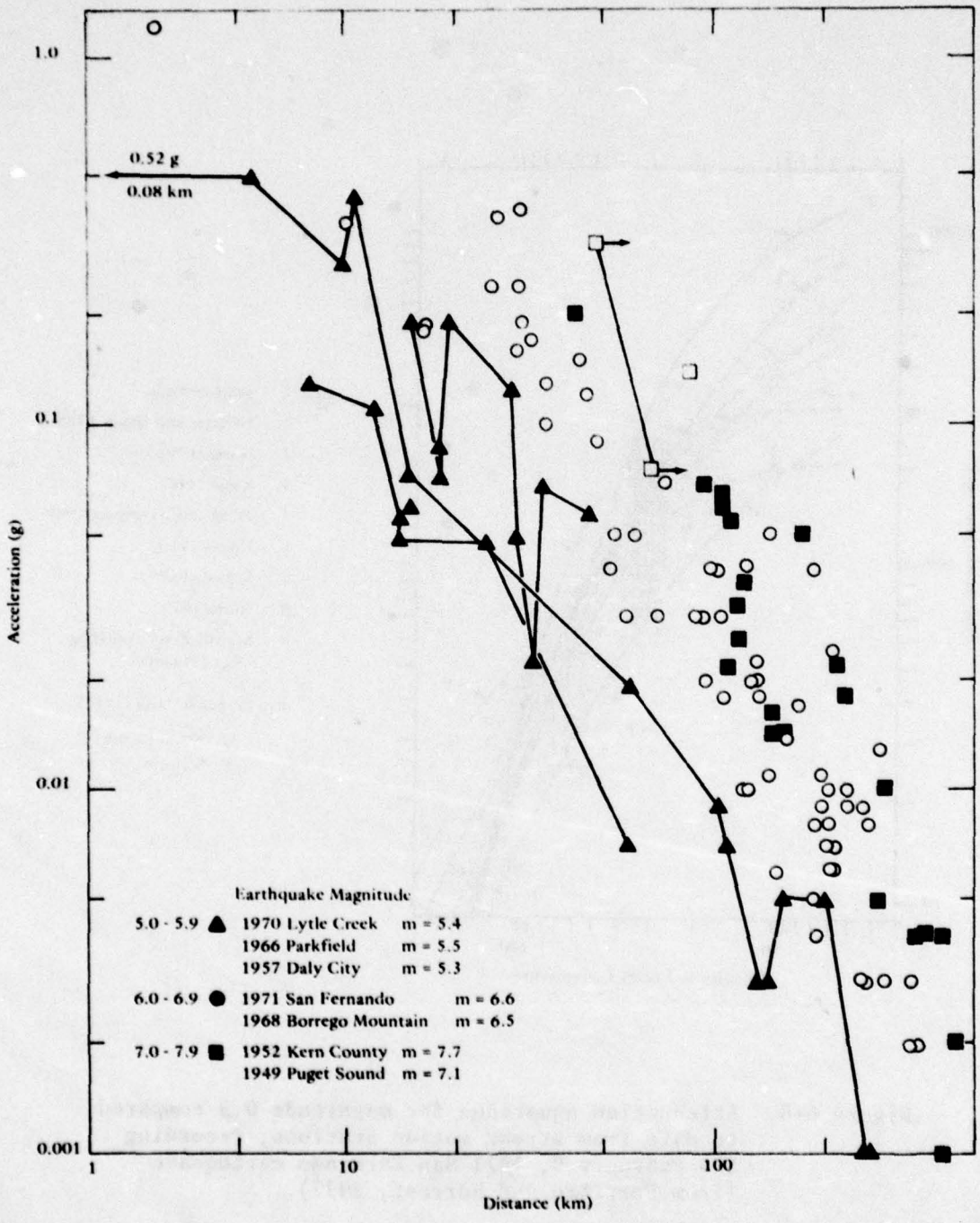

Figure 6-7. Peak horizontal acceleration versus distance to slipped fault as a function of magnitude.

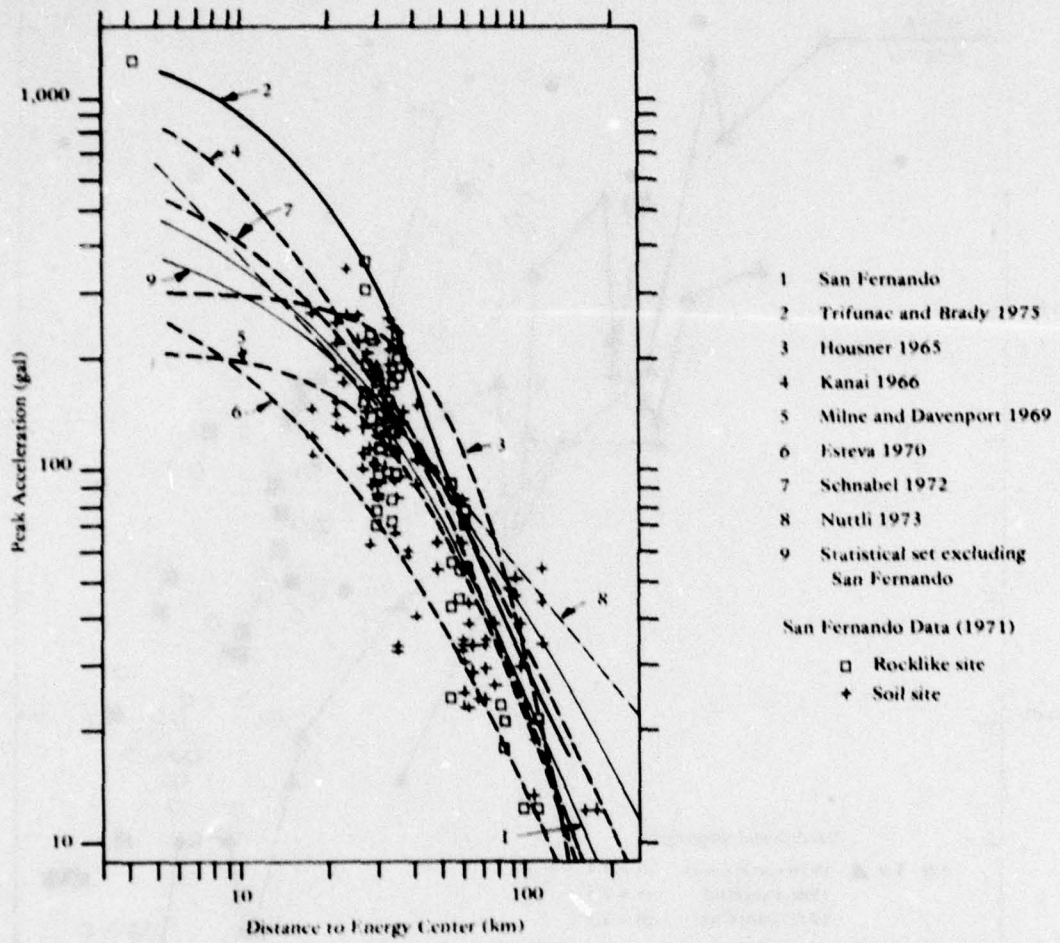

Figure 6-8. Attenuation equations for magnitude 0.5 compared to data from strong motion stations, recording the February 9, 1971 San Fernando earthquake (from Ferritto and Forrest, 1977).

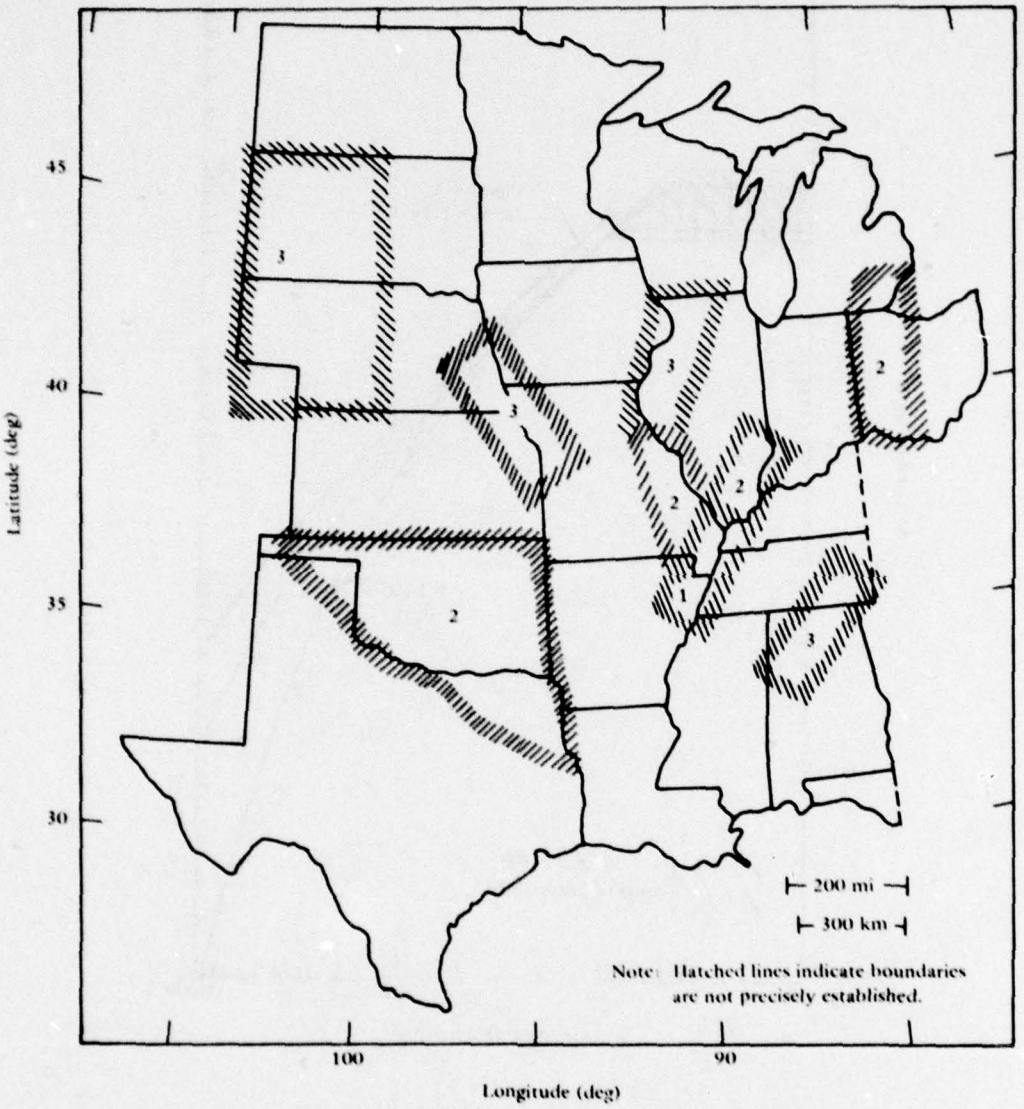

Figure 6-9. Approximate boundaries of seismic regions 1, 2, and 3 in the central United States.

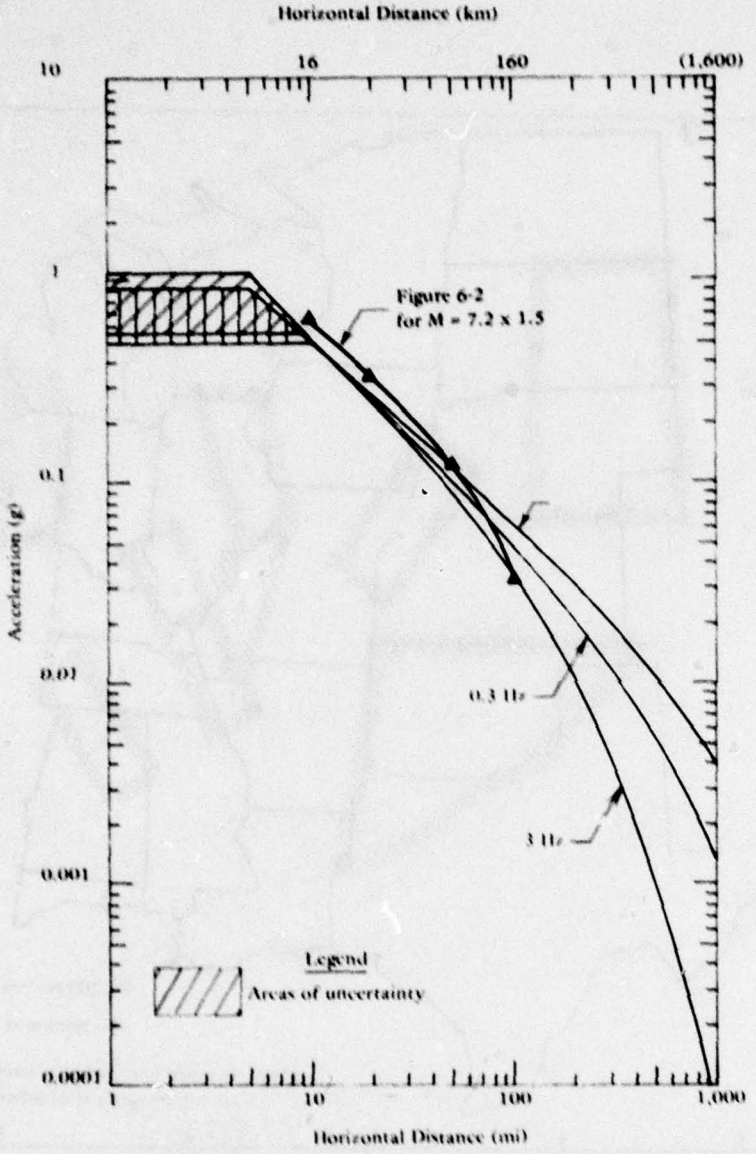

Figure 6-10. Ground accelerations on hard rock for the maximum credible earthquake of seismic region 1 (New Madrid faulted zone) (from Ferritto and Forrest, 1977). Accelerations for wave frequencies of 0.3, 1, and 3 Hz are the resultants of the vertical and horizontal components of the sustained maximum surface-wave motion.

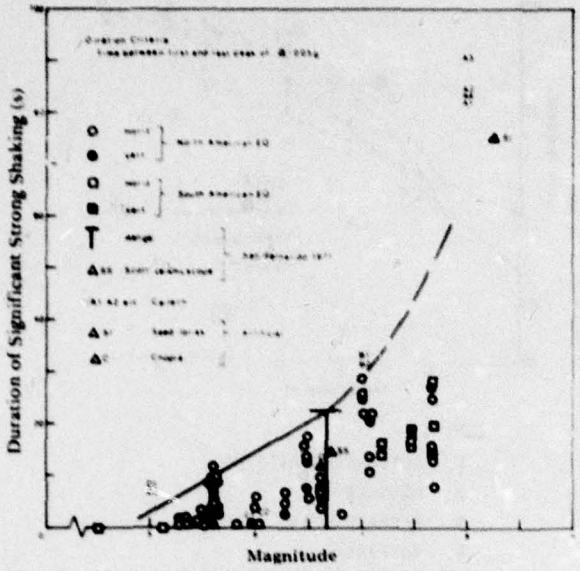

Figure 6-11. Lee and Chan (1972) results for duration.

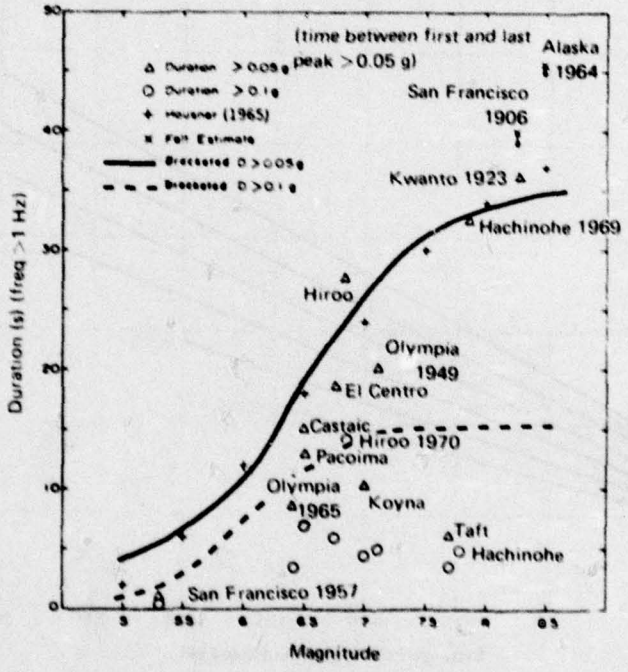

Figure 6-12. Bolt (1974) results for duration.

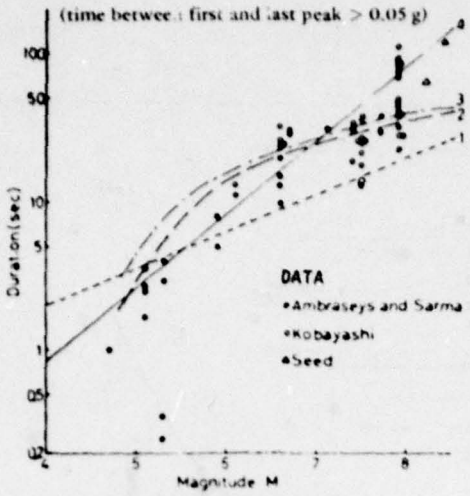

CURVES

1. GUTTENBERG-RICHTER
2. HOUSNER
3. AMBRASEYS AND SARMA
4. KOBAYASHI
   (JAPANESE EARTHQUAKES)

Figure 6-13. Kobayashi (1974) results for duration.

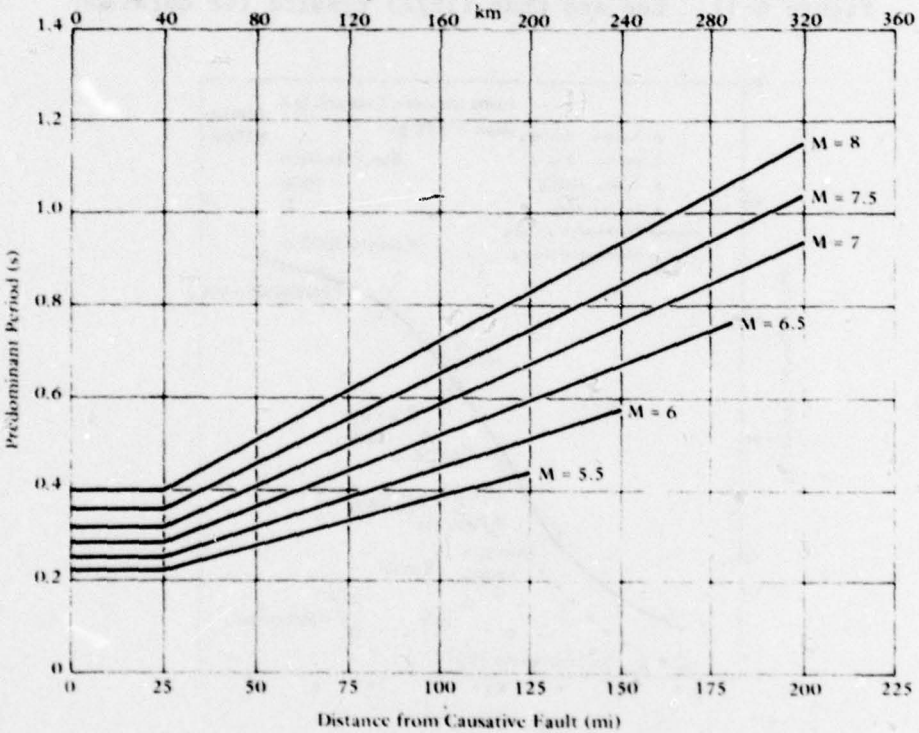

Figure 6-14. Predominant periods for maximum accelerations in rock (from "Characteristics of rock motions during earthquakes," by H. B. Seed, I. M. Idriss, and F. W. Kiefer, in Journal of the Soil Mechanics and Foundations Division, ASCE, vol 95, no SM5, Sep 1969, Figure 7).

CHAPTER 7 – DEVELOPMENT OF RECURRENCE ANALYSIS PROCEDURE

Requirements for Design

The current NAVFAC design procedure prescribes the selection of a design level earthquake with 10% chance of being exceeded in 25 years. As such, a probabilistic approach is specified which must relate site activity to structural design levels. Chapter 4 demonstrated the limitations of historic data when used as the sole data source for recurrence trends. Chapter 3 pointed out the use of slip rates in the computation of recurrence trends and the associated limitations. The best engineering estimate of earthquake recurrence can be made by use of historic data supplemented by fault slip data.

Computer Analysis

An automated procedure has been developed to perform the seismic analysis using the NOAA data base as input (Appendix A). The specific region of the study is specified in terms of bounding latitude and longitude. The general data file of earthquakes is sorted, and the subset of earthquakes in the region becomes the data base for the specific study. The location of the site is specified. The methodology proposed has been automated as a computer program. The program (Appendix B) determines the distance between the site and each epicenter in the study data base and, using the earthquake average magnitude and the Trifunac and Brady attenuation relationship, computes the site acceleration for all historic earthquakes; a histogram is created. The earthquake magnitudes are then plotted and a least-squares analysis used to obtain recurrence coefficients. A map of epicenters is plotted. These help in defining the regional seismicity.

Further study can be made by specifying the location of a fault in terms of coordinates of several points defining line segments. All earthquakes within a specified distance from the fault line under study are made a subset and the recurrence of the fault calculated as above. A probability analysis is then performed to calculate expected site acceleration and causative earthquake magnitude and epicentral distance. The program randomly selects the epicenter of an earthquake. Using the fault recurrence data in terms of Richter coefficients and maximum earthquake magnitude associated with the fault, the program determines an earthquake magnitude and the length of fault break which would occur. Using the random epicenter location and the fault break (assumed centered on the epicenter), the closest distance of the site to fault break is calculated. This distance, along with the acceleration-magnitude attenuation relationship, gives the site acceleration. The process is repeated to produce a list of site accelerations and related causative magnitude and epicentral distance. A Poisson distribution is used to compute a probability distribution. Random location, magnitude and acceleration level are all considered in the determination of site acceleration. Provisions are included to use recurrence data from slip analysis or regional seismicity in lieu of fault specific data. Further provision is included for floating earthquakes.

Experts disagree on whether main shocks alone or main shocks and aftershocks may be used to estimate recurrence; decision on which to use is independent of the computer analysis. It is felt that the use of aftershocks is a valid procedure since these events do represent the release of strain energy. Further, the inclusion of aftershocks will yield conservative results.

As stated above a single recent large event may release strain built up over hundreds or thousands of years. As such it might indicate a period of less activity in the immediate future. However, since the data base is relatively short, the return for this event might be erroneously indicated as much greater. For example, if this were a 500-year

event and occurred during a 50-year data base its return might be estimated at 0.02 rather than 0.002. The plotted data points and line of best fit are determined by the computer analysis using regression analysis techniques. These should be reviewed and judgment used to adjust this type of data point which will clearly plot significantly higher than the linear portion of the recurrence data.

Comparison With Fault Slip Data

Chapter 3 presents procedures for estimating recurrence data based on fault slip. Table 3-1 gives estimates of recurrence data for several faults based on slip rate and fault length. Figures 7-1, 7-2, and 7-3 show maps locating the faults and epicenters associated with the regions. Figure 7-4 gives plots of the recurrence data showing the data points based on historic earthquakes and estimates based on slip rate. For the most part agreement seems reasonable. Although this may not be the case for all faults, agreement between slip data and historic data gives confirmation and added assurance of the recurrence coefficients.

The San Andreas fault slip data were adjusted for the length of fault actually covered in the region where historic data were taken. It should be noted that the activity over its great length is quite variable, covering the whole range from locked to very active.

The White Wolf fault is predominantly a reverse fault. The fault was most active during the Pleistocene and Holocene period. The slip rate was estimated based on 10,000 feet (3,000 meters) of vertical displacement of Miocene rock over a period of 7 million years. This averaging is probably insufficient to account for more geologically recent activity exhibited. The historic data is biased by the 1952 Kern County earthquake magnitude 7.7 and its aftershocks which resulted in vertical displacement of up to 1.2 m (Lamar et al., 1973). The Garlock fault has had relatively little historic activity. The slip rate indicates recurrence intervals greater than historic data.

Combination of Fault Slip Data With Historical Data

The combination of the recurrence data based on fault slip rates and the recurrence data based on the historical data is an area involving a great deal of judgment. Judgment may be used directly to adjust the recurrence coefficients.

An alternative technique developed by Campbell (1977) utilizes a Bayesian technique for estimation of seismic risk. This technique combines the two data bases, which are founded on the uncertainty associated with each. Campbell (1977) has derived a procedure for estimating slip based on seismic moment, shear modulus, fault area, and the historical magnitude-frequency coefficients. Although based on empirical data in part, this model has not as yet been extensively validated against known fault behavior. The calculated mean rate of occurrence and coefficient of variation based on fault slip is used as the prior estimate. This is "updated" by the historical data. Although the approach has been automated, considerable judgment is still required. Great care is required to avoid arbitrarily biasing the results in favor of either the slip rate estimates or historic data. The size of the historic data base can totally dominate the procedure. Only main shocks are used in this procedure. This will limit the number of events considerably for less active faults.

The procedure developed by Campbell (1977) does provide a rigorous means of combining seismotectonic data with local historic seismicity. The procedure may be an improvement if applied with good judgment where data are available.

Case Study

The Naval Construction Battalion Center (NCBC), Port Hueneme is located in southern California at longitude 11.2W, latitude 34.15N. The time period for the study was 25 years to comply with the NAVFAC design instruction. During the 60 years of historic data, 3,394 earthquakes

occurred in the region around NCBC; most were very minor. The largest event was the 1952 7.7 magnitude earthquake in the White Wolf fault. This event produced a site acceleration of about 0.04g. The highest site acceleration was from the 1973 magnitude 5.6 Point Mugu earthquake and is estimated to have had a ground acceleration of 0.15g.

As an example of the methodology developed the following is presented. Figure 7-3 shows the California coast (longitude 118 to 120N, latitude 33.5 to 35N), NCBC, and all epicenters and faults. Figure 7-5 gives an outline of the computational procedures. Figures 7-4 and 7-6 give the regional recurrence data; Figure 7-7 the regional probability data. The regional recurrence data although interesting are limited in its applicability to engineering analysis. Further, the data are very dependent on the area (or radius from the site) of coverage. Figure 7-8 shows the epicenters associated with the Big Pine fault. Figure 7-9 gives the recurrence data for the Big Pine fault. Also shown is the recurrence data from fault slip studies (Chapter 3). As can be seen, agreement is very good in this case. Figure 7-10 gives probability of occurrence as a function of magnitude; Figure 7-11 gives probability of acceleration from an event on the Big Pine fault at the NCBC site not being exceeded. Associated with the probability of acceleration is the related causative earthquake magnitude and epicentral distance. In a similar manner Table 7-1 was prepared for all the faults affecting the site.

With the probability-acceleration data for each fault (such as Figure 7-11) it is possible to compute the total risk P of not exceeding an acceleration level from all the faults by

$$P = \prod_{i=1}^{n} (P_i)$$

where i = 1 to n faults

P_i = probability of not exceeding acceleration

In this example, Table 7-2 summarizes the data.

This example shows a procedure for determining site acceleration. Response spectra can be produced using the site acceleration for each fault, which should be examined to determine local characteristics for structural design. This will be discussed in the next section.

It is important to note that the procedure expresses a cumulative total seismic risk and results in values of acceleration at a confidence level in excess of those for any individual fault. The more traditional design procedure in use would simply utilize Table 7-1 directly in constructing a design spectrum assuming the acceleration produced on one or several faults would govern structural design. The selection of individual fault risk or total risk is independent of the procedures specified herein. It is not the intent of this report to prescribe a design criteria.

Table 7-1. Site Acceleration

Fault	Maximum Peak Site Acceleration in 25 yr			$M_{10\%\ 25\ yr}$[a]	$M_{max\ cred}$
	Confidence Level				
	50%	84%	90%		
Big Pine	0.04	0.10	0.13	7.1	7.5
Malibu Canyon	0.05	0.09	0.10	6.3	7.5
Oakridge	0.08	0.14	0.17	5.7	7.5
Santa Ynez	0.05	0.10	0.13	6.3	7.5
Arroyo Parida	0.09	0.13	0.16	(6.8)	6.5
San Andreas	0.03	0.06	0.07	6.4	8.25
San Gabriel	0.07	0.13	0.16	(7.9)	7.7
Santa Cruz	0.07	0.16	0.28	(8.3)	7.2
Santa Susana	0.08	0.13	0.14	(7.5)	6.5

[a]Limited by maximum credible event as shown in parentheses.

Table 7-2. Probability of Not Exceeding Acceleration in 25 Years

Fault	Site Acceleration a, g									
	0.05	0.10	0.15	0.20	0.25	0.30	0.35	0.40	0.45	0.50
Big Pine	0.54	0.820	0.920	0.968	0.987	0.991	0.994	0.999	0.9999	0.9999
Malibu Canyon	0.52	0.873	0.968	0.981	0.986	0.988	0.995	0.999	0.9999	0.9999
Oak Ridge	0.40	0.630	0.850	0.954	0.982	0.986	0.988	0.991	0.994	0.996
Santa Ynez	0.50	0.840	0.918	0.970	0.990	0.993	0.997	0.9999	0.9999	0.9999
Arroyo Parida	0.40	0.600	0.867	0.951	0.970	0.987	0.992	0.994	0.998	0.9999
San Andreas	0.72	0.965	0.992	0.998	0.9999	0.9999	0.9999	0.9999	0.9999	0.9999
San Gabriel	0.40	0.667	0.878	0.942	0.981	0.989	0.997	0.9999	0.9999	0.9999
Santa Cruz	0.40	0.667	0.814	0.873	0.917	0.942	0.965	0.984	0.994	0.996
Santa Susana	0.40	0.663	0.923	0.995	0.9999	0.9999	0.9999	0.9999	0.9999	0.9999
Total Risk Probability Not Exceeding a	0.001	0.065	0.394	0.682	0.826	0.881	0.942	0.967	0.986	0.992
Probability Exceeding a	0.999	0.935	0.606	0.318	0.174	0.119	0.058	0.033	0.014	0.008

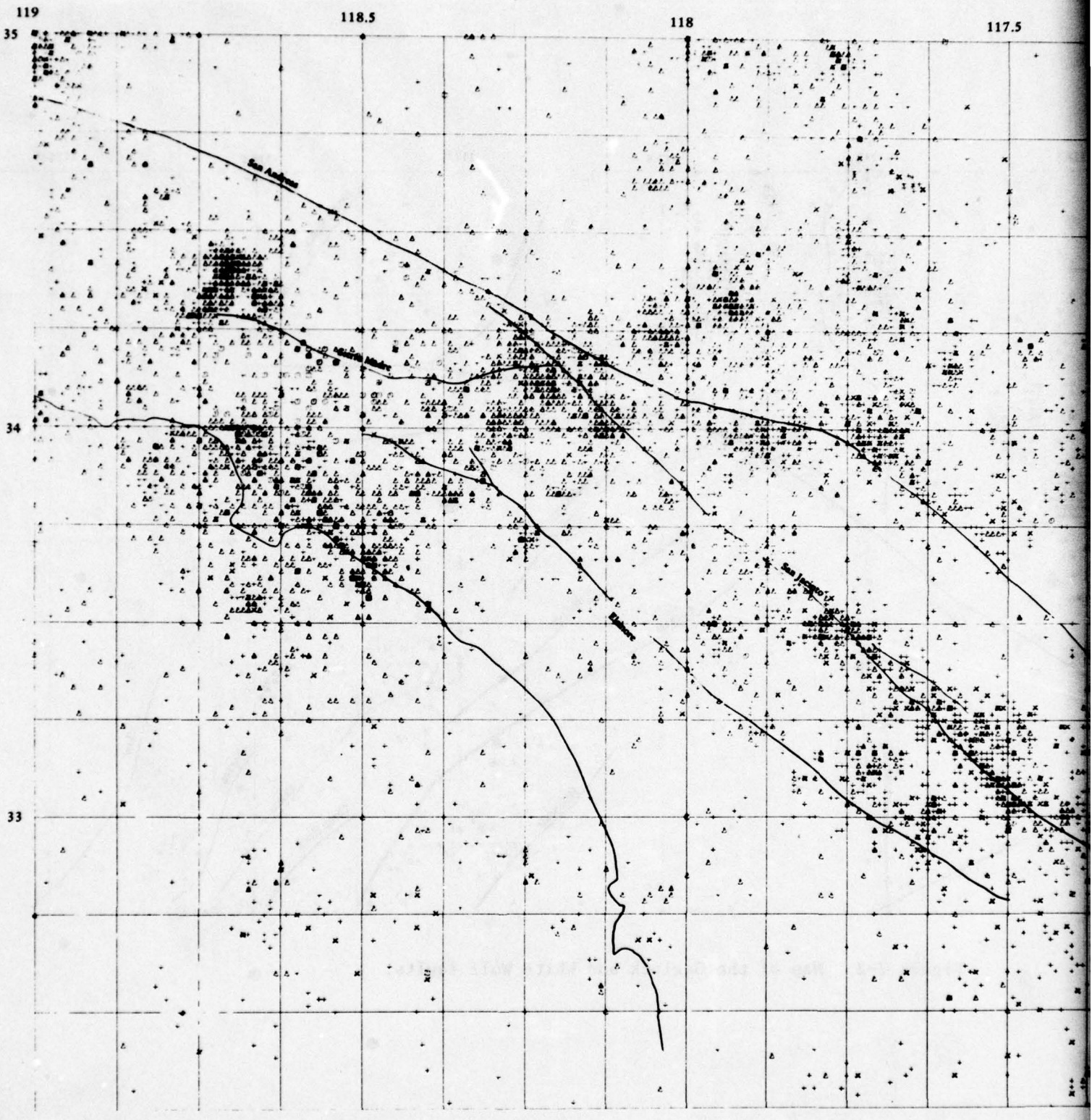

Figure 7-1. Map of the San Andreas, Elsinore, San Jacinto, and Sierra Madre faul

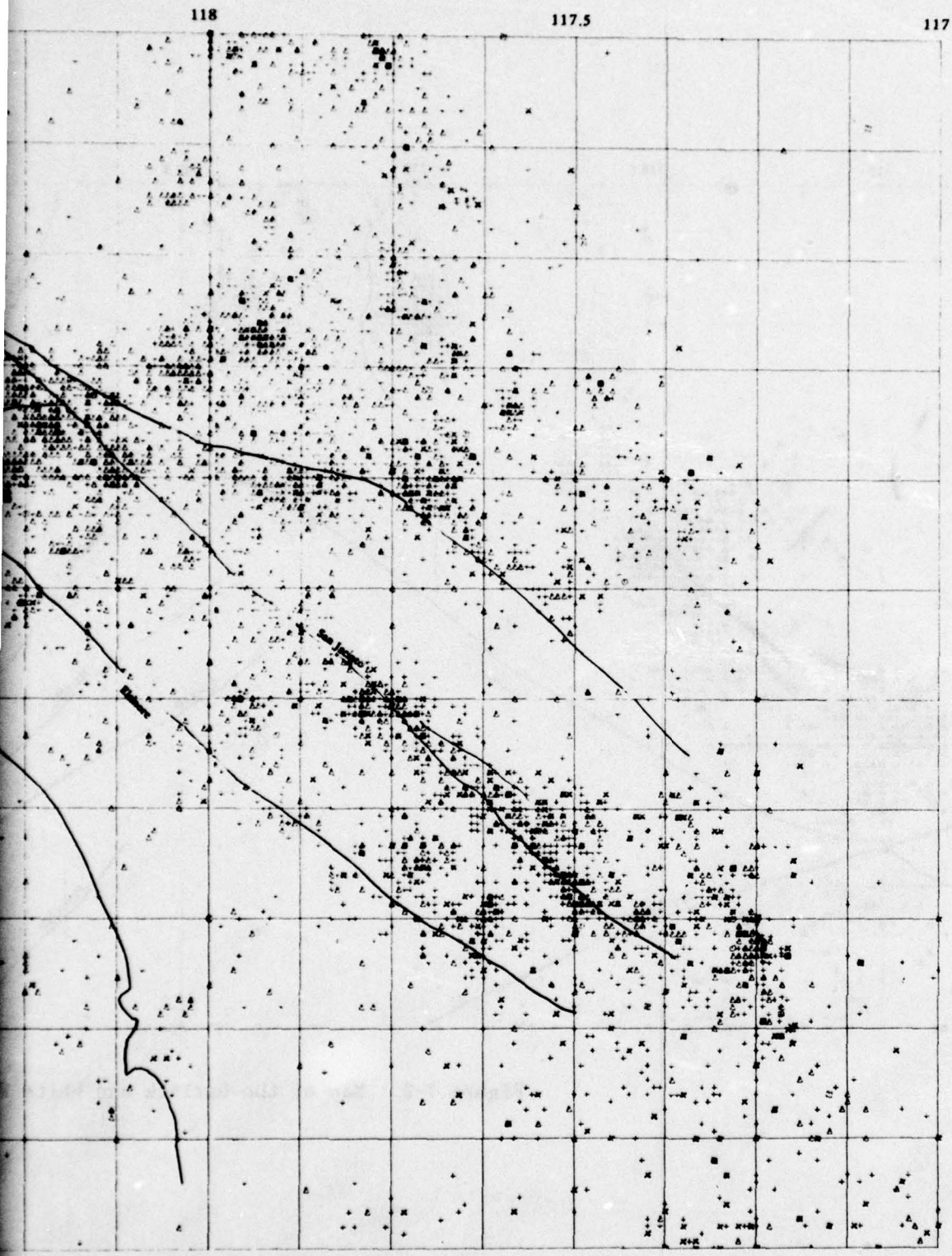

n Andreas, Elsinore, San Jacinto, and Sierra Madre faults.

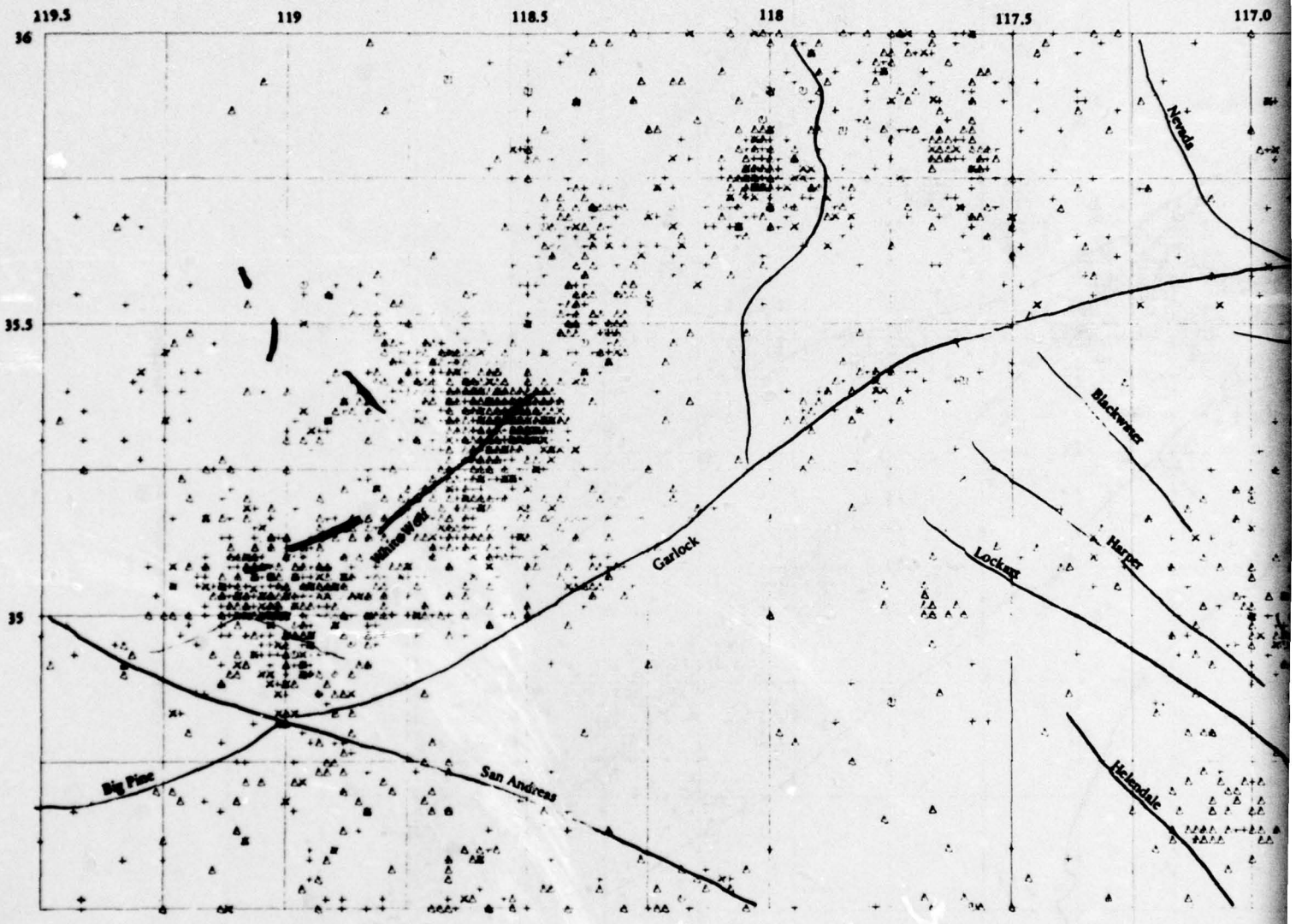

Figure 7-2. Map of the Garlock and White Wolf fau

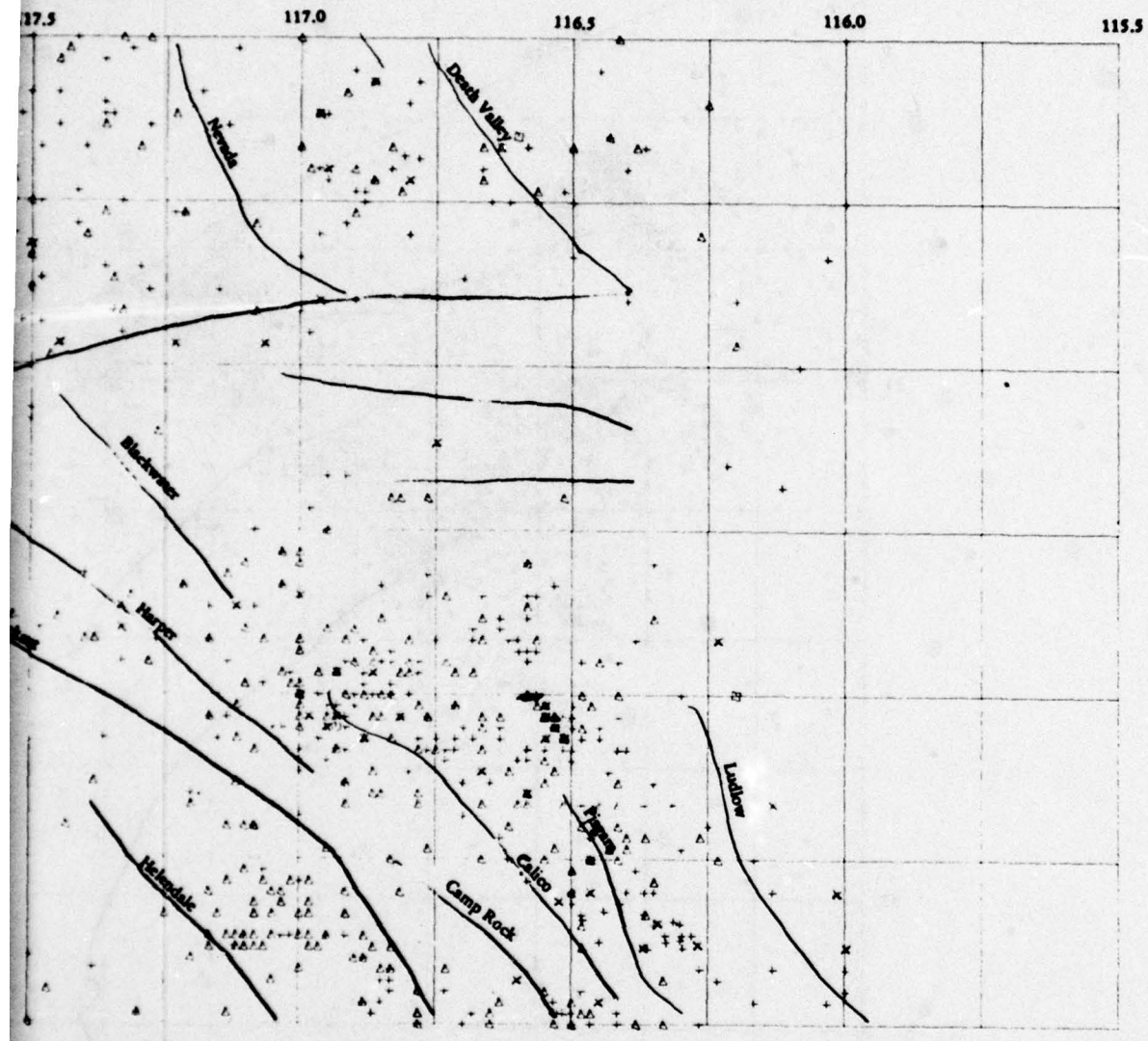

lock and White Wolf faults.

2

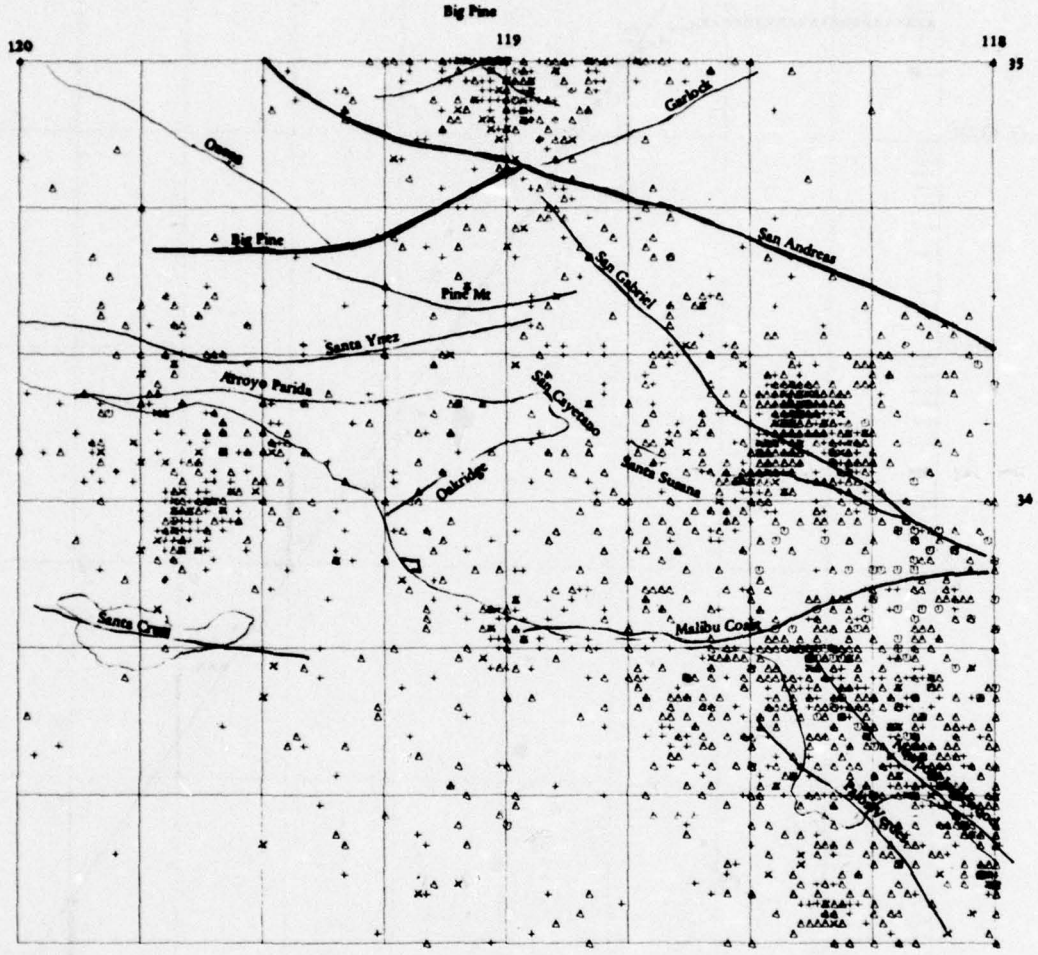

Figure 7-3. Map of the Big Pine fault.

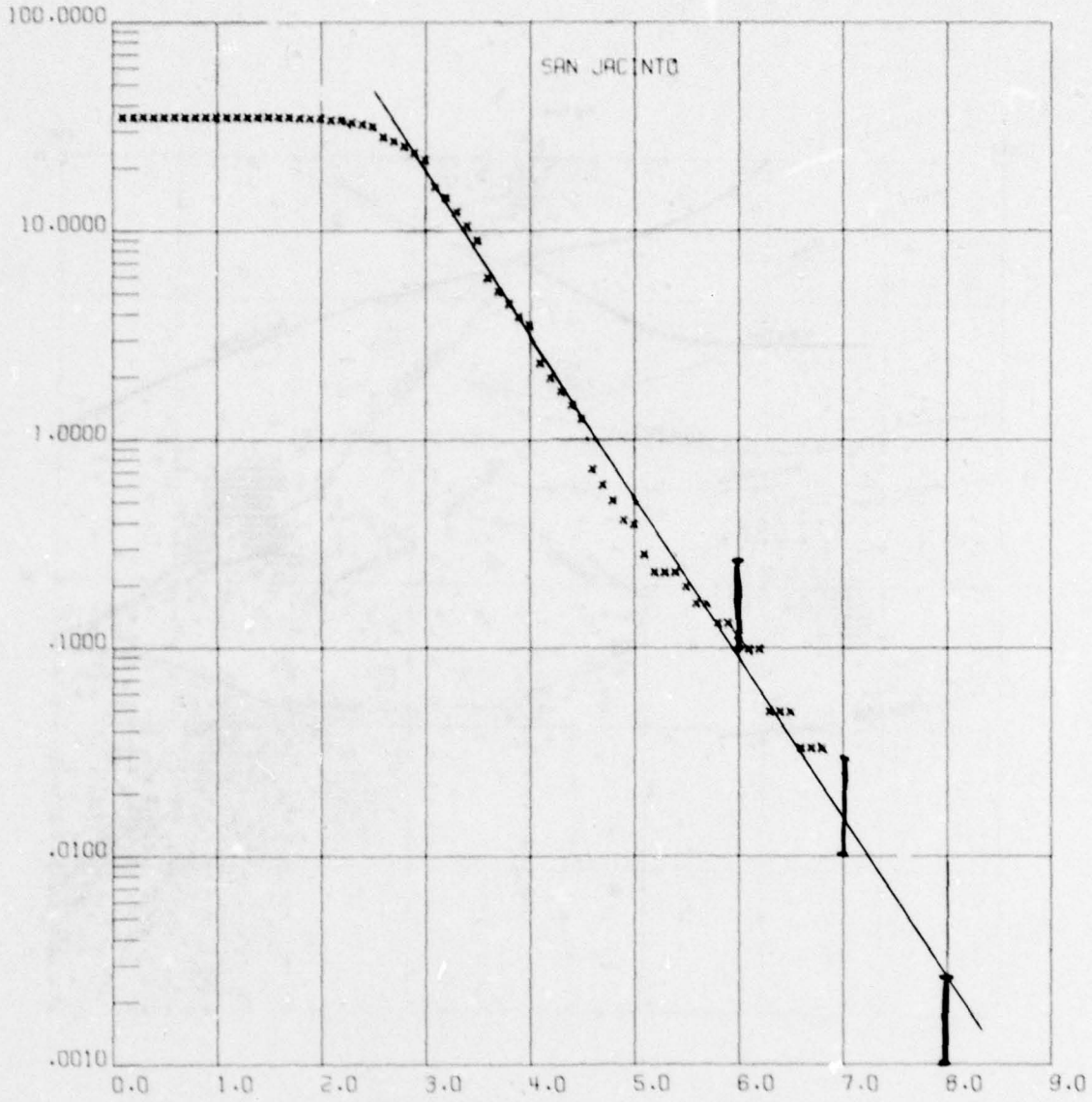

(a) San Jacinto.

Figure 7-4. Recurrence data.

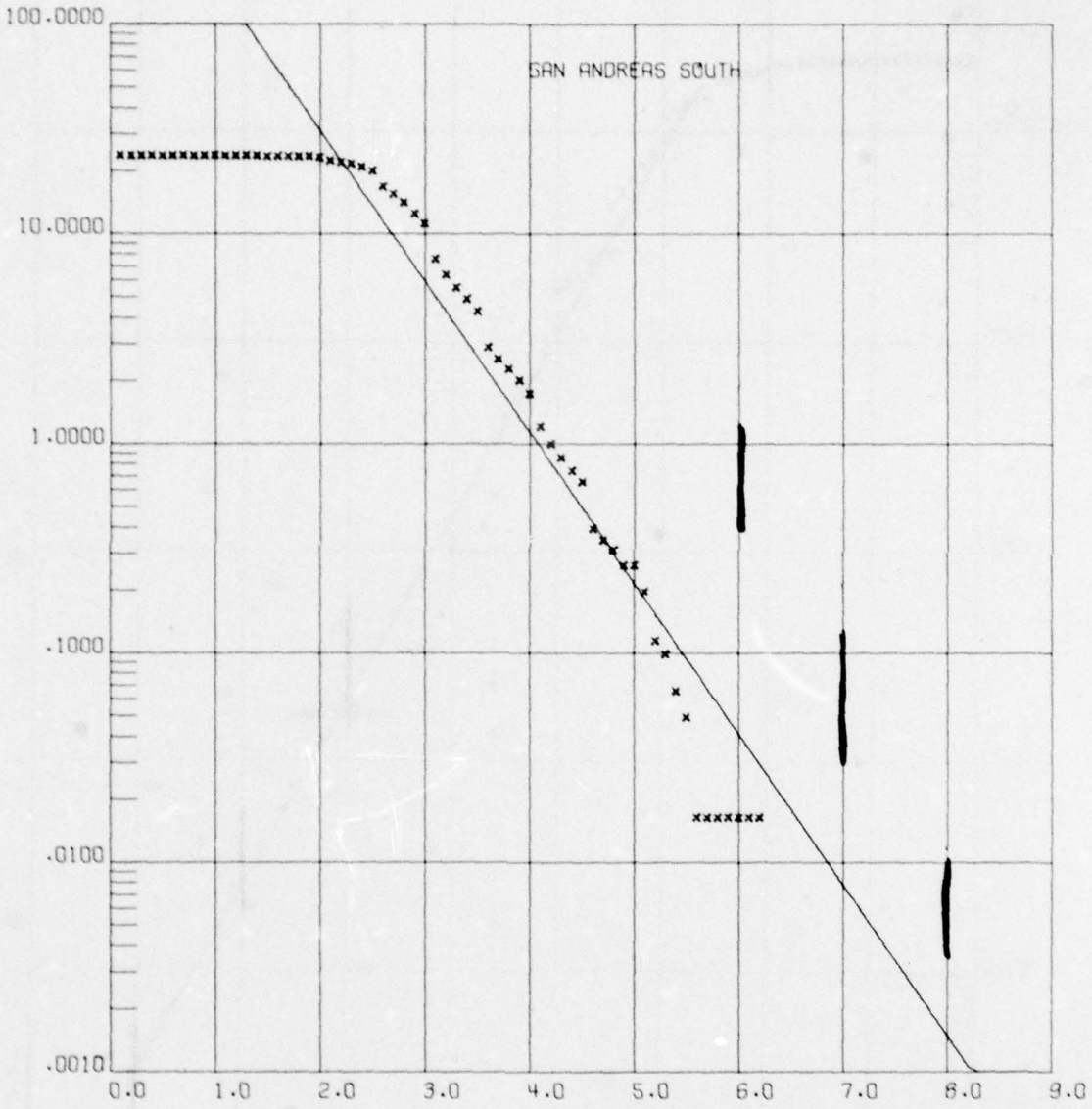

(b) San Andreas South.

Figure 7-4. Continued.

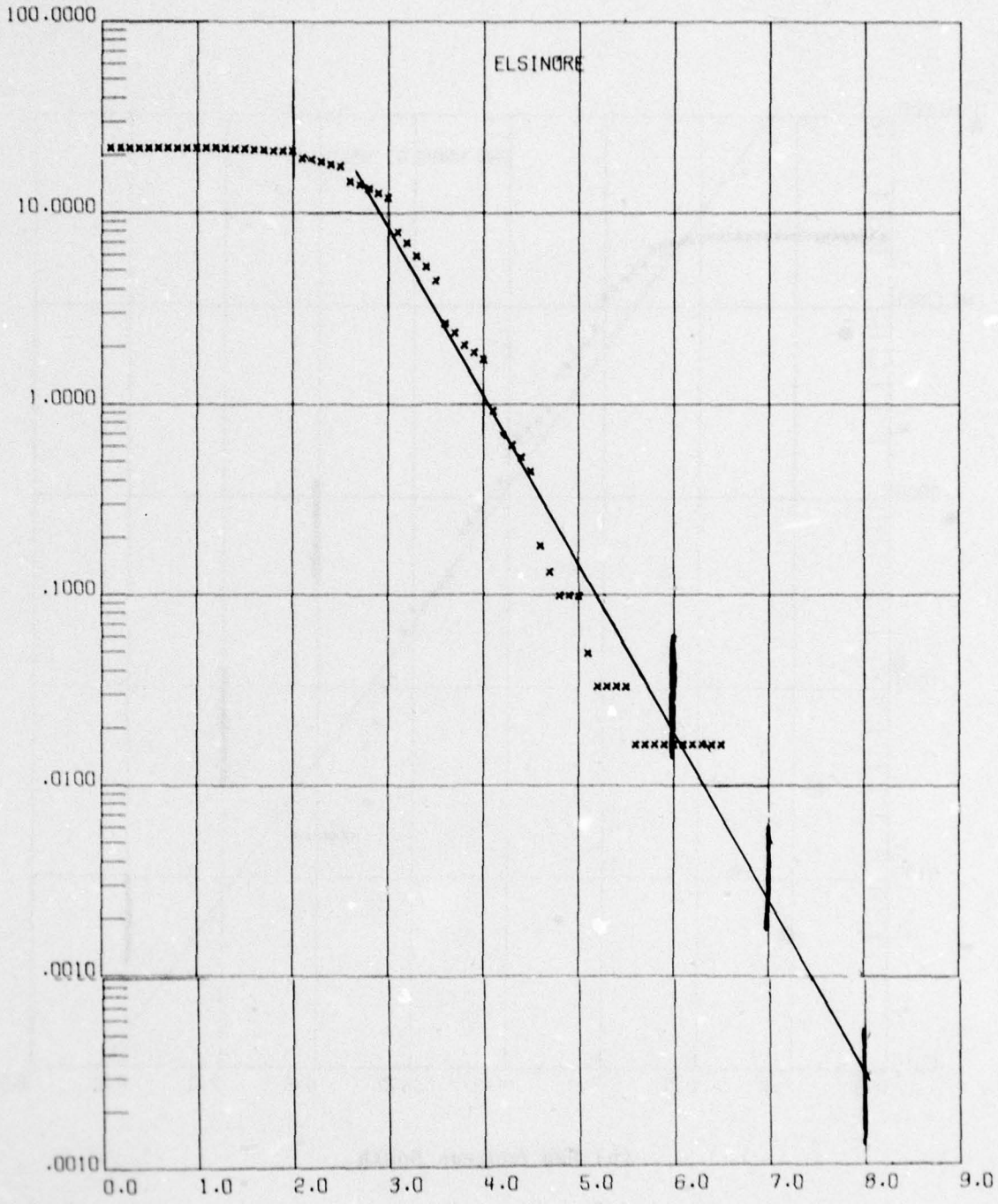

(c) Elsinore.

Figure 7-4. Continued.

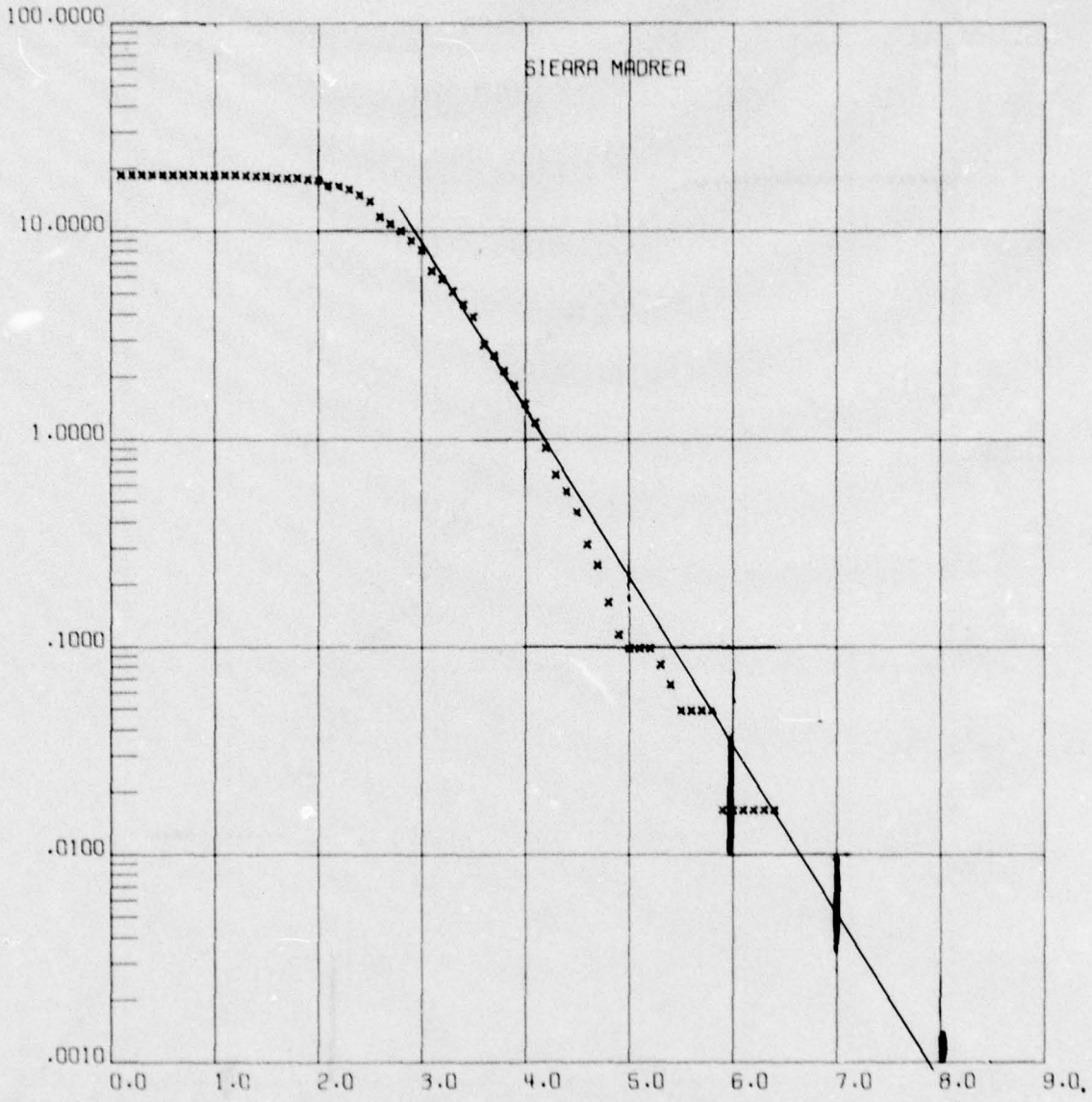

(d) Sierra Madre.

Figure 7-4. Continued.

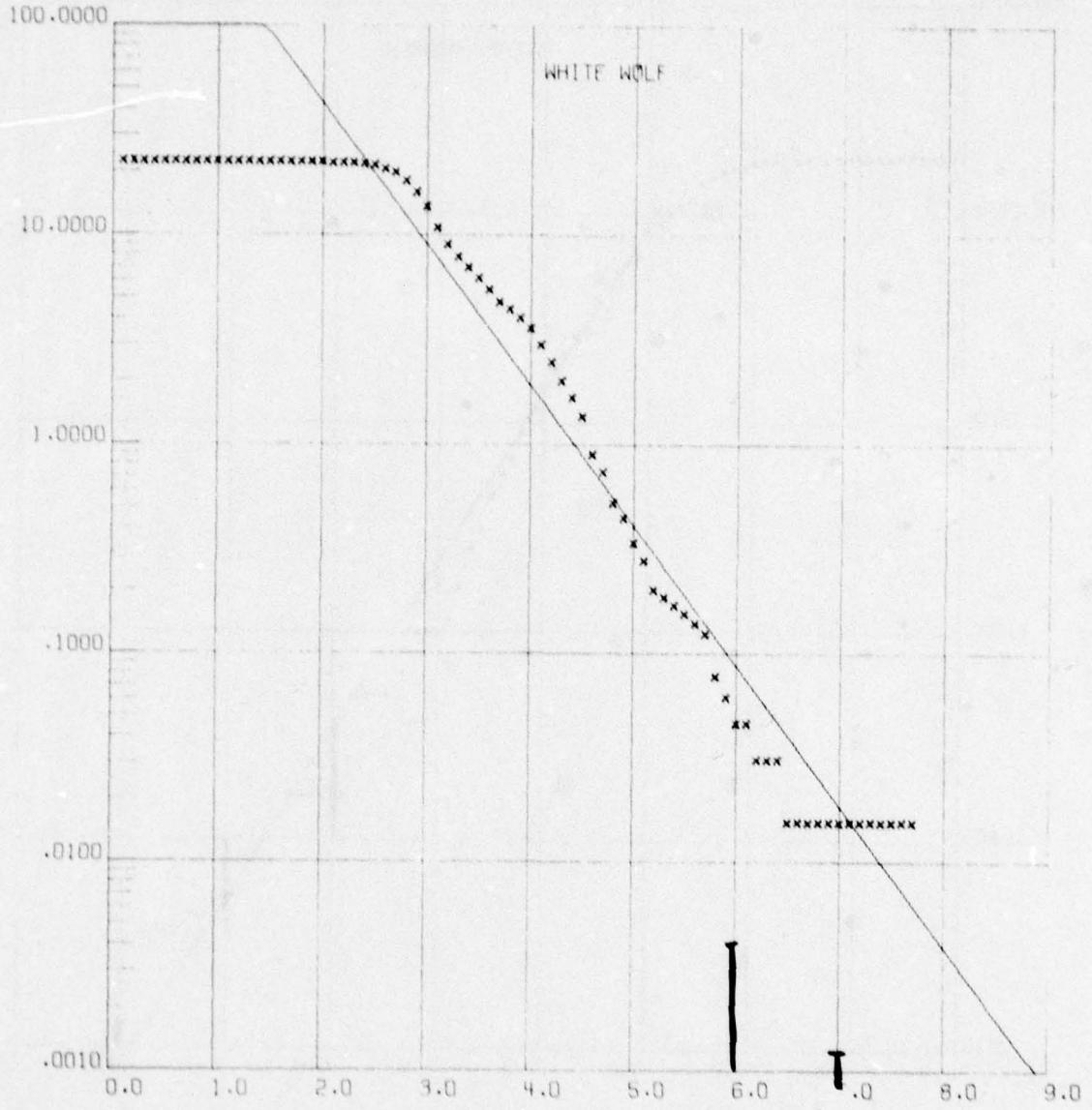

(e) White Wolf.

Figure 7-4. Continued.

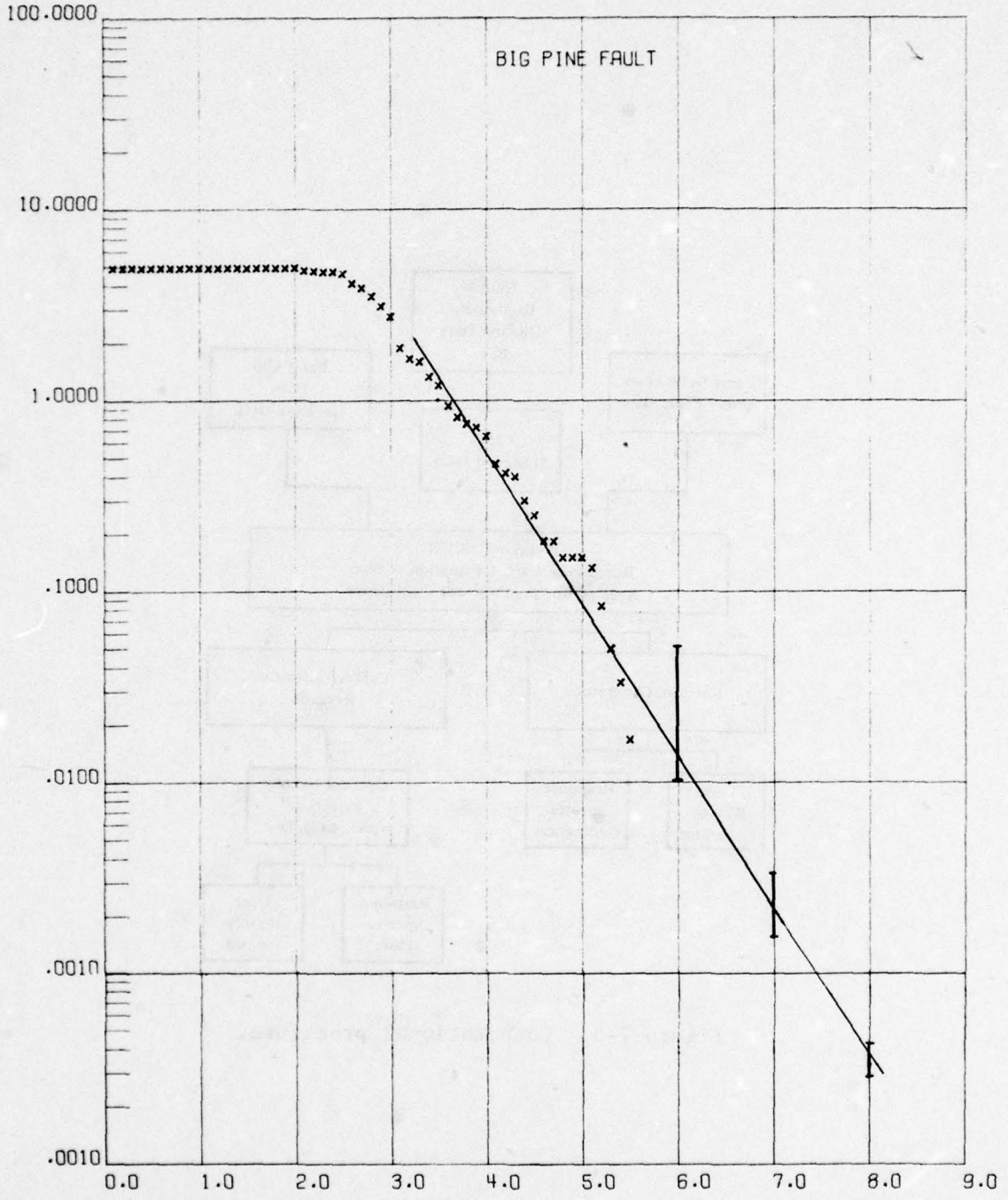

(f) Big Pine.

Figure 7-4. Continued.

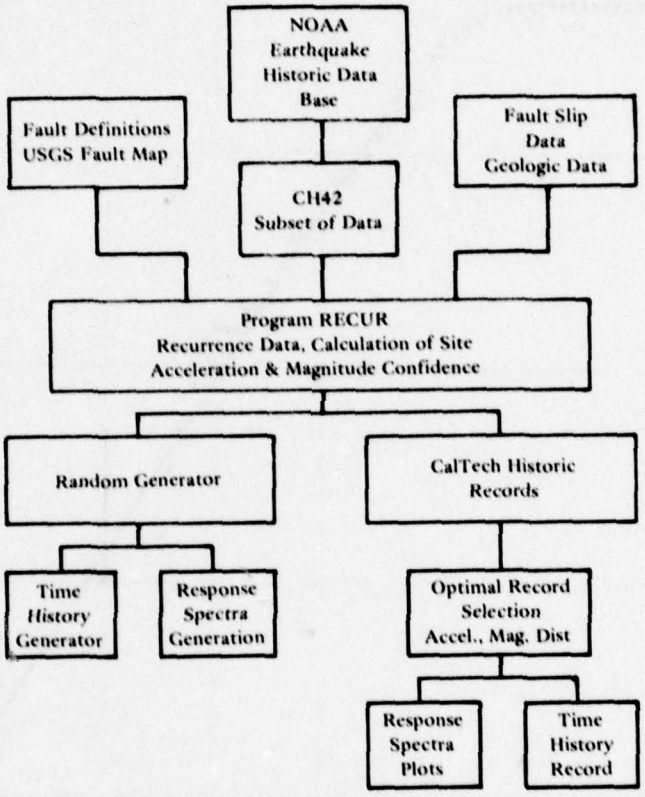

Figure 7-5. Computational procedure.

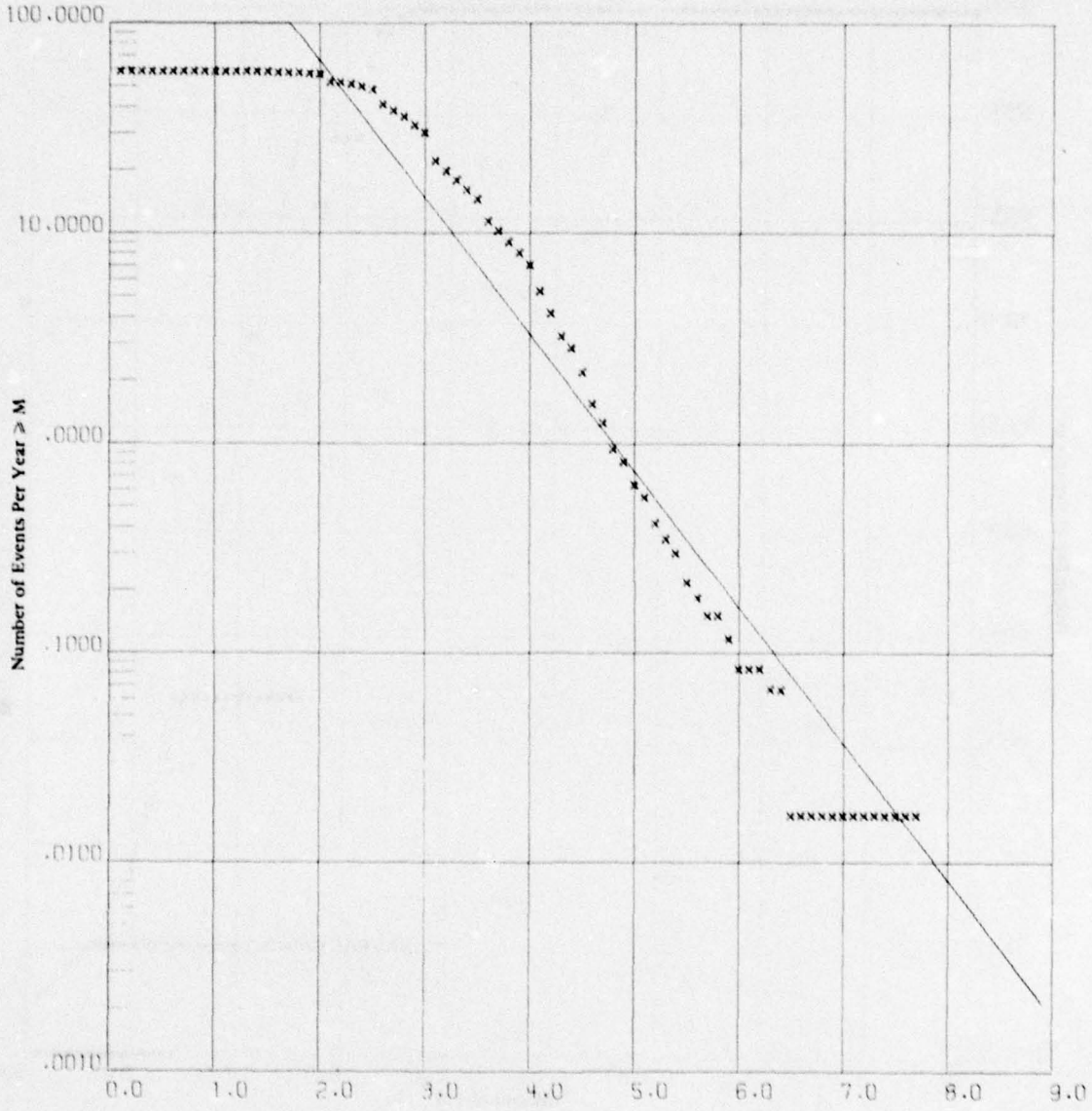

Figure 7-6. Regional recurrence data, 118-120 W, 33.5-35.0 N.

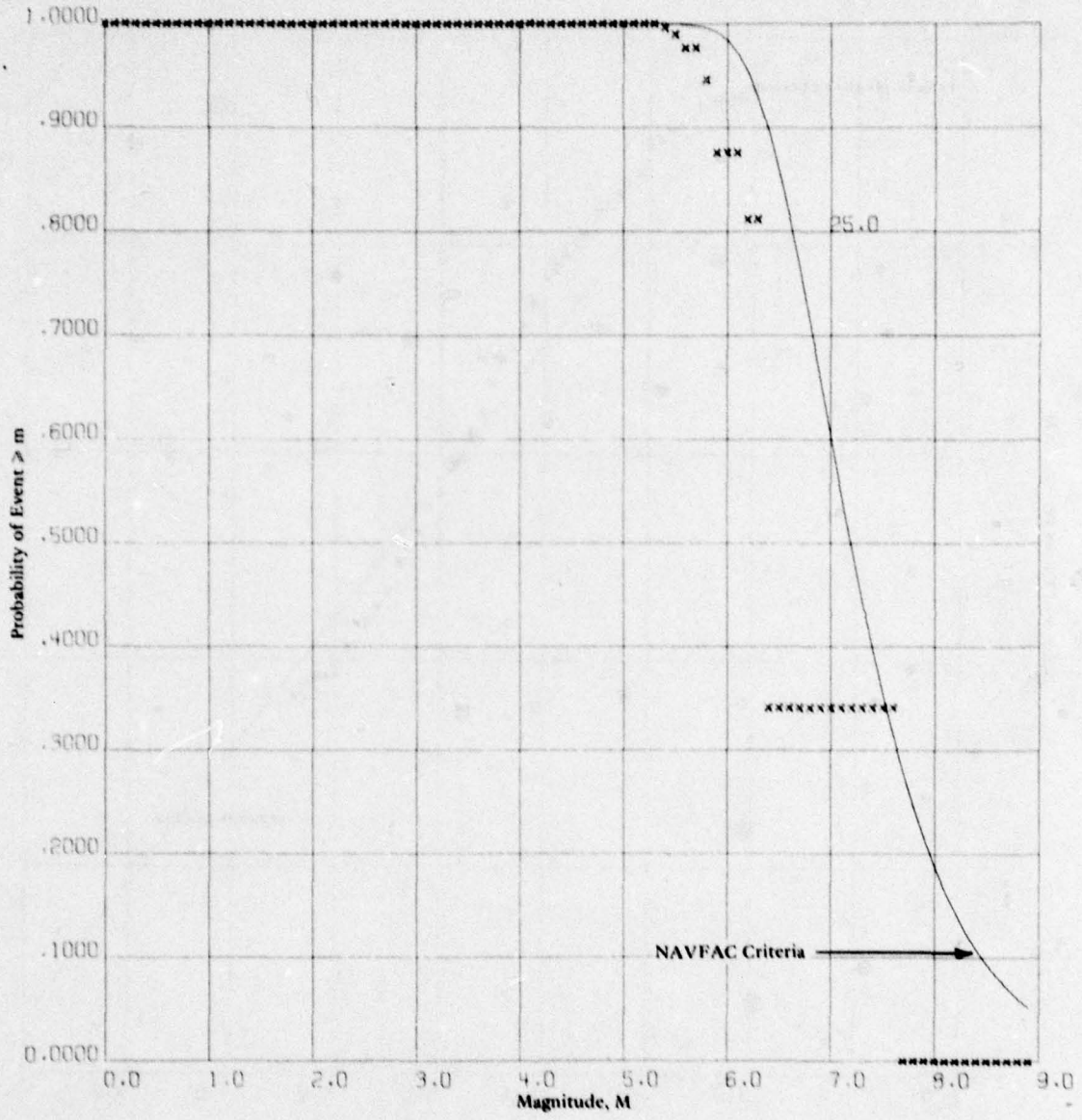

Figure 7-7. Probability of occurrence, Region 118-120 W, 33.5-35.0 N, 25 years.

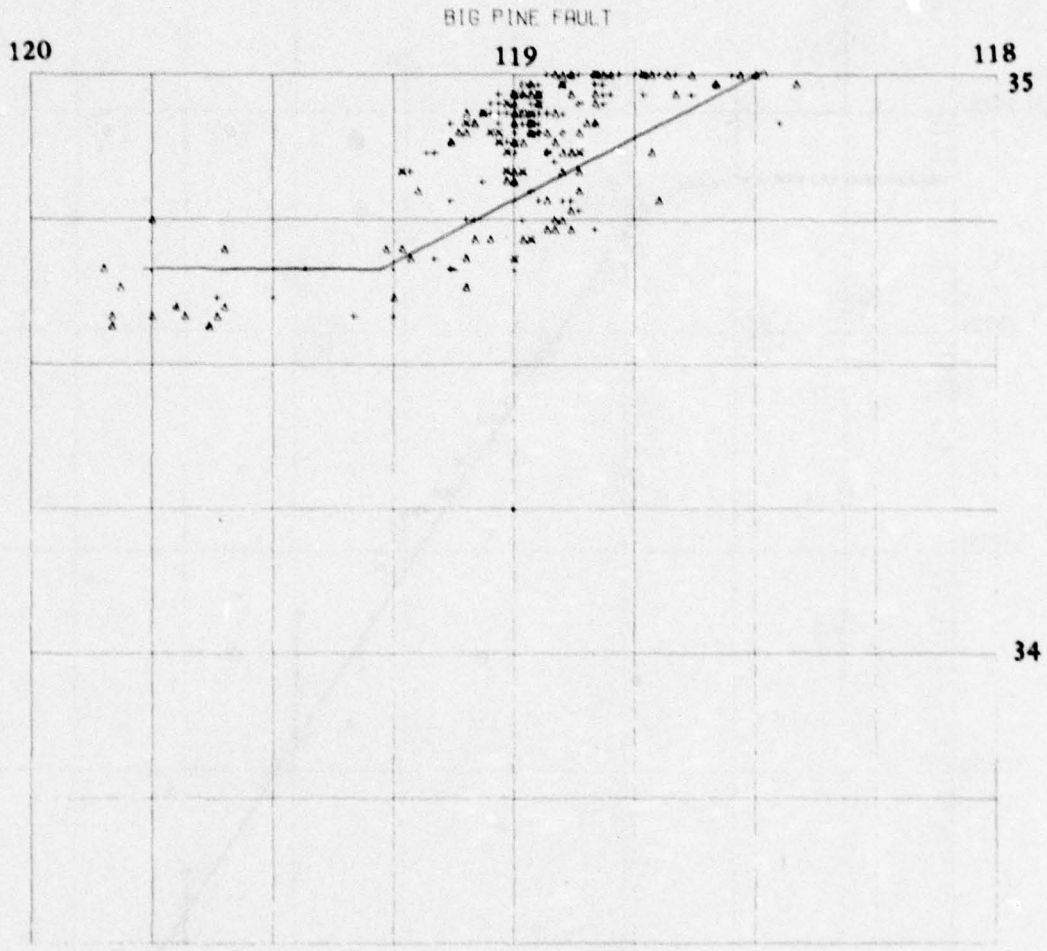

Figure 7-8. Portion of map showing epicenters associated with Big Pine fault.

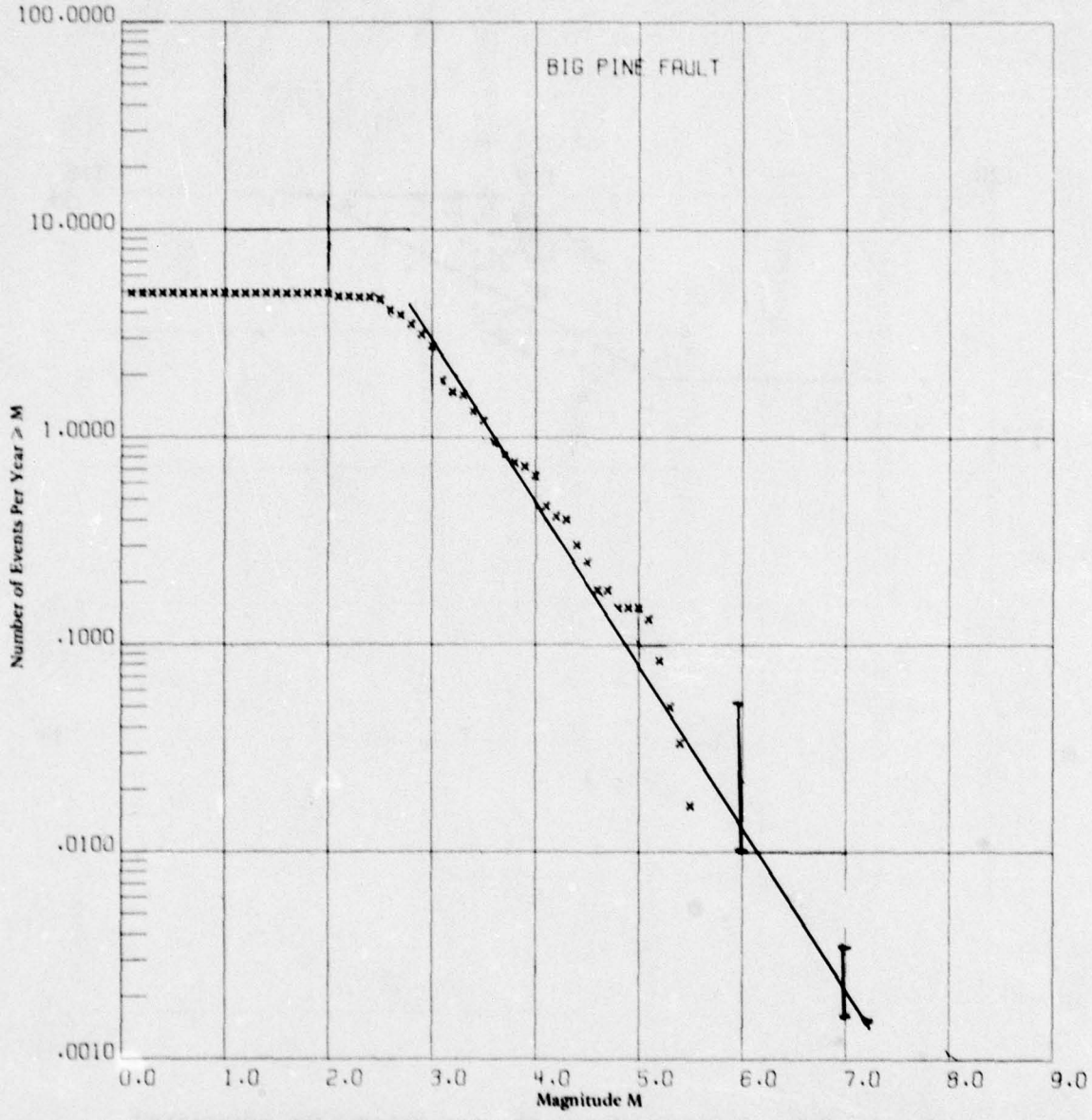

Figure 7-9. Recurrence data, Big Pine fault.

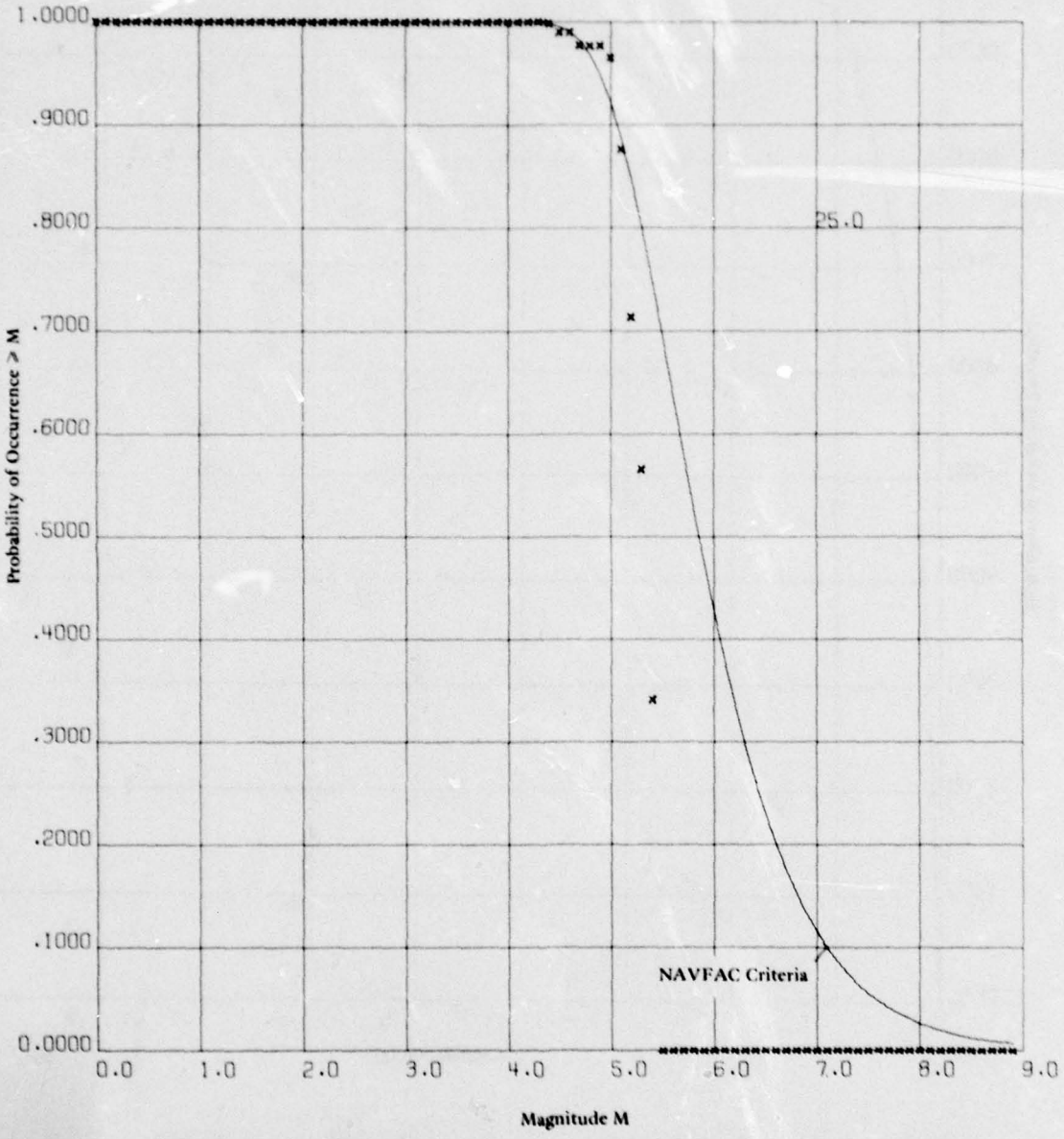

Figure 7-10. Probability of occurrence, Big Pine fault, 25 years.

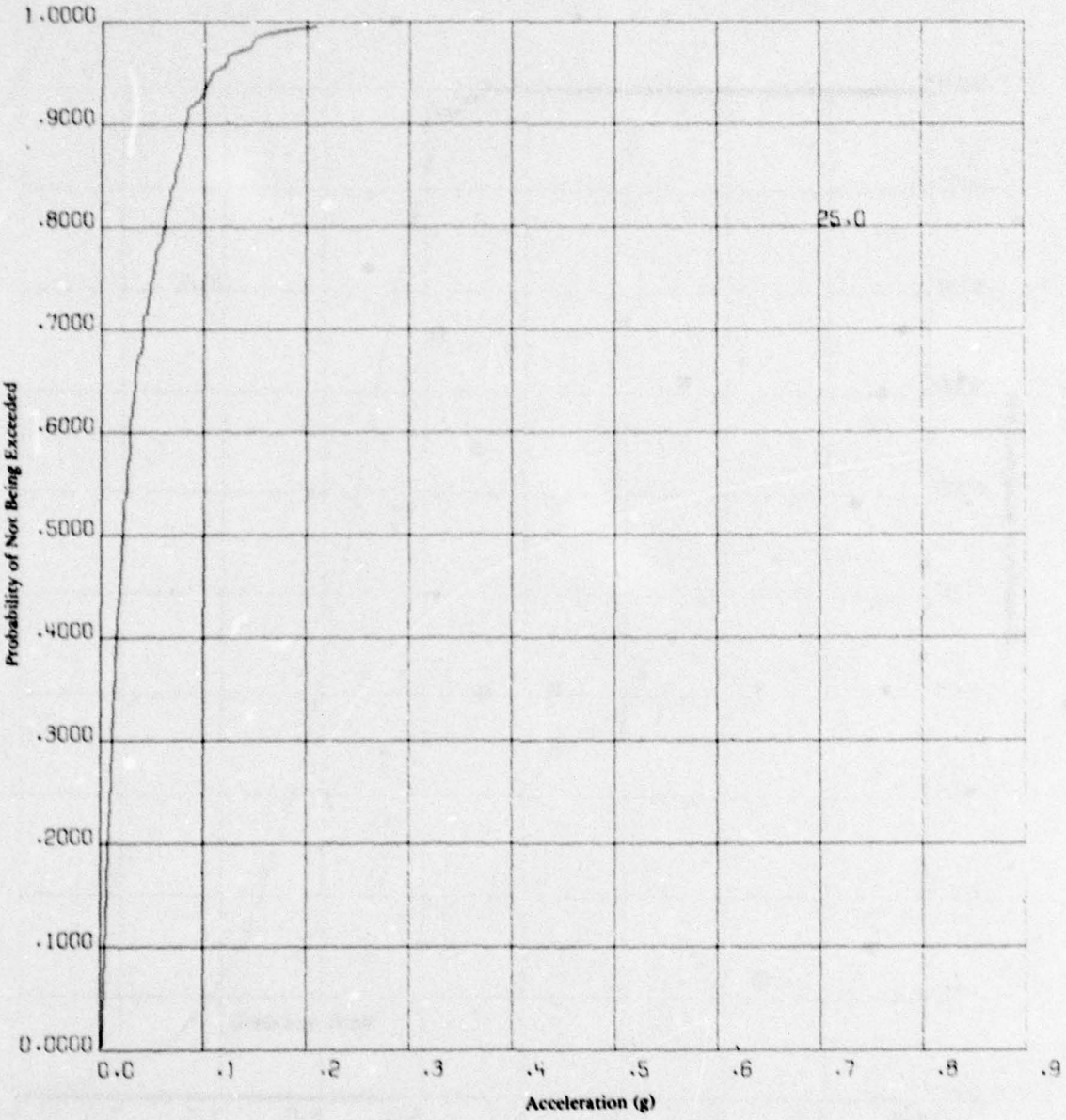

Figure 7-11. Probability of site acceleration not being exceeded in 25 years, Big Pine fault.

CHAPTER 8 - RESPONSE SPECTRA AND ANALYTICAL TECHNIQUES

Spectra

Engineers have found it useful to examine the frequency content of earthquake-induced ground motion. Strong motion accelerograms have been analyzed as a means of obtaining further insight into ground motion.

The first technique available is Fourier analysis. The Fourier spectrum of an acceleration shows the significant frequency characteristics of the recorded motion. The Fourier spectrum is defined as

$$F(\omega) = \int_0^T z(\tau)\, e^{-i\omega\tau}\, d\tau$$

over the interval $0<\tau<T$. The acceleration is zero outside the limits 0 to T. The Fourier amplitude spectrum is given by the square root of the sum of the squares of the real and imaginary parts of $F(\omega)$. Associated with the magnitude $F(\omega)$ is the phase angle $\phi(\omega)$, defined as the arc tangent of the imaginary part divided by the real part. Units of the spectrum reflect the time integration; thus, for an acceleration in ft/sec^2, the spectrum magnitude will be in feet per second and the phase angle will be in radians. The Fourier spectrum magnitude and phase angle represent only the input motion. Through convolution this may be combined with transfer functions for other elements (such as soil structure interaction) assuming elastic behavior. The Fourier spectrum magnitude and phase are a complete record which is unique and maintains the total time history record. The time history record may be recreated by reverse transformation. Generally, only the magnitude of the Fourier spectrum is shown in reference illustrations.

In earthquake engineering it is important to be able to determine the magnitude of maximum response of a structure. This has given rise to the response spectra technique. A single-degree-of-freedom, spring-mass-damper system can be analyzed and its time history of displacement calculated to determine relative displacement between the mass (the structure) and the excited base (the ground). Relative velocity and relative acceleration may also be calculated. However, of primary interest for engineering applications is the maximum absolute values of structure relative-displacement, structure relative-velocity and absolute structure acceleration. These values SD, SV, SA are functions of the critical damping. Plots of SD, SV, SA versus the undamped natural period of vibration and for various fractions of critical damping are called response spectra. In typical engineering structures the damping is small and for harmonic excitation the following holds

$$SD = \left(\frac{T}{2\pi}\right)SV$$

$$SA = \left(\frac{2\pi}{T}\right)SV$$

For earthquake-like excitations which are not strictly harmonic excitation an engineering assumption is made that the above is still accurate. The following definitions are used

$$PSV \equiv \left(\frac{2\pi}{T}\right)SD$$

$$PSA \equiv \left(\frac{2\pi}{T}\right)^2 SD$$

where PSV is the pseudo-relative velocity and PSA is the pseudo-absolute acceleration. The term "pseudo" is used to recognize the assumptions made concerning small damping and harmonic motion. Thus SD, PSV, PSA and T make up a set of data; knowing any two makes it possible to determine the other two. This unique relationship makes it possible to plot

response spectra in tripartile form. The response spectra shows the response of a single-degree-of-freedom system (structure) as a function of damping of the system and period for the given input acceleration.

A comparison of Fourier and pseudo-velocity response spectrum reveals that both are of the same units. For an undamped oscillator a similar mathematical relationship exists between the Fourier amplitude spectrum and exact relative velocity response spectrum. (The Fourier spectrum may be viewed as the maximum velocity of the undamped oscillator in the free vibration following the earthquake; however, the exact velocity response spectrum is the maximum velocity during both the earthquake and the subsequent free vibration.)

The Fourier amplitude spectrum is the quantity most frequently used by seismologists in their investigations of the earthquake ground motion. The response spectrum is generally used by structural engineers in the design of structures. Generally the pseudo-velocity response spectrum is the upper envelope of the Fourier spectrum.

In summary the most representative measure of the driving ground motion is the Fourier spectrum, which may be plotted in tripartile form. The response spectrum gives the response of a single-degree-of-freedom structure to the ground motion. Amplification of motion occurs where resonant components of motion interact with the structure. The response spectrum is most widely used in structural engineering with the modal analysis technique. This approach determines the eigenvalues and mode shapes for a number of the modes of structure, and using the modal period determines the acceleration to be used in computing an equivalent maximum static force to be applied to the structure. A response spectrum cannot be used directly as input to a dynamic structural analysis to generate a time history response because the response spectrum does not contain a measure of the duration of excitation. The Fourier spectrum does contain the full earthquake representation and may be used in conjunction with transfer functions to compute the structure response. This technique is not used in general structural engineering because of the difficulty in determining the transfer function. The more common

structural analysis techniques which produce dynamic time histories of response require input acceleration histories. Random analysis programs exist to generate time histories from a given spectral envelope; however, the duration must be specified. The resulting randomly generated signal is not unique, and any number may be generated from a single spectral envelope.

Time history records of actual earthquakes are available from the California Institute of Technology National Earthquake Information Center. These may be used when required for time history input of ground motion. Care is needed in selection since most records are recorded in structures which may influence the recording. Also the region around the site may influence the site response. The propagation of seismic waves is influenced by the local geology and soil conditions. The greater the extent of softer soils over bedrock, the less the boundary effects of the bedrock will have on the site. The depth of soil overlaying bedrock affects the period of vibration of the ground. This establishes a fundamental soil frequency of particular importance on soil-structure interaction. Further, this is a factor in determining the frequencies of waves filtered out by the soil, thus directly affecting the time history record.

Newmark-Hall Procedures for Elastic Spectra

Newmark (1967) based on studies of response spectra noted that response spectra could be related to peak ground acceleration, velocity, and displacement. From this study it was possible to develop standard shapes for use in structural analysis. The standard ground motion spectra (1g, 48 in./sec, 36 in.) could be scaled, based on peak horizontal ground acceleration expected at the site. Figure 8-1 gives amplification factors which could then be applied to estimate structural response.

McGuire (1977) also demonstrates ratios of damped spe ra. He found that the 5% damped pseudo-velocity spectra have values approximately 70% to 80% of the 2% damped spectra and that the 10% damped

spectra have values of approximately 55% to 65% of the 2% damped spectra. These ratios are constant throughout frequency range independent of the type of earthquake distance from site and magnitude. This confirms the Newmark-Hall approach.

At a frequency of about 6 cps, the amplified acceleration region line intersects a line sloping down toward the maximum ground acceleration value and intersecting that line at various frequencies, depending on the damping. The intersection is at a frequency of about 30 cps for 2% damping. These lines are designated as the acceleration transition region of the spectra. Finally, beyond the intersection with the maximum ground acceleration line, the response spectrum continues with the maximum ground acceleration value for higher frequencies.

The spectra so determined can be used as design spectra for elastic responses. The spectra are completely described when the maximum ground motion values are given for the three components of ground motion, and the damping is known. When only the maximum ground acceleration is given, the values used for maximum ground velocity and displacement are taken as proportional to those in the figure, or as scaled by the same scale factor relative to the maximum ground acceleration compared with 1g.

An assumption is made that acceleration, velocity, and displacement values are proportional to one another, independent of magnitude of motion. The shape is thought correct for sites on firm ground, soft rock, or competent sediments. However for soft sediments, the velocities and displacements must be increased. Garcia and Roesset (1970) performed studies comparing actual spectra with those estimated by the Newmark-Hall procedure. Results show favorable comparison indicating the utility of the Newmark-Hall procedure.

Vertical spectra may be estimated by taking two-thirds of the horizontal spectra when fault movements are horizontal and by taking horizontal spectra when large vertical motions are expected.

Newmark-Hall Procedures for Inelastic Response Spectra

The elastic spectra discussed in the previous section may be adjusted to approximate inelastic behavior of a structure. The displacement region and the velocity region are divided by the structure ductility μ to obtain yield displacement D' and velocity V' (Figure 8-2). The acceleration region (right side) is relocated by choosing it at a level which corresponds to the same energy absorption for elasto-plastic behavior as for elastic for the same period of vibration.

The extreme right-hand portion of the spectrum, where the response is governed by the maximum ground acceleration, remains at the same acceleration level as for the elastic case, and therefore at a corresponding increased total displacement level. The frequencies at the corners are kept at the same values as in the elastic spectrum. The acceleration transition region of the response spectrum is now drawn also as a straight line transition from the newly located amplified acceleration line and the ground acceleration line, using the same frequency points of intersection as in the elastic response spectrum.

In all cases the "inelastic maximum acceleration" spectrum and the "inelastic maximum displacement" spectrum differ by the factor μ at the same frequencies. The design spectrum so obtained is shown in Figure 8-2. Both the maximum displacement and maximum acceleration bounds are shown for comparison with the elastic response spectrum.

The solid line $DVAA_o$ shows the elastic response spectrum. The heavy circles at the intersections of the various branches show the frequencies which remain constant in the construction of the inelastic design spectrum.

The dashed line $D'V'A'A_o$ shows the inelastic acceleration, and the line $DVA''A''_o$ shows the inelastic displacement. These two differ by a constant factor μ for the construction shown, but A and A' differ by the factor $\sqrt{2\mu-1}$, since this is the factor that corresponds to constant energy.

Applied Technology Council Spectra Example

Using the Newmark-Hall procedure the Applied Technology Council (1974) developed basic response spectra for the "damage threshold" and "collapse threshold" earthquakes. Using a structure life of 70 years ground acceleration was selected for that study (representative for a number of sites in southern California) such that probabilities of occurrence of 50% and 10% for damage and collapse thresholds respectively (Figures 8-3 and 8-4). Ground acceleration values of 0.24g for the damage threshold and of 0.28g for the collapse threshold were used for their specific site.

Table 8-1 shows three categories of structure with ductility μ' and damping β' specified. Figures 8-5, 8-6 and 8-7 show inelastic design spectrum for the three types of structures.

Regulatory Guide 1.60 Procedures

Newmark (1973), Blume (1973), and Newmark, Blume and Kapur (1973) presented studies of the response spectra. These form the basis for the Nuclear Regulatory Commission (AEC) Regulatory Guide 1.60 (1973). The approach is similar to the Newmark-Hall procedure. The response spectra are summarized in Shannon and Wilson (1975) quoted as follows:

> The response spectra bounds are established by five straight lines, similar to the Newmark-Hall method, but the control points are designated by letters A, B, C, and D, and have definite assigned frequencies for all horizontal spectra. Amplification factors for constructing the response spectra are again a function of the percentage of critical damping, and are specified in *** [Figure 8-8] for the four control frequencies. Response spectra for 0.1g maximum horizontal ground acceleration have been constructed according to Regulatory Guide 1.60, and are provided in *** [Figure 8-8].

Vertical response spectra are constructed in the same manner as horizontal response spectra; however, the frequency for control point C is at 3.5 Hz rather than at 2.5 Hz, and the amplification factors are different *** [Figure 8-9]. Also, the maximum horizontal components of displacement and acceleration are used as scaling factors in constructing the vertical response spectra ***. The amplification factors in Figure *** [8-9] have been established so that the resulting vertical response spectra will be two-thirds of the values computed for the horizontal spectra, at frequencies below 0.25 Hz. In the range of frequencies from 0.25 Hz to 3.5 Hz, the ratio of vertical to horizontal spectral amplitudes varies from two-thirds to one; whereas, for frequencies between 3.5 Hz and 33 Hz, the horizontal and vertical response spectra are identical. Beyond 33 Hz, the vertical spectral accelerations decrease from a value equal to the peak horizontal ground acceleration at 33 Hz to two-thirds of the horizontal acceleration at 50 Hz.

This specification of the vertical spectral acceleration amplitudes above 33 Hz represents a correction to that currently indicated in Revision 1 of Regulatory Guide 1.60. As pointed out by Valera (1974), this correction results in a vertical spectrum shape that is consistent with the original Newmark, Blume and Kapur (1973) paper. The resulting family of vertical response spectra are shown in Figure 8-9.

Approximately one-quarter of the records considered in the development of the Regulatory Guide 1.60 spectra were recorded on rock sites, several were recorded on deep cohesionless soil sites, and the remaining records were obtained on stiff soil sites. It should be noted that Newmark Services (1973), and Blume and Associates (1973), in the course of their independent investigations that led to Regulatory Guide 1.60, considered potential effects of local soil conditions; in fact, the Newmark study provided spectra that indicated important differences

between motions recorded on sediments and on competent rock, particularly for frequencies below about 3 Hz. However, the recommended design spectra contained in the subsequent paper by Newmark, Blume, and Kapur (1973) and in Regulatory Guide 1.60 do not differentiate between various local soil profiles and, therefore, represent a statistical sample in which the subsurface soil conditions are an uncontrolled variable.

Site-Matched Records

The data base of strong motion records can be a useful source of seismic data. Records may be selected to represent seismologic, geologic, and local site conditions. Selection is complicated by a number of factors. Ideally, the records should be selected to match source-site transmission path source mechanism and local site conditions. These are not readily quantifiable. Thus, reliance is made on earthquake magnitude site acceleration level, site classification, and duration of motion. Judgment is an important factor in selecting and scaling records.

Appendix C presents a CEL program which uses the available data optimizing the selection considering magnitude distance, acceleration, and site category. This should assist in reducing the problem of selecting the closest records available. Appendix D describes a CEL plotting program. Appendix E describes a CEL program to plot time histories.

Guzman and Jennings (1975a and b) describe a procedure for developing criteria spectra based on site-matched records. Geological and seismological factors should be evaluated. A group of strong motion records is selected representing comparable magnitude, distance geology, and soil conditions. Accelerograms are added to the group until conditions under which they were recorded are no longer representative of the earthquake or until no additional reliability is obtained by further additions. Attenuation curves are used to adjust the peak acceleration magnitude and distance more closely to the desired earthquake.

Seed, Ugas and Lysmer (1974) studied 104 records broadly classified into rock (28 records), stiff soil (31 records), deep cohesionless soil (30 records), and soft to medium soil (15 records). The spectra were normalized to 5% damping ratio and 0.1g zero-period acceleration. Figures 8-10 and 8-11 show the effect of site conditions. The soft-to-medium soil sites and deep cohesionless soil sites show larger amplitudes than the others for frequencies less than 3 Hz. The Applied Technology Council (1976) have normalized these spectra as shown in Figures 8-12 and 8-13. The spectra have been compared to Regulatory Guide 1.60 by Shannon and Wilson (1975) as follows:

> These comparisons indicate that differences between the site-dependent spectra and Regulatory Guide 1.60 are most pronounced for frequencies below 2 to 3 Hz; less significant but still noticeable differences are noted at higher frequencies. For rock, stiff soil, or deep cohesionless soil sites, higher frequency components of composite spectra differ from Regulatory Guide 1.60 by as much as 25%. Higher frequency components of spectra from soft-to-medium soil sites exhibit larger differences relative to Regulatory Guide 1.60. Figure 8-14 shows the effect of shaking intensity.

Variability in Site-Matched Records

Practical limitations in the number of records available limit the selection process. Figures 8-15a and b show the extent of variation possible. The differences are probably caused by variations in the source mechanism and transmission path. It is only through obtaining a number of records that it is possible to achieve sufficient reliability.

The scaling of spectral shapes implies that the shapes are independent of the intensity of motion. McGuire (1977) has performed a regression analysis giving interesting information. It is known that larger magnitude events tend to produce relatively more or stronger long period

motions than do small magnitude events. Further, the high frequency components of ground motion attenuates with distance at a faster rate than the low frequency component.

Figure 8-16 shows the mean psuedo-velocity spectra computed for earthquakes of several magnitudes and distances, expressed as a percentage of the maximum pseudo-velocity observed at any frequency for that value of M and R. McGuire (1977) notes the following:

> In general, it is observed that longer hypocentral distances imply decreased relative spectra in the high frequency region, and a lower frequency at which the spectral velocity is a maximum. Small magnitude earthquakes have higher relative spectra in the high frequency region, and lower relative spectra at low frequencies, than do large earthquakes observed at the same distance.

Influence of Site Conditions on Response Spectra

Seed and Idriss (1969) give response spectra for sites whose soil conditions are shown during the same or similar magnitude earthquakes, Figure 8-17. All of these represent motions recorded at very considerable distances from the epicentral regions. The spectra are arranged in sequence from A to F, corresponding to increasing degrees of "softness" of the soil conditions underlying the recording stations. To eliminate the influence of different amplitudes of surface accelerations, the ordinates of the spectra have been normalized by dividing the spectral accelerations by the maximum ground acceleration at each site. Thus the different forms of the normalized spectra reflect primarily the different frequency characteristics of the motions from which they were obtained.

It may be seen that for the recording made at Site A, the peak ordinate of the response spectrum is developed at a period of about 0.3 second, indicating a predominantly high frequency in the ground motion.

However, for the still stiff (note high values of standard penetration resistance) but slightly softer soil deposit at Site B, the peak ordinate of the spectrum occurs at 0.5 second; and, as the ground conditions become progressively softer, as evidenced by the presence of increasingly greater depths of soft and medium stiff clays and silts, the periods at which the peak spectral accelerations are developed change as follows:

Sites	Approximate Period
A	0.3
B	0.5
C	0.6
D	0.8
E	1.3
F	2.5

The sites are arranged in increasing order of softness of soil conditions. The period is that at which maximum spectral acceleration is developed. It is thus apparent that the frequency components of the motions at the different sites and the form of the response spectra change in a reasonably consistent fashion, depending on the softness or hardness of the soil conditions. The natural period of structures in seconds may be crudely estimated by dividing the number of stories by 10.0. For the sites underlain by deposits of stiff soils, the peak ordinates of the acceleration response spectra tend to occur at a low value of the fundamental period, say 0.4 or 0.5 second (see Figure 8-17), indicating that at these locations the maximum accelerations would be induced in relatively stiff structures five or six stories in height. On the other hand, for the sites underlain by deep deposits of softer soils, the peak ordinates of the acceleration response spectra tend to occur at a rather high value of the fundamental period, say 1.5 to 2.5 seconds (see Figure 8-17), indicating that at these sites the maximum accelerations would be induced in multistory structures 15 to 25

stories in height. Thus, lateral forces on structures and related building damage in the same general area may develop selectively; multistory structures may be severely affected where they rest on relatively soft soil deposits but adjacent stiffer structures on the same deposits may be hardly affected at all; conversely, multistory buildings on shallow, stiff soil deposits may be only slightly affected while adjacent stiff structures are subjected to large lateral forces (Seed and Idriss, 1969).

Seed and Idriss (1969) also demonstrate the effect of local and distant earthquakes of magnitudes to produce the same level of site ground motion. One example they cite is as follows. A strong local earthquake may produce high frequency rock motions having a maximum acceleration of about 0.13g and a predominant period of about 0.25 second. On the other hand, a great earthquake located some 75 miles away might also induce a maximum acceleration in the rock of about 0.13g, but the motions would have a lower frequency and a somewhat longer predominant period, perhaps of the order of 0.7 second. The computed ground surface accelerations at the site during two such earthquakes are listed:

Type of Earthquake	Maximum Acceleration in Underlying Rock	Maximum Ground Surface Acceleration	Amplification Factor
Strong Local Shock	0.13g	0.08g	0.6
Great Distant Earthquake	0.13g	0.13g	1.0

The acceleration response spectra for these ground surface motions are shown in Figure 8-18. The maximum ground surface accelerations differ by some 70% but more significantly, the spectral accelerations corresponding to the fundamental period of the building of the site, about 1.3 seconds, differ by several hundred percent. Clearly other modal effects need to be considered, but these figures indicate the potential significance of the characteristics of the basic rock motions in determining ground surface and structural response (Seed and Idriss, 1969).

The influence of the characteristics of the base rock motion on ground response, as indicated by the spectra in Figure 8-18 is somewhat typical of that found for other site analyses. In some cases the acceleration spectrum shows its major peak at a period corresponding approximately to the fundamental period of the soil deposit, while in other cases the peak seems to develop at a period corresponding approximately with the predominant period of the base rock motions. Which of these situations will develop in any given case will probably depend in large measure on: (1) the difference between the predominant period of the base motion and the natural period of the deposit and (2) the duration of the ground shaking. Because there will always be some uncertainty concerning the form of the base motions likely to develop at any given site, it is clearly desirable that analyses should be made for a range of possible, but realistic, base excitations to bracket the range of surface accelerations to be expected. It is clearly shown that because the predominant period of the rock motions for the strong distant earthquake would be larger than that for the local earthquake, a soft soil deposit would tend to emphasize these long period effects, producing a much higher damage potential for multistory buildings than would the shorter period motions of the local earthquake. Such a result would be expected since the large amplitude motions produce greater strains in the transmitting soil deposit, resulting in correspondingly lower moduli and a longer fundamental period of the soil deposit (Seed and Idriss, 1969). Short period structures develop their highest damage potential when they are situated on shallow or stiff deposits. Long period structures develop their highest damage potential when they are situated on deep or soft soil deposits. Both reflect the undesirable effects of similarities in the fundamental period of a structure and the soil deposit on which it is constructed. Seed et al. (1975), Figure 8-19, gives approximate relationships between maximum accelerations for different soil types for the same depth to bedrock. For low intensity motion virtually all soil deposits tend to amplify underlying rock accelerations. For extremely high intensity motions many soil deposits

may attenuate underlying rock acceleration. Soft soil deposits are more effective in attenuating peak rock accelerations than shallow stiff soils.

Gates (1976) reports the influence of soil depth (Figure 8-20) based on analytical procedures. A Soil Amplification Factor was determined as a function of acceleration level and site description. The Soil Amplification Factor is the spectral ratio between the computed surface motions and the input rock motion for various frequencies for 5% damping. The ratio is primarily dependent on the soil properties and is not influenced to a great extent by the frequency content of the input motion.

Computer Analysis Techniques, One-Dimensional Models

A soil profile may be analyzed as a one-dimensional shear wave problem, assuming the stress wave to be only a vertically propagating shear wave (generally this is true for deep alluvium sites and not true for shallow sites near the fault). The differential equations of motion can be solved in closed form for linear elastic soil properties. This has been done by Seed and Idriss (1969) and Kanai (1961) to provide a one-dimensional analysis of sites of simple geometry. However, the stress-strain characteristics of a site are highly nonlinear, hysteretic, and strain-dependent.

Streeter et al. (1974) developed a computer program using the method of characteristics for calculating one-dimensional dynamic behavior of soils. A soil profile is divided into layers down to bedrock. Dynamic excitation of the soil is introduced at the rock-soil interface. The response of the soil can be evaluated on the basis of elastic, viscoelastic, or nonlinear (Ramberg-Osgood) soil behavior. The program determines shear, velocity, and displacement information.

An analytical technique for analyzing the response of horizontal soil profiles to earthquake motion is described by Seed and Idriss (1969, 1970a, 1970b) and Idriss and Seed (1968, 1970). The soil profile

is idealized by a series of discrete masses and springs with linear viscous dampers. The nonlinear and hysteretic stress-strain characteristics of the soil are introduced by using an equivalent shear modulus and an equivalent viscous damping factor which can vary with each layer of soil profile and with the strain level within the layer. The equivalent shear modulus for a given strain level is taken as the slope of the diagonal line (average slope) drawn through the hysteresis loop, which is shown in Figure 8-21 for a cyclically loaded laboratory specimen. The average equivalent viscous damping coefficient is proportional to the ratio of area of the hysteretic loop, as shown in the figure, to the maximum stored energy during the cycle.

An iterative procedure is used to obtain strain compatible values for shear modulus and damping. The response of the soil profile modeled as discrete masses is computed, and strains are determined.

Another automated-analysis technique, more widely used today for treating horizontal soil layers, has been developed by Schnabel, Lysmer, and Seed (1972), based on the one-dimensional wave propagation method. This program, SHAKE, can compute the responses for a given horizontal earthquake acceleration specified anywhere in the system. The analysis incorporates nonlinear soil behavior, the effect of the elasticity of the base rock, and variable damping. It computes the responses in a system of homogeneous viscoelastic layers of infinite horizontal extent, subject to vertically traveling shear waves. The program is based on the continuous solution of the wave-equation adapted for use with transient motions through the Fast Fourier Transform algorithm. Equivalent linear soil properties are obtained by an iterative procedure for values of modulus and damping compatible with the effective strains in each layer. The following assumptions are made:

1. The soil layers extend infinitely in the horizontal direction.

2. The layers are completely defined by shear modulus, critical-damping ratio, density, and thickness.

3. The soil values are independent of frequency.

4. Only vertically propagating, horizontal shear waves are considered.

The soil model is similar to that developed by Seed and Idriss (1970c), using data similar to Hardin and Drnevich (1970). The absolute range of soil parameter variation may be stipulated by merely in-putting factors whose numerical values may be derived from simple soil strength properties. These strength properties may be the undrained shear strength of a clay or the relative density for sands. The program requires the definition of the soil profile down to bedrock (assumed as seismic velocity 2,500 ft/sec) as well as an earthquake time history record in digital form.

The motion used as a basis for the analysis can be given in any layer in the system, and new motions can be computed in any other layer. Maximum stresses and strains, as well as time histories, may be obtained in the middle of each layer. Response spectra may be obtained and amplification spectra determined.

Effects of Soil and Site Parameters

Frequently, the parameters needed in the response studies are poorly defined at a given location. Often, the values of these parameters must be assumed in order to perform the ground response analyses. Experience has shown that variations in the value of any one of the parameters may affect the solution differently from site to site, and no general rules may be formulated at this time to establish the influence of the variables.

Earthquake motions are produced by a stress wave, which is transmitted more rapidly and with less energy loss through the bedrock than through the overlying soils. When the bedrock has a horizontal surface of great extent and the overlying soil layers are also horizontal, it is

frequently assumed that the earthquake motion within the soil is produced essentially by horizontal shear waves which propagate upward through the soil from the bedrock surface. This assumption greatly simplifies the analysis since the problem can be reduced to a one-dimensional shear wave problem. This is a simplification, since vertical components of the earthquake motion are always present and the wave transmission problem may be more complex than can be simulated in a one-dimensional model.

When the bedrock or soil layers are inclined, a one-dimensional shear wave assumption is questionable, and a two-dimensional model may be required to account for the more complex geometry and wave motion.

Lysmer, Seed, and Schnabel (1970) have shown that under identical boundary conditions, the lumped mass solution and the wave propagation solution are basically the same. Arango and Dietrich (1972) have investigated the variation of parameters for the two methods. They note close agreement in peak levels of motion with some differences in computed time histories.

Depth to Bedrock

In many cases the depth to bedrock is not well-defined. A preliminary analysis may be required to assess the influence of depth to bedrock on the ground response. Dezfulian and Seed (1969) have shown that an increase in thickness of the deposit may or may not cause a substantial change in surface motion. Their studies show that for shallow deposits, an increase in thickness of medium sand from 38 to 50 feet (12 to 15.6 meters) reduced the response significantly. Increasing the thickness to 80 feet (25 meters) reduced the response still more, but a further increase from 80 to 100 feet (25 to 31.2 meters) did not produce any additional reduction in the response.

For much deeper deposits, 1,000 feet (330 meters), Kiefer et al. (1970) analyzing the conditions at Osaka, found that the response was not very sensitive to the range of depths investigated.

Arango and Dietrich (1972) studied the variation for depths to bedrock equal to 600, 800, and 900 feet (180, 250, and 270 meters). The values of the maximum acceleration and the velocity and acceleration spectra are shown in Figure 8-22. The acceleration spectra for two depths to bedrock at Study Site A are also shown in Figure 8-22.

The above examples show that for shallow soil deposits, the depth to bedrock may or may not significantly affect the response; deep soil deposits are, in general, less sensitive. Preliminary studies using a reasonable range of depth to bedrock should precede any ground response calculation when uncertainties regarding the actual depth are present.

Influence of Soil Profile

The frequency characteristics of the ground motions and the form of the ground response spectra may be influenced by the nature of the soil conditions underlying the sites. This is illustrated by the studies by Arango and Dietrich (1972). Different soil profiles were used in the response analysis as shown in Figure 8-23. The values of the maximum acceleration and displacement obtained are shown in Figure 8-24. The corresponding response spectra are shown in Figure 8-25. Significant changes in response can result from variation in soil profile, and great care must be placed on the correct site stratigraphic representations. The importance of the time history of the ground motion on the response values is also apparent by comparing the spectra from Figure 8-25a to that of Figure 8-25b.

Soil Rigidity

Since the stiffness of the soil deposits can only be approximated, it is often desirable to run preliminary response analyses using the most reasonable values of the shear moduli for the various soils and values (say 50% to 100%) greater than those judged to be the most reasonable. Arango and Dietrich (1972) calculated the maximum ground

surface acceleration, ground displacement, the fundamental period of the soil column, and the response spectra by using the average values of the shear moduli and values 50% higher. The results of the calculations are shown in Figure 8-26. In some cases, errors in the estimated shear moduli cause minor differences in the calculated ground response which have no practical significance for engineering purposes. In other cases, however, it has been found that great differences may occur as a result of varying the values of the shear moduli.

Amplitude of Rock Acceleration

Schnabel and Seed (1972) have indicated that spectral acceleration values are often not significantly influenced by substantial reductions in maximum acceleration levels in rock. It was found that generally a reduction of 15% to 25% in maximum rock acceleration values will affect the spectral acceleration by less than 10%.

Frequency Content of the Rock Motions

The form and frequency characteristics of the base input may have a very significant influence on the response of soils. Arango and Dietrich (1972) studied a site under two different earthquakes (Figure 8-27). As shown at the right side of Figure 8-27, the two acceleration histories applied to the outcrop rock had the same peak acceleration and the spectra were similar. However, the small differences in frequency caused the motion to be amplified differently in the three soil columns. Therefore, two or more histories of acceleration should be considered in any given response study in order to define the relative magnitude of the ground response at any given location.

Computer Analysis Techniques, Two-Dimensional Models

As pointed out earlier, when the ground surface or the soil layers are inclined, one-dimensional wave assumptions may not be valid and a two-dimensional model may be required to represent the more complex geometry. Although two-dimensional liquefaction analyses are not in routine soil practice, the same procedures for evaluation of a stress history can be utilized. Finite element representations have been used to study dams and embankments.

Idriss et al. (1973) have developed a two-dimensional finite element program – QUAD-4 – for the evaluation of seismic response of soil deposits. This program allows for variable damping in each element using a Rayleigh damping expression for that element. The damping matrix for the entire assemblage of elements is obtained by appropriate addition of the damping submatrices of all the elements.

The response is evaluated by the solution of the equations of motion using direct numerical integration methods with a time increment small enough to provide stability. The program uses plane strain quadrilateral and triangular elements. An iteration procedure is used to determine the strain-dependent modulus and damping for each element, based on the average strain developed in that element. The relation of modulus and damping is based on Seed and Idriss (1970c). The solution is obtained using the modulus and damping for each element which is compatible with the average strain. The developers of the program report that comparison with one-dimensional methods shows that the finite element solution values of shear stress are about 10% greater. The response spectra of one- and two-dimensional methods are of similar shape. Major differences on response spectra occur only when the input motion has large amounts of high frequency components or when the finite element model is very coarse. The addition of variable damping makes the response calculation results in better agreement with recorded data.

Lysmer et al. (1974) have developed a two-dimensional finite element program, LUSH (revised version called FLUSH), which solves the transient response problem in soil sites by complex frequency response. It can calculate the response of sloping soil layers and can include the soil-structure interaction effect. The program accounts for the nonlinear effects which occur in soil masses by a combination of the equivalent linear method described in the section on one-dimensional analyses (Seed and Idriss, 1969) and the method of complex response with complex moduli allowing for different damping properties in all elements.

The model consists of plane quadrilateral or triangular elements. Three different material types are provided for: nonlinear clays and sands, elastic solids, and rigid solids. Typical relationships between stiffness, damping, and effective shear strains for sand and clay are provided within the program. These are similar to the curves used in SHAKE. Viscous damping is introduced by using complex moduli in the formation of the stiffness matrix which leads to the same amplitude response as nodal analysis with a uniform fraction of critical damping. The initial soil properties are specified at low strain level ($\gamma = 10^{-4}$% strain) and the program iterates to find material properties at strain levels compatible with the specified motion.

The mesh size of elements in the model should be small compared with the wavelength of shear waves propagating through the model. A suggested maximum height element is

$$h = (1/5)\,\lambda = 1/5\left(\frac{V_s}{w}\right)$$

where h = element height

λ = wavelength of shortest shear wave

V_s = velocity of shear wave at strain level of earthquake

w = highest frequency of the analysis

Case Study

Chapter 7 presented a portion of a case study as an example of the computational procedure. This section will demonstrate the preparation of response spectra. Assume it is of interest to generate the response spectra associated with motion from the Santa Cruz fault. Table 7-1 shows a 90% confidence level of 0.283g. Associated with the acceleration is a causitive magnitude 7.2 and epicentral distance 25 miles. This information is used as input to Program OPTIREC. The program using the weighting specified by the user (in this case equal weights), searches the list of records, and produces an ordered list of records representing the site conditions. Table 8-2 gives the first eight entries. Figure 8-28 shows time histories of the records obtained by Program TIMHIS. Figure 8-29a gives the response spectra for 5% damping for each record. Figure 8-29b gives the mean value and the mean plus one standard deviation. Figure 8-29c gives the maximum envelope of points. These were obtained using the Program RESPLOT.

As can be seen by Figure 8-29a there is some variability in the group of records. Previously, the randomness of the site acceleration in terms of attenuation and dispersion, source description, epicentral location and size of event have been considered. This section must only consider site characteristics which may cause amplification of motion. The best choice of spectra from a design viewpoint would probably be a mean plus one standard deviation. Care must be taken that the inclusion of acceleration dispersion not be taken twice; however, there is no practical way of separation of these effects. Superimposed on Figure 8-29b is the response spectra which would be indicated by the Newmark-Hall procedure. Judgment would indicate that the mean plus one standard deviation should be appropriate for design usage.

The results in Figure 8-29 were dominated by the San Fernando earthquake. Additional data were included from Santa Barbara, Long Beach, Eureka, and Taft earthquakes. Results remained essentially the same.

Table 8-1. Structure Categories and Modification Factors
(from Applied Technology Council, 1974)

Structural Categories	Spectral Modification Factors				Project Buildings	
CATEGORY A					NO.	LATERAL FORCE SYSTEM
Space Frame Ductile Moment Resisting—Concrete (Code K = 0.67)					1	5 stories ductile reinforced concrete frame
	Damage		Collapse		2	19 stories ductile steel frame E-W (See also Category B)
Space Frame Ductile Moment Resisting—Steel (Code K = 0.67)	μ'_D	β'_D	μ'_C	β'_C	3	10 stories ductile reinforced concrete frame N-S, ductile reinforced concrete frame with shear walls E-W
	1.50	10%	4.00	10%		
Ductile Moment Resisting Concrete Frame with Concrete Shear Walls (Code K = 0.80)					10	2 stories ductile steel frame
CATEGORY B					NO.	LATERAL FORCE SYSTEM
Ductile Moment Resisting Steel Frame with Vertical Bracing (Code K = 0.80)					2	19 stories braced steel frame N-S (See also Category A)
	Damage		Collapse			
Concrete Shear Walls with Vertical Load-Bearing Frame (Code K = 1.00)	μ'_D	β'_D	μ'_C	β'_C	8	9 stories reinforced concrete frame with shear walls
	1.50	7%	2.00	7%		
CATEGORY C					NO.	LATERAL FORCE SYSTEM
Vertical Load Steel Frame With Vertical Bracing (Code K = 1.00)					4	14 stories concrete shear walls
					5	7 stories concrete shear walls
	Damage		Collapse		6	2 stories steel frame with vertical bracing
Concrete Shear Bearing Walls With Rigid Diaphragm (Code K = 1.33)	μ'_D	β'_D	μ'_C	β'_C	7	3 levels masonry shear walls
	1.50	5%	2.00	5%		
					9	1 story concrete tilt-up shear walls
Flexible Diaphragms on Masonry or Tilt-up Walls (Code K = 1.33)					11	1 story masonry shear walls

Table 8-2. Earthquake Records From San Fernando Earthquake

(Magnitude was 6.6.)

CEL Record Identification	Epicentral Distance (mi)	A_{max} (g)
682	25.23	0.245
557	25.16	0.242
292	25.64	0.239
683	25.23	0.224
173	22.13	0.210
322	23.86	0.201
622	17.44	0.246
293	25.64	0.195

Percent of Critical Damping	Displacement	Velocity	Acceleration
0	2.5	4.0	6.4
0.5	2.2	3.6	5.8
1	2.0	3.2	5.2
2	1.8	2.8	4.3
5	1.4	1.9	2.6
7	1.2	1.5	1.9
10	1.1	1.3	1.5
20	1.0	1.1	1.2

(a) Relative values of spectrum amplification factors (from "Seismic design spectra for nuclear power plants," by N. M. Newmark, J. A. Blume, and K. K. Kapur, in Journal of the Power Division, ASCE, vol 99, no. PO2, Nov 1973, table 5).

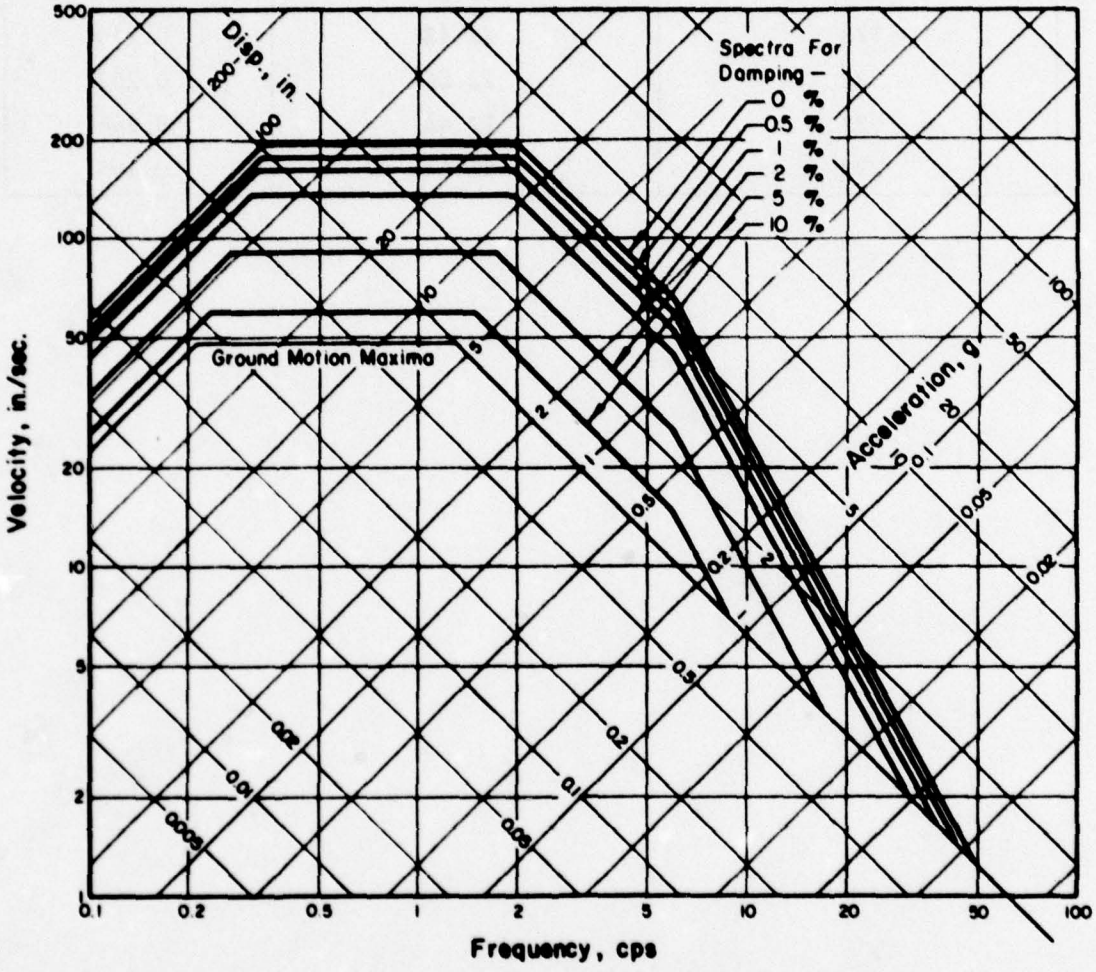

(b) Velocity versus frequency.

Figure 8-1. Basic design spectra normalized to 1.0g (from Applied Technology Council, 1974).

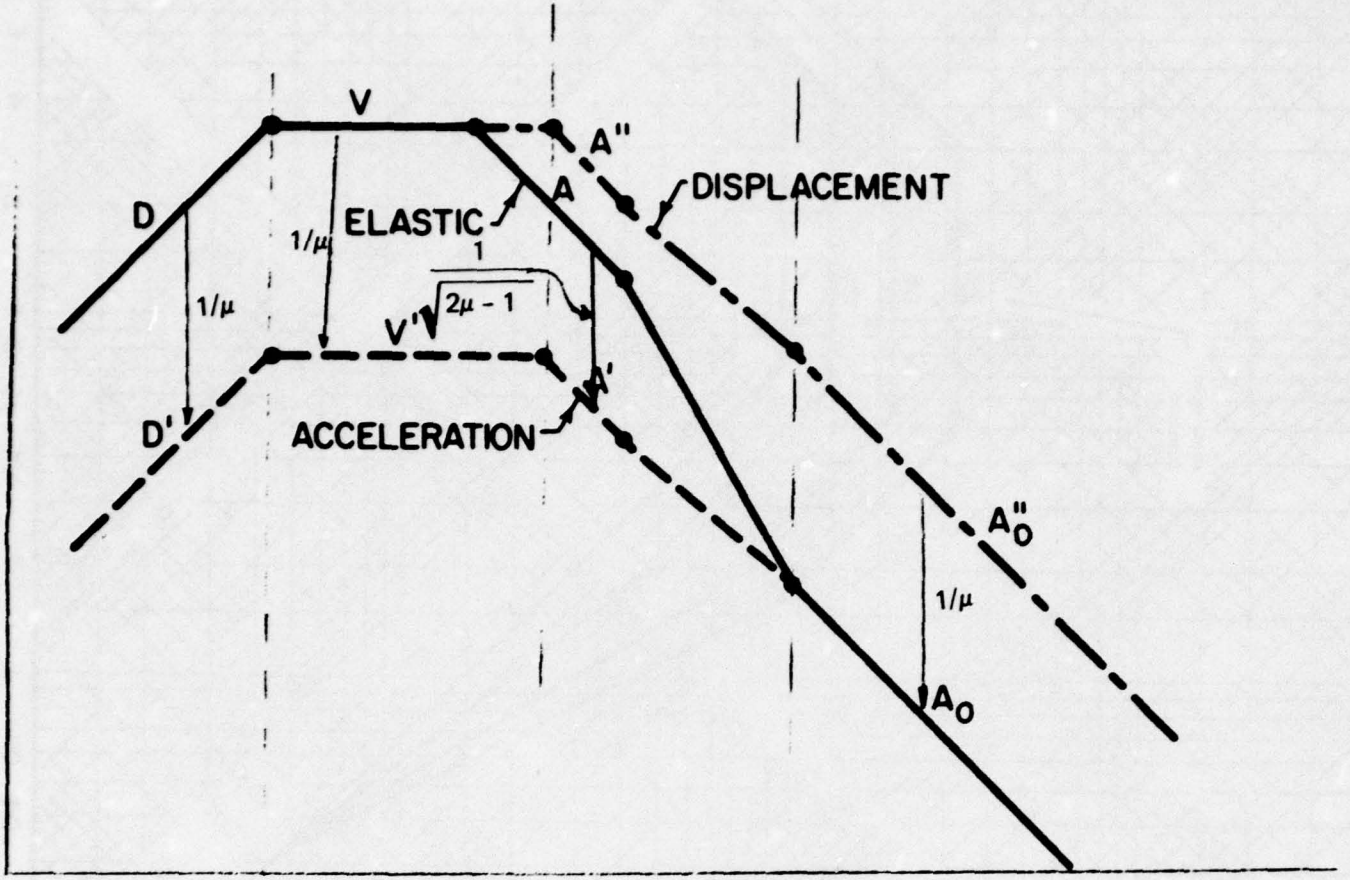

FIG. 9(N-H) Design Spectra

Figure 8-2. Design spectra for inelastic analysis (from Applied Technology Council, 1974).

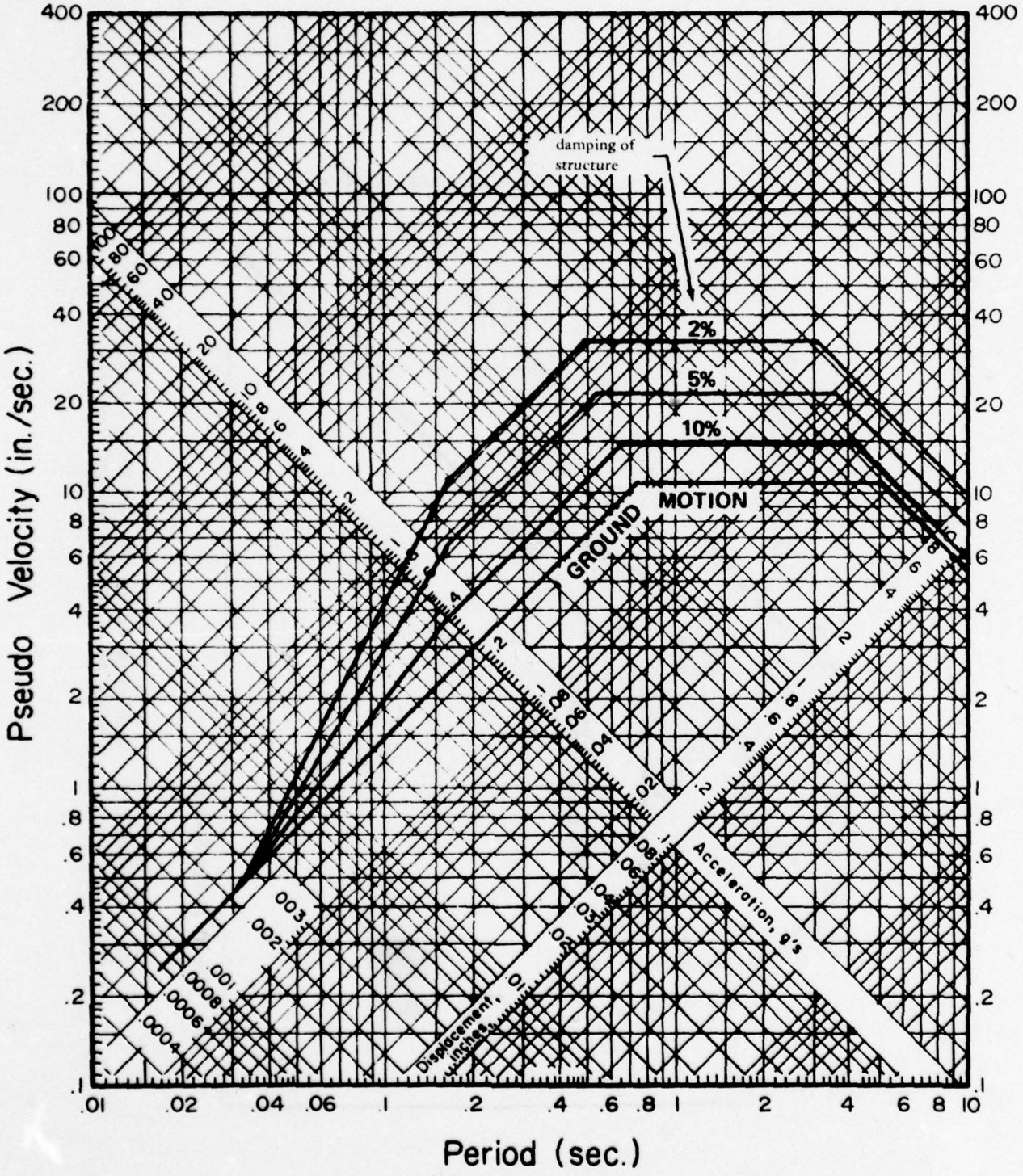

Figure 8-3. Elastic response spectra, damage threshold level (from Applied Technology Council, 1974).

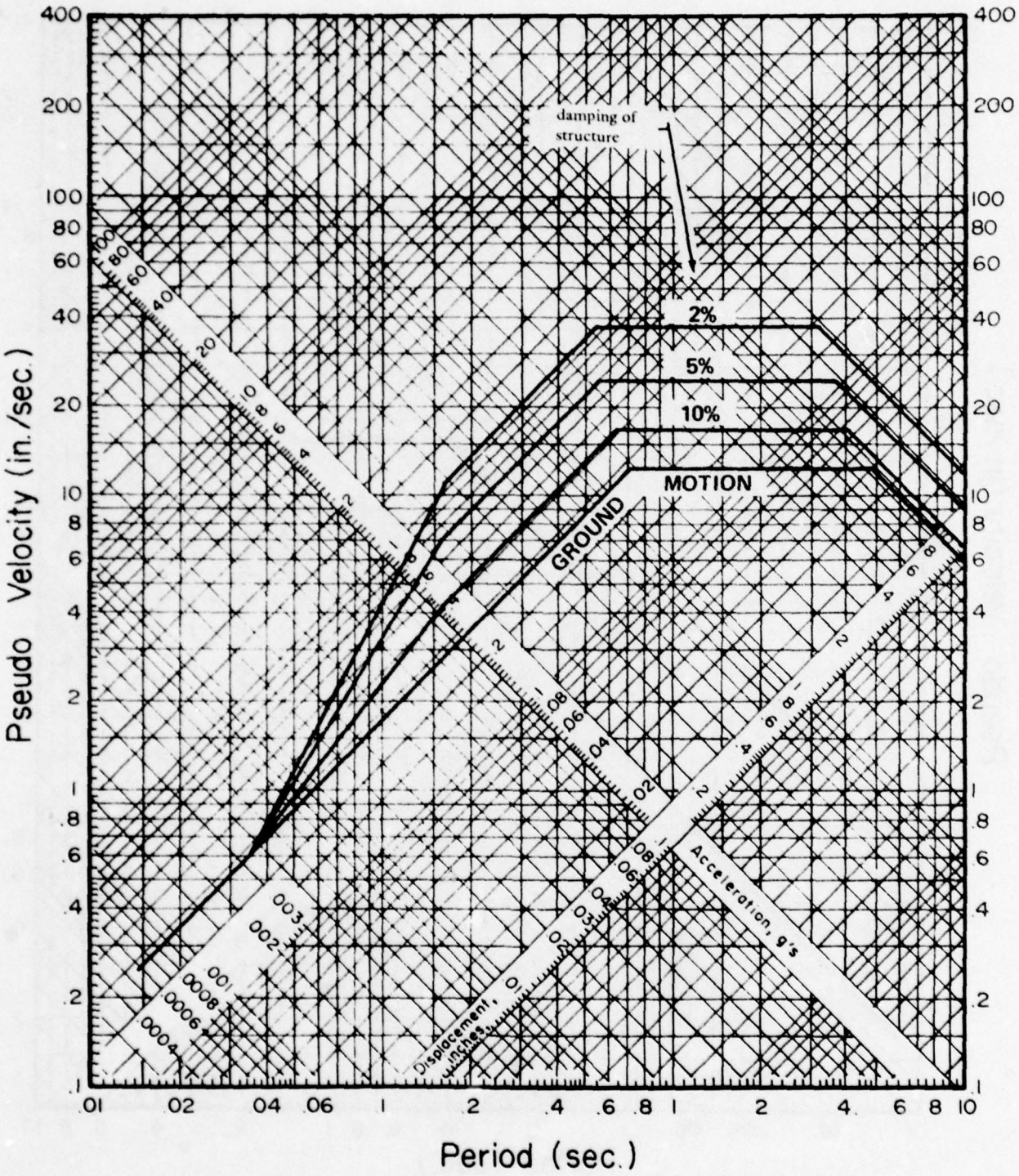

Figure 8-4. Elastic response spectra, collapse threshold level (from Applied Technology Council, 1974).

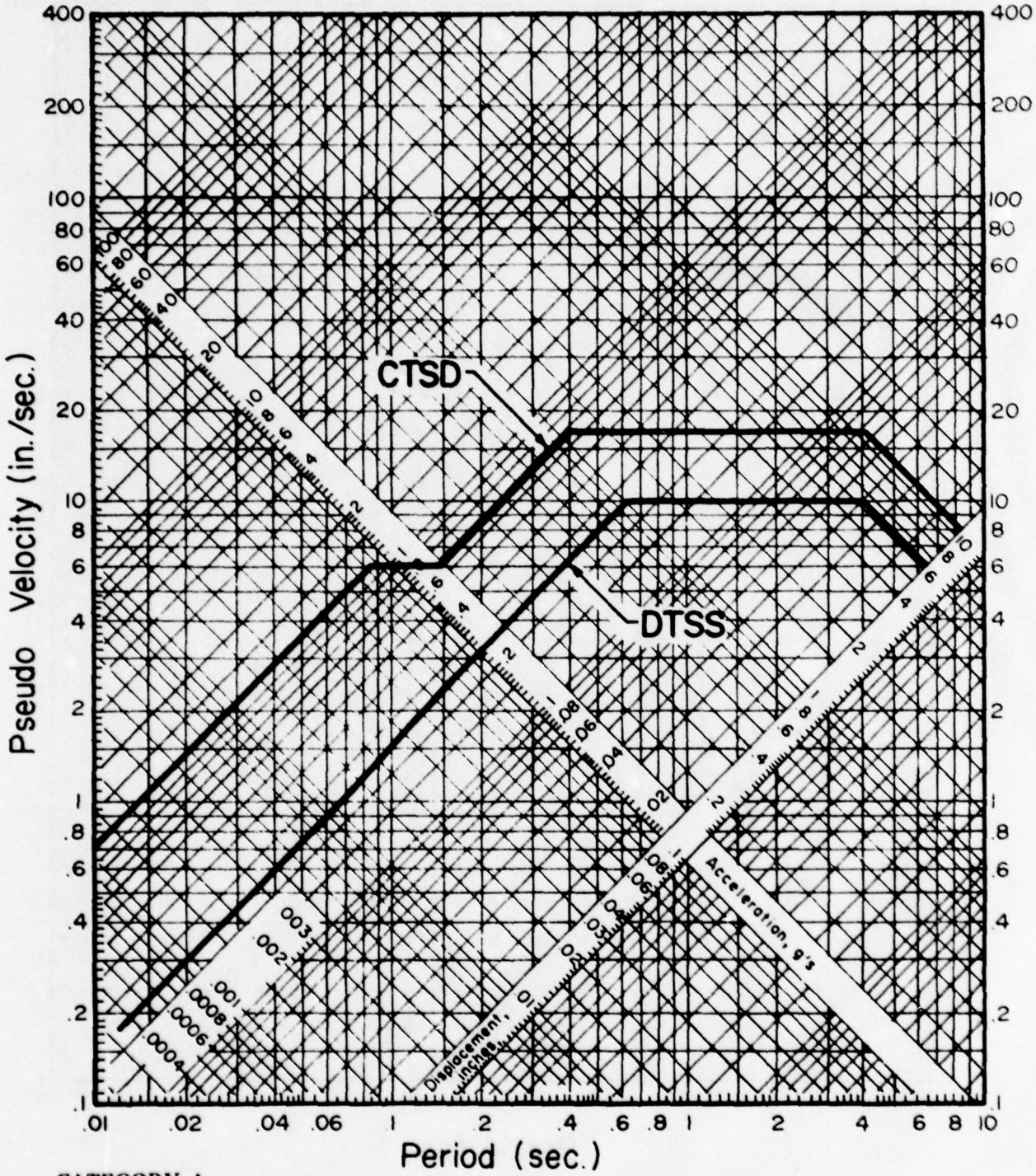

CATEGORY A

DTSS—Damage Threshold Spectrum for Strength $\mu'_D = 1.5$ $\beta'_D = 10\%$

CTSD—Collapse Threshold Spectrum for Deformation $\mu'_C = 4.0$ $\beta'_C = 10\%$

Figure 8-5. Modified design spectra for Category A buildings (from Applied Technology Council, 1974).

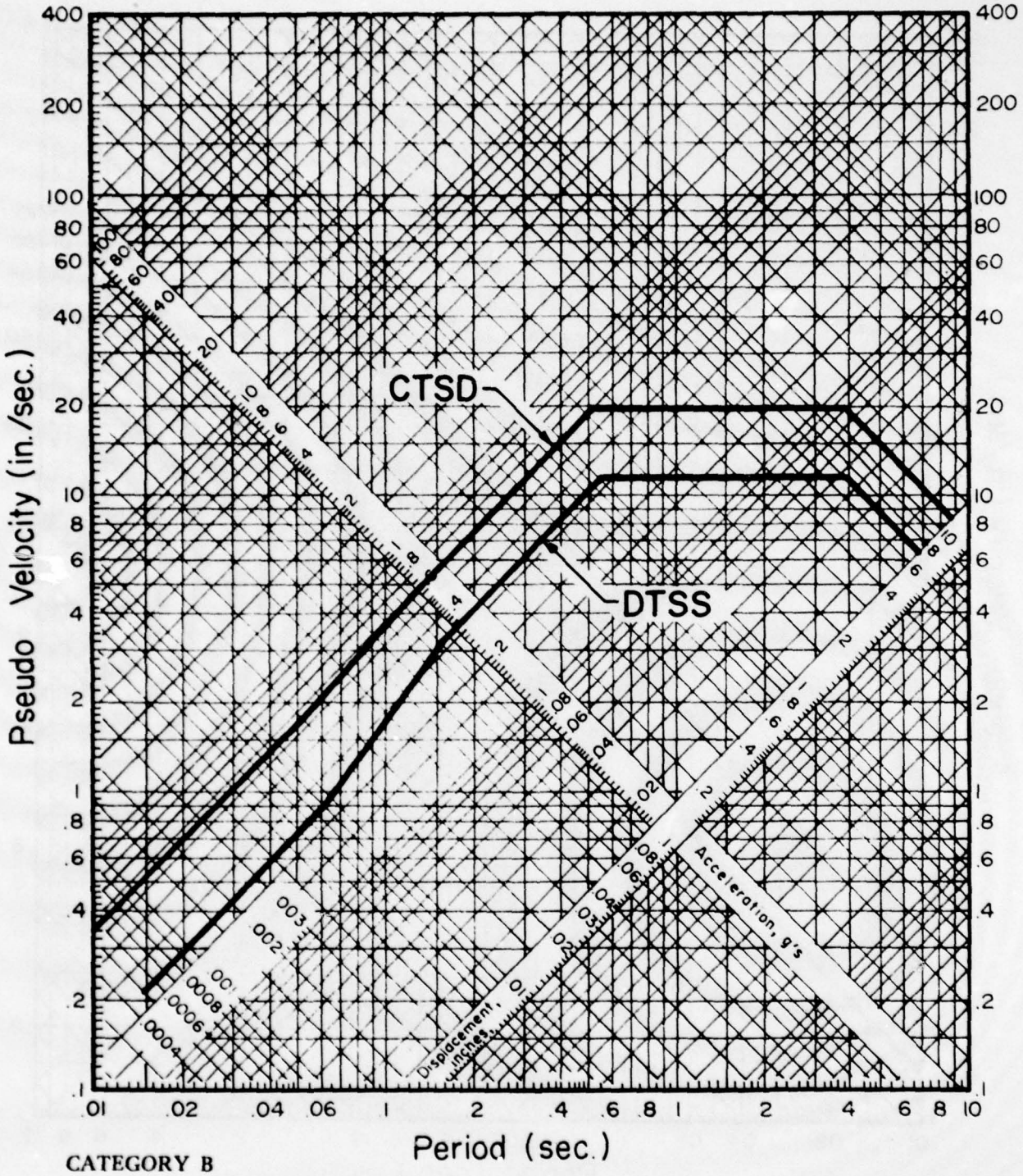

CATEGORY B

DTSS—Damage Threshold Spectrum for Strength	$\mu'_D = 1.5$	$\beta'_D = 7\%$
CTSD—Collapse Threshold Spectrum for Deformation	$\mu'_C = 2.0$	$\beta'_C = 7\%$

Figure 8-6. Modified design spectra for Category B buildings (from Applied Technology Council, 1974).

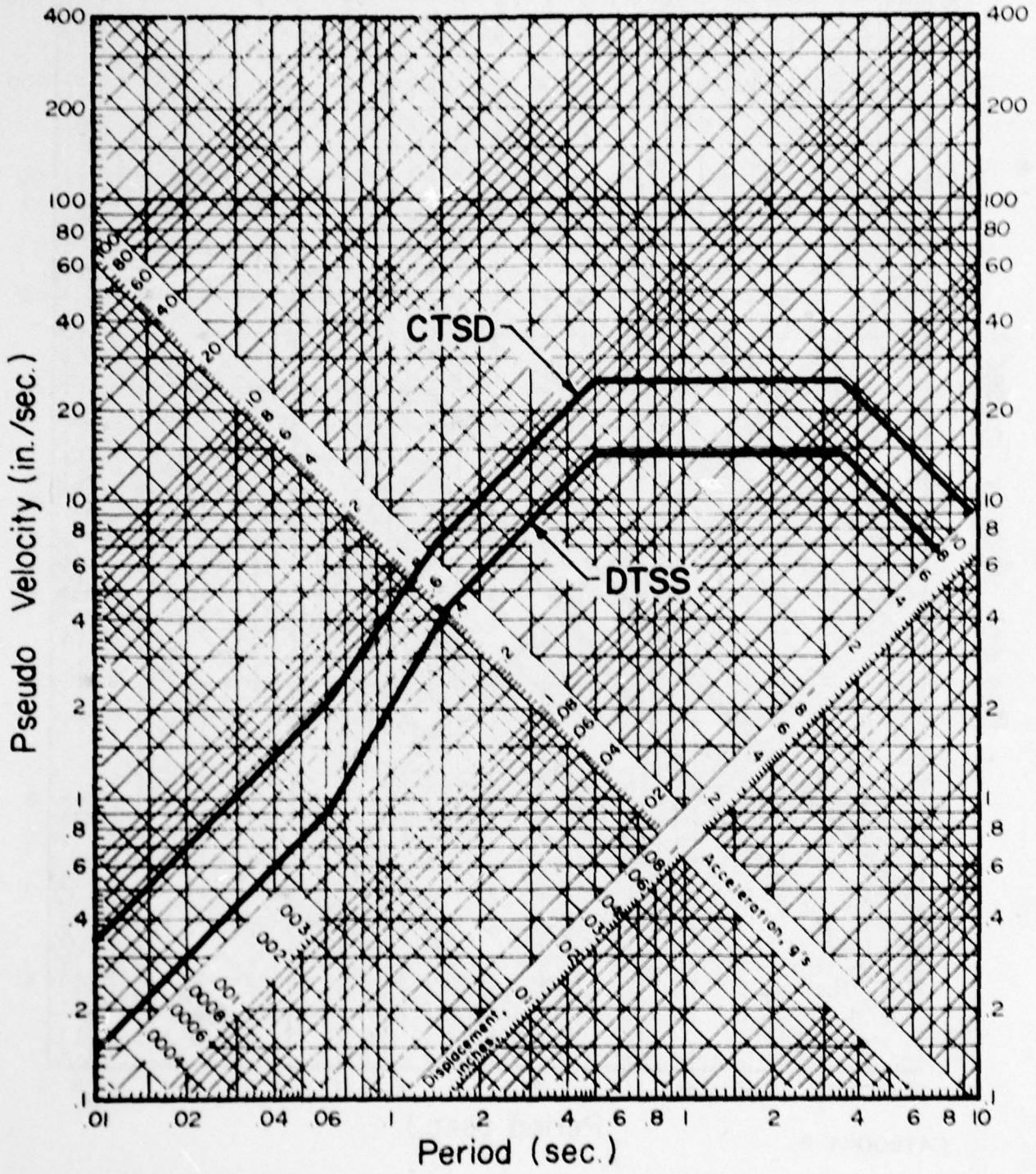

CATEGORY C

DTSS—Damage Threshold Spectrum for Strength	$\mu'_D = 1.5$	$\beta'_D = 5\%$
CTSD—Collapse Threshold Spectrum for Deformation	$\mu'_C = 2.0$	$\beta'_C = 5\%$

Figure 8-7. Modified design spectra for Category C buildings (from Applied Technology Council, 1974).

Percent of Critical Damping	Amplification Factors for Control Points			
	Acceleration[1]			Displacement[1]
	A(33 Hz)	B(9 Hz)	C(2.5 Hz)	D(0.25 Hz)
0.5	1.0	4.96	5.95	3.20
2.0	1.0	3.54	4.25	2.50
5.0	1.0	2.61	3.13	2.05
7.0	1.0	2.27	2.72	1.88
10.0	1.0	1.90	2.28	1.70

[1] Maximum ground displacement is taken proportional to maximum ground acceleration, and is 36 in. for ground acceleration of 1.0 gravity.

(a) Amplification factors.

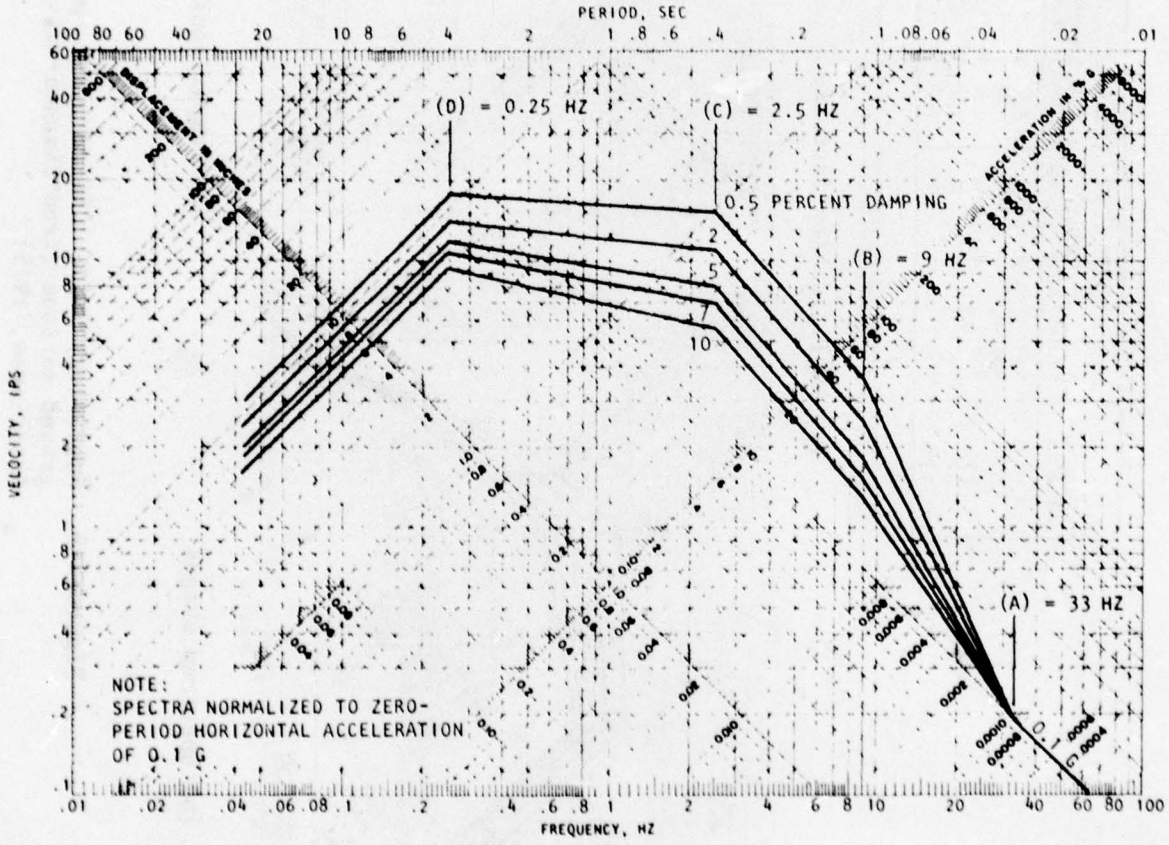

(b) Spectrum shapes.

Figure 8-8. Regulatory Guide 1.60 response spectra--horizontal ground motions (from Shannon-Wilson and Agbabian Associates, 1975).

Percent of Critical Damping	Amplification Factors for Control Points				
	Acceleration[1]				Displacement[1]
	(A' (50 Hz)	A(33 Hz)	B(9 Hz)	C(3.5 Hz)	D(0.25 Hz)
0.5	0.67	1.0	4.96	5.67	2.13
2.0	0.67	1.0	3.54	4.05	1.67
5.0	0.67	1.0	2.61	2.98	1.37
7.0	0.67	1.0	2.27	2.59	1.25
10.0	0.67	1.0	1.90	2.17	1.13

[1]Maximum ground displacement is taken proportional to maximum ground acceleration and is 36 in. for ground acceleration of 1.0 gravity.

(a) Amplification factors.

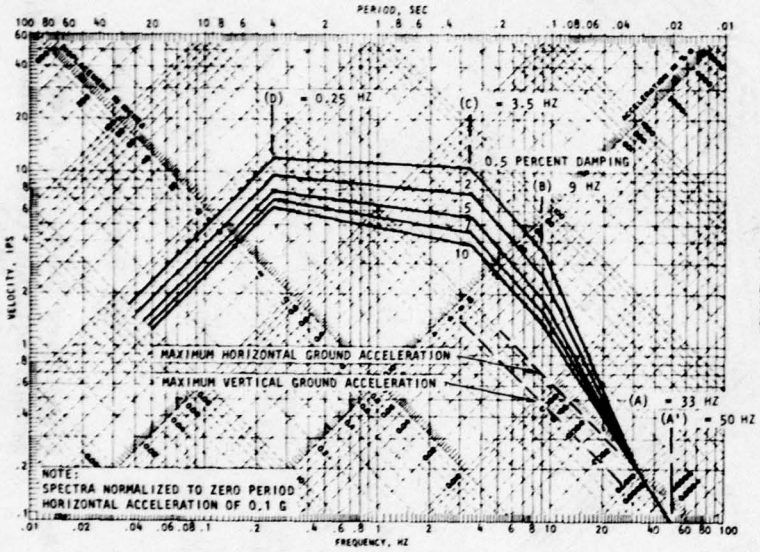

(b) Spectrum shapes.

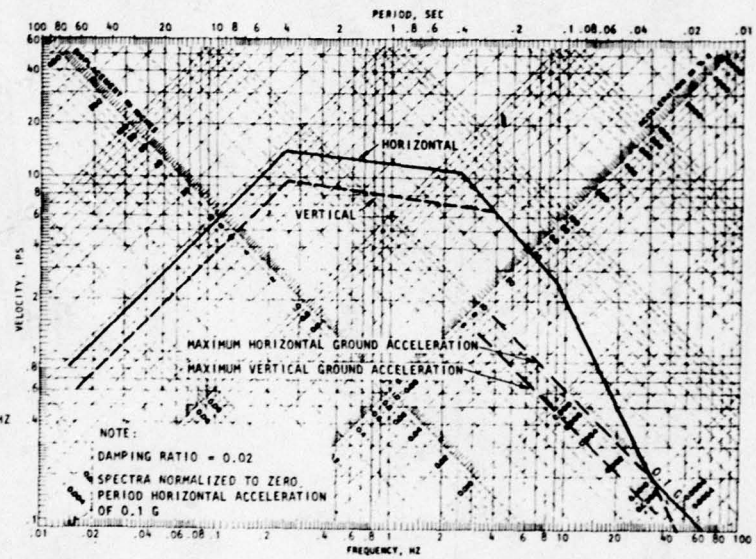

(c) Comparisons of horizontal and vertical spectra.

Figure 8-9. Regulatory Guide 1.60 response spectra--vertical ground motions (from Shannon-Wilson and Agbabian Associates, 1975).

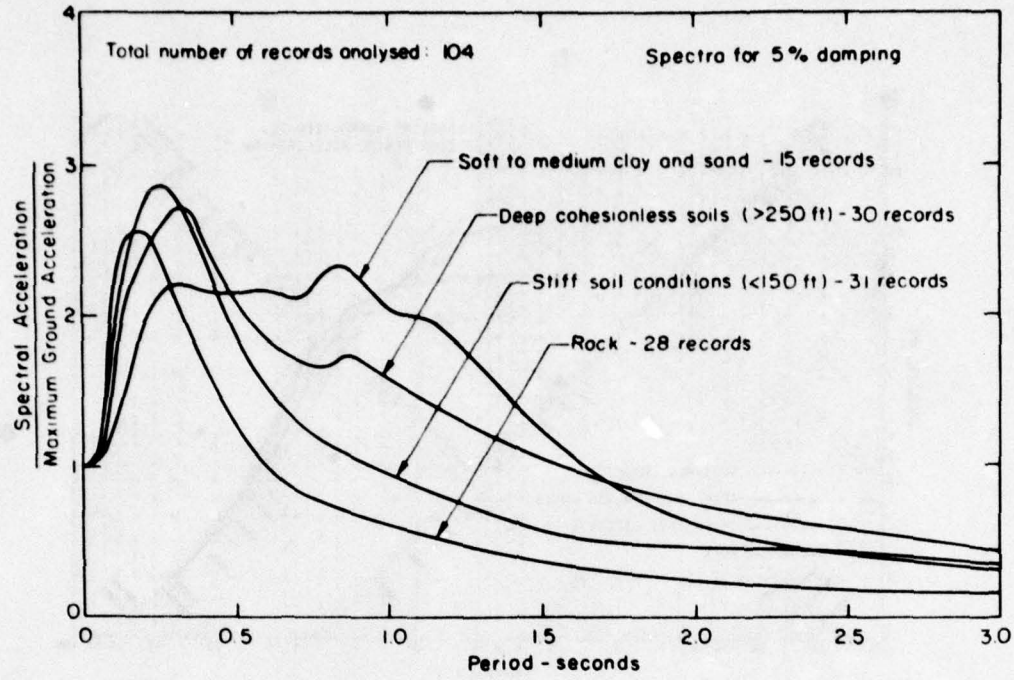

(a) Average acceleration spectra for different site conditions.

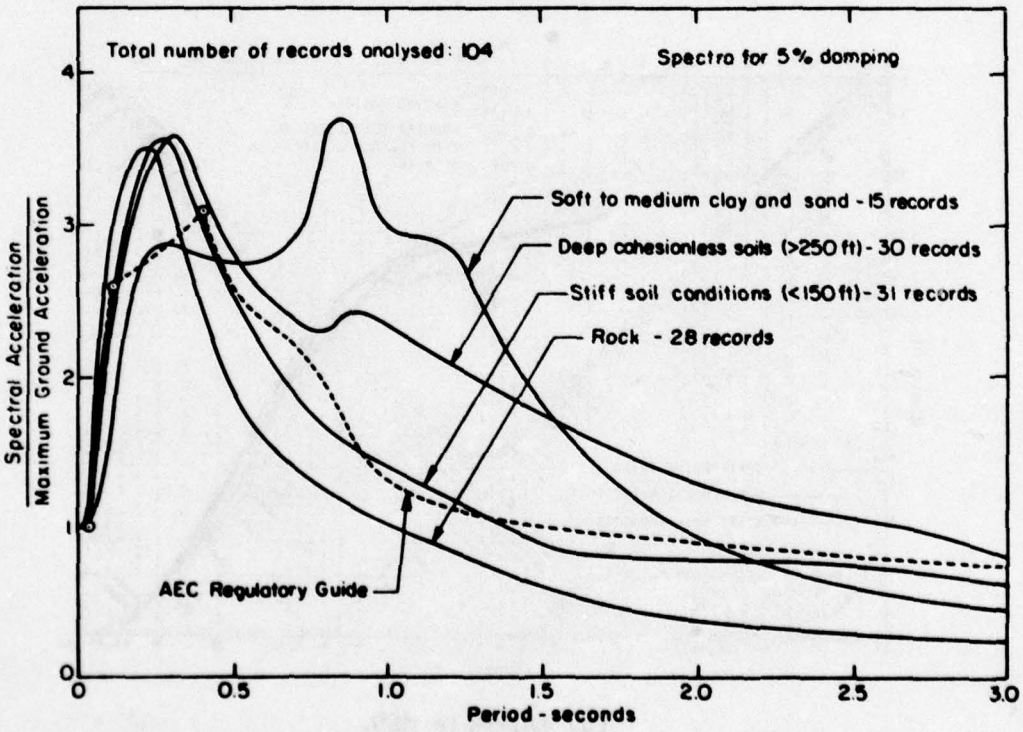

(b) 84th percentile acceleration spectra for different site conditions.

Figure 8-10. Seed-Ugas-Lysmer spectrum shapes (arithmetic plot) (from Seed, Ugas, and Lysmer, 1974).

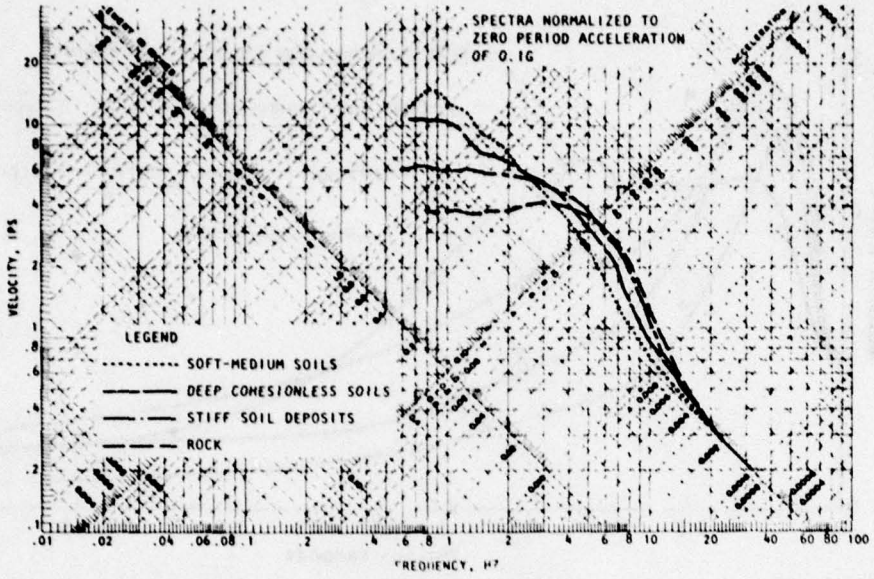

(a) Ensemble average.

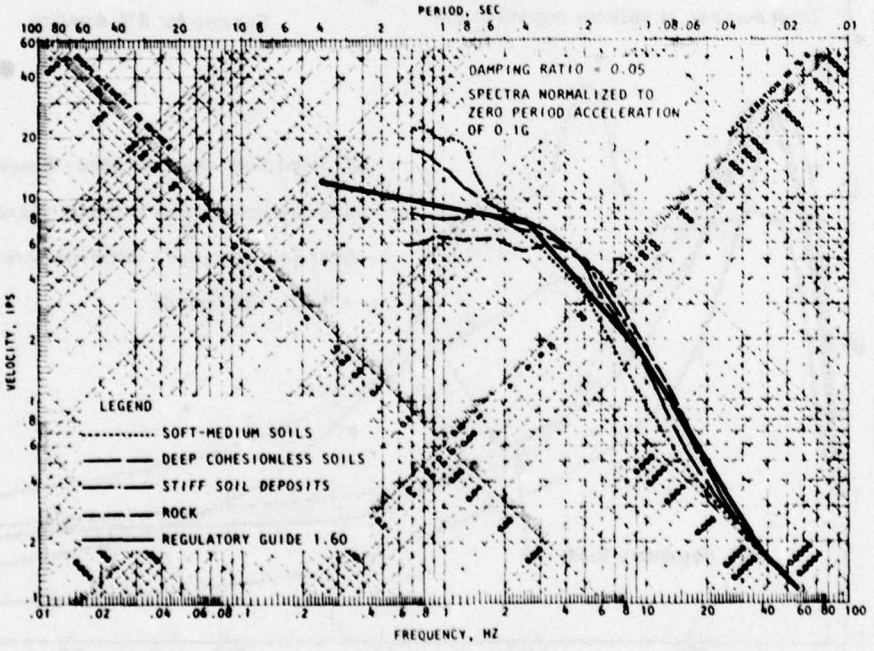

(b) Ensemble MSD.

Figure 8-11. Seed-Ugas-Lysmer spectrum shapes based on local soil conditions (from Shannon-Wilson and Agbabian Associates, 1975).

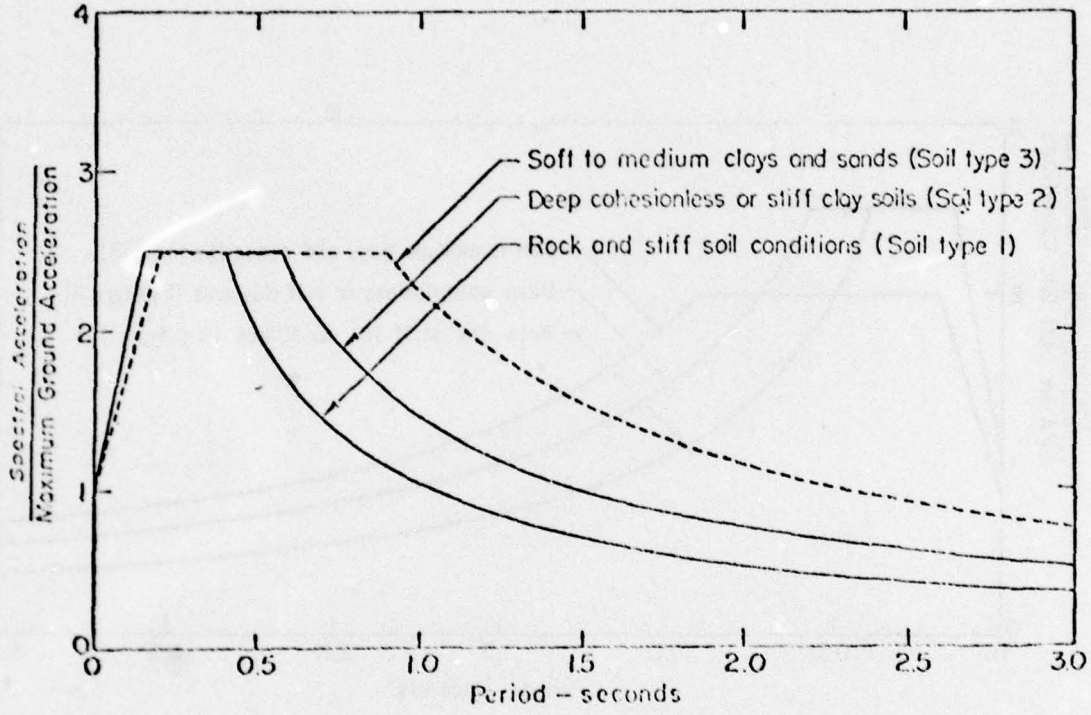

Figure 8-12. Normalized spectral curves recommended for use in building code (from Applied Technology Council, 1976).

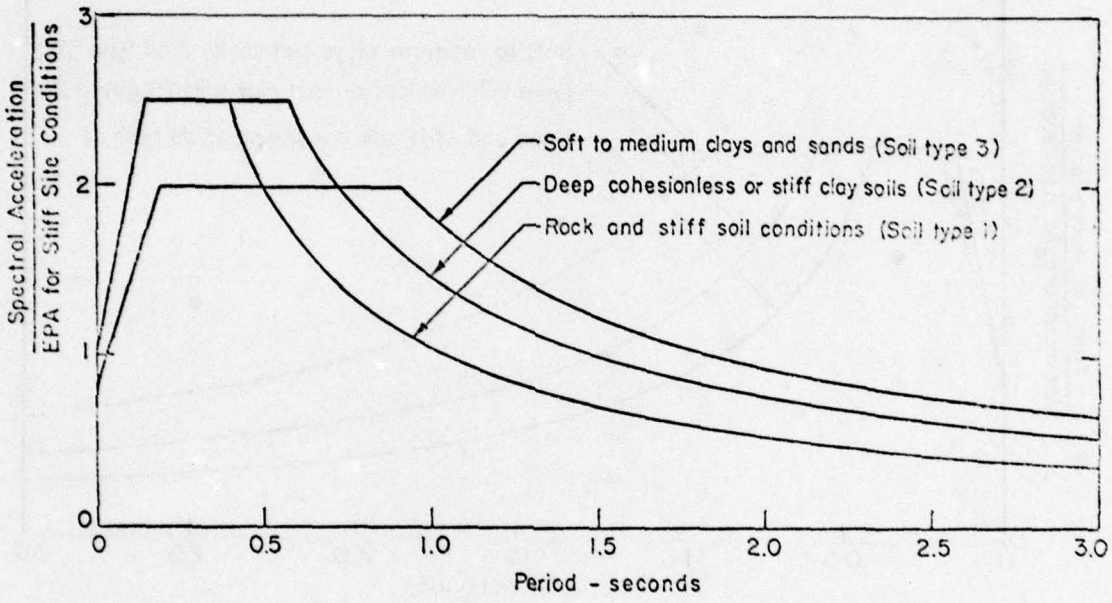

Figure 8-13. Spectral curves for use in building code normalized to EPA for stiff site conditions (from Applied Technology Council, 1976).

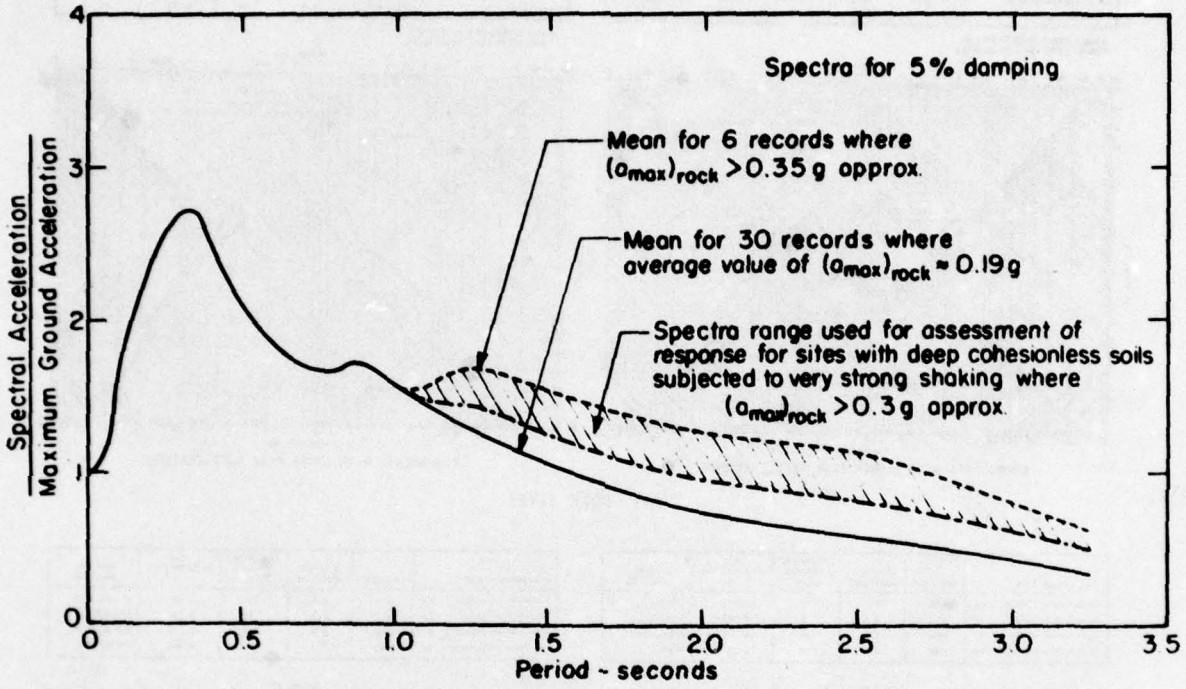

Figure 8-14. Effect of shaking intensity on normalized acceleration spectra for deep cohesionless soil sites (from Seed, Ugas, Lysmer, 1974).

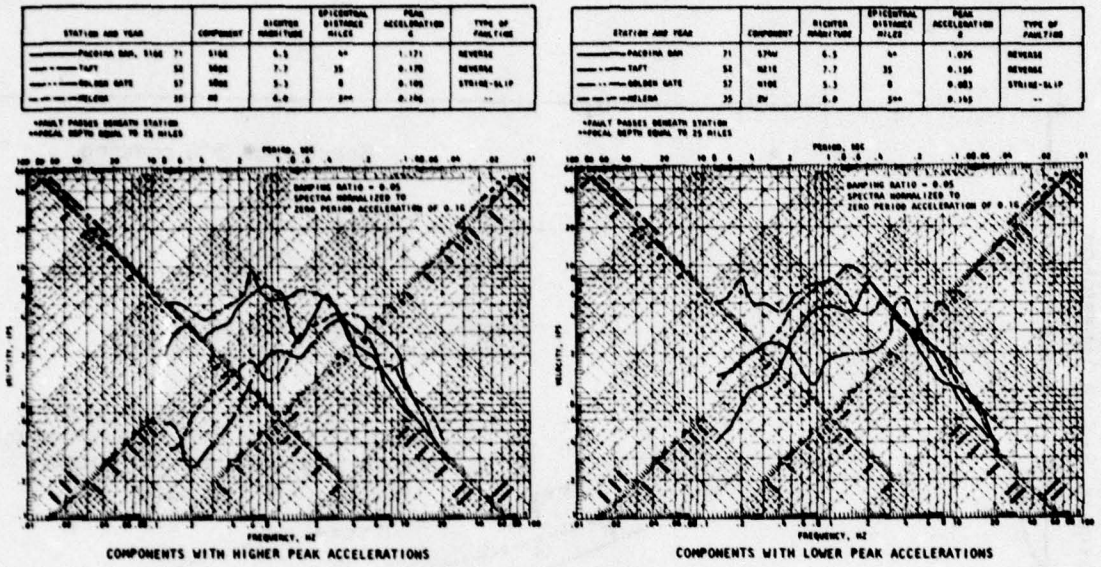

(a) ROCK SITES

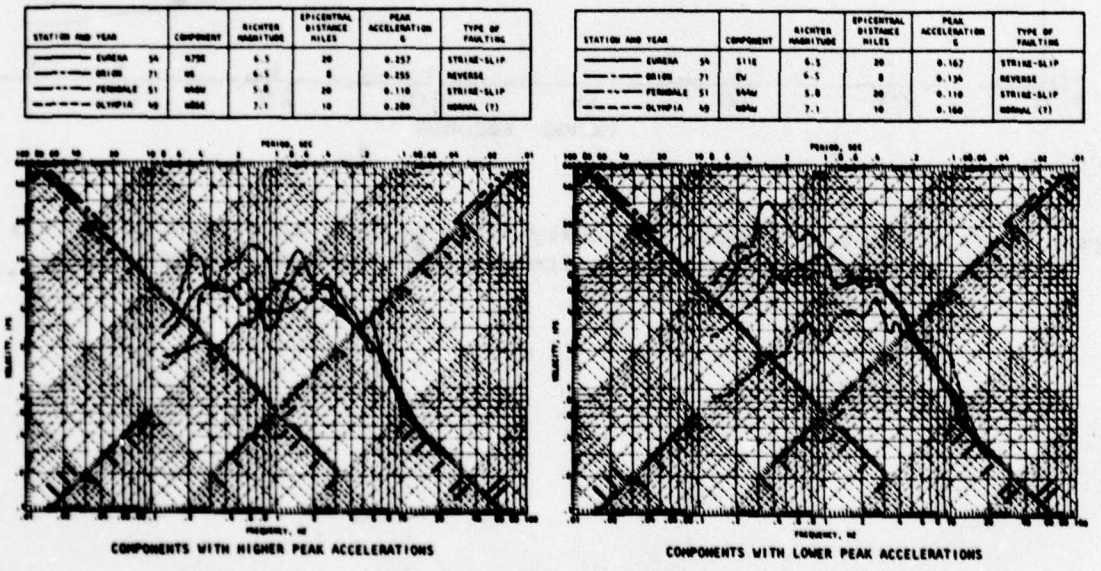

(b) DEEP-COHESIONLESS SOIL SITES

Figure 8-15. Comparisons of individual spectra with similar site conditions (from Shannon-Wilson and Agbabian Associates, 1975).

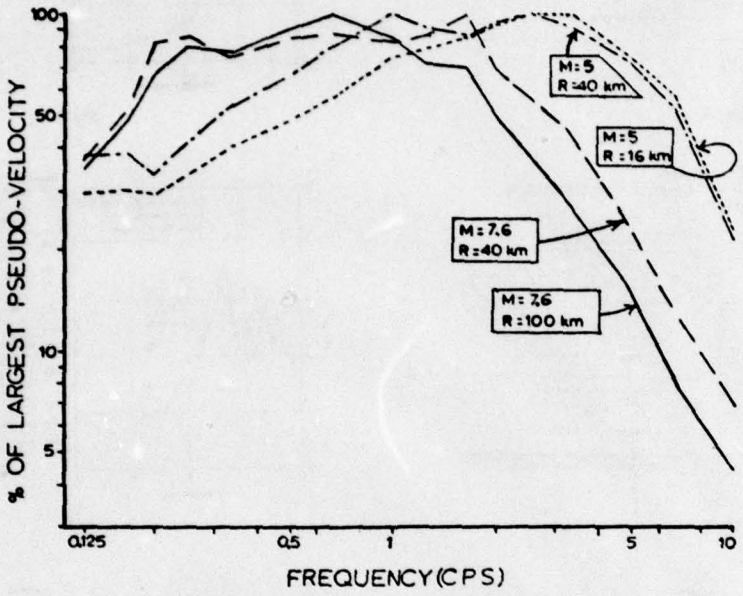

Figure 8-16. Predicted pseudo-velocities at different frequencies for earthquakes of several magnitudes and distances, normalized to maximum pseudo-velocity at any frequency for that magnitude and distance (reproduced with permission from "Seismic design spectra and mapping procedures using hazard analysis based directly on oscillator response," by R. K. McGuire, Earthquake Engineering and Structural Dynamics, 5 211-234, 1977. Copyright © 1977, John Wiley & Sons Limited).

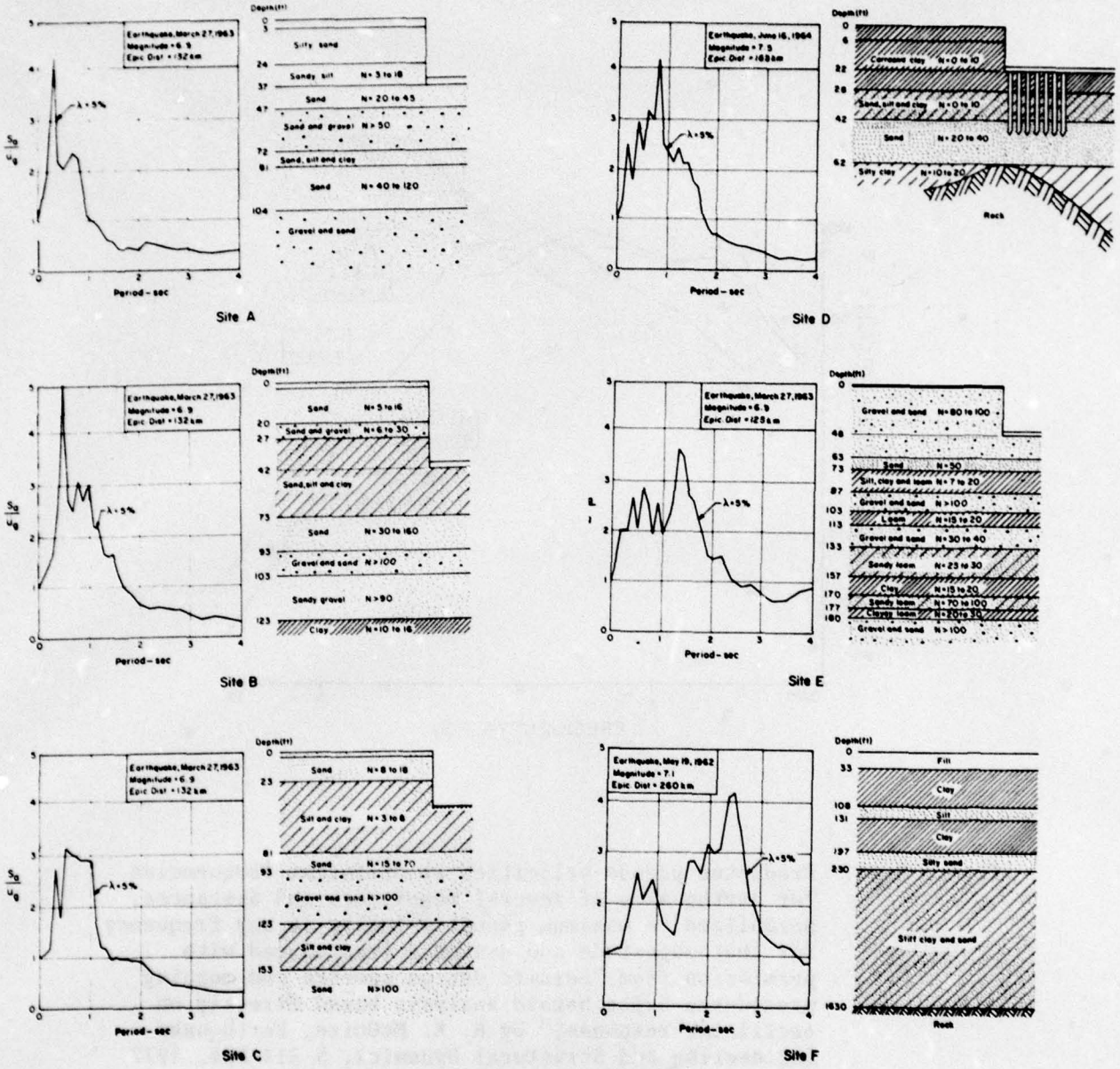

Figure 8-17. Effect of soil conditions on form of response spectra (from "Influence of soil conditions on ground motion during earthquakes," by H. B. Seed and I. M. Idriss, in Journal of the Soil Mechanics and Foundations Division, ASCE, vol 95, no. SM1, Jan 1969, figure 7).

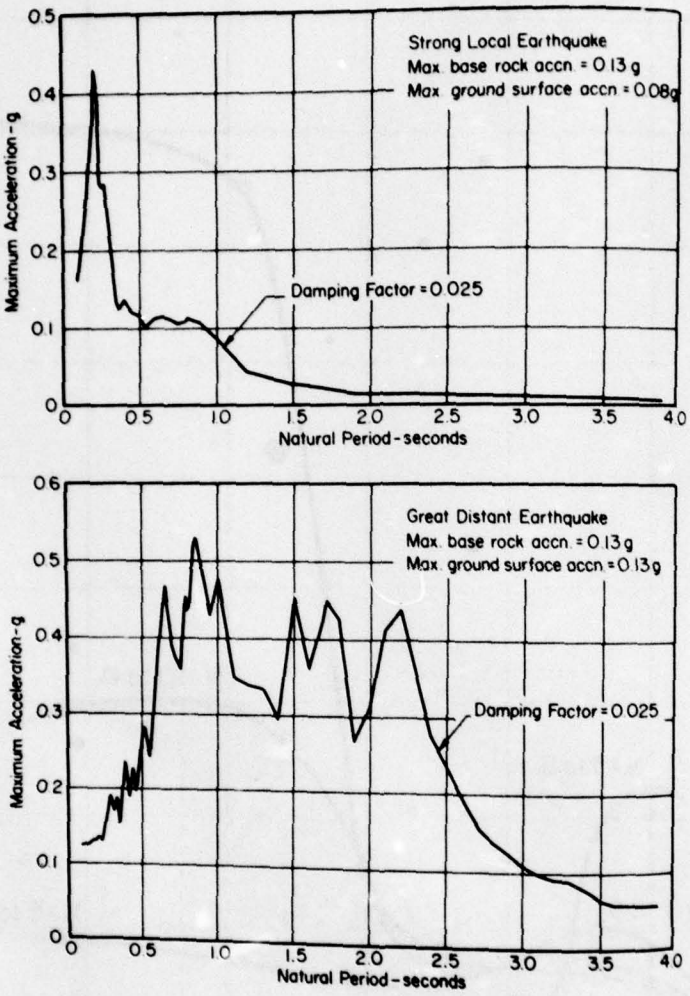

Figure 8-18. Acceleration spectra for computed ground surface accelerations at a site during two earthquakes with equal maximum base rock accelerations (from "Influence of soil conditions on ground motions during earthquakes," by H. B. Seed and I. M. Idriss, in Journal of the Soil Mechanics and Foundations Division, ASCE, vol 95, SM1, Jan 1969, figure 25).

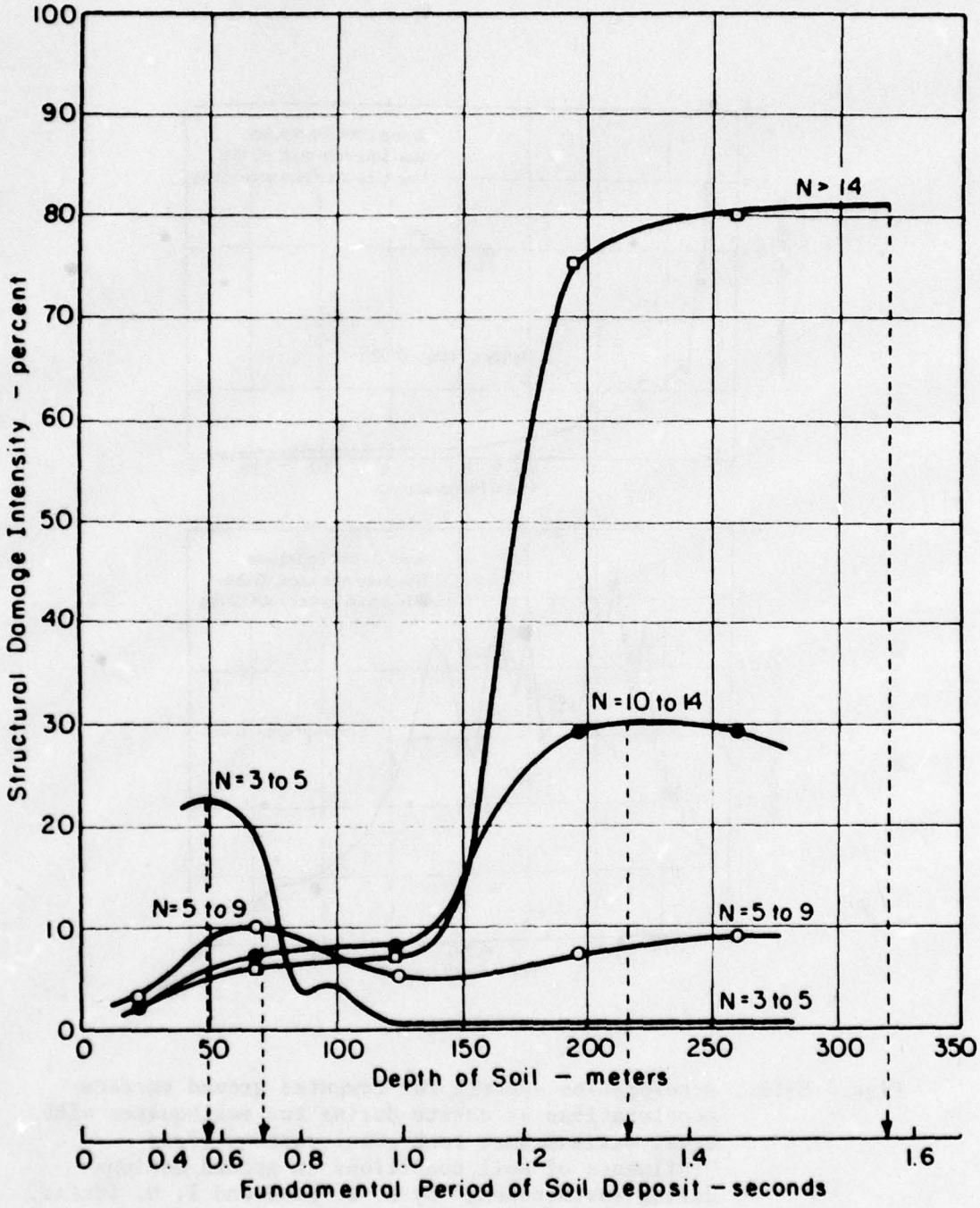

Figure 8-19. Relationship between structural damage intensities and computed fundamental periods of soil deposits (from Seed, 1975).

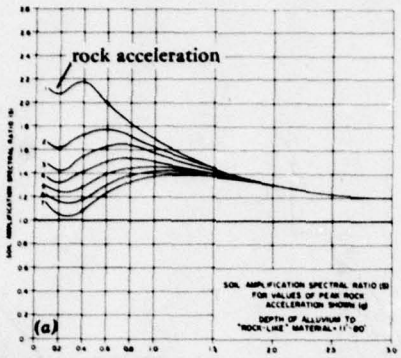

(a) Shallow stiff.

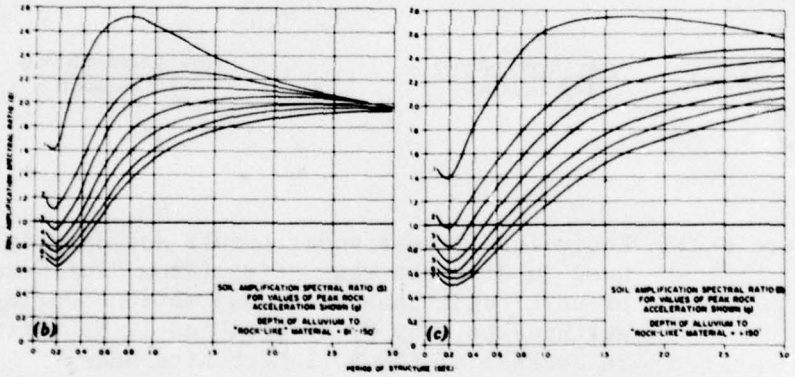

(b) Medium.

(c) Deep soft.

Figure 8-20. Soil amplification spectral ratio (from "California seismic design criteria for bridges," by J. H. Gates, in Journal of the Structural Division, vol 102, no. ST12, Dec 1976, figure 4).

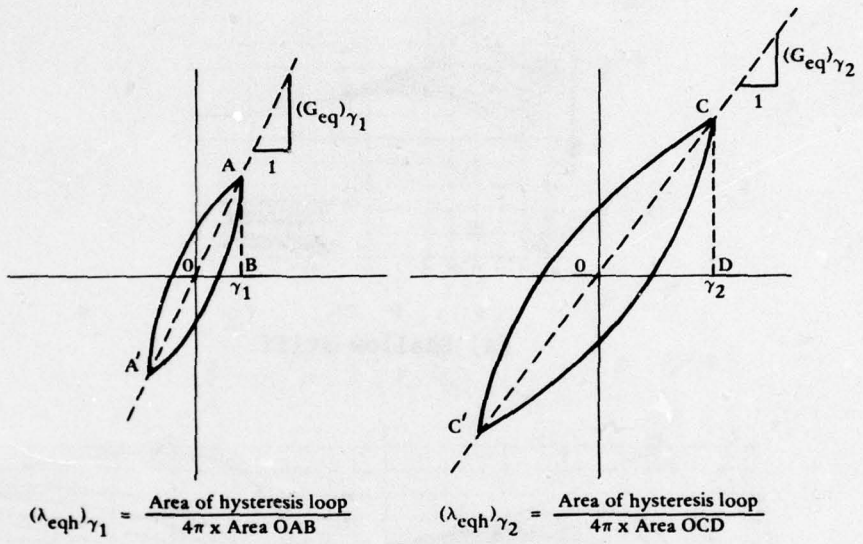

Figure 8-21. Equivalent linear shear moduli and damping used in discrete mass model (from "Influence of soil conditions on ground motions during earthquakes," by H. B. Seed and I. M. Idriss, in Journal of the Soil Mechanics and Foundations Division, ASCE, vol 95, no. SM1, Jan 1969, figure 13).

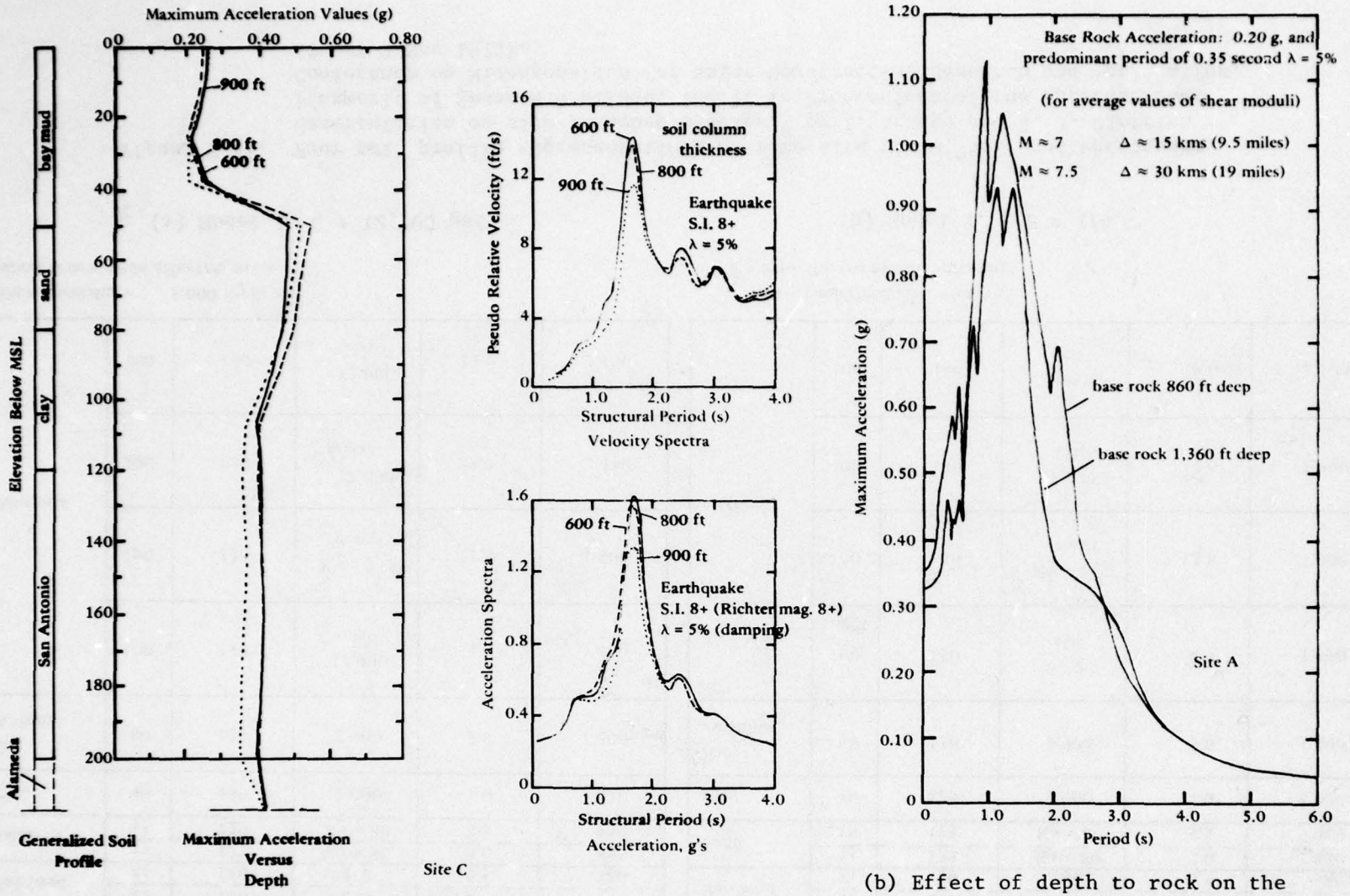

(a) Influence of depth to bedrock.

(b) Effect of depth to rock on the acceleration response spectra.

Figure 8-22. Response spectra and maximum surface accelerations (from "Soil and earthquake uncertainties on site response studies," by I. Arango and R. J. Dietrich [formerly of Shannon & Wilson, Inc.], in Proceedings of the International Conference on Microzonation for Safer Construction Research and Application, 30 Oct-3 Nov 1972).

Layer Classification	Layer Thick-ness (ft)	Unit Weight γT pcf	Strength Su (psf) or K_2*	Shear Modulus g x 10^6 (psf)	Shear Wave Velocity, Vs fps
Bay Mud	21	110	200	0.4	340
	21	110	250	0.5	380
Sand	15	125	K_2 = 80	3.0	880
	15	125	K_2 = 80	3.6	960
Clay	40	130	2,000	4.0	1,020
San Antonio	80	130	2,900	5.8	1,200
Alameda	100	130	12,000 clay	4.0	2,400
	100	130	K_2 = 115 gravel	12.8	1,800
	100	130	12,000 clay	24.0	2,440
	100	130	12,000 clay	24.0	2,440

*Shear modulus = $1{,}000\ K_2\ (\sigma' m)^{1/2}$
where $\sigma' m$ = mean effective stress.

(a) Model 1, C + 12,000 psf.

Layer Classification	Layer Thick-ness (ft)	Unit Weight γT pcf	Strength Su (psf) or K_2*	Shear Modulus g x 10^6 (psf)	Shear Wave Velocity, Vs fps
Bay Mud	21	110	200	0.4	340
	21	110	250	0.5	380
Sand	15	125	K_2 = 80	3.0	880
	15	125	K_2 = 80	3.6	960
Clay	40	125	2,000	4.0	1,020
San Antonio	80	130	2,900	5.8	1,200
Alameda	100	130	3,700 clay	7.4	1,350
	100	130	K_2 = 115 gravel	12.8	1,800
	100	130	7,300 clay	14.6	1,900
	100	130	9,000 clay	18.0	2,100

C = Su = Undrained clay strength.
P = Effective overburden pressure.

(b) Model 2, C/P = 1/4.

Figure 8-23. Four soil profile representations of same site (from "Soil and earthquake uncertainties on site response studies," by I. Arango and R. J. Dietrich [formerly of Shannon & Wilson, Inc.], in Proceedings of the International Conference on Microzonation for Safer Construction Research and Application, 30 Oct-3 Nov 1972).

Layer Classification	Layer Thick-ness (ft)	Unit Weight γT pcf	Strength Su (psf) or K_2*	Shear Modulus g x 10^6 (psf)	Shear Wave Velocity, Vs fps
Bay Mud	21	110	200	0.4	340
	21	110	250	0.5	380
Sand	15	125	K_2 = 80	3.0	880
	15	125	K_2 = 80	3.6	960
Clay	40	130	2,000	4.0	1,020
San Antonia	80	130	2,900	5.8	1,200
Alameda	100	130	6,000 clay	12.0	1,730
	100	130	K_2 = 115 gravel	12.8	1,780
	100	130	10,000 clay	20.0	2,240
	100	130	10,000 clay	20.0	2,240

***Strength between Models 1 and 2.

(c) Model 3, Intermediate properties.

Layer Classification	Layer Thick-ness (ft)	Unit Weight γT pcf	Strength Su (psf) or K_2*	Shear Modulus g x 10^6 (psf)	Shear Wave Velocity, Vs fps
Bay Mud	21	110	200	0.4	340
	21	110	250	0.5	380
Sand	15	125	K_2 = 80	3.0	880
	15	125	K_2 = 80	3.6	960
Clay	40	130	2,000	4.0	1,020
San Antonio	80	130	2,900	5.8	1,200
Alameda	100	130	4,950 clay	9.9	1,560
	100	130	7,240 clay	14.5	1,900
	100	130	9,500 clay	19.0	2,170
	100	130	10,750 clay	21.5	2,320

(d) Model 4, C/P = 1/3.

Figure 8-23. Continued.

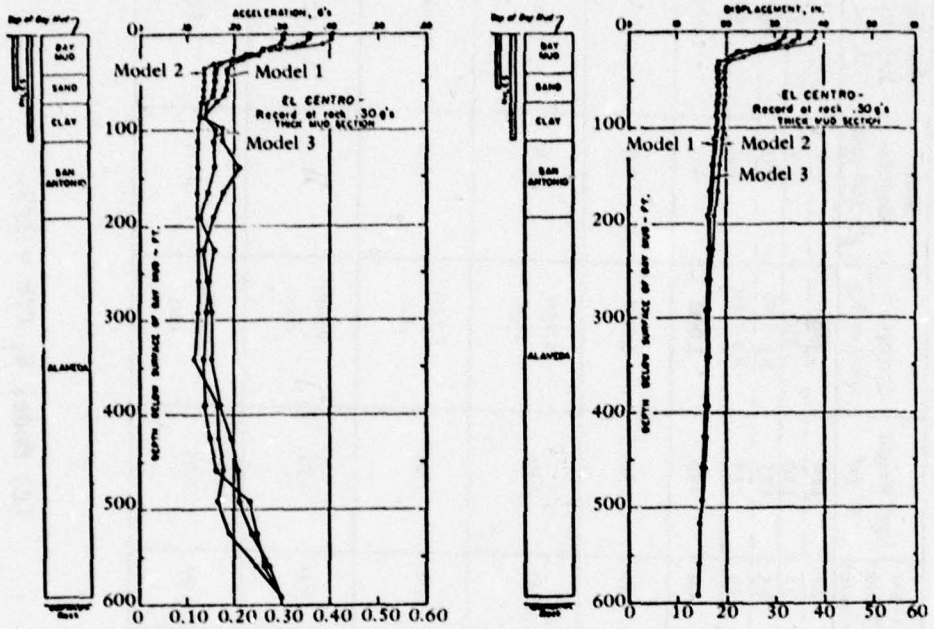

(a) El Centro earthquake.

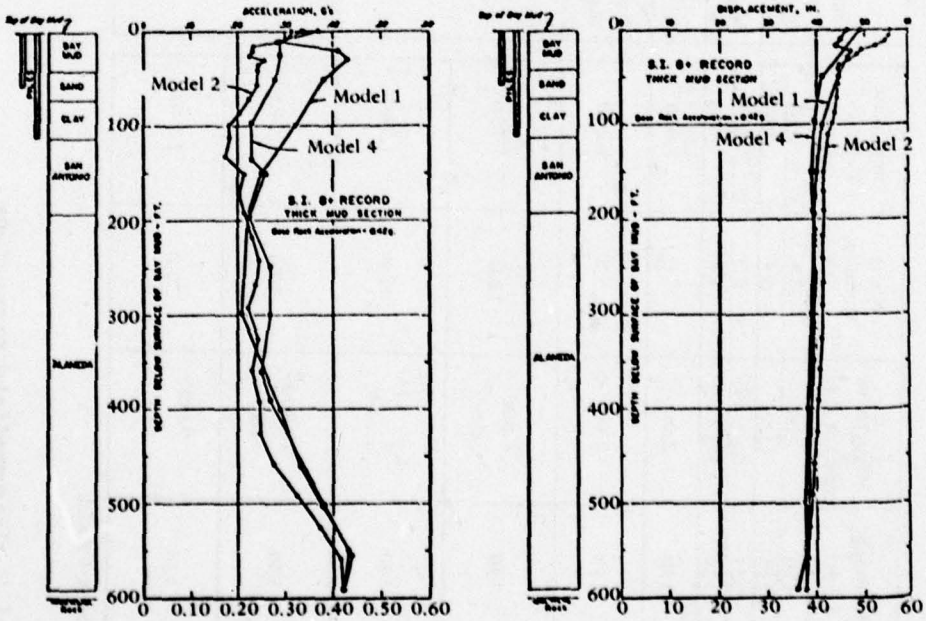

(b) Site intensity = 8+ earthquake.

Figure 8-24. Response of soil models (from "Soil and earthquake uncertainties on site response studies," by I. Arango and R. J. Dietrich [formerly of Shannon & Wilson, Inc.], in Proceedings of the International Conference on Microzonation for Safer Construction Research and Application, 30 Oct-3 Nov 1972).

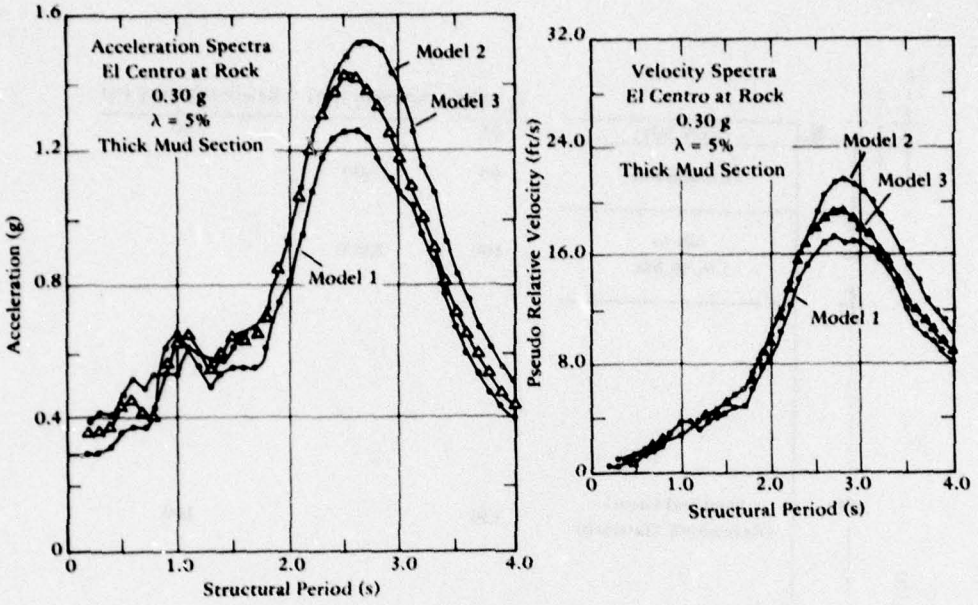

(a) El Centro earthquake.

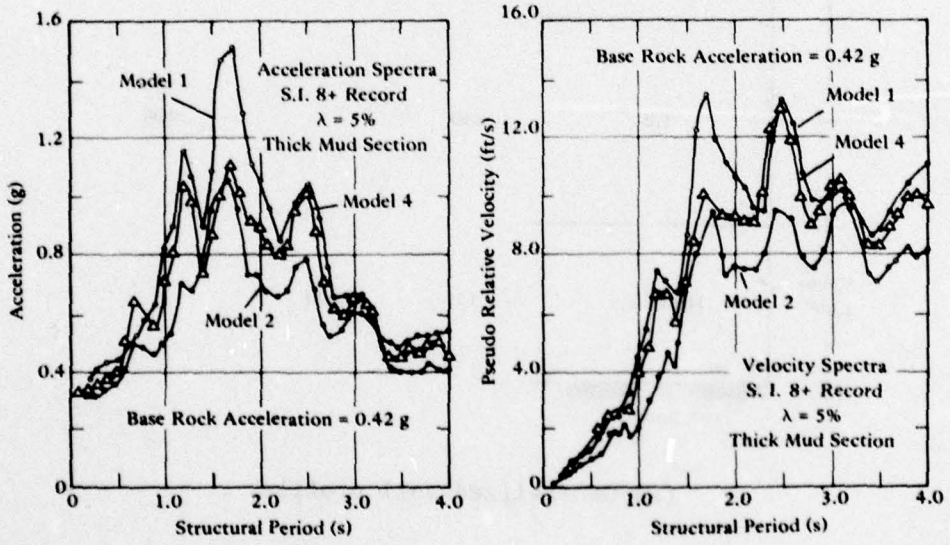

(b) Site intensity = 8+ earthquake.

Figure 8-25. Response spectra (from "Soil and earthquake uncertainties on site response studies," by I. Arango and R. J. Dietrich [formerly of Shannon & Wilson, Inc.], in Proceedings of the International Conference on Microzonation for Safer Construction Research and Application, 30 Oct-3 Nov 1972).

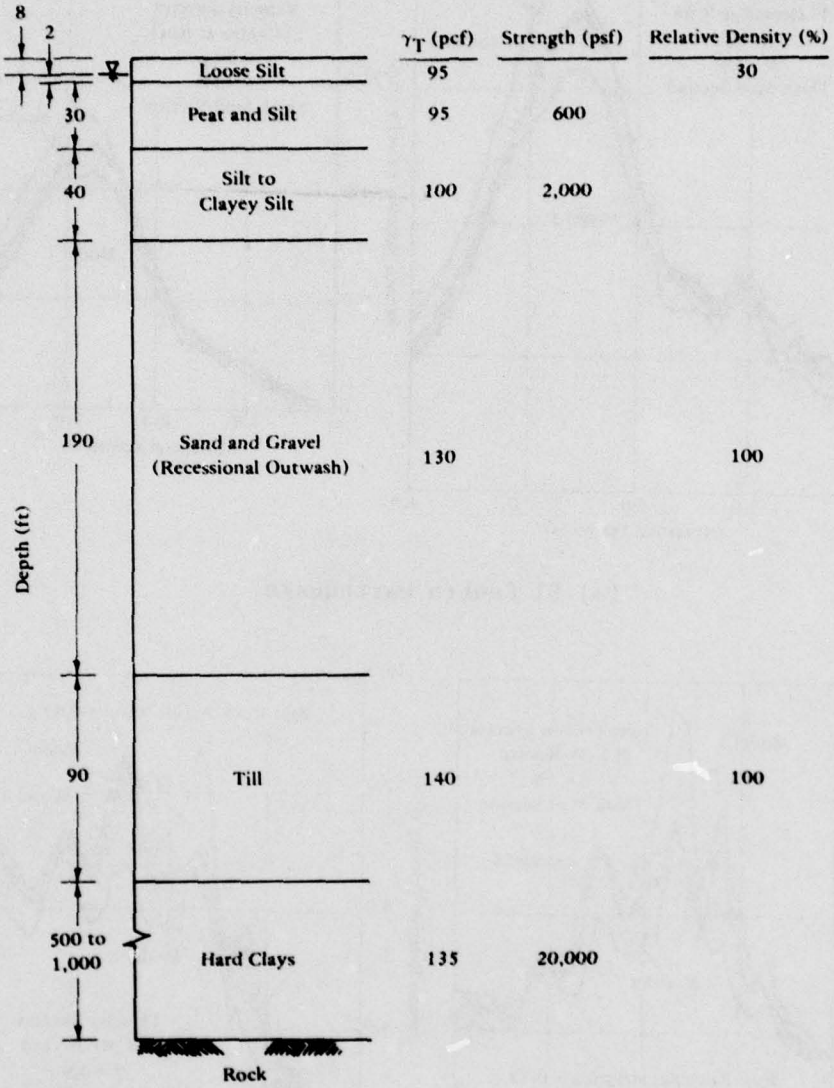

(a) Generalized soil profile.

Figure 8-26. Effect of variation of material properties (from "Soil and earthquake uncertainties on site response studies," by I. Arango and R. J. Dietrich [formerly of Shannon & Wilson, Inc.], in Proceedings of the International Conference on Microzonation for Safer Construction Research and Application, 30 Oct-3 Nov 1972).

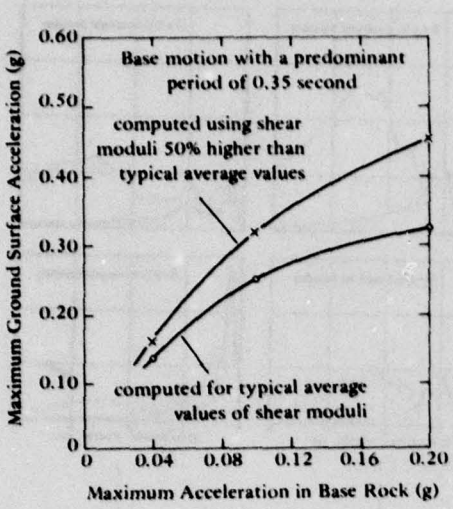

(b) Relationship between maximum ground surface displacement and maximum base rock acceleration.

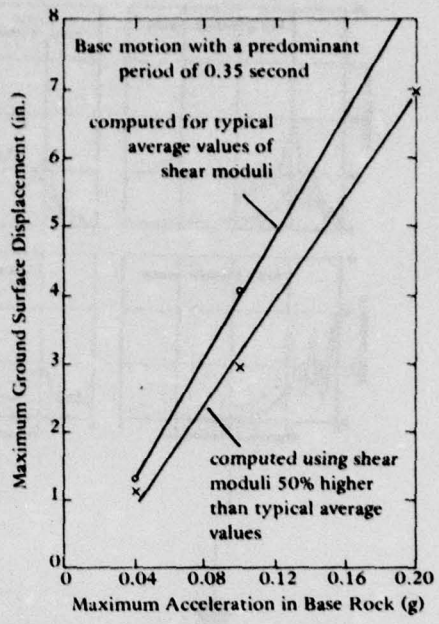

(c) Relationship between maximum ground surface displacement and maximum base rock acceleration.

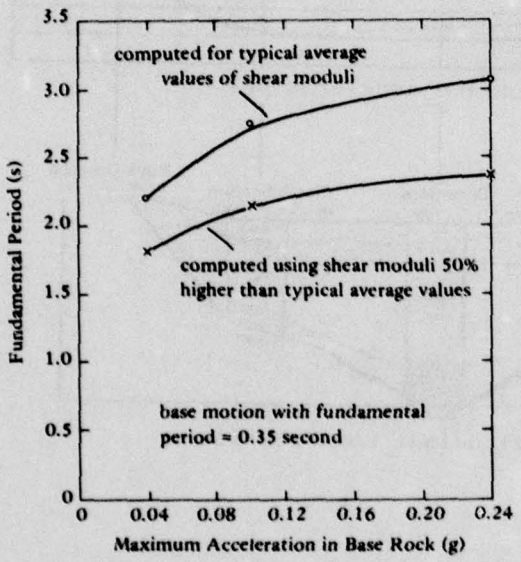

(d) Fundamental period of soil deposit.

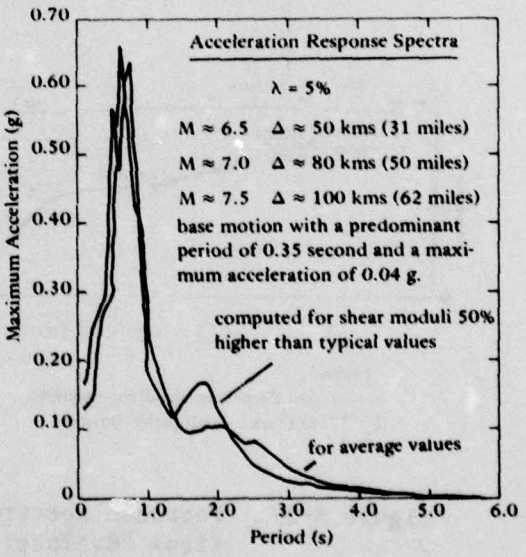

(e) Effect of soil moduli on the acceleration response spectra.

Figure 8-26. Continued.

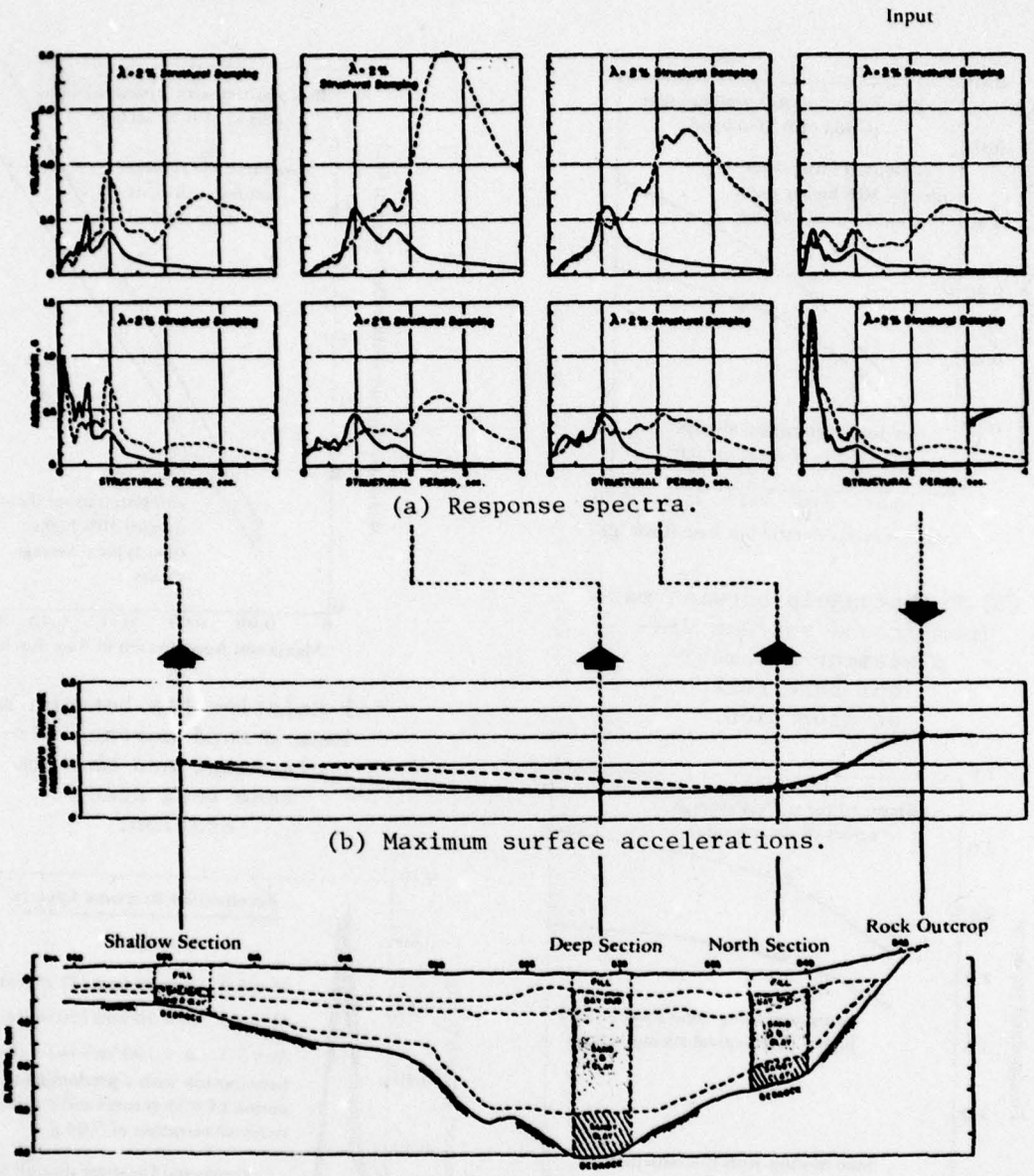

Figure 8-27. Response spectra and maximum surface accelerations (from "Evaluation of soil liquefaction effects on level ground during earthquake," by H. B. Seed in ASCE Preprint 2752, Liquefaction Problems in Geotechnical Engineering, ASCE Annual Convention, Philadelphia, Pa., 27 Sep-1 Oct 1976).

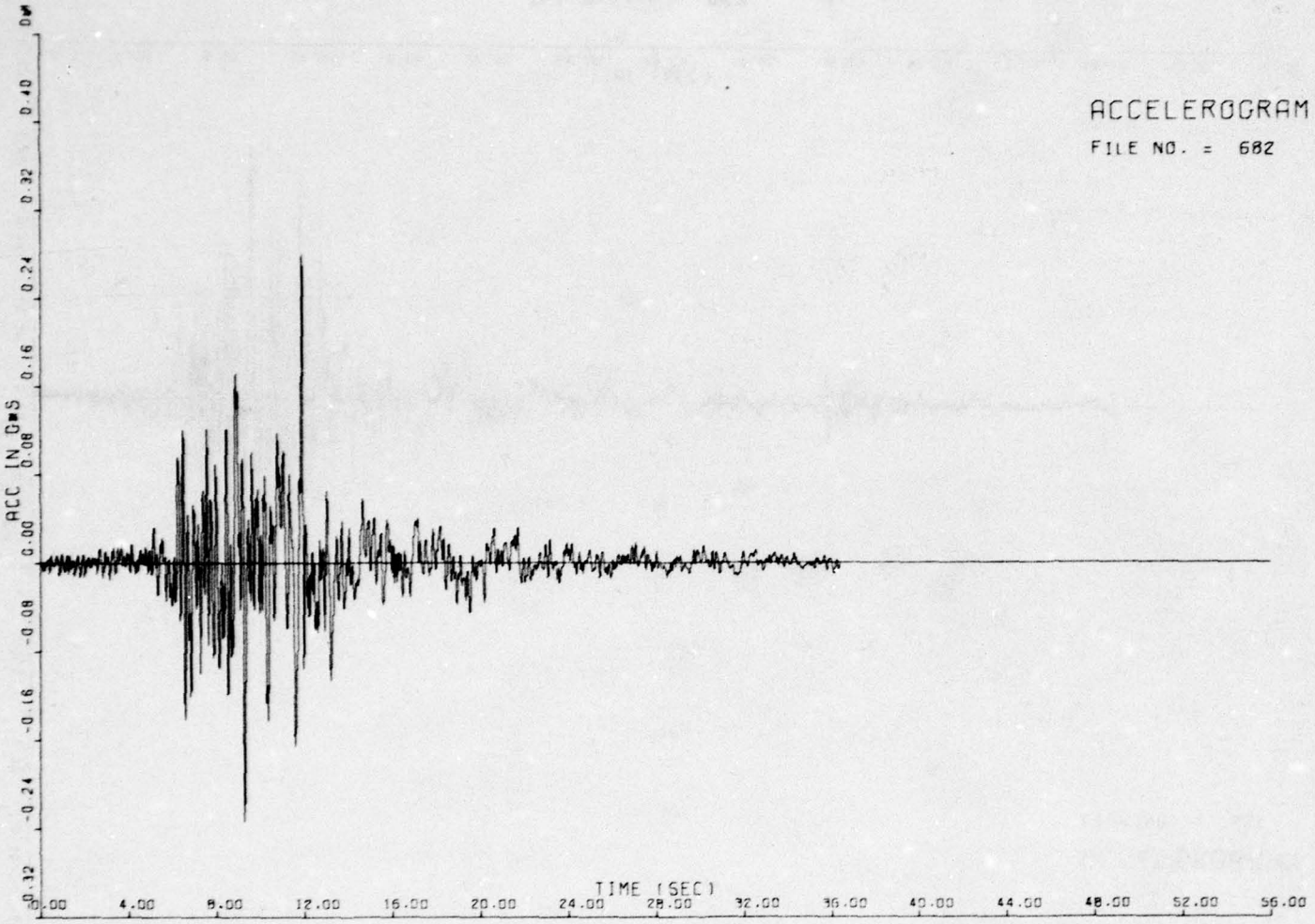

(a) File no. 682.

Figure 8-28. Time histories of records.

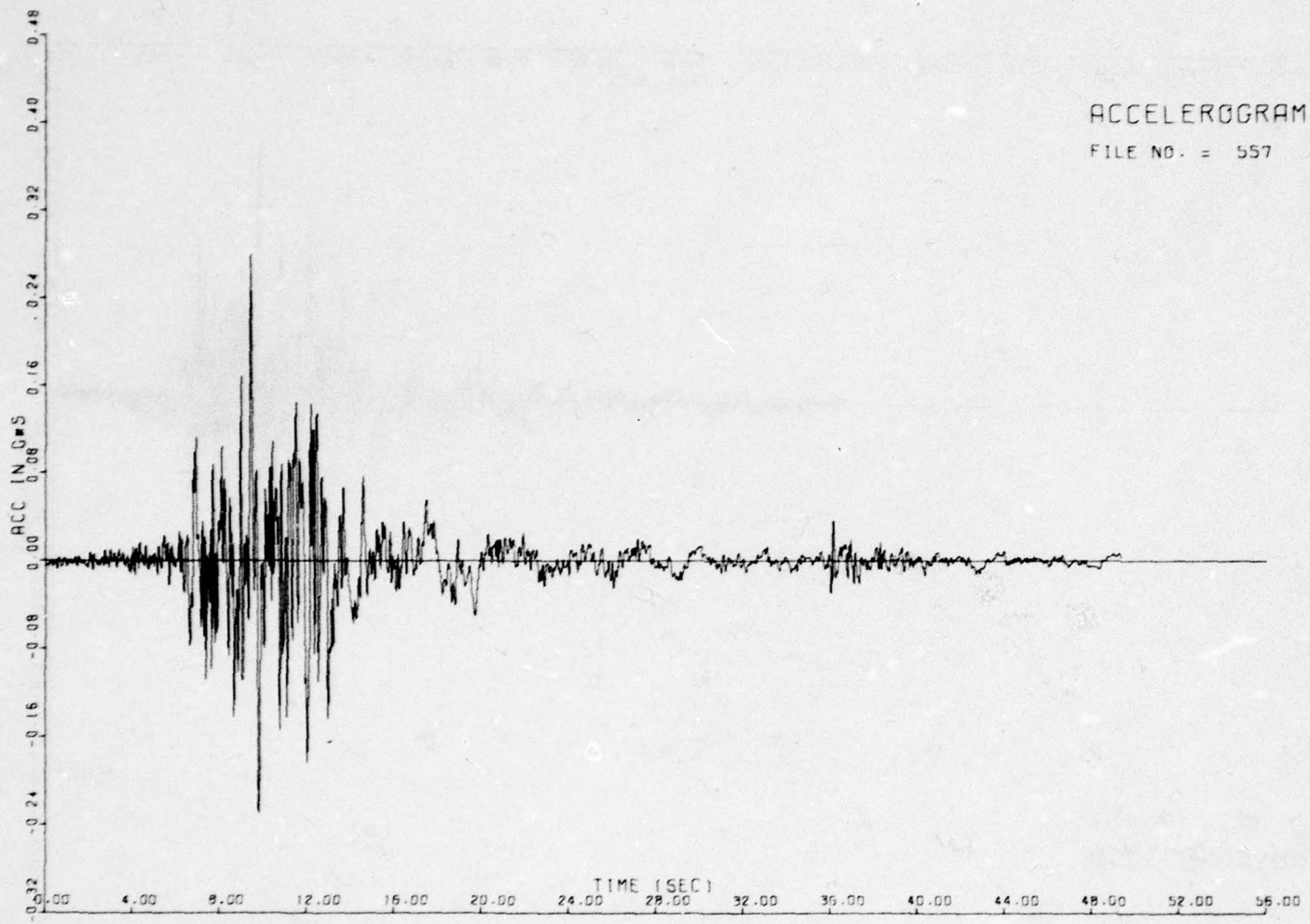

(b) File no. 557.

Figure 8-28. Continued.

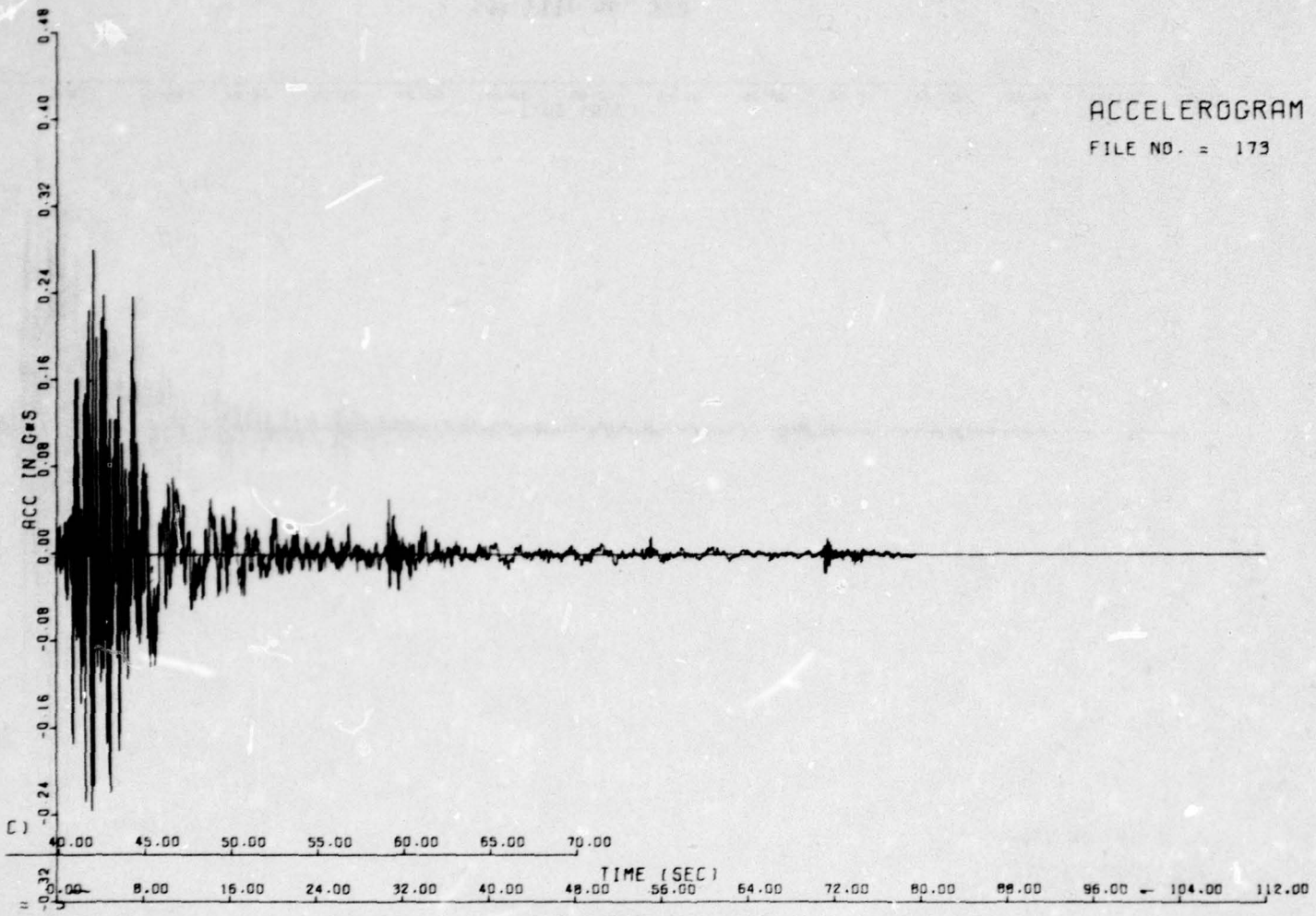

(c) File no. 173.

Figure 8-28. Continued.

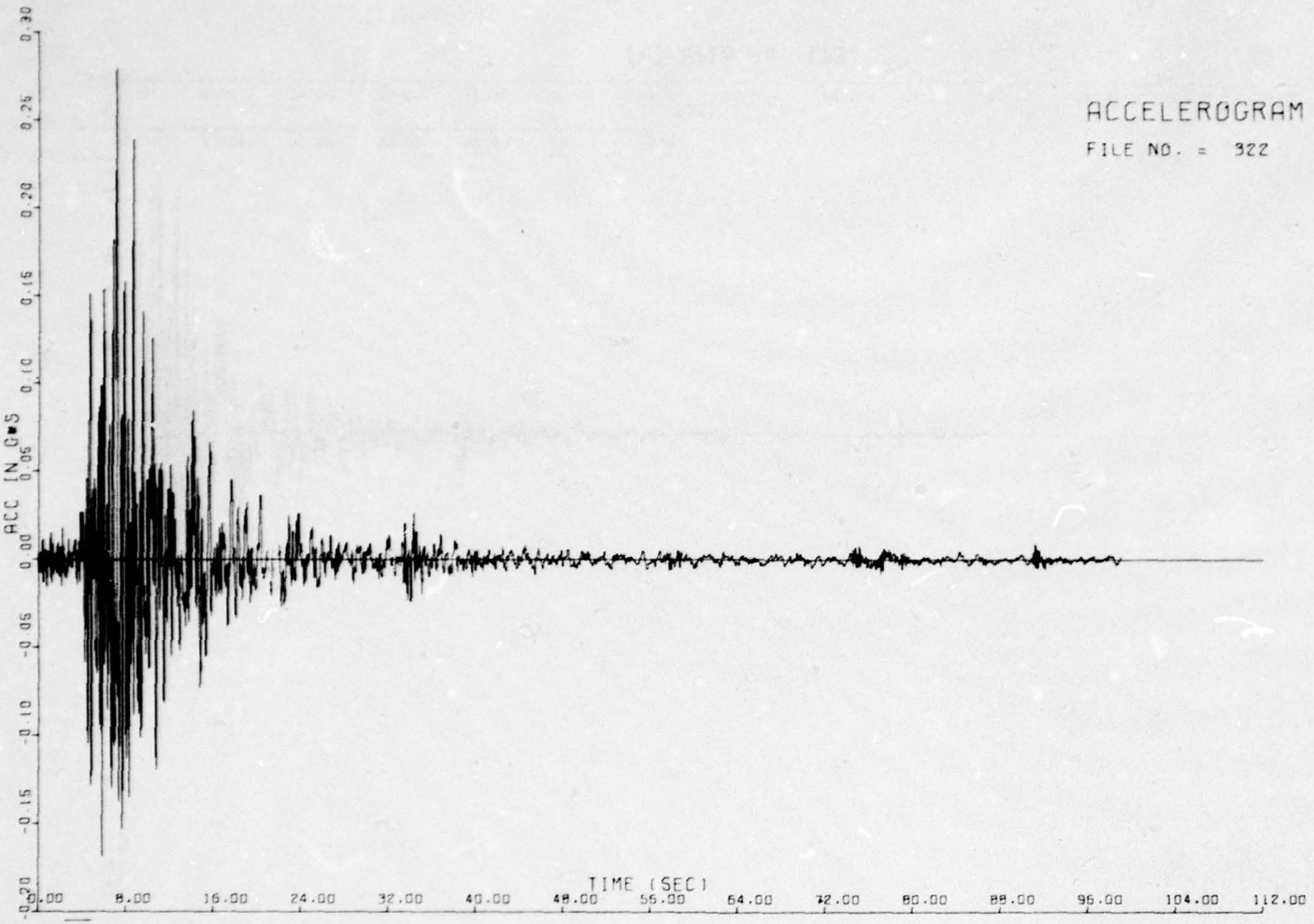

(d) File no. 322.

Figure 8-28. Continued.

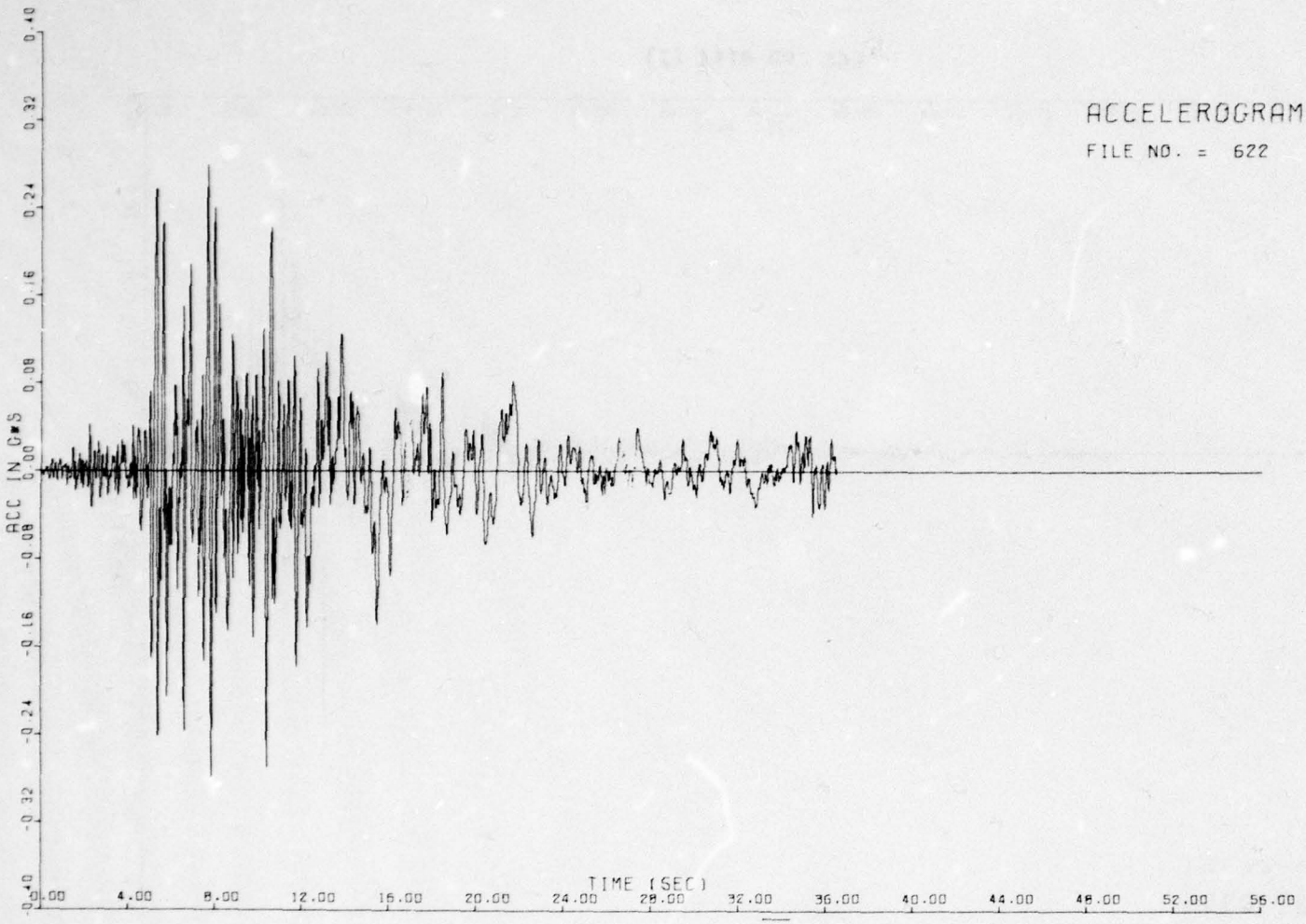

(e) File no. 622.

Figure 8-28. Continued.

AD-A060 204 CIVIL ENGINEERING LAB (NAVY) PORT HUFNEME CALIF F/G 8/11
A PROBABILISTIC PROCEDURE FOR ESTIMATING SEISMIC LOADING BASED --ETC(U)
AUG 78 J M FERRITTO

UNCLASSIFIED CEL-TR-867 NL

3 OF 3
AD
A060 204

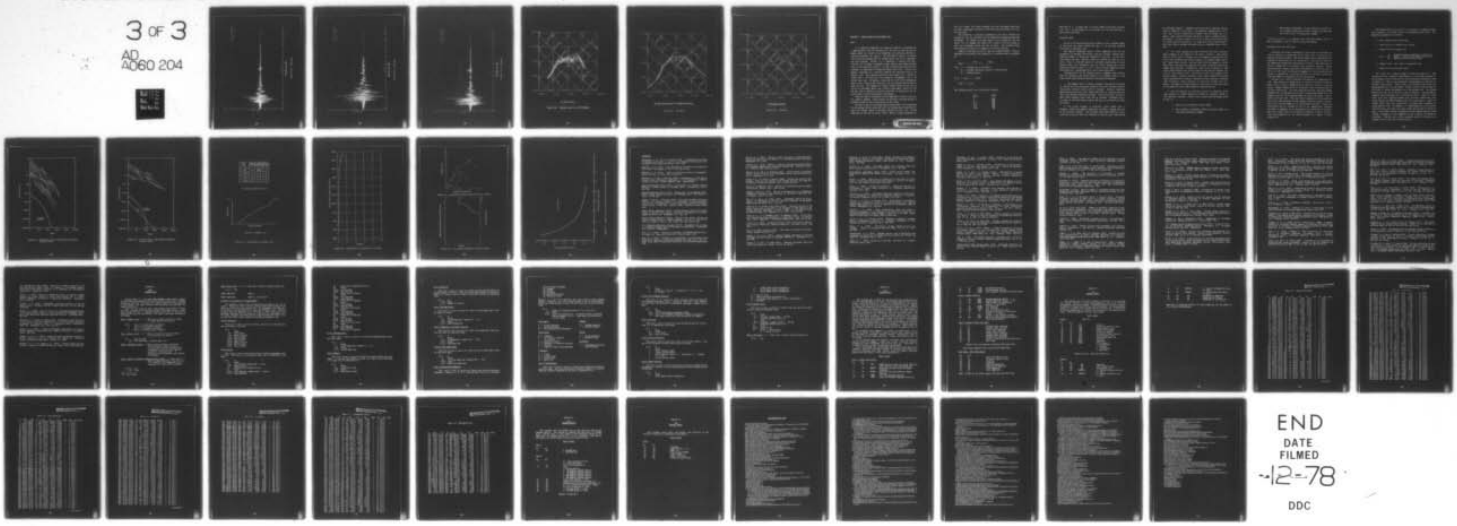

END
DATE
FILMED
12-78
DDC

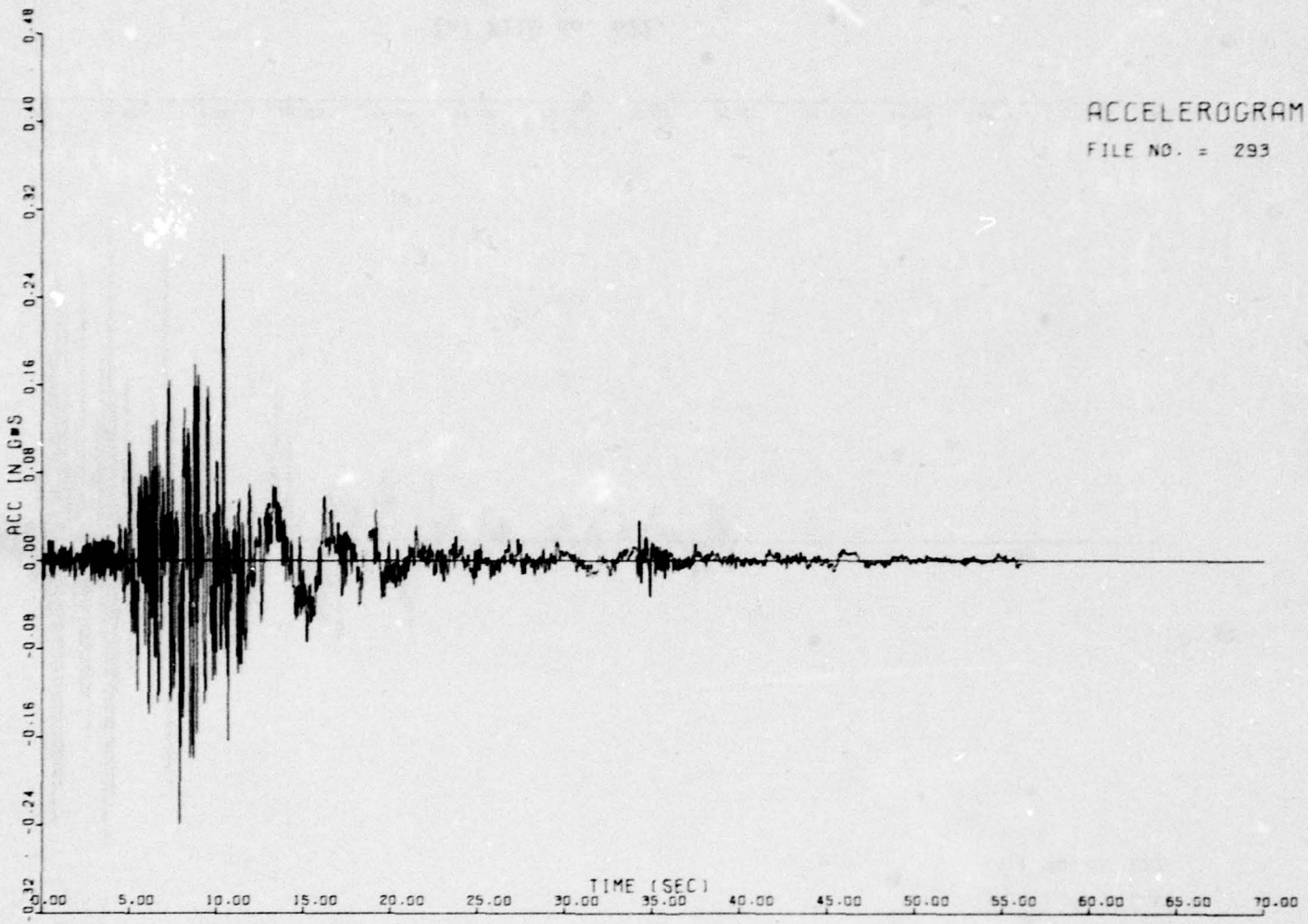

(f) File no. 293.

Figure 8-28. Continued.

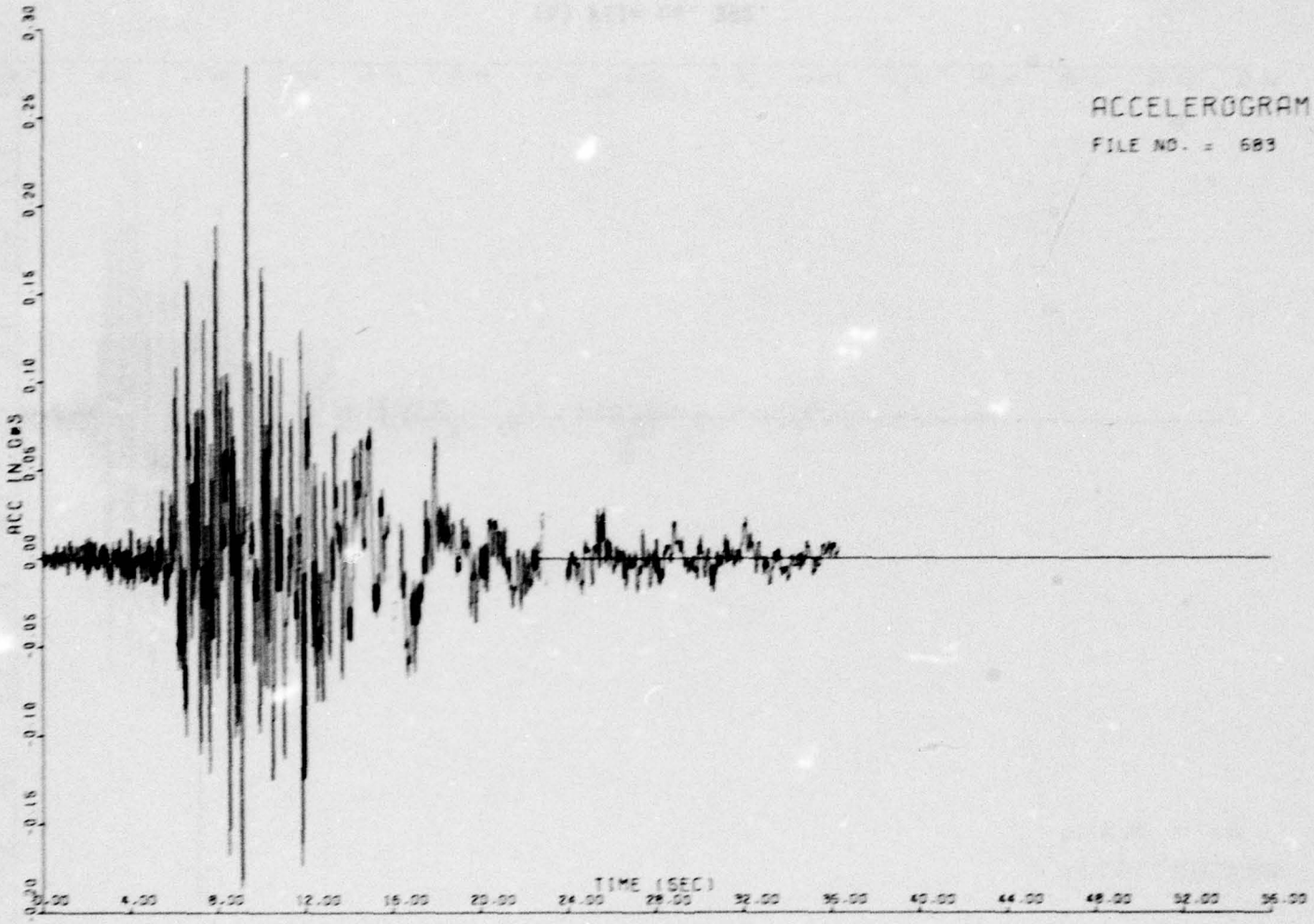

(g) File no. 683.

Figure 8-28. Continued.

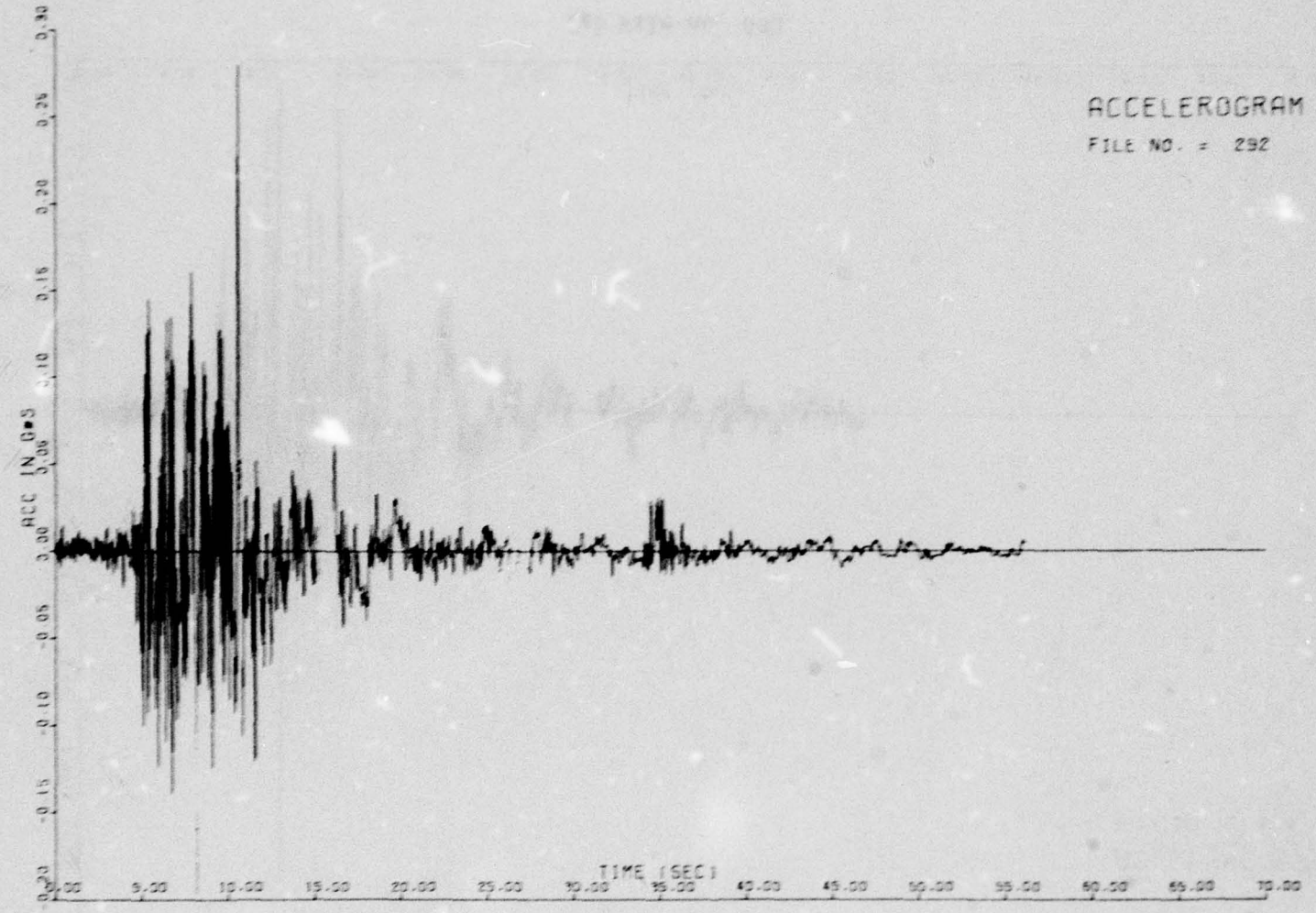

(h) File no. 292.

Figure 8-28. Continued.

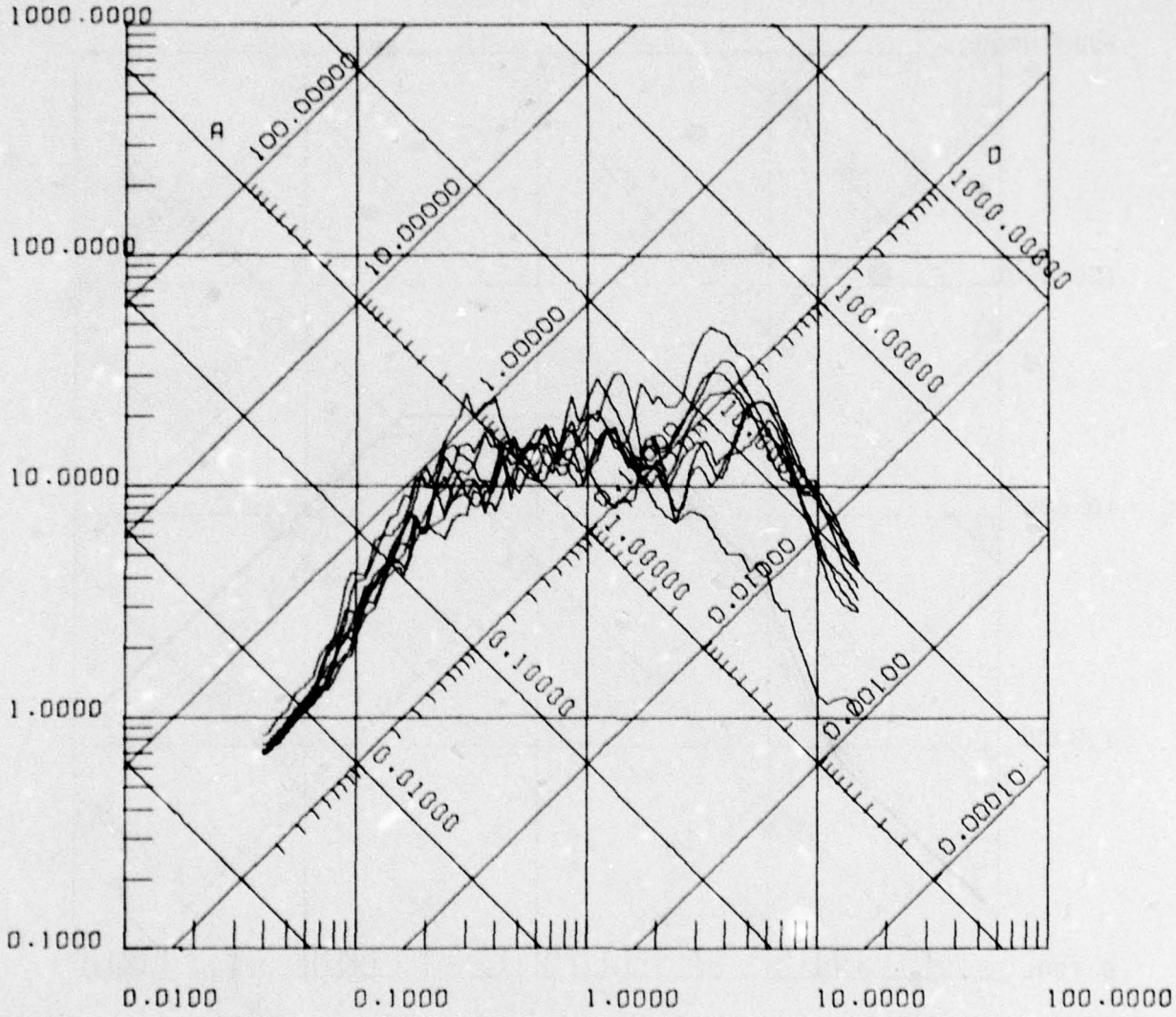

(a) Each record.

Figure 8-29. Response spectra with 5% damping.

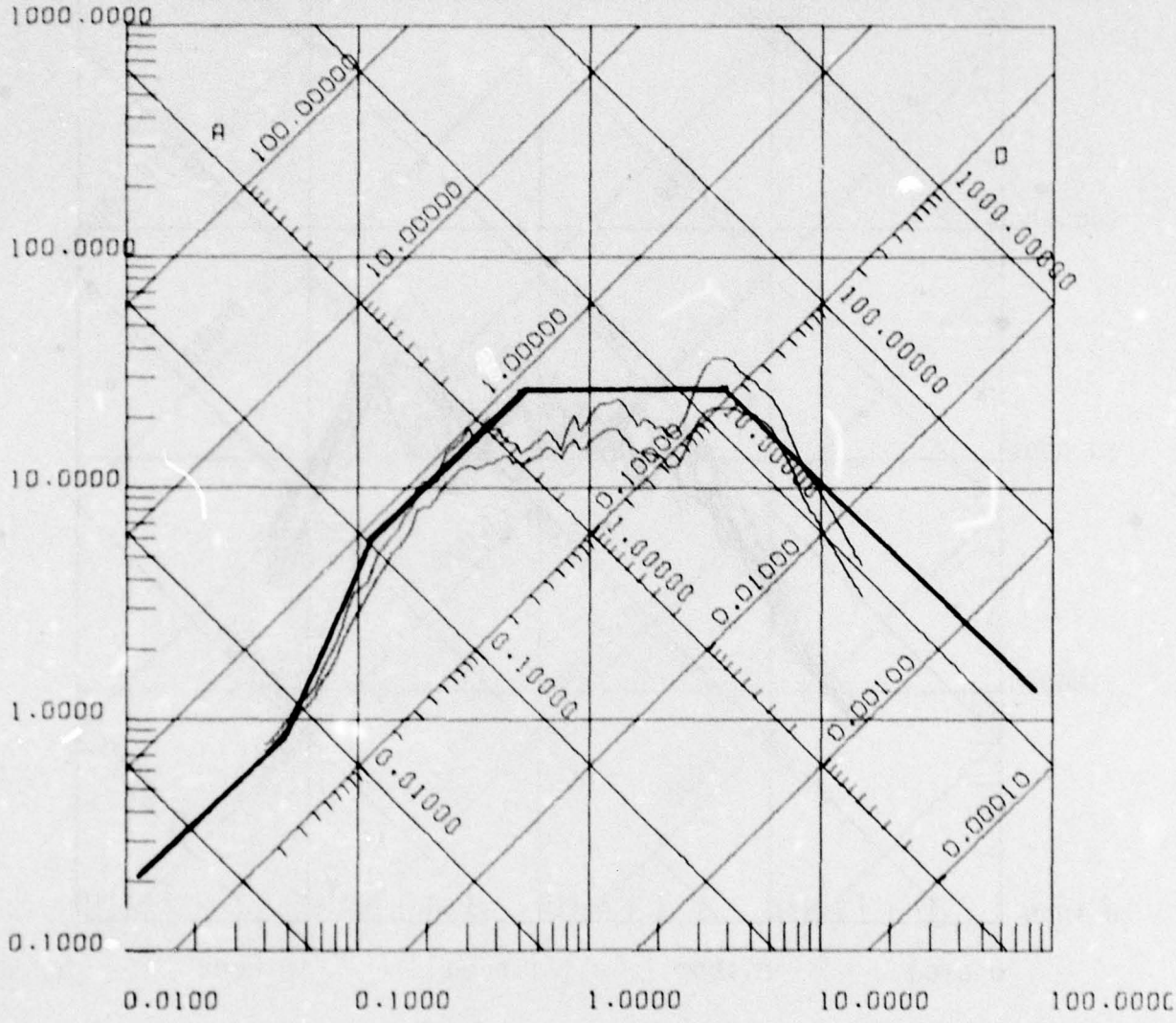

(b) Mean and mean plus 1 standard deviation.

Figure 8-29. Continued.

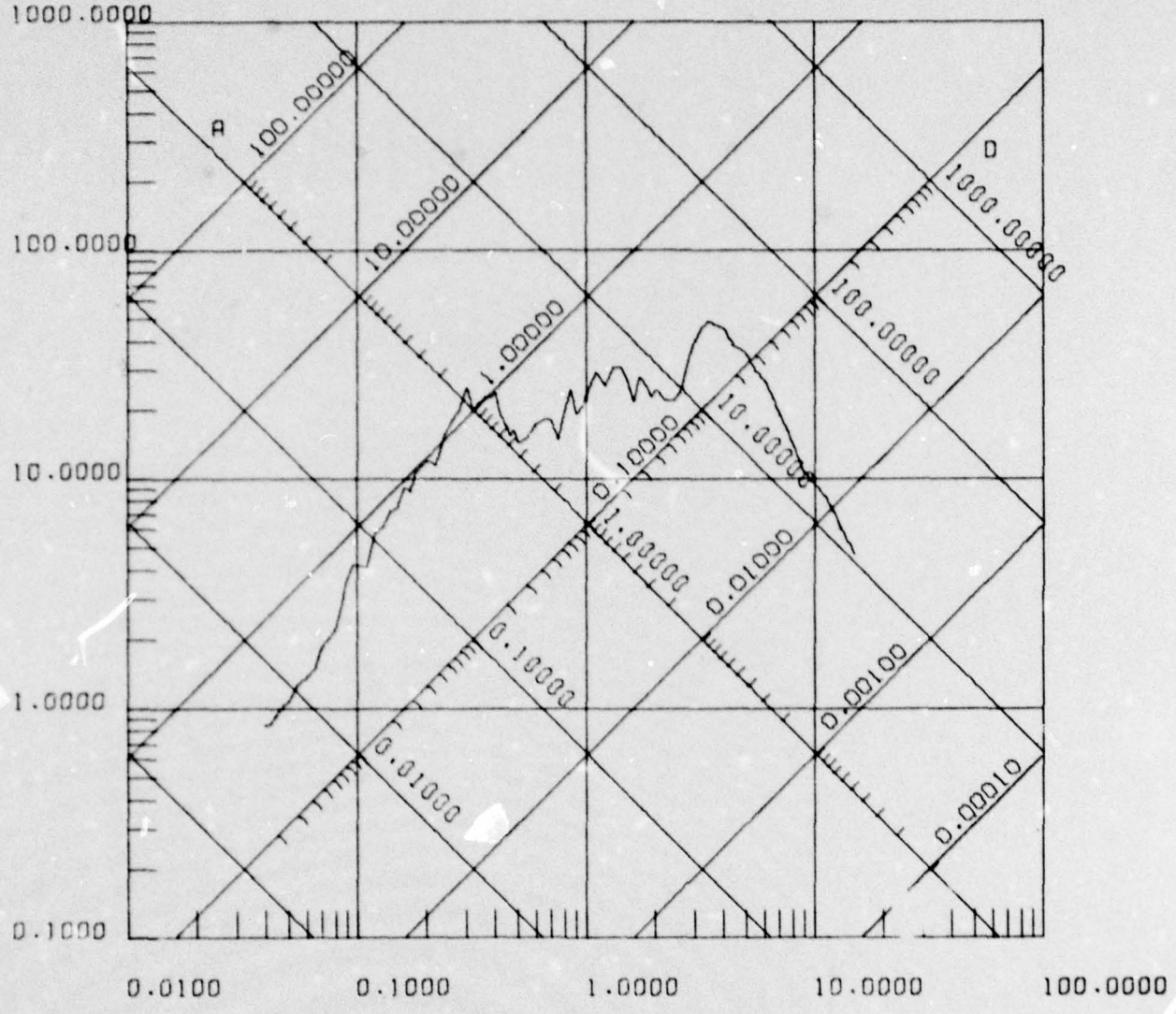

(c) Maximum envelope.

Figure 8-29. Continued.

CHAPTER 9 – DESIGN LEVELS AND ALLOWABLE RISK

Risk

It is generally impossible to design and construct a building with a 100% guarantee that the building will not fail in some way and endanger people as a result of an earthquake; the resources available to construct buildings are limited. The anticipated benefits of various life protecting programs must be weighed against the cost of implementing such programs. Further, it is impossible to specify with exact certainty the strongest earthquake ground shaking that might possibly occur at any specified location. As long as uncertainties exist in the loading it is impossible to design for exactly zero risk. A decision to design a building for a specified capacity has associated with it an implicit risk. This implied risk may be quite small (e.g., 1 chance in 10,000 that a building will fail during an earthquake), but it is greater than zero. In general, losses may be in the form of damage and repair costs, injuries and fatalities, and the indirect adverse effects upon the area. The emphasis of seismic design should be the risk of failure of buildings, where such a failure would imply a threat to life and the risk of failure of critical facilities to function at the required level to insure operational requirements.

Both the time of occurrence and the magnitude to affect a particular region is unknown. Future losses are uncertain, and some measure of probability must be used in evaluation of the losses.

One way is the use of average annual losses, which can be expressed as the average dollar losses per year, the average major casualties per year, the average number of building failures per year, etc. Losses expressed in this way are annual risks. However, large earthquakes are

PRECEDING PAGE BLANK

very rare events, and losses averaged over such infrequent events may not give a meaningful portrayal of the large loss that might occur over one such event.

The second way is to define a threshold of loss and to estimate the probability that the threshold will be equalled or exceeded during some earthquake. For example, we might speak of the probability that the dollar cost of damages and repairs will exceed $1 billion during at least one earthquake during the next 50 years. The threshold might alternatively be failure of a number of critical facilities.

Chapter 5 discusses the use of time as a random variable. Using an exponential distribution the probability of exceedence may be expressed as:

$$P[E] = 1 - e^{-\lambda T_e} = 1 - e^{-T_e/T_r}$$

where λ = average rate of occurrence

T_r = average recurrence interval or return period

T_e = exposure period

If $\lambda T = T_e/T_r \ll 1$, then:

$$P[E] \cong \lambda T_e/T_r$$

The following results are of particular interest:

T_e/T_r	P[E]
2	86%
1	63%
0.5	39%
0.2	18%
0.1	10%
0.05	5%

Note that $T_e = T_r$ means that it is quite (63%) certain that the event will occur. If the probability of the event is to be less than 10%, T_r must be more than $10T_e$.

Acceptable Risk

No law in the United States puts an amount on the acceptable number of fatalities per person exposed per year, or on any other proposed definition of acceptable risk.

The Applied Technology Council (1976) summarizes data for the probability of man-made and natural disasters causing a greater-than-specified number of fatalities (Figures 9-1 and 9-2). If the total "man-caused" and total "natural" curves are reduced by 1,000 (so as to give a level of risk that would not contribute significantly to total overall risk), the "acceptable" rate of events causing 100 or more fatalities would be about 5×10^{-4}. With a 50-year exposure period, there would be a 2.5% probability of one or more such events.

Considering all of the relevant factors, judgment would indicate that the following risk levels should not be exceeded; that is, risk levels above those indicated should be considered unacceptable.

1. The highest level of safety attainable with present technology is required for critical mission essential facilities and those containing nuclear material which could be released. Further, explosives manufacturing facilities with large quantities of sensitive material that could detonate should be included. Critical sea walls, failure of which could inundate a base, must also be included. Redundant facilities must be considered when a high enough level of survivability cannot be assured.

2. The second category of structures – those needed after a disaster – should also embody a high level of safety, although less than in the previous category. The principal safety goal should be structures and facilities that will continue to function after experiencing

an earthquake disaster. Examples would be sea walls, important utility centers, hospitals, fire, police, and emergency communication facilities, and critical transportation elements such as bridges and overpasses. These should be designed and built as safely as modern technology permits. An extra project cost of 5% to 25% to provide that level of safety would not be excessive. In some cases, where present technology cannot assure maximum attainable safety, redundance may be necessary.

3. In a third category are other structures that have occasional high occupancy or are needed for use after a disaster. These should have as little risk of collapse as is economically possible and also protect the occupants from serious hazard to the highest degree possible. Under these criteria, such structures could be damaged to a point where their functions were impaired; but their continued functioning, though under difficult circumstances, would still be possible. Some injury would possibly occur from falling articles and other hazards, but loss of life would be rare. Facilities in this risk category would include schools, churches, theaters, other places normally attracting large concentrations of people, secondary utility structures, extremely large structures, roads, alternate or noncritical bridges and overpasses. The degree of safety required in this class of structures would be attainable by a 5% to 15% increase in construction cost.

4. The vast majority of structures consist of industrial buildings, quarters, or family housing, for which an "ordinary" degree of risk should be acceptable. These criteria require that buildings should be able to:

a. Resist minor earthquakes without damage

b. Resist moderate earthquakes without structural damage, but with some nonstructural damage

c. Resist major earthquakes, of the intensity or severity of the strongest experienced without collapse, but with some structural as well as nonstructural damage

In most structures, it is expected that structural damage, even in a major earthquake, could be limited to repairable damage.

Building Failure and Total Risk

Exceeding the design earthquake by itself does not determine the risk of failure of a structure; total risk is also a function of the inherent building strength. The seismic hazard may be represented by a probability distribution of site acceleration. This must be related to the damage done during each acceleration occurrence. The probability of facility damage may be estimated from structural analysis. Having defined both the seismic hazard and the probability of facility failure, the total risk could be obtained by summing for all accelerations the product of probability of facility failure at a specific acceleration times the number of occurrences of that acceleration.

Whitman et al. (1975) illustrate one approach for computing total risk. They construct a damage matrix (a variation of which is shown in Figure 9-3a) in which a damage state is shown as a function of ground motion. Damage probabilities are estimated, based on uncertainties of facility construction. For each ground motion level individual damage probabilities are multiplied with their corresponding damage ratio and summed to give the total expected damage for that acceleration. This is plotted in Figure 9-3b. This data can be combined with the probability that a site will experience various ground acceleration levels to determine total risk and damage for all ground motion possible. Thus, site acceleration may be included by use of the computational technique described in Appendix B for determining site microzonation analysis. One of the output items in this analysis technique is data on acceleration and probability of not being exceeded in a number of years (Figure 9-4).

With Figures 9-3b, 9-4, and 9-5 it is possible to examine minimum loss conditions for various levels of earthquake ground motion. The methodology proposed is as follows:

1. Select design level acceleration

2. Using Figure 9-5, estimate cost increase

3. Estimate loss for design level

$$\text{Loss} = \sum_{i=1}^{n}$$

Probability site acceleration a_i (Figure 4)
Damage a_i (Figure 9-3b) summed over n increments in site acceleration level

4. Compute total: Cost = Loss + Construction Cost

5. Repeat for various design levels

The result for a typical example is shown in Figure 9-6. They indicate the most economical approximation is about 95% confidence of not exceeding a site acceleration for the acceleration probability shown in Figure 9-4. This is also expressed as approximately an event with a 500-year return period. These results are extremely crude using only approximations for cost and damage. Further effort should be spent in this area to obtain the maximum return and minimum risk. The optimum design level will be a function of site acceleration. The problem was repeated using different site acceleration levels. Figure 9-7 shows least total cost (expected damage plus increased construction cost) return periods for 90% confidence level site acceleration. Figure 9-7 clearly shows with site acceleration it becomes more economical to accept greater risk. For example, if a 90% probability site acceleration were 0.2g, the least cost event return period would be about 210 years. This event could be determined from the computer program output listing. Economics is not suggested as the criterion for design of structures. However, any criteria proposed should be reviewed on an economic basis as well as a structural basis.

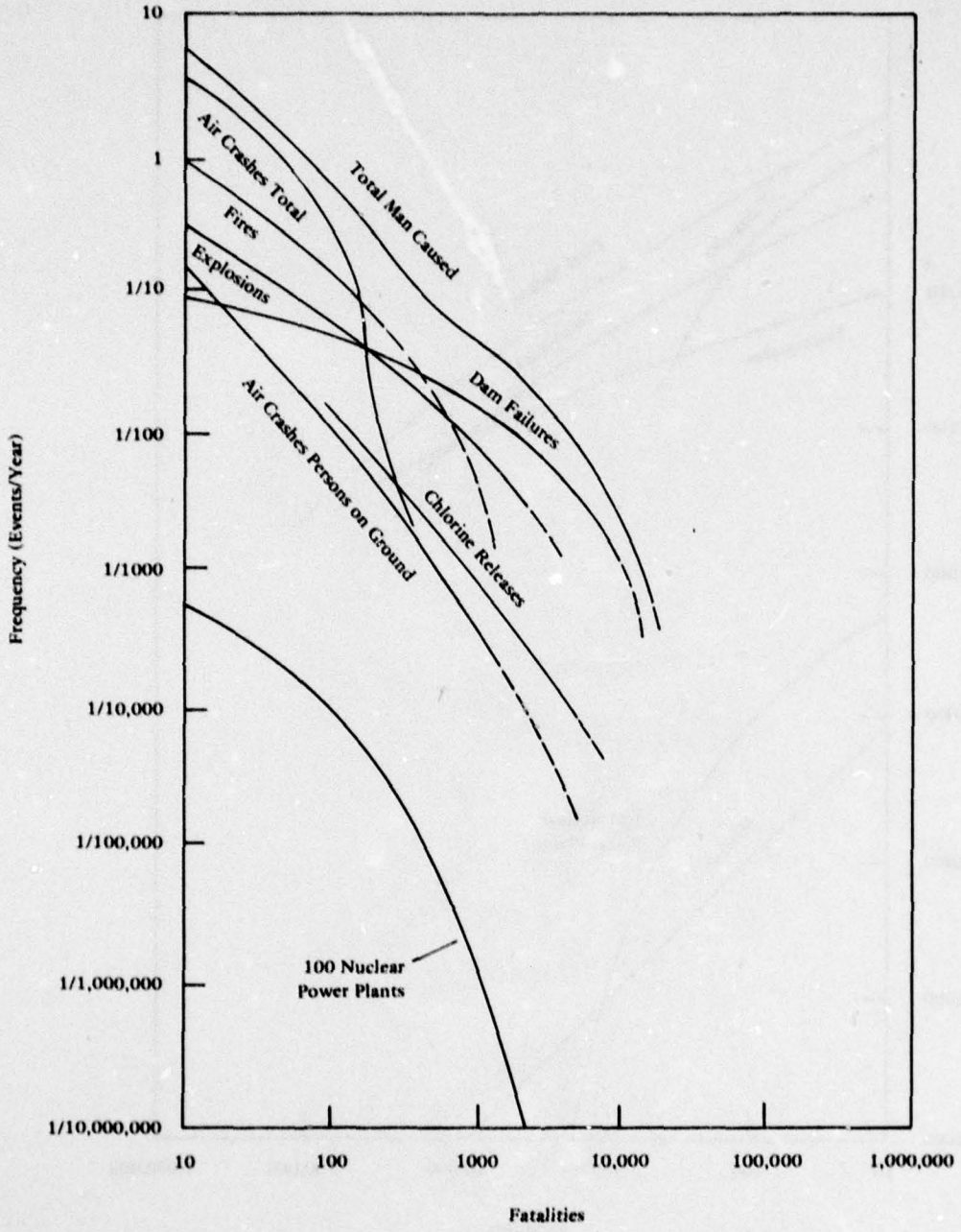

Figure 9-1. Man-caused events (from Applied Technology Council, 1976).

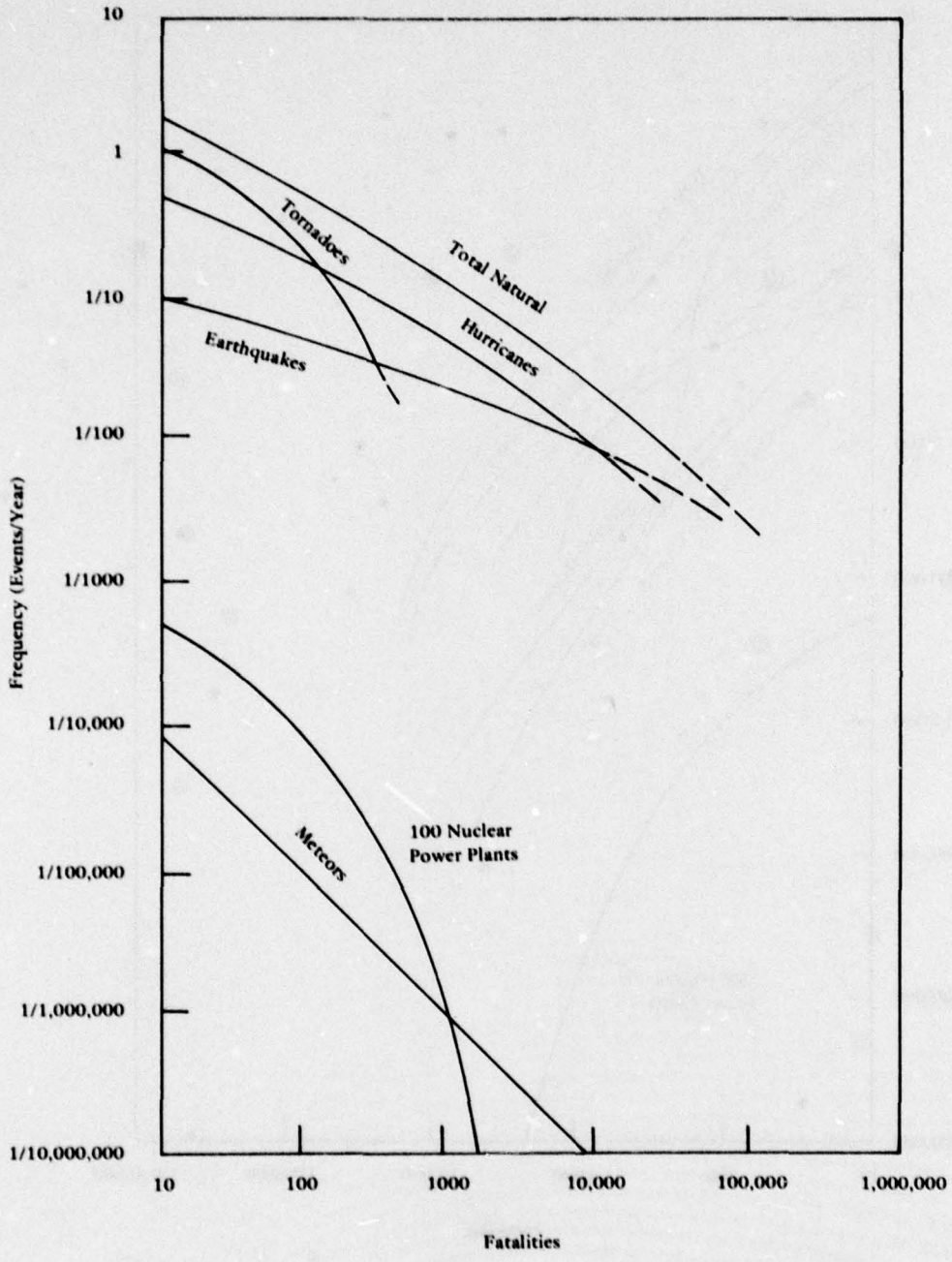

Figure 9-2. Natural events (from Applied Technology Council, 1970).

Damage State	Damage Ratio (%)	Ground Acceleration				
		g_1	g_2	g_3	g_4	g_5
O – None	0					
L – Light	0.3		P_{DSL}			
M – Moderate	5					
H – Heavy	30					
T – Total	100					
C – Collapse	100					

(a) Damage probability matrix

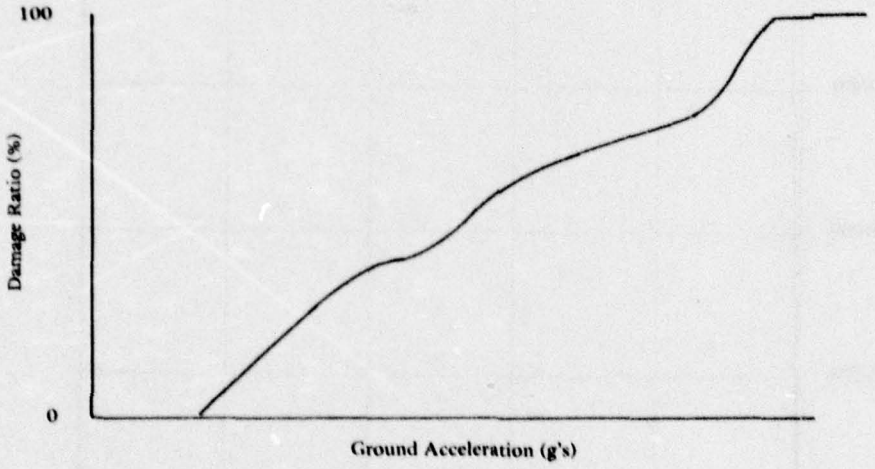

(b) Plot of damage ratio

Figure 9-3. Determination of damage ratio.

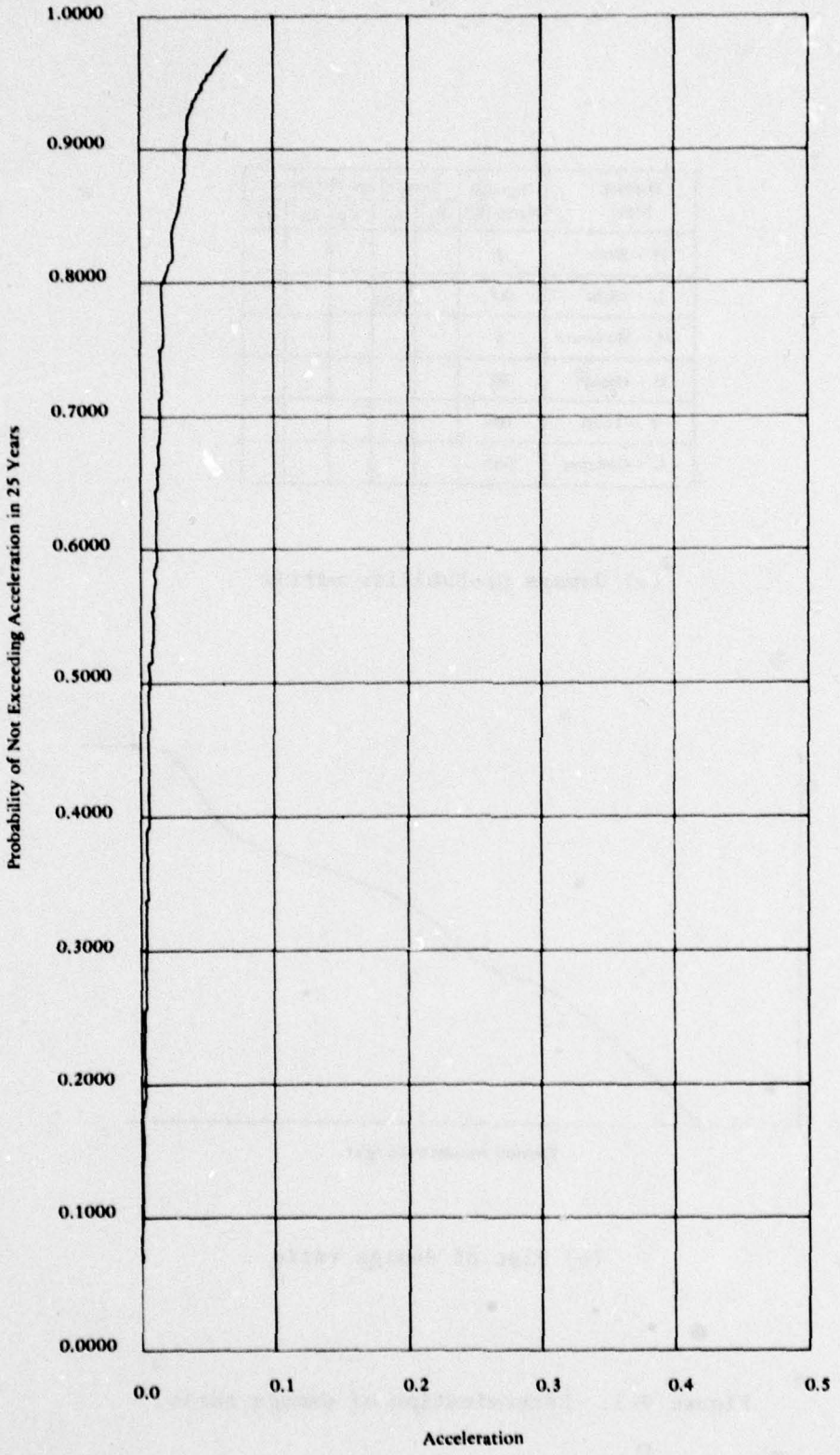

Figure 9-4. Probability of acceleration in 25 years.

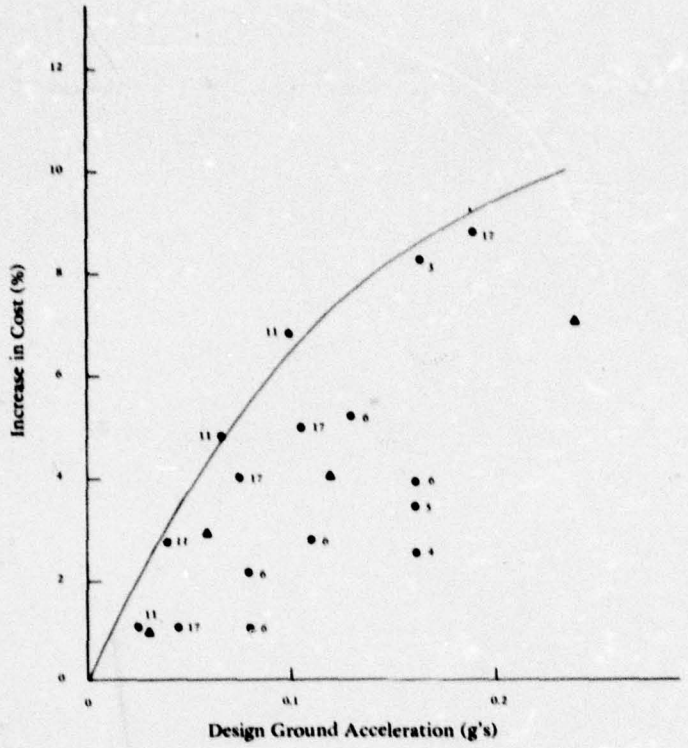

Figure 9-5. Acceleration versus construction cost increase.

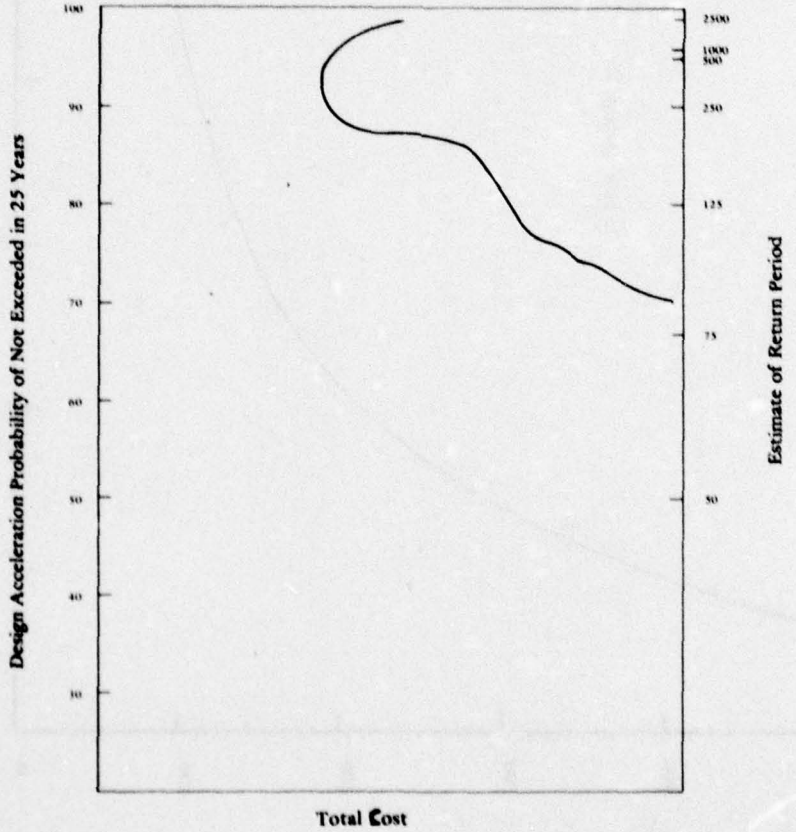

Figure 9-6. Cost versus probability or return period.

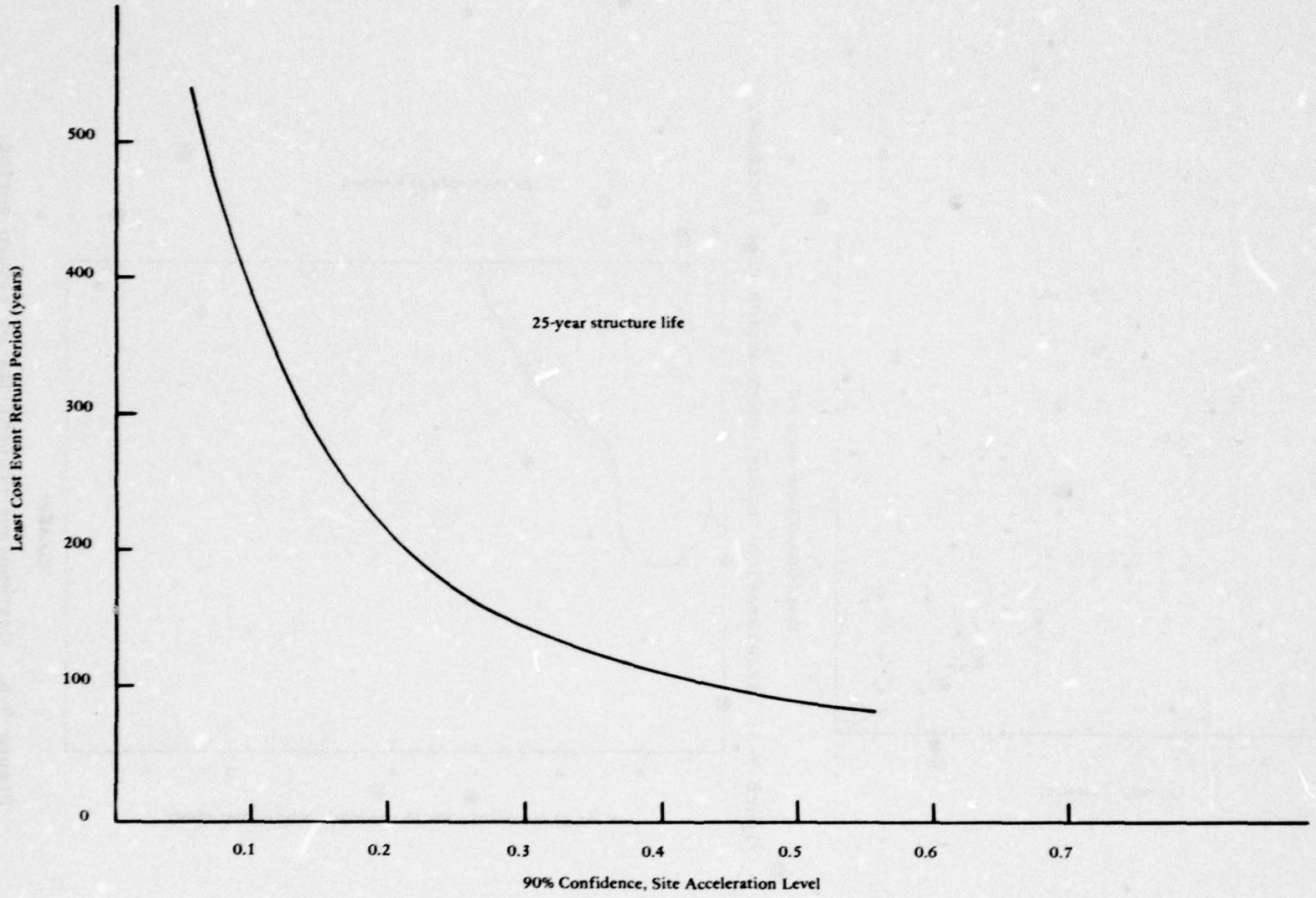

Figure 9-7. Least total cost return period versus acceleration levels.

REFERENCES

Algermissen, S. T. and D. M. Perkins (1976). A probabilistic estimate of maximum acceleration in rock in the contiguous United States, U.S. Geological Survey, Open File Report 76-416, 1976.

Ambraseys, N. N. (1970). "Some characteristic features of the Anatolian fault zone," Tectonophysics, vol 9, 1970, pp 143-165.

Ambraseys, N. N. (1971). "Value of historical records of earthquakes," Nature, vol 232, no. 5310, 1971, pp 375-379.

Ambraseys, N. N. and J. Tchalenko (1968). Documentation of faulting associated with earthquakes, Department of Civil Engineering, Imperial College of Science. London, England, 1968. (unpublished)

Applied Technology Council (1974). An evaluation of a response spectrum approach to seismic design of buildings, ATC-2. San Francisco, Calif., Sep 1974.

Applied Technology Council (1976). Working draft of recommended comprehensive seismic design provisions for buildings, ATC-3. San Francisco, Calif., 31 Jan 1976.

Arango, I. and R. J. Dietrich (1972). "Soil and earthquake uncertainties on site response studies," in Proceedings of the International Conference on Microzonation for Safer Construction Research and Application, 30 Oct - 3 Nov 1972. Seattle, Wash., National Science Foundation.

Atomic Energy Commission (1973a). Design response spectra for seismic design of nuclear power plants, Directorate of Regulatory Standards, Regulatory Guide 1.60. Washington, D.C., Dec 1973.

Atomic Energy Commission (1973b). "Nuclear power plants; seismic and geologic siting criteria," Federal Register, vol 36, no. 228, 25 Nov 1971, p. 22,602; vol 38, no. 218, 13 Nov 1973, pp 31,281-31,282.

J. A. Blume and Associates, Engineers (1973). Recommendations for shape of earthquake response spectra, Government Printing Office. Washington, D.C., Feb 1973. (WASH-1254)

Bolt, B. A. (1970). "Causes of earthquakes," Earthquake Engineering, R. L. Wiegel, ed. Englewood Cliffs, N.J., Prentice Hall, 1970.

Bolt, B. A. (1974). "Duration of strong motion," in Proceedings of the Fifth World Conference on Earthquake Engineering, Rome, Italy, Jun 1974. Rome, Italy, Rome International Association for Earthquake Engineering, 1974.

Bonilla, M. G. (1967). "Historic surface faulting in continental United States and adjacent parts of Mexico," U.S. Geological Survey, TID-24124. Washington, D.C., 1967.

Bonilla, M. G. (1970). Chapter 3, "Surface faulting and related effects in earthquake engineering," Earthquake Engineering. Englewood Cliffs, N.J., Prentice Hall, 1970, pp 47-74.

Bonilla, M. G. and J. M. Buchanan (1970). "Interim report on worldwide historic surface faulting," U.S. Geological Survey, Open File Series No. 16113. Washington, D.C., 1970.

Brown, R. D., Jr. and R. E. Wallace (1968). "Current and historic fault movement along the San Andreas fault between Paicines and Camp Dix, California," Geological Sciences, vol 11, 1968, pp 22-41.

Bureau of Reclamation (1972). Method for estimating design earthquake rock motions. Denver, Colo., 1972, 114 pp.

Campbell, Kenneth W. (1977). The use of seismotectonics in the Bayesian estimation of seismic risk, University of California, UCLA ENG 7744. Los Angeles, Calif., Jun 1977.

Chou, E. H. and J. A. Fisher (1975). "Earthquake hazards and confidence," in Proceedings of the U.S. National Conference on Earthquake Engineering, Ann Arbor, Mich., Jun 1975.

Clark, M. M., A. Grantz, and M. Rubin (1972). "Holocene activity of the Coyote Creek fault as recorded in the sediments of Lake Cahuilla," The Bollego Mountain Earthquake of April 9, 1968, U.S. Geological Survey Professional Paper 787. Washington, D.C., 1972, pp 1112-1130.

Cluff, R. S., D. B. Slemmons, and E. B. Waggoner (1970). "Active fault zone hazards and related problems of siting works of man," in Proceedings, Fourth Symposium of Earthquake Engineering, 1970, pp 401-410.

Cornel, C. T. (1974). Stochastic process models in structural engineering, Stanford University, Technical Report 34. Palo Alto, Calif., May 1974.

Cox, D. R. and H. D. Miller (1970). The theory of stochastic processes. London, England, Methuen, 1970.

Culver, C. G. et al. (1975). Natural hazards evaluation of existing buildings, National Bureau of Standards, NBS BSS 61. Washington, D.C., Jan 1975.

Davies, G. F. and J. H. Brune (1971). "Regional and global fault slip rates from seismicity," Nature, vol 229, pp 101-107.

Dezfulian, H. and H. B. Seed (1969). Seismic response on soil deposits underlain by sloping rock boundaries, University of California, Earthquake Engineering Research Center, EERC Report No. 69-9. Berkeley, Calif., Jul 1969.

Donovan, N. C. (1974). Earthquake hazards for buildings, Dames and Moore, Engineering Bulletin 46. Los Angeles, Calif., Dec 1974.

Environmental Development Agency (1975). Seismic safety element, San Diego Council General Plan, County of San Diego. San Diego, Calif., Jan 1975.

Esteva, L. (1968). Bases para la formulacion de decisiones de diseno dismico, Universidad Nacional Autonoma de Mexico, Instituto de Ingineria, no. 182. Mexico City, Mexico, May 1968.

Esteva, L. (1969). "Seismicity prediction: A Bayesian approach," in Proceedings of Fourth World Conference on Earthquake Engineering, Santiago, Chile, 1969.

Ferraes, S. G. (1973). "Earthquake magnitude probabilities and statistical independence for Mexico City earthquake," Bulletin of Seismological Society of America, vol 63, no. 6, Part 1, Dec 1973.

Ferritto, J. M. and J. B. Forrest (1977). Determination of seismically induced soil liquefaction potential at proposed bridge sites, Federal Highway Administration, Offices of Research and Development, FHWA RD 77-128. Washington, D.C., Aug 1977.

Figueroa, J. A. (1960). "Some considerations about the effect of Mexican earthquakes," in Proceedings of the Second World Conference on Earthquake Engineering, Tokyo and Kyoto, Japan, vol 3, Jul 1960. Tokyo, Japan, Science Council of Japan, 1960, pp 1553-1561.

Garcia, F. and J. M. Roesset (1970). Influence of damping on response spectra, Massachusetts Institute of Technology, Department of Civil Engineering, R70-4. Cambridge, Mass., Jan 1970.

Gates, T. H. (1976). "California's seismic design criteria for bridges," Journal of Structures Division, ASCE, vol 102, no. ST12, Dec 1976.

Greensfelder, R. W. (1974). Maximum credible rock accelerations from earthquakes in California, California Division of Mines and Geology, map sheet 23. Sacramento, Calif., 1974.

Gumbel, E. J. (1958). Statistics of extremes. New York, N.Y., Columbia University Press, 1958.

Guttenberg, B. and C. F. Richter (1954). Seismicity of the earth and associated phenomena, Second Ed. Princeton, N.J., Princeton University Press, 1954.

Guzman, R. and P. C. Jennings (1975a). Determination of design earthquakes for nuclear power plants, Fugro Inc., Consulting Engineers, Technical Report 50. Long Beach, Calif., 1975.

Guzman, R. A. and P. C. Jennings (1975b). "Determination of design spectra for nuclear power plants," preprint of paper presented at American Society of Civil Engineers, National Structural Engineering Conference, New Orleans, La., Apr 1975.

Hardin, B. and V. Drnevich (1970). Shear modulus and damping in soils, University of Kentucky, College of Engineering, Soil Mechanics Series Technical Report UKY 26-70-CE2. Lexington, Ky., Jul 1970.

Hofmann, R. B. (1968). "Geodimeter fault movement investigations in California," California Department of Water Resources, Bulletin No. 116-6. Sacramento, Calif., May 1968, p. 74.

Housner, G. W. (1965). "Intensity of earthquake ground shaking near the causative fault," in Proceedings of Third World Conference on Earthquake Engineering, New Zealand, vol 1. Wellington, New Zealand, New Zealand National Committee on Earthquake Engineering, 1965, pp III: 95-115.

Hudson, D. E. (1972). "Strong motion seismology," in Proceedings of the International Conference on Microzonation for Safer Construction Research and Application, Seattle, Wash., 30 Oct - 3 Nov 1972. Seattle, Wash., National Science Foundation, 1972, pp 39-60.

Idriss, I. M. and H. B. Seed (1968). "Seismic response of horizontal soil layers," Journal of the Soil Mechanics and Foundations Division, ASCE, vol 94, no. SM4, Jul 1968, pp 1030-1031.

Idriss, I. M. and H. B. Seed (1970). "Seismic response of soil deposits," Journal of the Soil Mechanics and Foundations Division, ASCE, vol 96, no. SM2, Mar 1970, pp 631-638.

Idriss, I. M. et al. (1973). QUAD 4: A computer program for evaluating the seismic response of soil structures by variable damping finite element procedures, University of California, Earthquake Engineering Research Center, EERC Report No. 73-16. Berkeley, Calif., Jul 1973.

Iida, K. (1965). "Earthquake magnitude, earthquake fault, and source dimensions," Journal of Earth Sciences, Nagoya University, vol 13, no. 2, 1965, pp 115-132.

International Atomic Energy Agency (1972). Earthquake guidelines for reactor siting, Technical Report Series No. 139. Vienna, Austria, 1972, pp 9-10.

Kanai, K. (1961). "An empirical formula for the spectrum of strong earthquake motions," Bulletin, Tokyo University Earthquake Research Institute, vol 39, 1961.

Kiefer, F. W., H. B. Seed, and I. M. Idriss (1970). "Analysis of earthquake ground motions at Japanese sites," Bulletin of the Seismological Society of America, vol 60, no. 6, Dec 1970, pp 2057-2070.

Knopoff, L. (1964). "The statistics of earthquakes in southern California," Bulletin of the Seismological Society of America, vol 54, no. 6-a, 1964, pp 1871-1873.

Kobayashi, Y. (1974). "Prepared discussion on duration of strong motion by B.A.B.H.," in Proceedings of the Fifth World Conference on Earthquake Engineering, Rome, Italy, Jun 1974. Rome, Italy, Rome International Association for Earthquake Engineering, 1974.

Krinitzsky, E. (1974). Fault assessment in earthquake engineering, Army Engineering Waterways Experiment Station, Miscellaneous Paper S-73-1. Vicksburg, Miss., May 1974.

Lamar, D. L., P. M. Merifield, and R. J. Proctor (1973). Earthquake recurrence intervals on major faults in southern California, geology seismicity and environmental impact, Association of Engineering Geologists, Special Publication. Los Angeles, Calif., University Publishers, 1973.

Lee, K. L. and K. Chan (1972). "Number of equivalent significant cycles on strong motion earthquakes," in Proceedings of the International Conference on Microzonation for Safer Construction Research and Application, Seattle, Wash., 30 Oct - 3 Nov 1972. Seattle, Wash., National Science Foundation, 1972.

Lomnitz, C. (1969). "Earthquake risk map of Chile," in Proceedings of Fourth World Conference on Earthquake Engineering, Santiago, Chile, 1969.

Lomnitz, C. (1974). "Global tectonics and earthquake risk," Developments in Geotectonics 5. New York, N.Y., Elsevier Scientific Publishing Company, 1974.

Lysmer, J., H. B. Seed, and P. B. Schnabel (1970). Influence of base rock characteristics on ground response, University of California, Earthquake Engineering Research Center, EERC Report No. 70-7. Berkeley, Calif., Nov 1970.

Lysmer, J., T. Udaka, H. B. Seed, R. Hwang (1974). LUSH: A computer program for complex response analysis of soil structure systems, University of California, Earthquake Engineering Research Center, EERC Report No. 74-4. Berkeley, Calif., Apr 1974.

Mark, R. K. and M. G. Bonilla (1977). Regression analysis of earthquake magnitude and surface fault length using the 1970 data of Bonilla and Buchanan, U.S. Geological Survey, USGS Open File Report 77-614. Menlo Park, Calif., 1977.

McGuire, R. K. (1976). FORTRAN computer program for seismic risk analysis, U.S. Geological Survey, Open File Report 76-67. Menlo Park, Calif., 1976.

McGuire, R. (1977). "Seismic design spectra and mapping procedures," Earthquake Engineering and Structural Dynamics, vol 5. New York, Wiley Publications, 1977, pp 211-234.

Mertz, H. A. and C. A. Cornell (1973). "Seismic risk analysis based on a quadratic magnitude-frequency law," Bulletin of Seismological Society of America, vol. 63, no. 6, Part 1, Dec 1973.

Milne, A. and A. G. Davenport (1969). "Distribution of seismic risk," Canada Bulletin of Seismological Society of America, vol 59, no. 2, Apr 1969.

Newmark, N. M. (1967). Design criteria for nuclear reactors subjected to earthquake hazards, University of Illinois, Department of Civil Engineering. Urbana, Ill., May 1967.

Newmark, N. M., J. A. Blume, and K. K. Kapur (1973). "Seismic design spectra for nuclear power plants," Journal of the Power Division, ASCE, vol 99, no. P02, Nov 1973.

Newmark, N. M. and W. J. Hall (1969). "Seismic design criteria for nuclear reactor facilities," in Proceedings of the Fourth World Conference on Earthquake Engineering, Santiago, Chile, 1969.

Newmark, N. and E. Rosenblueth (1971). Fundamentals of earthquake engineering. Englewood Cliffs, N.J., Prentice Hall, 1971.

N. M. Newmark Consulting Engineering Services (1973). A study of vertical and horizontal earthquake spectra. Washington, D.C., Government Printing Office, Apr 1973. (WASH-1255)

Nuttli, O. W. (1973a). "Seismic wave attenuation and magnitude relations for eastern North America," Journal of the Geophysical Research Division, ASCE, vol 75, no. 5, Feb 1973, pp 876-885.

Nuttli, O. W. (1973b). State-of-the-art for assessing earthquake hazard in the United States, design earthquakes for the central United States, Army Engineering Waterways Experiment Station, Miscellaneous Paper S-73-1. Vicksburg, Miss., Jan 1973.

Nuttli, O. W. (1973c). "The Mississippi Valley earthquakes of 1811 and 1812: Intensities, ground motion and magnitudes," Bulletin of the Seismological Society of America, vol 63, no. 1, Feb 1973, pp 227-248.

Nuttli, O. W. (1974). "Magnitude-recurrence relations for central Mississippi Valley earthquakes," Bulletin of the Seismological Society of America, vol 64, no. 4, Aug 1974, pp 1189-1207.

Nuttli, O. and J. Zellweg (1974). "The relation between felt area and magnitude for central United States earthquakes," Bulletin of the Seismological Society of America, vol 64, no. 1, Feb 1974, pp 73-85.

Oliveira, C. S. (1975). Seismic risk analysis for a site and a metropolitan area, University of California, Earthquake Engineering Research Center, EERC Report No. 75-3. Berkeley, Calif., Feb 1975.

Page, R. A., et al. (1972). Ground motion values for use in the seismic design of the trans-Alaska pipeline system, U.S. Geological Survey, Circular 672. Washington, D.C., 1972.

Reid, H. F. (1911). The elastic rebound theory of earthquakes, University of California, Department of Geology, Bulletin 6 (19). Berkeley, Calif., 1911.

Richter, C. F. (1958). Elementary seismology. San Francisco, Calif., W. H. Freeman Co., 768 pp.

Rosenblueth, E. (1973). "Analysis of risk," in Proceedings of Fifth World Conference on Earthquake Engineering, Rome, Italy, 1973.

Schnabel, P. B. and H. B. Seed (1972). Accelerations in rock for earthquakes in the western United States, University of California, College of Engineering, Earthquake Engineering Research Center, EERC Report No. 72-2. Berkeley, Calif., Feb 1972.

Schnabel, P. B., J. Lysmer, and H. B. Seed (1972). SHAKE: A computer program for earthquake response analysis of horizontally layered sites, University of California, Earthquake Engineering Research Center, EERC Report No. 72-12. Berkeley, Calif., Dec 1972.

Seed, H. B. (1975). "Chapter 6. Soils coefficient 'S' and period 'T_s'," in Earthquake Symposium, Los Angeles, Calif., Jun 1975. Los Angeles, Calif., Structural Engineers Association of Southern California, 1975.

Seed, H. B. and I. M. Idriss (1969). "Influence of soil conditions on ground motions during earthquakes," Journal of the Soil Mechanics and Foundations Division, ASCE, vol 95, no. SM1, Jan 1969, pp 99-137.

Seed, H. B. and I. M. Idriss (1970a). A simplified procedure for evaluating soil liquefaction potential, University of California, Earthquake Engineering Research Center, EERC Report No. 70-9. Berkeley, Calif., Nov 1970.

Seed, H. B. and I. M. Idriss (1970b). "Analysis of ground motions at Union Bay, Seattle, during earthquakes and distant nuclear blasts," Bulletin of the Seismological Society of America, vol 60, no. 1, Feb 1970, pp 125-136.

Seed, H. B. and I. M. Idriss (1970c). Soil moduli and damping factors for dynamic response analysis, University of California, Earthquake Engineering Research Center, EERC Report No. 70-10. Berkeley, Calif., Dec 1970.

Seed, H. B., I. M. Idriss and F. S. Kiefer (1969). "Characteristics of rock motions during earthquakes," Journal of the Soil Mechanics and Foundations Division, ASCE, vol 95, no. SM5, Sep 1969, pp 1199-1218.

Seed, H. B., R. Murarka, J. Lysmer, and I. M. Idriss (1975). Relationships between maximum acceleration, maximum velocity distance from source, and local site conditions for moderately stray earthquakes, University of California, Earthquake Engineering Research Center, EERC Report No. 75-17. Berkeley, Calif., Jul 1975.

Seed, H. B., C. Ugas, and J. Lysmer (1974). Site-dependent spectra for earthquake-resistant design, University of California, Earthquake Engineering Center, EERC Report No. 74-12. Berkeley, Calif., Nov 1974.

Shannon & Wilson Co. and Agbabian Associates (1975). Procedures for evaluation of vibratory ground motions of soil deposits at nuclear power plant sites, Nuclear Regulatory Commission, NUREG 75/072. Seattle, Wash., Jun 1975.

Streeter, V. L., E. G. Wylie, and F. E. Richart (1974). "Soil motion computations by characteristics method," Journal of the Geotechnical Division, ASCE, vol 100, no. GT3, Mar 1974, pp 247-263.

Tocher, D. (1958). "Earthquake energy and ground breakage," Bulletin of the Seismological Society of America, vol 48, 1958, pp 147-153.

Trifunac, M. D. and A. G. Brady (1975a). "On the correlation of seismic intensity scales with the peaks of recorded strong ground motion," Bulletin of the Seismological Society of America, vol 65, no. 1, Feb 1975, pp 139-162.

Trifunac, M. D. and A. G. Brady (1975b). "On the correlation of peak acceleration of strong motion with earthquake magnitude epicentral distance and site condition," in Proceedings of the U.S. National Conference of Earthquake Engineering, Ann Arbor, Mich., Jun 1975. Oakland, Calif., Earthquake Engineering Research Institute, 1975.

U.S. Geological Survey (1975). Studies for seismic zonation of the San Francisco Bay region; Basis for reduction of earthquake hazards, San Francisco Bay Region, California, R. D. Borcherdt, ed., Professional Paper 941-A. Reston, Va., 1975.

Valera, J. (1974). Revision to Regulatory Guide 1.60, Design response spectra for seismic design of nuclear power plants, Rev. 1., Atomic Energy Commission, Directorate of Regulatory Standards. Washington, D.C., Jan 1974.

Wallace, R. E. (1970). "Earthquake recurrence intervals on the San Andreas fault," Geological Society of America Bulletin, vol 81, 1970, pp 2875-2890.

Walper, T. L. (1976). State of the art for assessing earthquake hazards in the United States, Report 5, Plate tectonics and earthquake assessment, Army Engineering Waterways Experiment Station. Vicksburg, Miss., Mar 1976.

Wentworth, C. M. and R. F. Yerkes (1971). Geological setting and activity of faults in the San Fernando area in the San Fernando, California earthquake of February 9, 1971, U.S. Geological Survey, Professional Paper 733. Washington, D.C., 1971, pp 6-16.

Werner, S. D. (1970). A study of earthquake input motions for seismic design, Agbabian Jacobsen Associates, Report No. 6912-925. Los Angeles, Calif., Jun 1970.

Wesson, R. L. et al. (1975). Faults and future earthquakes studies for seismic zonation of the San Francisco Bay Region, U.S. Geological Survey, Professional Paper 941-A. Reston, Va., 1975.

Whitman, R. V., J. M. Biggs et al. (1975). "Seismic design decision analysis," Journal of Structures Division, ASCE, vol 101, ST5, May 1975.

Appendix A

NOAA
PROGRAM CH42C

Program CH42C is a CDC 6600 COBOL-FORTRAN program used to search the National and Geophysical and Solar-Terrestrial Data Center's (NGSDC) hypocenter data file. This data file contains hypocenter data from 1638 to the present. The tape records are 90 characters long (punched card images) blocked 50.

There are five types of input cards (search set) needed to search the file. As many as 50 different searches may be made during a single pass through the tape. A separate printout, card deck, or tape file is generated for each of the searches. The input cards must be sequenced as follows:

Type 1 (Output card)----------This card is used to specify the types of output desired for each set.

CC*1	use a 1 if tape output is desired
2	use a 1 if a listing is desired
3	use a 1 if punchout is desired
4	use a 1 if plotter tape is desired

Type 2 (Header card)----------This card is used to print a header on the printout for each set.

CC 1	must be blank
2-80	free form (area, customer name, etc.)

Type 3 (Parameter cards)------These cards are used to search the file for specific types of events. At least one of the 15 different types of parameter cards (A thru P) must be present for each search set. A description of the parameter card formats is attached.

Type 4 (Special Parameter Combination/"or" card)--------This card is used to combine parameter card sets in an "or" condition (e.g., magnitude 4.0 or intensity IV). This card is optional.

CC 1-2	or
3-80	blank

*CC - Card Column

Type 5 (End card)----------This card is used to end each search set.

CC 1-3 ZZZ

INPUT TAPE UNIT: TAPE 10.

OUTPUT TAPE UNIT: TAPE 11. for block 50

Parameter Card Formats for Program CH42C

The parameter cards A thru P described below may be in any sequence. Except for card K (of which there can be several) there can be only one of each for each search set. All parameter cards used in a search must be satisfied before a record is considered a hit. However, if more than one magnitude card (C,F,G,H) is used, only one of the magnitude cards need be satisfied for a record to be considered a hit. For those parameter cards with several items (cards B,I,K,L,M,N), a hit on only one of the items is needed to satisfy the parameter card.

Card A (Interval)

This card is used to search on dates, only the low and high year must be present on the card.

CC	1	A
	2	blank
	3-6	year (1964)
	7-8	month or blank
	9-10	day or blank
	11-12	hour or blank
	13-16	year (1973)
	17-18	month or blank
	19-20	day or blank
	21-22	hour or blank

Card B (Area)

This card is used to search for events in specific geographic area or areas. From one to four different areas can be indicated on this card.

CC	1	B
	2	blank
	3-5	low latitude, example 900 = 90.0°
	6-8	high latitude
	9	direction of latitude (N or S)
	10	blank
	11-14	low longitude, example 1500 = 150.0°
	15-18	high longitude

19	direction of longitude (E or W)
20	blank
21-23	low latitude
24-26	high latitude
27	direction of latitude
28	blank
29-32	low longitude
33-36	high longitude
37	direction of longitude
38	blank
39-41	low latitude
42-44	high latitude
45	direction of latitude
46	blank
47-50	low longitude
51-54	high longitude
55	direction of longitude
56	blank
57-59	low latitude
60-62	high latitude
63	direction of latitude
64	blank
65-68	low longitude
69-72	high longitude
73	direction of longitude

Card C (MB Magnitude)

This card is used to search for events with MB magnitudes within specified range.

CC 1	C
2	blank
3-4	low MB magnitude, example 55 = 5.5
5-10	blank
11-12	high MB magnitude

Card D (Depth)

This card is used to search for events with depth within specified range. If low and high depths are blank, all tape records with blank for a depth will be considered hits.

CC 1	D
2	blank
3-5	low depth (in km)
6-10	blank
11-13	high depth (in km)

Card E (Quality)

This card is used to search for events derived from the specified minimum number of stations. Any tape record whose number of stations is equal to or greater than the number indicated on the card is considered a hit.

CC 1	E
2-10	blank
11-13	number of stations

Card F (MS Magnitudes)

This card is used to search for events with MS magnitudes within the specified range.

CC 1	F
2	blank
3-4	low MS magnitude, example 55 = 5.5
5-10	blank
11-12	high MS magnitude

Card G (Magnitudes From Other Sources)

This card is used to search for events with magnitudes from other sources within the specified range.

CC 1	G
2	blank
3-5	low magnitude, example 500 = 5.00
6-10	blank
11-13	high magnitude

Card H (Local Magnitudes)

This card is used to search for events with local magnitudes within the specified range.

CC 1	H
2	blank
3-5	low local magnitude, example 500 = 5.00
6-10	blank
11-13	high local magnitude

Card I (Associated Phenomena)

This card is used to search for events with various associated phenomena. Whatever is in CC 2 indicates the field to be searched.

"D" diastrophic phenomena
"T" tsunamis
"S" seiches
"V" volcanism
"N" non-tectonic events
"O" infrasonic waves

Whatever is in CC 11-17 indicates what that field is being checked against. Therefore, this card allows search of one of six different fields and allows search of that field for from one to seven different items.

CC 1	I
2	field to be searched either D, T, S, V, N, or O
3-10	blank
11-17	item to be searched for. If search is made on only one item put symbol in CC 11. Items which can be selected are as follows:

Diastrophic

F = surface faulting
U = uplift/subsidence
D = faulting and uplift/subsidence

Tsunami

T = tsunami generated
? = possible tsunami

Non-Tectonic

R = rockburst
C = coal bump or rockburst in coal mine
M = meteoritic source
E = explosion or suspected explosion
I = collapse
L = lights or other visual phenomena

Seiche

S = seiche generated
? = possible seiche

Volcanism

V = earthquake associated with volcanism

Infrasonic

T = T-wave
A = acoustic wave
G = gravity wave
B = both A & G

Card J (Intensities)

This card is used to search for events with intensities within the specified range. Any tape record whose intensity is equal to or greater than the intensity indicated on the card is considered a hit.

CC	1	J
	2	blank
	3	intensity (1 thru 9 = I thru IX, X = X, E = XI, T = XII)

Card K (Flinn-Engdahl Regions)

This card is to search for events falling within the specified Flinn-Engdahl geographic region. Several K cards can be used; however, not more than 120 different Flinn-Engdahl geographic numbers may be used.

CC	1	K
	2	blank
	3-5	first Flinn-Engdahl geographic number
	6-80	next 25 Flinn-Engdahl geographic numbers (acceptable to have many K cards with less than the 26 F-E numbers)

Card L (Sources)

This card is used to search for events derived by specific sources. From 1 to 13 comparisons can be made.

CC	1	L
	2	blank
	3-5	first source
	9-41	next 12 sources

Card M (Cultural Effects)

This card is used to search for events with cultural effects. From one to four different cultural effects may be searched.

CC	1	M
	2	blank
	3	first cultural effect
	4	second cultural effect
	5	third cultural effect; C = casualties, D = damage, F = felt
	6	fourth cultural effect

Card N (Depth Control)

This card is used to search for events with specific Depth Control Designations. From one to four different depth control designations may be searched.

CC	1	N
	2	blank
	3	first depth control designation

4	second depth control designation
5	third depth control designation
6	fourth depth control designation

N = held at 33 km
G = depth restrained by geophysicist
D = restrained depth based on 2 or more reported pP's
A = assigned

Card P (Radius Card)

This card is used to search for events within the specified radius from the specified geographic point.

CC	1	P
	2	blank
	3-6	latitude, example 8900 = 89.00°
	7	latitude direction (N or S)
	8	blank
	9-13	longitude, example 10,000 = 100.00°
	14	longitude direction (E or W)
	15	filler
	16-20	radius in km
	21	blank = radius in km M = radius in miles

Type 5 (End Card)----------This card is used to end each search set.

CC	1-3	ZZZ

Appendix B

CEL
PROGRAM RECAL

This program uses a subset of data obtained from the NOAA historical data (see Appendix A) as input. The program computes and plots the annual recurrence interval as a function of magnitude for the region. It then, using this data and assuming a Poisson distribution, computes the cumulative probability of not exceeding a magnitude over a period of time. Faults may be defined as line segments, and all events within a specified distance are associated with that fault; recurrence data and cumulative probability are computed as above for each fault input. The program has options to omit or include regional analysis and to calculate an input fault recurrence. Using the fault recurrence, the program (by use of a Monte Carlo technique) assigns 2,000 years of earthquakes random in magnitude and epicentrally located to the fault. The shortest distance from the fault break to the site is calculated and an acceleration (mean and standard deviation) is determined. A Poisson distribution is used to account for acceleration uncertainty. Where faults are not clearly defined a floating earthquake may be assigned for the region.

In assigning line segments to a fault one should take care to assign all events in the area to specific faults; thus, events will not be overlooked or recurrence interval reduced. Uncertainties exist in the actual location of many epicenters. Further discussion of this is in the text.

It is intended that the historic recurrence data calculated be adjusted based on judgment, taking into account recurrence intervals estimated by other techniques such as slip rate, etc. Provisions are included to allow for input of recurrence coefficients.

Since the program uses random number generation and the Monte Carlo technique, there will be some variation in solution, particularly for values of confidence above 70%. However, below this number, sufficient samples have been taken to insure good repeatability.

User's Guide

Card 1 Format (I10 7F10.0)

Col	Col		
1	10	NPT	number points in data set if not specified seek blank card after earthquake data
11	20	SEALEX	scale for plotting inches per degree longitude
21	30	SCALEY	scale for plotting inches per degree latitude
31	40	XMAX	left side maximum longitude
41	50	XMIN	right side minimum longitude first plot

51	60	1/MAX	top maximum latitude
61	70	1/MIN	bottom minimum latitude
71	80	XMINN	last longitude covered for multiple plots

Card 2 Format (8 F10.0)

1	10	AMIN	minimum magnitude default = 0
11	20	AMAX	maximum magnitude default = 8.6
21	30	TIME	time interval for probability default = 25.0 years
31	40	SITEX	site longitude
41	50	SITEY	site latitude
51	60	FAC	plot scale miles per inch
61	70	R	distance from fault for inclusion default = 10 miles
71	75	OPT1	option to omit regional analysis
76	80	OPT3	option to perform regional analysis (floating earthquake)

Card 3 Format (7 F8.0, 4X, 2A10)

1	8	westmost fault longitude
9	16	westmost fault latitude
17	24	center fault longitude
25	32	center fault latitude
33	40	eastmost fault longitude
41	48	eastmost fault latitude
49	56	maximum fault magnitude
57	60	option to read A and B from next card
61	80	fault name

(Repeat Card 3 as required; end group with blank card.)

Data cards compatible with output from Program CH42.

Data Cards (All fixed point)

Col	Col	
5	6	first two digits of year
11	12	second two digits of year
20	25	latitude
26	32	longitude
36	38	body wave magnitude
54	55	surface wave magnitude
61	63	other magnitude
73	75	local magnitude

NOTE: If NPT not specified, supply one blank card after data.

Appendix C

CEL
PROGRAM OPTREC

This program uses the data in Tables C-1 through C-4 in selecting the closest records to a prescribed magnitude, epicentral distance, acceleration, and site category. Weighting factors are used to combine the effects of magnitude, distance, and acceleration. By assigning zero weight to a variable, that variable may be excluded, thus it is possible to search by magnitude or distance or acceleration or any combination of these. Default parameters consider equal weight.

User's Guide

Group 1 Data Set

Col	Col		
1	5	ID	record I
6	12	DIST	epicentral distance, miles
13	19	DUR	record duration, sec
20	24	NUM	CALTEC record number
25	29	DIR	direction, degrees
30	37	ACC	acceleration peak, cm/sq sec
38	45	VEL	velocity peak, cm/sec
46	53	DISP	displacement peak, cm
54	63	I1,I2	reference
64	68	AMAG	magnitude
69	70	ISITE	site category 0 unclassified 1 alluvium 2 intermediate 3 hard rock

(Repeat for all. End with blank card.)

Group 2

Col	Col		
1	10	SM	magnitude
11	20	SD	site distance, miles
21	30	SA	acceleration, g's
31	35	ICODE(1)	1 = include unclassified site; 0 = omit
36	40	ICODE(2)	1 = include alluvium sites; 0 = omit

41	45	ICODE(3)	1 = include intermediate sites; 0 = omit
46	50	ICODE(4)	1 = include hard rock sites; 0 = omit
51	60	WM	weighting for magnitude
61	70	WD	weighting for distance
71	80	WA	weighting for acceleration

Omitting all weighting defaults to equal weighting, set any weight to 0.0 to omit from weighting.

THIS PAGE IS BEST QUALITY PRACTICABLE
FROM COPY FURNISHED TO DDC

Table C-1. Unclassified Sites

ID	DIST	DUR	NUM	DIR	ACC	VEL	DISP	REF	MAG	SITE
7	85.95	77.30	3	180	-44.50	-6.23	2.69	1	1	7.7-0
8	85.95	77.40	3	270	-52.10	9.07	-2.88	1	1	7.7-0
10	25.81	54.40	4	21	153.00	-15.70	-6.70	1	1	7.7-0
11	25.81	54.40	4	111	174.00	-17.70	-9.15	1	1	7.7-0
16	97.53	82.40	6	180	-54.10	-6.12	-5.11	1	1	7.7-0
17	97.53	82.50	6	90	43.50	9.38	-5.89	1	1	7.7-0
19	97.53	78.60	7	180	-58.10	-6.57	-8.54	1	1	7.7-0
20	97.53	78.60	7	90	41.20	8.91	6.45	1	1	7.7-0
22	15.00	77.90	8	349	165.00	-31.60	12.00	1	1	6.5-0
23	15.00	79.60	8	79	-253.00	29.40	14.10	1	1	6.5-0
31	75.26	90.00	11	180	32.40	-3.97	-2.45	1	1	6.8-0
32	75.26	90.00	11	270	-50.10	-6.96	-4.09	1	1	6.8-0
34	75.26	88.10	12	180	-11.80	1.89	1.65	1	1	6.4-0
35	75.24	88.10	12	270	-15.40	2.67	-2.30	1	1	6.4-0
37	10.27	38.90	13	45	-45.90	-2.89	-1.10	1	1	5.3-0
38	10.27	39.00	13	315	-48.90	4.96	1.40	1	1	5.3-0
40	9.25	39.70	14	351	41.80	2.88	-1.31	1	1	5.3-0
41	9.25	39.60	14	81	-45.40	-2.12	1.00	1	1	5.3-0
52	13.81	40.50	18	181	-63.40	-7.77	-2.80	1	1	5.6-0
53	13.81	40.50	18	271	-174.00	17.10	3.80	1	1	5.6-0
55	85.80	87.40	19	180	-128.00	25.80	-12.20	1	1	6.5-0
56	85.80	87.20	19	270	-54.30	-10.70	-11.00	1	1	6.5-0
61	106.72	124.00	21	188	131.00	20.00	-15.50	1	2	6.3-0
62	106.72	124.00	21	278	-152.00	17.30	-17.50	1	2	6.3-0
67	23.68	75.00	23	0	32.10	-1.96	-.76	1	2	5.4-0
68	23.68	75.00	23	270	-24.40	-2.21	.88	1	2	5.4-0
70	41.14	90.30	24	180	-157.00	-20.90	-8.20	1	2	6.5-0
71	41.16	90.30	24	270	-179.00	11.60	-3.66	1	2	6.5-0
73	92.14	50.90	25	180	143.00	7.34	1.83	1	2	6.0-0
74	92.14	51.00	25	270	142.00	-13.30	-3.74	1	2	6.0-0
85	10.51	89.20	29	356	162.00	21.40	-8.58	1	2	7.1-0
86	10.51	89.10	29	86	-275.00	-17.10	10.40	1	2	7.1-0
118	36.77	45.20	40	33	40.00	-3.47	-1.65	1	2	6.5-0
119	36.77	45.20	40	303	-45.50	-8.20	-2.88	1	2	6.5-0
244	20.73	53.20	82	165	-203.00	22.20	-7.11	1	5	6.6-0
245	20.73	53.20	82	255	174.00	-18.10	-5.27	1	5	6.6-0
511	43.70	29.70	184	115	-43.10	-6.68	-1.24	1	13	6.6-0
512	43.70	29.60	184	205	-57.20	2.87	.73	1	13	6.6-0
745	7.82	76.60	274	0	28.20	-1.81	1.33	1	20	3.0-0
746	7.82	76.60	274	90	-48.80	-3.86	-3.08	1	20	3.0-0
748	20.00	30.00	275	0	33.30	-.94	.47	1	20	5.0-0
749	20.00	30.00	275	90	-24.00	-.82	.64	1	20	5.0-0
751	20.00	55.90	276	0	-8.38	.53	.81	1	20	4.0-0
752	20.00	55.90	276	0	-8.38	.53	.81	1	20	4.0-0
781	28.82	71.40	286	0	-58.50	-6.23	-4.28	1	20	6.5-0
782	28.82	71.30	286	90	-44.50	-6.05	-3.34	1	20	6.5-0
784	22.10	60.10	287	0	30.40	-2.99	-1.95	1	20	5.6-0
785	22.10	60.10	287	90	-27.60	-3.09	1.00	1	20	5.6-0
787	7.34	84.00	288	0	-7.21	-1.40	1.31	1	20	5.5-0
788	7.34	84.00	288	90	35.80	-6.32	-1.51	1	20	5.5-0
790	93.19	77.70	289	0	-28.20	3.77	-1.00	1	20	6.3-0
791	93.19	77.80	289	90	27.00	-3.17	2.67	1	20	6.3-0
793	14.40	68.00	290	0	-30.40	-1.15	.79	1	20	4.3-0
794	14.40	68.00	290	90	-15.00	-.91	1.15	1	20	4.3-0
796	14.40	68.30	291	0	-6.30	2.38	3.24	1	20	3.9-0
797	14.40	68.30	291	90	-7.10	.75	1.05	1	20	3.9-0
799	14.40	61.30	292	0	-62.50	-4.41	2.06	1	20	5.4-0

(continued)

THIS PAGE IS BEST QUALITY PRACTICABLE
FROM COPY FURNISHED TO DDC

Table C-1. Continued

800	14.40	43.80	292	90	-71.10	-5.14	2.20	1	20	5.4-0
802	92.14	75.40	293	0	-13.50	-2.44	2.03	1	20	6.3-0
803	92.14	75.30	293	90	-14.80	2.40	1.47	1	20	6.3-0
820	22.74	61.80	299	45	234.00	21.80	-3.74	1	21	5.0-0
821	22.74	61.80	299	135	172.00	21.70	-3.92	1	21	5.0-0
826	12.39	54.30	301	271	-104.00	11.70	-1.40	1	21	5.3-0
827	12.39	56.30	301	181	119.00	-8.27	1.72	1	21	5.3-0
838	14.73	57.30	305	271	52.00	4.20	2.25	1	21	5.3-0
839	16.73	57.40	305	181	48.90	4.53	1.36	1	21	5.3-0
844	4.96	74.70	307	271	-55.50	-5.25	1.85	1	21	5.0-0
845	4.96	74.70	307	181	-35.30	-3.64	-1.22	1	21	5.0-0
847	17.50	82.30	308	314	57.40	-3.12	1.21	1	21	5.7-0
848	17.50	82.30	308	224	73.60	-3.61	1.18	1	21	5.7-0
850	12.77	87.40	309	271	140.00	-10.80	3.00	1	21	5.7-0
851	12.77	87.60	309	181	-74.00	-4.28	-1.77	1	21	5.7-0
853	13.88	74.10	310	148	-52.20	5.60	-2.55	1	21	6.5-0
854	13.88	74.10	310	238	-77.40	9.36	-5.44	1	21	6.5-0
856	96.81	72.40	311	21	-8.11	2.10	2.53	1	21	5.6-0
857	96.81	72.40	311	111	11.20	-2.21	-1.50	1	21	5.6-0
859	19.01	93.00	312	314	103.00	11.80	-1.70	1	21	5.8-0
860	19.01	93.00	312	224	-232.00	11.90	1.66	1	21	5.8-0
865	35.67	110.00	314	30	62.30	-17.30	-8.21	1	22	6.3-0
866	35.67	110.00	314	300	95.40	-23.70	-14.30	1	22	6.3-0
868	17.66	131.00	315	180	103.00	-29.40	22.70	1	22	6.3-0
869	17.66	131.00	315	270	-154.00	16.50	11.90	1	22	6.3-0
871	2.13	66.60	316	0	30.70	-7.62	2.47	1	22	5.4-0
872	2.13	66.60	316	90	-53.70	9.32	3.57	1	22	5.4-0
880	47.27	48.80	319	324	52.90	3.36	-.80	1	22	6.0-0
881	47.27	48.90	319	234	-35.40	2.90	-1.27	1	22	6.0-0
883	9.90	35.70	320	45	-2.02	-.28	.32	1	22	3.8-0
884	9.90	35.70	320	315	2.42	.33	.43	1	22	3.8-0
901	14.43	29.40	324	24	2.47	-.42	-.24	1	22	4.4-0
902	14.43	29.40	324	114	-3.53	-.60	.34	1	22	4.4-0
907	11.31	26.30	325	45	2.07	-.42	-.38	1	22	4.0-0
908	11.31	26.20	325	315	-0.00	.91	-.48	1	22	4.0-0
913	212.64	86.30	330	70	-45.30	-3.52	1.71	1	22	5.0-0
914	212.64	86.20	330	160	-47.30	-2.67	-1.19	1	22	5.0-0
916	11.17	7.19	331	180	-40.40	2.12	.87	1	22	4.0-0
917	11.17	7.19	331	90	-35.90	-1.13	.42	1	22	4.0-0
925	8.23	16.70	334	115	139.00	-8.88	-2.21	1	23	5.4-0
926	8.23	16.70	334	205	194.00	-9.64	1.04	1	23	5.4-0
934	18.53	29.50	338	0	-114.00	-4.75	-1.76	1	23	5.4-0
935	18.53	29.50	338	90	-57.50	-3.10	1.66	1	23	5.4-0
937	19.53	42.00	339	180	-40.20	-2.55	-.95	1	23	5.4-0
938	19.53	42.00	339	90	-35.40	-1.37	-.70	1	23	5.4-0
940	34.79	23.30	342	0	-10.40	1.54	1.75	1	23	5.4-0
941	34.79	23.40	342	90	18.70	1.45	1.14	1	23	5.4-0
946	36.64	23.40	344	98	-14.50	1.03	-1.03	1	23	5.4-0
947	36.64	23.40	344	188	24.10	-2.00	2.38	1	23	5.4-0
952	90.95	44.90	370	180	-21.50	-3.53	4.25	1	25	6.4-0
953	90.95	44.80	370	90	28.10	2.71	-2.11	1	25	6.4-0
955	107.72	82.30	371	176	-13.20	-4.38	3.47	1	25	6.4-0
956	107.72	82.30	371	266	11.70	-4.28	-2.86	1	25	6.4-0
958	127.59	51.80	372	330	8.74	3.10	-4.98	1	25	6.4-0
959	127.59	51.80	372	240	0.51	-2.87	-2.12	1	25	6.4-0
961	137.04	42.40	373	98	7.36	-1.35	-.53	1	25	6.4-0
962	137.04	42.40	373	188	-7.03	-1.32	-.76	1	25	6.4-0
967	132.45	50.10	375	0	9.83	-2.20	1.71	1	25	6.4-0
968	132.45	51.80	375	90	-10.30	-2.25	-1.84	1	25	6.4-0
970	131.92	60.30	376	180	-7.00	2.10	2.03	1	25	6.4-0
971	131.92	60.30	376	270	10.10	-2.46	-1.62	1	25	6.4-0
979	132.06	62.10	379	277	18.50	4.27	-2.50	1	25	6.4-0

THIS PAGE IS BEST QUALITY PRACTICABLE
FROM COPY FURNISHED TO DDC

Table C-2. Alluvium Sites

ID	DIST	DUR	NUM	DIR	ACC	VEL	DISP	REF	MAG	SITE
1	7.16	53.70	1	180	342.00	33.40	10.90	1	1	6.5 1
2	7.16	53.50	1	270	210.00	-36.90	-10.80	1	1	6.5 1
4	35.00	55.90	2	224	-102.00	4.81	-2.38	1	1	6.0 1
5	35.00	55.90	2	314	110.00	-7.39	-2.74	1	1	6.0 1
13	55.01	75.50	5	42	-87.80	-11.80	4.65	1	1	7.7 1
14	55.01	75.50	5	132	129.00	19.30	-5.76	1	1	7.7 1
25	25.00	42.30	9	44	156.00	35.60	-14.20	1	1	6.5 1
26	25.00	42.40	9	314	197.00	-26.00	-9.62	1	1	6.5 1
28	5.97	49.50	10	320	-100.00	10.80	2.80	1	1	5.5 1
29	5.97	51.80	10	50	106.00	-4.44	-1.67	1	1	5.5 1
58	44.63	79.20	20	180	29.50	5.97	-4.44	1	1	6.5 1
59	64.63	79.20	20	90	28.90	4.07	-3.05	1	1	6.5 1
76	34.37	71.40	26	45	-141.00	-6.60	-3.80	1	2	5.5 1
77	34.37	71.40	26	135	-87.10	4.78	1.66	1	2	5.5 1
79	50.23	67.30	27	45	-61.30	-3.51	-1.99	1	2	6.4 1
80	50.23	67.30	27	135	38.40	-3.44	2.15	1	2	6.4 1
82	35.88	66.80	28	182	64.50	8.22	2.41	1	2	7.1 1
83	35.88	66.70	28	272	-65.90	7.94	2.67	1	2	7.1 1
88	26.78	58.00	30	44	-53.10	-4.95	2.04	1	2	5.5 1
89	26.78	58.00	30	134	74.10	-4.75	-1.86	1	2	5.5 1
91	26.68	66.00	31	21	-63.90	5.93	1.67	1	2	5.9 1
92	26.68	65.80	31	111	64.80	-3.68	1.06	1	2	5.9 1
94	37.92	82.10	32	176	134.00	8.06	-2.73	1	2	6.5 1
95	37.92	82.10	32	266	-104.00	13.10	-3.84	1	2	6.5 1
97	36.40	63.80	33	45	-480.00	-78.10	24.50	1	2	5.6 1
98	36.40	63.80	33	45	-480.00	-78.10	26.50	1	2	5.6 1
100	34.99	44.00	34	355	-348.00	-23.20	-5.31	1	2	5.6 1
101	34.99	44.00	34	85	-424.00	-25.40	-7.11	1	2	5.6 1
103	15.75	24.20	35	50	-233.00	10.80	4.42	1	2	5.6 1
104	15.75	24.20	35	320	-270.00	11.80	-3.93	1	2	5.6 1
106	33.33	44.30	36	50	-52.10	7.02	4.09	1	2	5.6 1
107	33.33	44.30	36	320	-63.20	-8.02	5.60	1	2	5.6 1
142	13.09	50.50	48	0	-250.00	-30.00	-14.90	1	3	6.6 1
143	13.09	50.60	48	270	-132.00	23.90	13.80	1	3	6.6 1
151	25.70	52.30	51	36	97.80	17.10	-9.22	1	3	6.6 1
152	25.70	52.30	51	306	123.00	21.90	11.60	1	3	6.6 1
169	22.13	82.10	57	180	104.00	-17.00	8.63	1	4	6.6 1
170	22.13	82.10	57	90	148.00	-19.40	-13.10	1	4	6.6 1
172	22.13	79.50	58	180	167.00	-16.50	8.05	1	4	6.6 1
173	22.13	79.50	58	90	-207.00	-21.10	-14.70	1	4	6.6 1
175	23.90	57.30	59	314	134.00	9.65	7.51	1	4	6.6 1
176	23.90	57.30	59	224	147.00	-16.70	-12.20	1	4	6.6 1
184	25.66	54.10	62	322	-118.00	16.10	12.00	1	4	6.6 1
185	25.66	54.20	62	232	-130.00	-17.60	6.94	1	4	6.6 1
193	23.88	41.10	65	180	-147.00	18.10	10.30	1	4	6.6 1
194	23.88	41.00	65	270	-156.00	22.10	12.90	1	4	6.6 1
202	20.81	36.90	68	0	81.20	12.40	-8.13	1	4	6.6 1
203	20.81	36.90	68	90	-98.00	-13.30	-7.17	1	4	6.6 1
211	54.29	29.80	71	180	-26.50	-1.87	1.41	1	5	6.6 1
212	54.29	29.80	71	90	25.30	-2.50	-2.08	1	5	6.6 1
223	24.01	43.70	75	0	-134.00	22.30	11.40	1	5	6.6 1
224	24.01	43.60	75	270	112.00	18.60	-11.60	1	5	6.6 1
247	23.97	62.60	83	180	-158.00	18.40	9.05	1	5	6.6 1
248	23.97	62.60	83	90	-162.00	-16.60	-10.40	1	5	6.6 1
256	29.77	78.10	86	277	105.00	17.50	14.80	1	6	6.6 1
257	29.77	78.00	86	187	80.50	-15.10	10.80	1	6	6.6 1
259	54.14	81.20	87	76	26.80	5.01	-3.57	1	6	6.6 1
260	54.14	81.20	87	266	28.20	-7.99	-5.69	1	6	6.6 1
245	26.48	59.20	89	127	-132.00	-20.80	-14.50	1	6	6.6 1
246	26.48	59.30	89	217	-130.00	-20.70	-11.60	1	6	6.6 1
283	22.39	64.60	95	92	-94.20	-16.80	-10.60	1	6	6.6 1
284	22.39	64.60	95	182	83.90	-17.90	12.10	1	6	6.6 1

(continued)

THIS PAGE IS BEST QUALITY PRACTICABLE
FROM COPY FURNISHED TO DDC

Table C-2. Continued

292	25.64	54.20	98	127	-236.00	-21.40	-13.20	1	6	6.6 1
293	25.64	54.20	98	217	-102.00	-18.50	13.50	1	6	6.6 1
301	46.36	0.52	101	180	37.50	-2.62	1.08	1	6	6.6 1
302	46.36	11.20	101	90	-30.00	2.21	-1.28	1	6	6.6 1
307	28.08	27.30	103	0	-91.50	4.43	-2.53	1	6	6.6 1
308	28.08	27.40	103	270	121.00	-5.44	2.40	1	6	6.6 1
313	23.21	63.60	105	180	83.10	-8.33	4.05	1	6	6.6 1
314	23.21	63.60	105	90	77.60	8.08	-4.95	1	6	6.6 1
319	23.88	28.60	107	0	93.50	-7.97	2.96	1	7	6.6 1
320	23.88	28.60	107	90	-107.00	14.30	-7.37	1	7	6.6 1
322	23.86	99.20	108	0	-198.00	-9.84	2.72	1	7	6.6 1
323	23.86	99.30	108	90	-182.00	-16.40	-6.90	1	7	6.6 1
334	25.50	52.00	112	38	102.00	17.00	11.00	1	7	6.6 1
335	25.50	51.90	112	338	78.50	-15.70	-9.25	1	7	6.6 1
340	20.27	57.70	114	120	111.00	14.20	-3.84	1	7	6.6 1
341	20.27	57.70	114	210	134.00	-9.35	2.76	1	7	6.6 1
343	17.43	40.30	115	11	221.00	-28.20	-13.50	1	8	6.6 1
344	17.43	40.30	115	281	-146.00	-23.50	-10.30	1	8	6.6 1
352	30.38	86.30	118	135	33.70	-11.90	8.83	1	8	6.6 1
353	30.38	86.30	118	225	-32.70	9.06	7.82	1	8	6.6 1
361	25.91	45.70	121	270	-110.00	-17.20	-8.68	1	8	6.6 1
362	25.91	45.70	121	180	112.00	-10.60	4.40	1	8	6.6 1
370	46.56	33.00	124	270	-34.00	4.42	2.13	1	8	6.6 1
371	46.56	33.10	124	180	-34.50	-5.80	-2.71	1	8	6.6 1
378	22.23	27.40	128	0	-60.90	13.20	-7.26	1	9	6.6 1
380	22.23	27.40	128	270	-91.60	15.00	8.10	1	9	6.6 1
388	22.87	48.30	131	50	-188.00	17.20	9.28	1	9	6.6 1
389	22.87	48.30	131	320	-161.00	-14.10	6.13	1	9	6.6 1
397	23.26	49.50	134	50	-97.90	16.70	11.00	1	9	6.6 1
398	23.29	49.50	134	140	-82.30	-10.70	-6.23	1	9	6.6 1
406	17.25	56.60	137	90	140.00	-16.10	-7.10	1	9	6.6 1
407	17.25	56.60	137	180	-120.00	22.30	-8.45	1	9	6.6 1
427	20.82	98.60	145	180	114.00	31.60	-17.60	1	10	6.6 1
428	20.82	98.60	145	270	103.00	-28.80	15.30	1	10	6.6 1
436	23.92	18.60	148	0	-108.00	14.20	7.32	1	10	6.6 1
437	23.92	18.60	148	270	112.00	17.50	-11.10	1	10	6.6 1
447	25.73	88.20	174	37	-83.40	20.90	13.80	1	13	6.6 1
448	25.73	88.20	176	127	-116.00	-17.80	-13.70	1	13	6.6 1
499	51.54	149.00	180	180	23.00	-5.71	-3.55	1	13	6.6 1
500	51.54	149.00	180	270	20.90	-8.46	6.55	1	13	6.6 1
517	32.74	58.70	184	143	95.70	-8.76	-4.94	1	14	6.6 1
518	32.74	58.70	186	233	-94.70	-9.74	5.02	1	14	6.6 1
520	44.27	30.00	187	15	-55.70	-3.08	-.71	1	14	6.6 1
521	44.27	30.00	187	285	75.90	-3.47	-.78	1	14	6.6 1
523	23.32	45.20	188	54	-114.00	17.00	10.80	1	14	6.6 1
524	23.32	45.00	188	324	127.00	12.20	5.43	1	14	6.6 1
544	75.37	99.50	195	33	-40.90	-3.56	-2.39	1	14	6.6 1
545	75.37	98.80	195	303	-31.00	4.64	-2.45	1	14	6.6 1
547	45.97	53.30	196	282	35.00	9.49	-7.97	1	14	6.6 1
548	45.97	53.30	196	102	-31.20	-9.24	6.74	1	14	6.6 1
550	114.85	42.50	197	45	-25.60	-2.19	-1.18	1	14	6.6 1
551	114.85	42.50	197	315	-35.40	-2.62	-1.00	1	14	6.6 1
596	25.16	49.40	199	28	138.00	-17.60	9.78	1	15	6.6 1
597	25.16	49.40	199	298	239.00	21.30	10.30	1	15	6.6 1
545	45.00	68.70	204	0	-24.00	-8.17	-5.82	1	15	6.6 1
546	45.00	68.70	204	90	20.80	9.58	-7.27	1	15	6.6 1
568	44.89	112.00	205	339	-28.40	-7.38	4.80	1	15	6.6 1
569	44.89	112.00	205	249	-28.10	10.40	-8.73	1	15	6.6 1
571	44.82	52.80	206	0	37.40	3.46	-1.31	1	15	6.6 1
572	46.82	52.80	206	90	-43.90	2.87	-1.06	1	15	6.6 1

(continued)

THIS PAGE IS BEST QUALITY PRACTICABLE
FROM COPY FURNISHED TO DDC

Table C-2. Continued

580	93.55	53.50	210	135	34.00	2.86	1.67	1	15	6.6	1
581	93.55	53.50	210	225	38.00	-2.70	-1.32	1	15	6.6	1
595	23.97	41.90	217	180	-108.00	-14.80	-9.94	1	16	6.6	1
596	23.97	41.90	217	90	-88.20	-16.20	9.09	1	16	6.6	1
610	49.25	58.10	222	180	-25.00	7.26	-4.94	1	16	6.6	1
611	49.25	58.10	222	270	25.20	5.51	-4.02	1	16	6.6	1
616	31.31	48.80	231	0	41.30	10.70	-8.28	1	16	6.6	1
617	31.31	48.80	231	270	37.80	13.30	10.30	1	16	6.6	1
622	17.48	36.90	233	192	-243.00	31.60	18.30	1	17	6.6	1
623	17.48	36.50	233	282	197.00	-17.80	9.47	1	17	6.6	1
631	20.75	42.30	234	180	-167.00	-13.50	-6.14	1	17	6.6	1
632	20.75	42.30	234	90	122.00	10.30	5.86	1	17	6.6	1
640	22.99	44.90	239	180	119.00	-17.20	-9.80	1	17	6.6	1
641	22.99	44.90	239	90	162.00	-19.10	-11.60	1	17	6.6	1
655	25.04	41.90	244	307	149.00	18.40	9.80	1	18	6.6	1
656	25.04	41.90	244	217	-127.00	-18.70	9.94	1	18	6.6	1
661	21.20	43.50	244	180	-116.00	-14.70	8.30	1	18	6.6	1
662	21.20	43.50	244	90	-107.00	-18.30	-10.50	1	18	6.6	1
667	21.22	45.00	248	180	188.00	-19.80	7.69	1	18	6.6	1
668	21.22	45.00	248	90	-174.00	-18.20	-10.20	1	18	6.6	1
670	23.50	41.20	249	44	-79.00	14.20	11.50	1	18	6.6	1
671	23.50	41.20	249	134	-84.20	10.10	-7.35	1	18	6.6	1
682	25.23	36.40	253	330	242.00	19.30	11.50	1	18	6.6	1
683	25.23	36.40	253	240	-221.00	18.10	-12.50	1	18	6.6	1
697	26.80	48.10	258	29	-56.40	17.20	-10.40	1	19	6.6	1
698	26.80	48.10	258	119	-83.80	-18.50	-10.50	1	19	6.6	1
706	23.74	38.90	261	59	-97.80	-18.30	-12.20	1	19	6.6	1
707	23.74	38.90	261	329	-104.00	11.20	5.93	1	19	6.6	1
721	23.94	41.90	264	0	154.00	-17.50	8.04	1	19	6.6	1
722	23.94	42.00	264	270	-130.00	21.50	-11.60	1	19	6.6	1
724	31.41	48.90	267	0	55.50	-13.50	8.49	1	19	6.6	1
725	31.41	48.70	267	90	61.50	-13.80	9.39	1	19	6.6	1
817	46.34	76.40	298	315	38.50	4.08	-.90	1	21	5.7	1
818	46.34	76.40	298	225	35.90	2.72	.99	1	21	5.7	1
823	40.47	67.90	300	315	-110.00	6.92	-2.94	1	21	6.4	1
824	40.47	67.90	300	225	114.00	-5.75	2.52	1	21	6.4	1
842	24.19	61.30	313	271	-13.10	2.68	-2.27	1	21	5.2	1
843	24.19	61.30	313	181	16.30	1.74	2.08	1	21	5.2	1
874	16.83	62.00	317	130	-14.90	1.33	.85	1	22	5.4	1
875	16.83	62.20	317	220	11.20	1.43	.49	1	22	5.4	1
889	10.70	48.70	322	45	8.56	-.83	-.40	1	22	4.4	1
890	10.70	48.70	322	315	-28.40	2.61	1.17	1	22	4.4	1
910	3.94	60.00	329	180	-164.00	-17.90	8.03	1	22	4.7	1
911	3.94	60.90	329	270	86.90	8.86	2.62	1	22	4.7	1
919	94.14	42.50	332	180	14.50	-1.57	-.70	1	22	6.3	1
920	94.16	42.50	332	90	-12.50	-1.75	-.75	1	22	6.3	1
973	136.12	43.60	377	308	7.67	-2.38	1.98	1	25	6.4	1
974	136.12	43.60	377	218	-11.90	-3.09	2.32	1	25	6.4	1
976	136.12	21.50	378	128	6.97	2.28	-1.07	1	25	6.4	1
977	136.12	21.50	378	218	-11.50	3.08	2.31	1	25	6.4	1

THIS PAGE IS BEST QUALITY PRACTICABLE
FROM COPY FURNISHED TO DDC

Table C-3. Intermediate Sites

ID	DIST	DUR	NUM	DIR	ACC	VEL	DISP	REF	MAG	SITE
43	7.13	39.90	15	10	-81.80	-4.92	-2.25	1	1	5.3 ?
44	7.13	39.90	15	100	-103.00	-4.61	-.83	1	1	5.3 ?
46	8.84	40.80	16	171	-83.80	-5.05	-1.14	1	1	5.3 ?
47	8.84	40.70	16	261	55.10	4.04	.92	1	1	5.3 ?
49	15.03	40.30	17	26	30.00	1.95	-1.50	1	1	5.3 ?
50	15.03	40.10	17	116	23.70	1.19	-1.13	1	1	5.3 ?
112	44.52	30.00	38	324	-14.30	-1.06	1.22	1	2	5.6 ?
113	44.52	29.90	38	234	11.40	.80	-.58	1	2	5.6 ?
115	31.44	30.10	39	160	-20.40	-2.32	-.89	1	2	5.8 ?
116	31.44	30.10	39	70	19.50	-2.82	1.36	1	2	5.8 ?
160	25.19	57.30	50	308	147.00	17.40	11.80	1	3	6.6 ?
161	25.19	57.30	50	218	-117.00	-17.30	11.80	1	3	6.6 ?
166	18.39	61.80	54	21	-309.00	-17.20	8.23	1	4	6.6 ?
167	18.39	61.90	54	291	-265.00	-27.80	9.49	1	4	6.6 ?
214	23.64	53.80	72	285	-82.20	20.90	14.70	1	5	6.6 ?
215	23.64	53.70	72	15	115.00	21.50	11.80	1	5	6.6 ?
252	25.53	54.80	78	310	124.00	23.40	13.70	1	5	6.6 ?
253	25.53	57.00	78	220	-169.00	-16.10	8.88	1	5	6.6 ?
241	20.77	50.50	81	172	213.00	9.88	7.02	1	5	6.6 ?
242	20.77	50.50	81	262	198.00	6.24	-4.60	1	5	6.6 ?
262	20.25	50.40	88	110	264.00	-30.80	11.10	1	6	6.6 ?
263	20.25	50.50	88	200	-200.00	23.50	-5.20	1	6	6.6 ?
274	25.87	33.70	92	118	44.20	-13.80	-10.30	1	6	6.6 ?
275	25.87	33.70	92	208	70.10	-11.60	6.32	1	6	6.6 ?
310	33.25	9.24	100	0	-85.20	8.50	-2.06	1	6	6.6 ?
311	33.25	11.00	104	270	103.00	6.12	2.35	1	6	6.6 ?
328	18.72	97.60	110	98	208.00	13.00	-4.98	1	7	6.6 ?
329	18.72	97.60	110	188	139.00	9.20	-2.89	1	7	6.6 ?
424	15.14	36.70	148	21	-346.00	14.70	1.77	1	10	6.6 ?
425	15.14	36.70	148	291	278.00	-12.80	8.86	1	10	6.6 ?
457	18.21	45.30	166	0	-164.00	12.00	-4.86	1	12	6.6 ?
458	18.21	45.20	166	270	148.00	15.00	-5.44	1	12	6.6 ?
472	86.09	52.50	171	33	12.00	1.81	2.06	1	12	6.6 ?
473	86.09	52.50	171	303	-15.90	2.81	-2.10	1	12	6.6 ?
496	44.74	12.60	179	180	20.80	-1.14	.74	1	13	6.6 ?
497	44.74	12.60	179	90	-44.70	2.84	.91	1	13	6.6 ?
508	43.70	20.00	183	295	42.40	3.83	1.22	1	13	6.6 ?
509	43.70	20.00	183	25	55.70	2.50	.87	1	13	6.6 ?
514	44.19	43.50	185	130	47.30	-3.46	1.71	1	14	6.6 ?
515	44.19	43.50	185	220	67.30	4.45	2.07	1	14	6.6 ?
532	41.35	70.20	191	45	-20.70	4.15	2.50	1	14	6.6 ?
533	41.35	70.20	191	135	-40.10	4.98	-3.76	1	14	6.6 ?
535	24.38	25.40	192	20	94.70	-14.80	7.72	1	14	6.6 ?
536	24.38	25.40	192	290	98.90	19.60	-7.87	1	14	6.6 ?
577	83.25	41.90	208	82	-16.50	2.69	1.66	1	15	6.6 ?
578	83.25	41.90	208	172	17.00	-3.47	2.32	1	15	6.6 ?
586	21.60	46.90	214	260	150.00	23.30	8.03	1	16	6.6 ?
587	21.60	47.00	214	170	156.00	16.30	7.95	1	16	6.6 ?
604	58.60	40.80	220	180	-24.20	-7.02	4.92	1	16	6.6 ?
605	58.60	60.90	220	90	34.30	-5.78	6.70	1	16	6.6 ?
646	25.09	89.80	241	57	84.80	17.90	9.23	1	17	6.6 ?
647	25.09	89.30	241	327	138.00	19.60	9.99	1	17	6.6 ?
676	25.08	47.10	251	37	194.00	16.80	8.93	1	18	6.6 ?
677	25.08	47.10	251	127	-188.00	-18.80	-9.89	1	18	6.6 ?
688	23.32	43.10	255	8	124.00	22.50	-15.90	1	19	6.6 ?
689	23.32	43.10	255	278	-128.00	22.00	10.90	1	19	6.6 ?
708	23.37	34.10	262	277	-68.40	25.70	-14.60	1	19	6.6 ?
710	23.37	34.10	262	187	93.70	-27.80	-13.80	1	19	6.6 ?
718	23.92	20.80	265	180	-104.00	-17.90	-8.69	1	19	6.6 ?
719	23.92	20.80	265	270	125.00	18.20	-12.70	1	19	6.6 ?
802	0.60	22.80	323	81	-15.70	-.82	-.24	1	22	4.4 ?
803	0.60	22.80	323	351	18.60	.98	-.72	1	22	4.4 ?
931	13.83	10.20	334	174	54.00	2.05	.78	1	23	5.4 ?
932	13.83	10.20	334	264	-60.80	3.06	-1.22	1	23	5.4 ?

THIS PAGE IS BEST QUALITY PRACTICABLE
FROM COPY FURNISHED TO DDC

Table C-4. Hard-Rock Sites

ID	DIST	DIR	NUM	DIR	ACC	VEL	DISP	REF	MAG	SITE
109	37.1A	30.40	37	295	-264.00	-14.50	4.66	1	2	5.6 S
110	37.1A	30.40	37	205	-341.00	22.50	-5.50	1	2	5.6 S
121	4.4A	41.80	41	164	-1150.00	-113.00	37.70	1	3	6.6 S
122	4.4A	41.70	41	254	1050.00	-57.70	-10.80	1	3	6.6 S
124	4.4A	12.60	42	254	-27.10	2.86	-1.74	1	3	5.8 S
125	4.4A	12.60	42	164	-20.70	-1.52	-.87	1	3	5.8 S
127	4.4A	17.10	43	254	-45.50	2.66	2.42	1	3	4.2 S
128	4.4A	17.10	43	164	-51.40	1.96	-1.66	1	3	4.2 S
130	4.4A	30.90	44	254	-110.00	-5.63	-2.17	1	3	4.1 S
131	4.4A	30.90	44	164	113.00	-4.74	-2.25	1	3	4.1 S
133	4.4A	13.10	45	254	-47.50	1.56	-.42	1	3	4.5 S
134	4.4A	13.30	45	164	-31.40	-1.31	-1.17	1	3	4.5 S
136	4.4A	19.50	46	254	-23.60	1.43	-1.51	1	3	4.2 S
137	4.4A	19.50	46	164	30.90	-1.03	-.83	1	3	4.2 S
139	4.4A	16.20	47	254	-18.20	-.97	.81	1	3	4.1 S
140	4.4A	16.20	47	164	27.50	.98	-1.27	1	3	4.1 S
304	43.3A	10.40	102	0	-24.60	-1.41	-.84	1	6	6.6 S
305	43.3A	10.40	102	90	-20.60	1.32	-.70	1	6	6.6 S
316	21.5A	101.00	104	180	-87.50	-6.00	1.65	1	7	6.6 S
317	21.5A	101.00	104	270	-189.00	-11.60	4.97	1	7	6.6 S
415	19.1A	60.20	141	21	-146.00	18.00	3.43	1	10	6.6 S
416	19.1A	60.20	141	111	109.00	-14.40	-2.96	1	10	6.6 S
418	17.3A	37.00	142	111	164.00	5.75	1.28	1	10	6.6 S
419	17.3A	37.00	142	201	-144.00	-8.62	1.74	1	10	6.6 S
421	17.2A	35.00	143	21	119.00	4.80	-1.98	1	10	6.6 S
422	17.2A	35.00	143	291	-109.00	4.50	-2.41	1	10	6.6 S
553	20.1A	43.00	198	180	-177.00	-20.50	7.28	1	15	6.6 S
554	20.1A	43.10	198	270	-167.00	14.60	-5.45	1	15	6.6 S
574	21.1P	61.10	207	96	-64.70	3.85	-1.24	1	15	6.6 S
575	21.1P	61.70	207	326	-97.10	8.36	1.72	1	15	6.6 S
583	235.5S	28.30	213	135	-.66	-.27	.21	1	15	6.6 S
584	235.5S	28.20	213	225	-1.23	.29	-.19	1	15	6.6 S
607	26.1A	29.70	221	3	-138.00	5.29	-3.15	1	16	6.6 S
608	26.1A	29.80	221	273	-166.00	-6.67	-5.92	1	16	6.6 S
613	39.6P	32.80	223	55	-69.70	4.60	-2.07	1	16	6.6 S
614	39.6P	32.80	223	325	53.30	-4.40	1.82	1	16	6.6 S
818	3.7D	45.00	297	0	-78.90	-3.22	-.84	1	21	6.6 S
819	3.7D	45.00	297	90	-83.10	-3.88	-.99	1	21	6.6 S
928	11.7A	38.10	335	95	-60.90	-5.55	-2.02	1	23	5.4 S
929	11.7A	38.10	335	185	58.90	1.97	-2.01	1	23	5.4 S

Appendix D

CEL
PROGRAM RESPLOT

This program uses the CALTEC spectra data and plot Fourier and response spectra. The program can produce SCR 4020 plots or CALCOMP plots. Options exist in the program to plot different records on the same plot, to average records or to plot an envelope. Data may be displayed in acceleration-period plots or tripartile plots.

User's Guide

Card 1

Col	Col	
1	10	0 CALCOMP plot 1 SCR 4020 plot

Card 2

Col	Col	
1		L = last of group for plot S = stop after plot
2	5	ID file (see Appendix C)
6	10	code 1 Fourier spectra 2 0% damping response spectra 3 2% damping response spectra 4 5% damping response spectra 5 10% damping response spectra 6 20% damping response spectra
11	20	scale value (default = 1.0)
21	30	response acceleration (scaling), g's
31	40	ground motion acceleration (scaling), g's
41	45	0 = plot acceleration-period; 1 = omit
46	50	0 = plot tripartile; 1 = omit
51	55	1 = average group; 0 = omit
56	60	1 = maximum group; 0 = omit

(Repeat as required.)

Appendix E

CEL
PROGRAM TIMHIS

This program scales plots and punches time histories of the California Institute of Technology accelerograms.

User's Guide

Card 1

Col	Col	
1	5	ID number
10	20	SCALE; default = 1.0
21	30	AMAX, g's
31	35	flag to plot CALCOMP
35	40	flag to PUNCH
41	45	flag to plot 4020
46	80	format for punch output

DISTRIBUTION LIST

AF HQ Prees Washington DC (R P Reid)
AFB AFCEC/XR,Tyndall FL; CESCH, Wright-Patterson; MAC/DET (Col. P. Thompson) Scott, IL; SAMSO/MNNF, Norton AFB CA; Stinfo Library, Offutt NE
ARCTICSUBLAB Code 54T, San Diego, CA
ARMY BMDSC-RE (H. McClellan) Huntsville AL; DAEN-MCE-D Washington DC; ERADCOM Tech Supp Dir. (DELSD-L) Ft. Monmouth, NJ; Tech. Ref. Div., Fort Huachuca, AZ
ARMY - CERL Library, Champaign IL
ARMY COASTAL ENGR RSCH CEN Fort Belvoir VA; R. Jachowski, Fort Belvoir VA
ARMY CORPS OF ENGINEERS MRD-Eng. Div., Omaha NE; Seattle Dist. Library, Seattle WA
ARMY ENG DIV ED-CS (S.Bolin) Huntsville, AL; HNDED-CS, Huntsville AL; Hnded-Sr, Huntsville, AL
ARMY ENG WATERWAYS EXP STA Library, Vicksburg MS
ARMY ENGR DIST. Library, Portland OR
ARMY ENVIRON. HYGIENE AGCY Water Qual Div (Doner), Aberdeen Prov Ground, MD
ARMY MATERIALS & MECHANICS RESEARCH CENTER Dr. Lenoe, Watertown MA
ARMY MISSILE R&D CMD Redstone Arsenal AL Sci. Info. Cen (Documents)
ARMY MOBIL EQUIP R&D COM Mr. Cevasco, Fort Belvoir MD
ARMY-PLASTEC Picatinny Arsenal (A M Anzalone, SMUPA-FR-M-D) Dover NJ
ASST SECRETARY OF THE NAVY Spec. Assist Energy (P. Waterman), Washington DC
BUREAU OF RECLAMATION Code 1512 (C. Selander) Denver CO
CINCLANT Civil Engr. Supp. Plans. Ofr Norfolk, VA
CNM NMAT 08T246 (Dieterle) Wash. DC
CNO Code NOP-964, Washington DC; OP987J (J. Boosman), Pentagon
COMOCEANSYSPAC SCE, Pearl Harbor HI
DEFENSE CIVIL PREPAREDNESS AGENCY J.O. Buchanan, Washington DC
DEFENSE DOCUMENTATION CTR Alexandria, VA
DEFENSE INTELLIGENCE AGENCY Dir., Washington DC
DNA STTL, Washington DC
DOD Explosives Safety Board (Library), Washington DC
DOE Dr. Cohen
DTNSRDC Code 1706, Bethesda MD; Code 172 (M. Krenzke), Bethesda MD
DTNSRDC Code 4121 (R. Rivers), Annapolis, MD
FLTCOMBATTRACENLANT PWO, Virginia Bch VA
HEDSUPPACT PWO, Taipei, Taiwan
MARINE CORPS BASE M & R Division, Camp Lejeune NC; PWO, Camp S. D. Butler, Kawasaki Japan
MARINE CORPS DIST 9, Code 043, Overland Park KS
MARINE CORPS HQS Code LFF-2, Washington DC
MCAS Facil. Engr. Div. Cherry Point NC; Code PWE, Kaneohe Bay HI; Code S4, Quantico VA; J. Taylor, Iwakuni Japan; PWD, Dir. Maint. Control Div., Iwakuni Japan; PWO Kaneohe Bay HI
MCDEC P&S Div Quantico VA
MCLSBPAC B520, Barstow CA
MCRD PWO, San Diego Ca
NAD Engr. Dir. Hawthorne, NV
NAF PWO Sigonella Sicily; PWO, Atsugi Japan
NAS CO, Guantanamo Bay Cuba; Code 114, Alameda CA; Code 183 (Fac. Plan BR MGR); Code 187, Jacksonville FL; Code 18700, Brunswick ME; Code 70, Atlanta, Marietta GA; Dir. Util. Div., Bermuda; ENS Buchholz, Pensacola, FL; Lead. Chief. Petty Offr. PW/Self Help Div, Beeville TX; PW (J. Maguire), Corpus Christi TX; PWD Maint. Div., New Orleans, Belle Chasse LA; PWD, Willow Grove PA; PWO (M. Elliott), Los Alamitos CA; PWO Belle Chasse, LA; PWO Chase Field Beeville, TX; PWO Key West FL; PWO Whiting Fld, Milton FL; PWO, Dallas TX; PWO, Glenview IL; PWO, Kingsville TX; PWO, Miramar, San Diego CA; SCE Lant Fleet Norfolk, VA; SCE Norfolk, VA; SCE, Barbers Point HI
NATL RESEARCH COUNCIL Naval Studies Board, Washington DC
NATPARACHUTETESTRAN PW Engr, El Centro CA
NAVACT PWO, London UK
NAVAEROSPREGMEDCEN SCE, Pensacola FL
NAVAL FACILITY PWO, Barbados; PWO, Brawdy Wales UK; PWO, Cape Hatteras, Buxton NC

NAVCOASTSYSLAB CO, Panama City FL; Code 423 (D. Good), Panama City FL; Code 715 (J. Quirk) Panama City, FL; Library Panama City, FL
NAVCOMMAREAMSTRSTA PWO, Norfolk VA; PWO, Wahiawa HI; SCE Unit 1 Naples Italy
NAVCOMMSTA Code 401 Nea Makri, Greece; PWO, Adak AK; PWO, Exmouth, Australia
NAVEDTRAPRODEVCEN Tech. Library
NAVEDUTRACEN Engr Dept (Code 42) Newport, RI
NAVFACENGCOM Code 043 Alexandria, VA; Code 044 Alexandria, VA; Code 0451 Alexandria, VA; Code 0453 (D. Potter) Alexandria, VA; Code 0454B Alexandria, Va; Code 04B5 Alexandria, VA; Code 101 Alexandria, VA; Code 10133 (J. Leimanis) Alexandria, VA; Code 1023 (T. Stevens) Alexandria, VA; Code 2014 (Mr. Taam), Pearl Harbor HI; Morrison Yap, Caroline Is.; P W Brewer Alexandria, VA; PC-22 (E. Spencer) Alexandria, VA; PL-2 Ponce P.R. Alexandria, VA
NAVFACENGCOM - CHES DIV. Code 101 Wash, DC; Code 402 (R. Morony) Wash, DC; Code 405 Wash, DC; Code FPO-1 (C. Bodey) Wash, DC; Code FPO-1 (Ottsen) Wash, DC; Code FPO-1SP (Dr. Lewis) Wash, DC; Code FPO-1SP13 (T F Sullivan) Wash, DC; Code FPO-1P12 (Mr. Scola), Washington DC; Scheessele, Code 402, Wash, DC
NAVFACENGCOM - LANT DIV.; Eur. BR Deputy Dir, Naples Italy; RDT&ELO 09P2, Norfolk VA
NAVFACENGCOM - NORTH DIV. (Boretsky) Philadelphia, PA; Code 09P (LCDR A.J. Stewart); Code 1028, RDT&ELO, Philadelphia PA; Design Div. (R. Masino), Philadelphia PA; ROICC, Contracts, Crane IN
NAVFACENGCOM - PAC DIV. Code 402, RDT&E, Pearl Harbor HI; Commander, Pearl Harbor, HI
NAVFACENGCOM - SOUTH DIV. Code 90, RDT&ELO, Charleston SC; Dir., New Orleans LA
NAVFACENGCOM - WEST DIV. Code 04B; RDT&ELO Code 2011 San Bruno, CA
NAVFACENGCOM CONTRACT AROICC, Point Mugu CA; AROICC, Quantico, VA; Eng Div dir, Southwest Pac, Manila, PI; OICC, Southwest Pac, Manila, PI; OICC/ROICC, Balboa Canal Zone; ROICC (Ervin) Puget Sound Naval Shipyard, Bremerton, WA; ROICC AF Guam; ROICC LANT DIV., Norfolk VA; ROICC, Diego Garcia Island; ROICC, Keflavik, Iceland; ROICC, Pacific, San Bruno CA
NAVHOSP LT R. Elsbernd, Puerto Rico
NAVMAG SCE, Guam
NAVMIRO OIC, Philadelphia PA
NAVOCEANSYSCEN Code 409 (D. G. Moore), San Diego CA; Code 5311(T) (E. Hamilton) San Diego CA; Code 6565 (Tech. Lib.), San Diego CA
NAVORDSTA PWO, Louisville KY
NAVPETOFF Code 30, Alexandria VA
NAVPGSCOL Code 61WL (O. Wilson) Monterey CA
NAVPHIBASE CO, ACB 2 Norfolk, VA; Code S3T, Norfolk VA; Harbor Clearance Unit Two, Little Creek, VA; OIC, UCT ONE Norfolk, Va
NAVREGMEDCEN Code 3041, Memphis, Millington TN; SCE (D. Kaye); SCE (LCDR B. E. Thurston), San Diego CA; SCE, Camp Pendleton CA
NAVSCOLCECOFF C35 Port Hueneme, CA; C44A (R. Chittenden), Port Hueneme CA; CO, Code C44A Port Hueneme, CA
NAVSEASYSCOM Code OOC (LT R. MacDougal), Washington DC
NAVSEC Code 6034 (Library), Washington DC
NAVSECGRUACT PWO, Torri Sta, Okinawa
NAVSHIPREPFAC Library, Guam; SCE Subic Bay
NAVSHIPYD Code 202.4, Long Beach CA; Code 202.5 (Library) Puget Sound, Bremerton WA; Code 400, Puget Sound; Code 404 (LT J. Riccio), Norfolk, Portsmouth VA; Code 410, Mare Is., Vallejo CA; Code 440 Portsmouth NH; Code 440, Norfolk; Code 440, Puget Sound, Bremerton WA; Code 440.4, Charleston SC; L.D. Vivian; Library, Portsmouth NH; PWO, Mare Is.; Tech Library, Vallejo, CA
NAVSTA CO Naval Station, Mayport FL; CO Roosevelt Roads P.R. Puerto Rico; Engr. Dir., Rota Spain; Maint. Div. Dir/Code 531, Rodman Canal Zone; PWD (LTJG.P.M. Motolenich), Puerto Rico; PWO Midway Island; PWO, Keflavik Iceland; PWO, Mayport FL; ROICC, Rota Spain; SCE, Guam; SCE, Subic Bay, R.P.; Utilities Engr Off. (LTJG A.S. Ritchie), Rota Spain
NAVSUBASE LTJG D.W. Peck, Groton, CT
NAVSUPPACT CO, Seattle WA; Code 413, Seattle WA; Engr. Div. (F. Mollica), Naples Italy; LTJG McGarrah, Vallejo CA
NAVSURFWPNCEN PWO, White Oak, Silver Spring, MD
NAVTECHTRACEN SCE, Pensacola FL
NAVWPNCEN Code 2636 (W. Bonner), China Lake CA; PWO (Code 26), China Lake CA; ROICC (Code 702), China Lake CA

NAVWPNSTA EARLE ENS G.A. Lowry, Fallbrook CA; PW Office (Code 09C1) Yorktown, VA
NAVWPNSUPPCEN Code 09 (Boennighausen) Crane IN
NCBU 405 OIC, San Diego, CA
NCBC CEL (CAPT N. W. Petersen), Port Hueneme, CA; CEL AOIC Port Hueneme CA; Code 10 Davisville, RI; Code 155, Port Hueneme CA; Code 156, Port Hueneme, CA; PW Engrg, Gulfport MS; PWO (Code 80) Port Hueneme, CA
NCBU 411 OIC, Norfolk VA
NCR 20, Commander
NMCB 133 (ENS T.W. Nielsen); 5, Operations Dept.; Forty, CO; THREE, Operations Off.
NORDA Code 440 (Ocean Rsch Off) Bay St. Louis MS
NRL Code 8400 (J. Walsh), Washington DC; Code 8441 (R.A. Skop), Washington DC; Rosenthal, Code 8440, Wash. DC
NSD SCE, Subic Bay, R.P.
NTC Code 54 (ENS P. G. Jackel), Orlando FL; Commander Orlando, FL
NUSC Code 131 New London, CT; Code EA123 (R.S. Munn), New London CT; Code TA131 (G. De la Cruz), New London CT
ONR Code 700F Arlington VA; Dr. A. Laufer, Pasadena CA
PHIBCB 1 P&E, Coronado, CA
PMTC Code 4253-3, Point Mugu, CA; Pat. Counsel, Point Mugu CA
PWC ACE Office (LTJG St. Germain) Norfolk VA; CO Norfolk, VA; CO, Great Lakes IL; Code 116 (LTJG. A. Eckhart) Great Lakes, IL; Code 120, Oakland CA; Code 120C (Library) San Diego, CA; Code 128, Guam; Code 200, Great Lakes IL; Code 200, Oakland CA; Code 220 Oakland, CA; Code 220.1, Norfolk VA; Code 30C (Boettcher) San Diego, CA; Code 400, Pearl Harbor, HI; Code 680, San Diego CA; Library, Subic Bay, R.P.; OIC CBU-405, San Diego CA; XO Oakland, CA
SPCC Code 122B, Mechanicsburg, PA; PWO (Code 120) Mechanicsburg PA
U.S. MERCHANT MARINE ACADEMY Kings Point, NY (Reprint Custodian)
US DEPT OF INTERIOR Bureau of Land MNGMNT - Code 733 (T.E. Sullivan) Wash, DC
US GEOLOGICAL SURVEY Off. Marine Geology, *Piteleki, Reston VA*
USAF SCHOOL OF AEROSPACE MEDICINE Hyperbaric Medicine Div, Brooks AFB, TX
USCG (G-ECV) Washington Dc; (G-ECV/61) (Burkhart) Washington, DC; G-EOE-4/61 (T. Dowd), Washington DC
USCG ACADEMY LT N. Stramandi, New London CT
USCG R&D CENTER D. Motherway, Groton CT; Tech. Dir. Groton, CT
USNA Ch. Mech. Engr. Dept Annapolis MD; Ocean Sys. Eng Dept (Dr. Monney) Annapolis, MD; PWD Engr. Div. (C. Bradford) Annapolis MD; PWO Annapolis MD
AMERICAN CONCRETE INSTITUTE Detroit MI (Library)
CALIF. DEPT OF NAVIGATION & OCEAN DEV. Sacramento, CA (G. Armstrong)
CALIFORNIA STATE UNIVERSITY LONG BEACH, CA (CHELAPATI); LONG BEACH, CA (YEN)
COLORADO STATE UNIV., FOOTHILL CAMPUS Fort Collins (Nelson)
CORNELL UNIVERSITY Ithaca NY (Serials Dept, Engr Lib.)
DAMES & MOORE LIBRARY LOS ANGELES, CA
DUKE UNIV MEDICAL CENTER B. Muga, Durham NC; DURHAM, NC (VESIC)
FLORIDA ATLANTIC UNIVERSITY BOCA RATON, FL (MC ALLISTER); Boca Raton FL (Ocean Engr Dept., C. Lin)
FLORIDA ATLANTIC UNIVERSITY Boca Raton FL (W. Tessin)
FLORIDA TECHNOLOGICAL UNIVERSITY ORLANDO, FL (HARTMAN)
GEORGIA INSTITUTE OF TECHNOLOGY Atlanta GA (School of Civil Engr., Kahn); Atlanta GA (B. Mazanti)
IOWA STATE UNIVERSITY Ames IA (CE Dept, Handy)
VIRGINIA INST. OF MARINE SCI. Gloucester Point VA (Library)
LEHIGH UNIVERSITY BETHLEHEM, PA (MARINE GEOTECHNICAL LAB., RICHARDS); Bethlehem PA (Fritz Engr. Lab No. 13, Beedle); Bethlehem PA (Linderman Lib. No.30, Fleckstein)
LIBRARY OF CONGRESS WASHINGTON, DC (SCIENCES & TECH DIV)
MICHIGAN TECHNOLOGICAL UNIVERSITY Houghton, MI (Haas)
MIT Cambridge MA; Cambridge MA (Rm 10-500, Tech. Reports, Engr. Lib.); Cambridge MA (Whitman)
NEW MEXICO SOLAR ENERGY INST. Dr. Zwibel Las Cruces NM
NORTHWESTERN UNIV Z.P. Bazant Evanston IL
NY CITY COMMUNITY COLLEGE BROOKLYN, NY (LIBRARY)
UNIV. NOTRE DAME Katona, Notre Dame, IN
OREGON STATE UNIVERSITY (CE Dept Grace) Corvallis, OR; CORVALLIS, OR (CE DEPT, BELL);

CORVALLIS, OR (CE DEPT, HICKS); Corvalis OR (School of Oceanography)
PENNSYLVANIA STATE UNIVERSITY UNIVERSITY PARK, PA (GOTOLSKI)
PURDUE UNIVERSITY Lafayette IN (Leonards); Lafayette, IN (Altschaeffl); Lafayette, IN (CE Engr. Lib)
SAN DIEGO STATE UNIV. I. Noorany San Diego, CA; Dr. Krishnamoorthy, San Diego CA
SEATTLE U Prof Schwaegler Seattle WA
SOUTHWEST RSCH INST King, San Antonio, TX; R. DeHart, San Antonio TX
STANFORD UNIVERSITY Engr Lib, Stanford CA; Stanford CA (Gene)
STATE UNIV. OF NEW YORK Buffalo, NY
TEXAS A&M UNIVERSITY COLLEGE STATION, TX (CE DEPT); College Station TX (CE Dept. Herbich)
UNIVERSITY OF CALIFORNIA BERKELEY, CA (CE DEPT, GERWICK); BERKELEY, CA (CE DEPT, MITCHELL); Berkeley CA (B. Bresler); Berkeley CA (Dept of Naval Arch.); Berkeley CA (R. Williamson); DAVIS, CA (CE DEPT, TAYLOR); LIVERMORE, CA (LAWRENCE LIVERMORE LAB, TOKARZ); La Jolla CA (Acq. Dept, Lib. C-075A); M. Duncan, Berkeley CA; SAN DIEGO, CA, LA JOLLA, CA (SEROCKI)
UNIVERSITY OF DELAWARE Newark, DE (Dept of Civil Engineering, Chesson)
UNIVERSITY OF HAWAII HONOLULU, HI (SCIENCE AND TECH. DIV.); Honolulu HI (Dr. Szilard)
UNIVERSITY OF ILLINOIS Metz Ref Rm, Urbana IL; URBANA, IL (DAVISSON); URBANA, IL (LIBRARY); URBANA, IL (NEWARK); Urbana IL (CE Dept, W. Gamble)
UNIVERSITY OF MASSACHUSETTS (Heronemus), Amherst MA CE Dept
UNIVERSITY OF MICHIGAN Ann Arbor MI (Richart)
UNIVERSITY OF NEBRASKA-LINCOLN Lincoln, NE (Ross Ice Shelf Proj.)
UNIVERSITY OF NEW MEXICO J Nielson-Engr Matls & Civil Sys Div, Albuquerque NM
UNIVERSITY OF TEXAS Inst. Marine Sci (Library), Port Arkansas TX
UNIVERSITY OF TEXAS AT AUSTIN AUSTIN, TX (THOMPSON); Austin TX (R. Olson); Austin, TX (Breen)
UNIVERSITY OF WASHINGTON Dept of Civil Engr (Dr. Mattock), Seattle WA; SEATTLE, WA (MERCHANT); SEATTLE, WA (OCEAN ENG RSCH LAB, GRAY); Seattle WA (E. Linger); Seattle, WA Transportation, Construction & Geom. Div
ALFRED A. YEE & ASSOC. Honolulu HI
AMETEK Offshore Res. & Engr Div
APPLIED TECH COUNCIL R. Scholl, Palo Alto CA
ARVID GRANT OLYMPIA, WA
ATLANTIC RICHFIELD CO. DALLAS, TX (SMITH)
AUSTRALIA Dept. PW (A. Hicks), Melbourne
BECHTEL CORP. SAN FRANCISCO, CA (PHELPS)
BELGIUM HAECON, N.V., Gent
BETHLEHEM STEEL CO. Dismuke, Bethelehem, PA
BROWN & CALDWELL E M Saunders Walnut Creek, CA
BROWN & ROOT Houston TX (D. Ward)
CANADA Mem Univ Newfoundland (Chari), St Johns; Surveyor, Nenninger & Chenevert Inc., Montreal; Warnock Hersey Prof. Srv Ltd, La Sale, Quebec
CF BRAUN CO Du Bouchet, Murray Hill, NJ
CHEVRON OIL FIELD RESEARCH CO. LA HABRA, CA (BROOKS)
CONCRETE TECHNOLOGY CORP. TACOMA, WA (ANDERSON)
CONRAD ASSOC. Van Nuys CA (A. Luisoni)
DRAVO CORP Pittsburgh PA (Giannino); Pittsburgh PA (Wright)
NORWAY DET NORSKE VERITAS (Library), Oslo
EVALUATION ASSOC. INC KING OF PRUSSIA, PA (FEDELE)
FORD, BACON & DAVIS, INC. New York (Library)
FRANCE Dr. Dutertre, Boulogne; L. Pliskin, Paris; P. Jensen, Boulogne
GEOTECHNICAL ENGINEERS INC. Winchester, MA (Paulding)
GLIDDEN CO. STRONGSVILLE, OH (RSCH LIB)
GRUMMAN AEROSPACE CORP. Bethpage NY (Tech. Info. Ctr)
HALEY & ALDRICH, INC. Cambridge MA (Aldrich, Jr.)
HONEYWELL, INC. Minneapolis MN (Residential Engr Lib.)
HUGHES AIRCRAFT Culver City CA (Tech. Doc. Ctr)
ITALY M. Caironi, Milan; Sergio Tattoni Milano; Torino (F. Levi)
MAKAI OCEAN ENGRNG INC. Kailua, HI
JAMES CO. R. Girdley, Orlando FL
LAMONT-DOHERTY GEOLOGICAL OBSERV. Palisades NY (McCoy); Palisades NY (Selwyn)

LOCKHEED MISSILES & SPACE CO. INC. Mgr Naval Arch & Mar Eng Sunnyvale, CA; Sunnyvale CA (Rynewicz); Sunnyvale, CA (Phillips)
LOCKHEED OCEAN LABORATORY San Diego CA (F. Simpson)
MARATHON OIL CO Houston TX (C. Seay)
MC CLELLAND ENGINEERS INC Houston TX (B. McClelland)
MCDONNEL AIRCRAFT CO. Dept 501 (R.H. Fayman), St Louis MO
MEDALL & ASSOC. INC. J.T. GAFFEY II SANTA ANA, CA
MEXICO R. Cardenas
MOBIL PIPE LINE CO. DALLAS, TX MGR OF ENGR (NOACK)
MUESER, RUTLEDGE, WENTWORTH AND JOHNSTON NEW YORK (RICHARDS)
NEW ZEALAND New Zealand Concrete Research Assoc. (Librarian), Porirua
NEWPORT NEWS SHIPBLDG & DRYDOCK CO. Newport News VA (Tech. Lib.)
NORWAY DET NORSKE VERITAS (Roren) Oslo; I. Foss, Oslo; J. Creed, Ski; Norwegian Tech Univ (Brandtzaeg), Trondheim
OFFSHORE DEVELOPMENT ENG. INC. BERKELEY, CA
PACIFIC MARINE TECHNOLOGY Long Beach, CA (Wagner)
PORTLAND CEMENT ASSOC. SKOKIE, IL (CORELY); Skokie IL (Rsch & Dev Lab, Lib.)
PRESCON CORP TOWSON, MD (KELLER)
RAND CORP. Santa Monica CA (A. Laupa)
RAYMOND INTERNATIONAL INC. E Colle Soil Tech Dept, Pennsauken, NJ
RIVERSIDE CEMENT CO Riverside CA (W. Smith)
SANDIA LABORATOkIES Library Div., Livermore CA
SCHUPACK ASSOC SO. NORWALK, CT (SCHUPACK)
SEATECH CORP. MIAMI, FL (PERONI)
SHELL DEVELOPMENT CO. Houston TX (E. Doyle)
SHELL OIL CO. HOUSTON, TX (MARSHALL)
SOUTH AMERICA N. Nouel, Valencia, Venezuela
SWEDEN GeoTech Inst; VBB (Library), Stockholm
TIDEWATER CONSTR. CO Norfolk VA (Fowler)
TRW SYSTEMS CLEVELAND, OH (ENG. LIB.); REDONDO BEACH, CA (DAI)
UNITED KINGDOM Cement & Concrete Assoc Wexham Springs, Slough Bucks; Cement & Concrete Assoc. (Lit. Ex), Bucks; D. New, G. Maunsell & Partners, London; Library, Bristol; Shaw & Hatton (F. Hansen), London; Taylor, Woodrow Constr (014P), Southall, Middlesex; Univ. of Bristol (R. Morgan), Bristol
WATT BRIAN ASSOC INC. Houston, TX
WESTINGHOUSE ELECTRIC CORP. Annapolis MD (Oceanic Div Lib, Bryan); Library, Pittsburgh PA
WISS, JANNEY, ELSTNER, & ASSOC Northbrook, IL (D.W. Pfeifer)
WOODWARD-CLYDE CONSULTANTS (A. Harrigan) San Francisco; PLYMOUTH MEETING PA (CROSS, III)
AL SMOOTS Los Angeles, CA
BARA, JOHN P. Lakewood, CO
BROWN, ROBERT University, AL
BULLOCK La Canada
F. HEUZE Boulder CO
CAPT MURPHY Sunnyvale, CA
GREG PAGE EUGENE, OR
R.F. BESIER Old Saybrook CT
T.W. MERMEL Washington DC